NACA
L-553

MR Oct. 1943

L-553

NATIONAL ADVISORY COMMITTEE FOR AERONAUTICS

WARTIME REPORT

ORIGINALLY ISSUED

October 1943 as
Memorandum Report

PRESSURE-DISTRIBUTION MEASUREMENTS ON VARIOUS SURFACES OF A 0.2375-SCALE MODEL OF THE DOUGLAS XA-26 AIRPLANE IN THE 19-FOOT PRESSURE TUNNEL

By C. Dixon Ashworth

Langley Memorial Aeronautical Laboratory
Langley Field, Va.

JPL LIBRARY
CALIFORNIA INSTITUTE OF TECHNOLOGY

WASHINGTON

NACA WARTIME REPORTS are reprints of papers originally issued to provide rapid distribution of advance research results to an authorized group requiring them for the war effort. They were previously held under a security status but are now unclassified. Some of these reports were not technically edited. All have been reproduced without change in order to expedite general distribution.

L-553

MEMORANDUM REPORT

for the

Army Air Forces, Materiel Command

PRESSURE-DISTRIBUTION MEASUREMENTS ON VARIOUS SURFACES OF A 0.2375-SCALE MODEL OF THE DOUGLAS XA-26 AIRPLANE IN THE 19-FOOT PRESSURE TUNNEL

By C. Dixon Ashworth

SUMMARY

Pressure-distribution measurements on a 0.2375-scale model of the Douglas XA-26 airplane were conducted in the NACA 19-foot pressure tunnel.

The measurements were made on the spinner-cowl-nacelle assembly and the fuselage for angles of yaw from -10° to 10° and at angles of attack from -8° to 8°. Pressures were also measured on the main-wheel door, nose-wheel door, and bomb-bay door at door angles from closed to full open through various ranges of angle of yaw and angle of attack. These tests were made at an airspeed of approximately 95 miles per hour with the air in the tunnel compressed to 35 pounds per square inch absolute, corresponding to a Reynolds number and Mach number of approximately 3,900,000 and 0.12, respectively.

The results of the pressure measurements on the doors are presented as loads and hinge moments, whereas the measurements obtained on the nacelle and fuselage are shown as pressures on isometric diagrams. The latter method of presenting data was used to eliminate tedious tables.

Tests of the model indicate that no critical pressures should be encountered in the high-speed level-flight condition of the airplane at 17,000 feet unless the spinner is removed; removing the spinner introduces critical pressures at 265 miles per hour. The nose-wheel door over most of the range tested will tend to close while the main-wheel and bomb-bay doors tend to open due to the aerodynamic loads.

INTRODUCTION

Efficient aerodynamic and structural design of modern high-speed aircraft is often dependent on a knowledge of the static pressures acting on the surface of the airplane. To obtain such information for application to the design of the XA-26 airplane, the NACA has conducted an extensive investigation of the pressure distribution over various surfaces of a 0.2375-scale model of that airplane. The investigation was requested by the Army Air Forces, Materiel Center, and was conducted in the 19-foot pressure tunnel at Langley Memorial Aeronautical Laboratory.

Pressure distribution measurements were made at angles of yaw from -10° to 10° and at angles of attack from -8° to 8° to determine:

(1) pressures acting on the cowl with and without spinner, on the nacelle, and on the fuselage

(2) the effect of flaps on the pressure distribution over the nacelle and fuselage at 0° yaw

(3) the loads and hinge moments on the main-wheel, nose-wheel, and bomb-bay doors at various door angles

(4) the loads acting on the upper and lower two-gun turrets

The load and hinge-moment data for the various doors are of particular interest because it is believed that this is the first time such complete information has been made available.

APPARATUS AND TESTS

The principal dimensions of the 0.2375-scale model of the Douglas XA-26 airplane are shown in figure 1. The model was tested as shown there except for one configuration with the spinner removed. All pressure-distribution tests were made with the propellers off.

The method of mounting the model in the wind tunnel is shown in figure 2(a) (yaw support on which all surfaces were tested) and figure 2(b) (normal supports where the

tests were made on the bomb-bay door because of the severe interference effects between the yaw strut and the door). The tests were made in the 19-foot pressure tunnel which has a closed circular test section.

The model is of all-metal construction following very closely the lines of its prototype. As tested, it was sprayed with several coats of lacquer, sanded, and waxed to produce a smooth finish. The pressure orifices were installed in such a way that clean, smooth orifices flush with the surface of the model were produced.

Simultaneous measurement of the pressure acting at every orifice could not be obtained because of the great number of orifices (nearly 1000) and the limitation of handling but 120 orifices at one time. Consequently, various surfaces were tested individually; for example, measurements were made on the spinner and cowl, then the forward part of the nacelle, and lastly the aft part of the nacelle. For ease in changing from one surface to another, headers for each surface were located in the fuselage and were accessible through the bomb bay.

From one side of the headers, which were small flat plates, suitable tubes lead to the surface of the model. To the other side a similar flat plate was bolted which contained copper tubes that extended from the model to the control room below. In the control room the tubes were connected to two multiple-tube manometers.

Simultaneous records of the pressures acting on a particular surface were obtained by photographing each manometer. In order to provide a reference line on each record one tube on each manometer was connected to the reference pressure which for these tests was the static pressure in the tunnel test section.

The locations of the pressure orifices on the spinner-cowl-nacelle assembly are shown in figure 3. Figure 4 locates the orifices on the fuselage and on the General Electric two-gun turrets. Figures 5, 6, and 7 show the orifice locations on the left outboard main-wheel, left nose-wheel, and left bomb-bay doors.

By locating orifices on both surfaces of the doors an accurate picture of the forces acting on them is obtained. If the internal pressures on the model

and the airplane are similar, correlation between wind-tunnel and flight data should be good when the doors are closed. As soon as the doors are opened, a similar condition exists between the model and the airplane and thus the internal pressures should be the same. Only on the doors were the internal pressures of the model taken into account.

All tests were made at a tunnel airspeed of approximately 95 miles per hour with the exception of the cowl tests with the spinner removed which were made at approximately 78 miles per hour. It was necessary to drop the tunnel airspeed in order to record the peak pressures on the manometer.

In general, pressure-distribution measurements over the various surfaces were obtained through an angle-of-attack range from -8° to 8° and at yaw angles from -10° to 10°. The tests herein reported were made with the air in the tunnel compressed to 35 pounds per square inch absolute and are listed in detail in table I.

SYMBOLS AND METHOD OF ANALYSIS

The coefficients and symbols used in this report are defined as follows:

p/q pressure coefficient

C_L lift coefficient, L/qs (corrected for support-tare and interference effects)

R Reynolds number, $\rho Vc/\mu$

M Mach number, V/V_s

where

p static pressure difference between the model surface and free stream

q dynamic pressure, $\frac{1}{2}\rho V^2$

L-553

L	lift
S	wing area (30.488 sq ft)
c	mean aerodynamic chord (1.930 ft)
ρ	mass density of air
V	airspeed
μ	coefficient of viscosity of air
V_s	sonic velocity

and

α'	geometric angle of attack of model fuselage with respect to centerline of tunnel
ψ	angle of yaw, degrees
δ_f	flap deflection, degrees
θ	door deflection, degrees

Subscripts

m	main-wheel door
n	nose-wheel door
b	bomb-bay door

The following example illustrates the method used to obtain the door moments and loads:

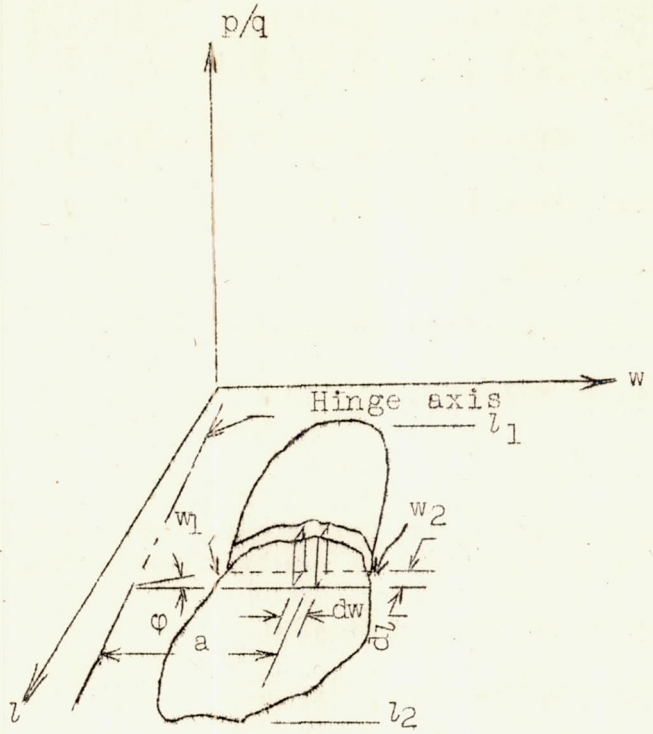

$$\Delta F = q \int_{w_1}^{w_2} \frac{p}{q}\, dw$$

$$F = \int_{l_1}^{l_2} \Delta F\, dl \qquad \text{or} \qquad F = q \int_{l_1}^{l_2} \int_{w_1}^{w_2} \frac{p}{q}\, dl\, dw$$

$$\Delta M = q \int_{w_1}^{w_2} \frac{p}{q}\, a \cos\varphi\, dw$$

$$M = \int_{l_1}^{l_2} \Delta M\, dl \qquad \text{or} \qquad M = q \cos\varphi \int_{l_1}^{l_2} \int_{w_1}^{w_2} \frac{p}{q}\, a\, dl\, dw$$

where

F door load

M door hinge moment

l length of door parallel to the vertical plane of the fuselage reference line

w width of door perpendicular to l

a distance from hinge axis to centroid of pressure diagram angle between hinge axis and orifice row

φ angle between hinge axis and orifice row

Graphical solutions of the equations for door loads and hinge moments were obtained by plotting the values of p/q in each orifice row perpendicular to the appropriate plane against the distance of each orifice from the hinge axis. In the case of the left outboard main-wheel door, an average plane was taken which passed through the hinge axis and the outer edge of the door. For the left nose-wheel door a plane was chosen parallel to the outer flat surface of the door. Two planes were used with the left bomb-bay door, one parallel to the outer flat surface of the door and the other perpendicular to the first plane. The use of two planes for the bomb-bay door gave the normal and transverse moments and loads, respectively.

The section loads and moments were obtained from the pressure diagrams by means of a mechanical integrator and were plotted against the distance from the leading edge of the door to each orifice row. The area under the section moment and load curves was again integrated to obtain values of total door load and hinge moment.

For convenience in obtaining a graphical solution of the moments on the nose-wheel door, the cos φ term was neglected. Thus the moments are in error by about 1.0 percent.

In this report the door loads and hinge moments per unit dynamic pressure are presented against door length. Positive values of the loads and moments were arbitrarily chosen to mean that the forces acting tended to close the door.

Pressure orifices were located on only one-half of the upper and lower gun turrets; thus it was necessary to assume symmetry and use data from both positive and negative angles of yaw to obtain the loads for a particular angle of yaw.

The turret loads are given by the following expressions:

(1) Vertical load

$$F_v = q\int_o^R \int_o^{2\pi} \frac{p}{q}\, r\, dr\, d\epsilon$$

(2) Side load

$$F_s = q\int_o^h \int_o^{l_t} \frac{p}{q}\, dh\, dl_t$$

(3) Longitudinal load

$$F_l = q\int_o^h \int_o^{w_t} \frac{p}{q}\, dh\, dw_t$$

where

R maximum radius of turret

r radius of turret at any orifice row (orifice rows lie in planes which are perpendicular to the axis of rotation of the turret)

ϵ angular displacement of orifices as seen from a top or bottom view of the turret in question

h height of turret

l_t length of turret (measured along the longitudinal axis of the model)

w_t width of turret perpendicular to l_t

The equation for vertical loads was solved graphically by plotting values of p/q against the circumference of the turret at every row of orifices. Integration of these pressure diagrams gives values of section load which when plotted against the maximum radius of the turret and again integrated solve the equation.

In like manner the equations for side and longitudinal loads are solved by plotting p/q against the appropriate diameter of the turret, integrating these curves, plotting the section loads against the height of the turret and, by again integrating, the total loads are obtained.

All turret loads are measured with respect to the body axis of the model and are presented as loads per unit dynamic pressure. Positive vertical loads are compressing loads parallel to the axis of rotation of the turret. Side loads are measured perpendicular to a vertical plane through the fuselage reference line and are positive to the right. Longitudinal loads are parallel to the vertical plane of the fuselage reference line and are positive aft.

Vertical, side, and longitudinal loads were obtained for the upper turret but due to asymmetrical orifice locations on the lower turret only vertical loads are presented.

Accuracy

Individual pressures could be read from the photographs to ± 0.1 cm. Values of p/q are accurate to within 0.001.

The accidental errors that exist in the final loads and hinge moments are due to fairing curves and integrating these curves. From the results of the total door loads and hinge moments it would appear that these are about $0.01/q$ for the loads and $0.002/q$ for moments.

RESULTS AND DISCUSSION

In order to estimate the lift coefficient at which the tests were made, figure 8 is presented. The lift

coefficient has been plotted as a function of geometric angle of attack at 0° yaw because the geometric angle of attack remains constant throughout the yaw range.

Spinner-cowl-nacelle assembly and fuselage.- Values of the external pressure coefficient, p/q, for the spinner-cowl-nacelle assembly and the fuselage are shown in figures 9(a) through 20(e). Presentation of data in this manner is rather unusual but it was used because it not only gives the value of p/q at each orifice, but provides for easy comparison with the pressures acting at other orifices in the same vicinity. For a particular model attitude all the pressures acting on the unit can be obtained from one diagram.

The pressures measured on the spinner, cowl, and nacelle are presented for the following angles of yaw: -10°, figure 9; -5°, figure 10; 0°, figure 11; 5°, figure 12; 10°, figure 13; and 0° with wing flaps deflected 55°, figure 14. At each angle of yaw the results are given for an angle-of-attack range from -8° to 8°. The cowl-alone data are presented on the same diagrams as the spinner-cowl-nacelle pressures at 0° yaw, figure 11. For all tests made with the spinner in place the cowling-entrance-velocity ratio V_I/V was approximately 0.28. The entrance-velocity ratio was not measured when the spinner was removed.

The fuselage pressures including the wing fillet and the upper and lower turrets are shown for angles of yaw from -10° to 10° at angles of attack from -8° to 8° in figures 15(a) through 19(e). Values of p/q over a portion of the fuselage with the flaps down at 0° yaw are shown in figure 20.

These diagrams indicate that no critical pressures should be encountered in the high-speed level-flight condition of the airplane at 17,000 feet, unless the spinner is removed. When the spinner is removed critical pressures occur at 265 miles per hour.

The following table lists some values of the critical pressures on the spinner-cowl-nacelle assembly and on the fuselage:

Surface	Fig.	ψ (deg)	α' (deg)	$\frac{p}{q}$	Critical M (2)	Critical velocity at 17,000 ft (mph)
Cowl with spinner	9(d)	-10	4	-2.09	0.46	330
Cowl alone	11(a)	0	-8	-4.82	.32	230
Cowl with spinner[1]	11(e)	0	0	-.66	.65	466
Cowl alone[1]	11(e)	0	0	-3.54	.37	265
Nacelle	13(e)	10	8	-2.42	0.43	309
Nacelle $\delta_f = 55^\circ$	14(e)	0	8	-3.30	.38	273
Nacelle[1]	11(e)	0	0	-.55	.68	488
Fuselage (fillet)	19(e)	10	8	-4.46	.33	237
Fuselage $\delta_f = 55^\circ$	20(e)	0	8	-2.71	.41	294
Fuselage (upper turret)[1]	17(e)	0	0	-.75	.63	452

[1]High-speed level-flight attitude.

[2]The values of critical Mach number presented in the table have been estimated by the von Kármán-Tsien relation from low-speed pressure coefficients.

Main-wheel, nose-wheel, and bomb-bay doors.- Diagrams of the pressures acting on the main-wheel door, nose-wheel door, and bomb-bay door for a few representative cases are presented in figures 21, 22, and 23. The main-wheel and nose-wheel door pressures are shown for four door angles from closed to full open at 4° angle of attack and yaw angles of -10°, 0°, and 10°. The bomb-bay-door diagrams represent the results of tests made at 0° yaw, -8°, -4°, 0°, 4°, and 8° angles of attack, and door angles of 0°, 10°, and 60°. These pressure diagrams are presented to give a picture of how various door attitudes affect the pressures. They are not intended to be used for determining exact values of p/q.

Section moments (lb-ft per ft of length/q) and sections loads (lb per ft of length/q) for the three doors are presented in figures 24 through 29. These curves are particularly valuable in showing how the moments and loads vary along the length of each door. As might be expected, at the higher door angles, the curves near the leading edge of the door are very erratic.

Figures 30 and 31 present the total moments and loads for the main-wheel and the nose-wheel doors. The total moments and the normal and transverse loads on the bomb-bay door are presented in figure 32. It is of interest to note the similarity of results for the main-wheel and the nose-wheel doors. The magnitude of the moments and loads are different, but the slope and displacement of the curves are very much alike. The results indicate that throughout most of the range tested the nose-wheel door will tend to close but the main-wheel and bomb-bay doors tend to open due to the aerodynamic loads.

Turret loads.- The vertical loads on the upper and lower-gun turrets and the longitudinal and side-force loads on the upper turret are given in table II. Some of the values of total loads on the turrets, especially the side load and longitudinal loads, do not appear as would be expected. For example, the side load on the upper turret at 0° yaw is 0 because symmetry was assumed, at -10° yaw the side loads are negative while at -5° yaw they are positive when it would appear that they should be negative. Considering the same limit of accuracy for the turret as set up for the door loads (0.01/q) the results lie within the experimental accuracy of the measurements.

Scale factor.- All results in this report are given in terms of the model. To change from model to airplane loads and moments the scale factor must be taken into account. For example, suppose the total load and the total hinge moment were desired on the airplane nose-wheel door for the following conditions:

$$q = 300 \text{ lb/sq ft}; \quad \theta_n = 0^\circ; \quad \psi = 0^\circ;$$

and $\alpha' = 0^\circ$. Figure 31 gives the values of the model load and moment at $\theta_n = 0^\circ$, $\psi = 0^\circ$, and $\alpha' = 0^\circ$. Multiply these values by the desired airplane q (300 lb/sq ft) and by (1/model scale)^3 for moments and (1/model scale)^2 for loads.

$$M(\text{airplane}) = M/q \text{ (model)} \times 300 \times \left(\frac{1}{0.2375}\right)^3$$

$$= 0.0232 \times 300 \times 74.62$$

$$= 518 \text{ lb-ft}$$

$$F(\text{airplane}) = F/q \text{ (model)} \times 300 \times \left(\frac{1}{0.2375}\right)^2$$

$$= 0.107 \times 300 \times 17.72$$

$$= 569 \text{ lb}$$

CONCLUSIONS

Pressure-distribution measurements of the model indicate that:

1. In the airplane's high-speed level-flight condition at 17,000 feet no critical pressures should be encountered unless the spinner is removed. With the spinner removed, critical pressures were reached on the cowl at 265 miles per hour.

2. Throughout most of the range tested the nose-wheel door tends to close, whereas the main-wheel and bomb-bay doors tend to open due to the aerodynamic loads.

3. The longitudinal and side loads on the upper turret are small and generally lie within the experimental accuracy of the measurements.

Langley Memorial Aeronautical Laboratory,
National Advisory Committee for Aeronautics,
Langley Field, Va., October 2, 1943.

L-553

Table I
Tests and Figures

NATIONAL ADVISORY COMMITTEE FOR AERONAUTICS

Surface	Angle of yaw, deg									Door Angle, deg	δ_f (deg)	Approx Vel (mph)	R	M	Figs
	$\alpha'=-8°$	$\alpha'=-6°$	$\alpha'=-4°$	$\alpha'=-2°$	$\alpha'=0°$	$\alpha'=2°$	$\alpha'=4°$	$\alpha'=6°$	$\alpha'=8°$						
spinner, cowl, and nacelle	-10,-5, 0, 5,10	0	-10,-5, 0, 5,10	0	-10,-5, 0, 5,10	0	-10,-5, 0, 5,10	0	-10,-5, 0, 5,10	—	0	95	3.89 x10^6	0.12	9-13
cowl with spinner off	0	0	0	0	0	0	0	0	0	—	0	79	3.30	.10	11
nacelle	0	—	0	—	0	—	0	—	0	—	55	90	3.72	.12	14
fuselage	-10,-5, 0, 5,10	0	-10,-5, 0, 5,10	0	-10,-5, 0, 5,10	0	-10,-5, 0, 5,10	0	-10,-5, 0, 5,10	—	0	95	3.98	.12	15-19
fuselage	0	—	0	—	0	—	0	—	0	—	55	89	3.75	.12	20
main wheel door	-10,-5, 0, 5,10	0	-10,-5, 0, 5,10	0	-10,-5, .0, 5,10	0	-10,-5, 0, 5,10	0	-10,-5, 0, 5,10	0	0	94	3.99	.12	21 24 25 30
main wheel door	—	—	-10, 0,10	—	-10, 0,10	—	-10, 0,10	—	-10, 0,10	1,3	0	94	3.98	.12	
main wheel door	—	—	-10,-5, 0,5,10	—	-10,-5, 0,5,10	—	-10,-5, 0,5,10	—	-10,-5, 0,5,10	5,10,30, 50, 72	0	94	3.94	.12	
nose wheel door	-10,-5, 0, 5,10	0	-10,-5, 0, 5,10	0	-10,-5, 0, 5,10	0	-10,-5, 0, 5,10	0	-10,-5, 0, 5,10	0	0	94	4.04	.12	22 26 27 31
nose wheel door	—	—	-10, 0,10	—	-10, 0,10	—	-10, 0,10	—	-10, 0,10	1, 3	0	95	4.04	.12	
nose wheel door	—	—	-10,-5, 0,5,10	—	-10,-5, 0,5,10	—	-10,-5, 0,5,10	—	-10,-5, 0,5,10	5,10,30, 60,86	0	95	3.92	.12	
*	0	0	0	0	0	0	0	0	0	0	0	96	3.64	.12	23 28 29 32
*	0	—	0	—	0	—	0	—	0	1,3,5,10,40, 60,88.7	0				

* bomb bay door tested on normal supports

NATIONAL ADVISORY
COMMITTEE FOR AERONAUTICS

Table II

Loads on Upper and Lower Turrets

Type of load	ψ (deg)	α' (deg)	Magnitude of load (lb/q)
Upper turret			
Side	-10	-8	-0.029
		-4	-0.028
		0	-0.024
		4	-0.004
		8	0
Side	-5	-8	0.001
		-4	0.002
		0	0.003
		4	0.004
		8	0.004
Longitudinal	-10	-8	0.018
		-4	0.017
		0	0.017
		4	0.017
		8	0.013
Longitudinal	-5	-8	0.021
		-4	0.020
		0	0.018
		4	0.018
		8	0.014
Longitudinal	0	-8	0.011
		-4	0.010
		0	0.009
		4	0.020
		8	0.018
Vertical	-10	-8	-0.186
		-4	-0.211
		0	-0.232
		4	-0.250
		8	-0.262
Vertical	-5	-8	-0.172
		-4	-0.195
		0	-0.218
		4	-0.238
		8	-0.247
Vertical	0	-8	-0.136
		-4	-0.178
		0	-0.199
		4	-0.249
		8	-0.267
Lower turret			
Vertical	-10	-8	-0.073
		-4	-0.067
		0	-0.065
		4	-0.064
		8	-0.059
Vertical	-5	-8	-0.052
		-4	-0.052
		0	-0.055
		4	-0.054
		8	-0.047
Vertical	0	-8	-0.049
		-4	-0.037
		0	-0.030
		4	-0.029
		8	-0.025

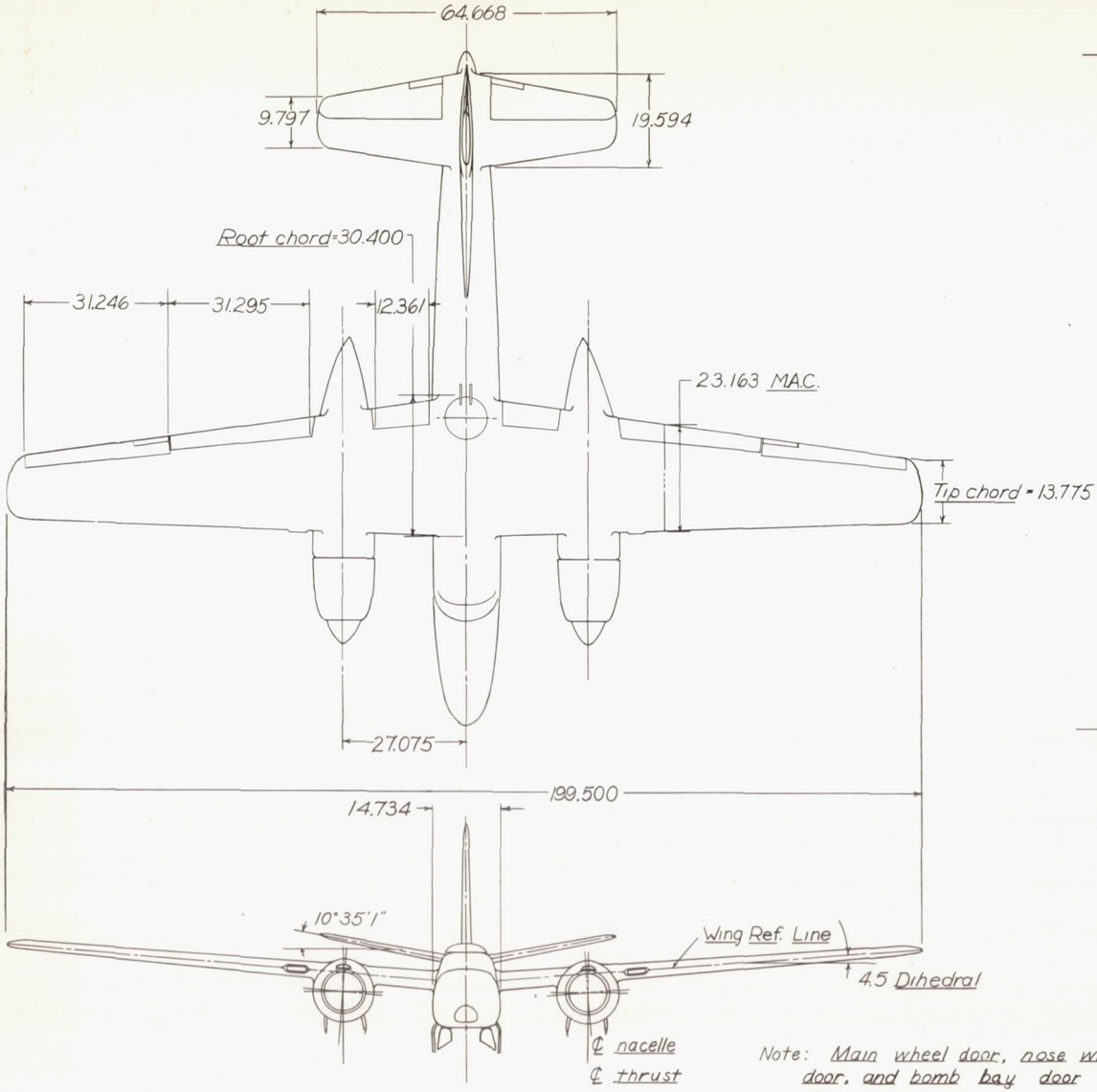

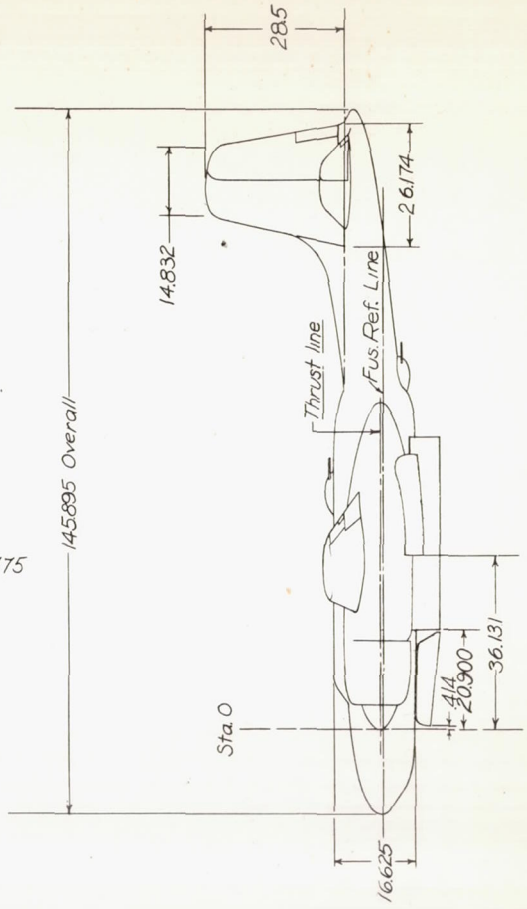

All dimensions in inches

Note: Main wheel door, nose wheel door, and bomb bay door shown full open.

NATIONAL ADVISORY COMMITTEE FOR AERONAUTICS

Figure 1 — Plan and elevations of the 0.2375-scale model of the Douglas XA-26 airplane.

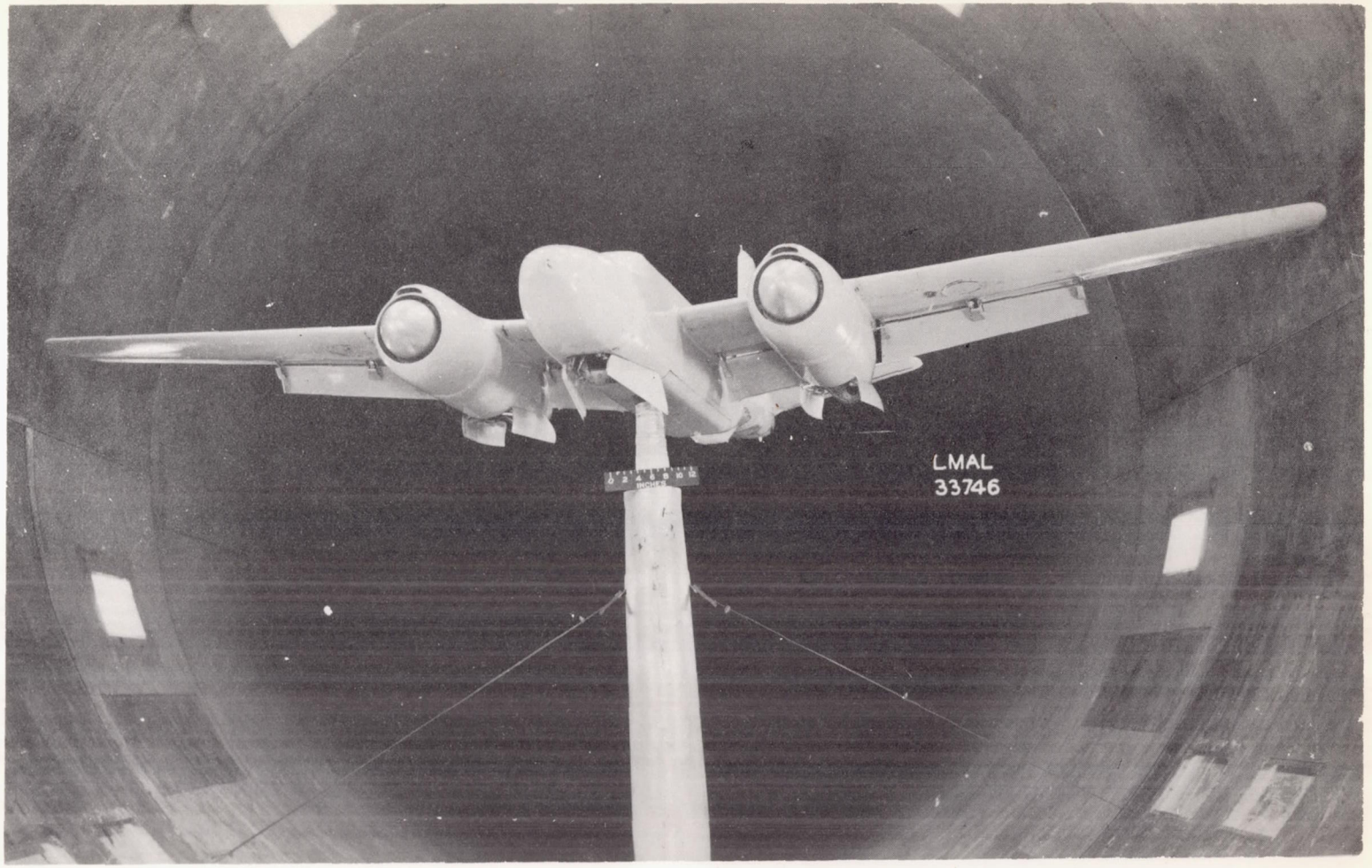

Figure 2(a).- 0.2375-scale model Douglas XA-26 airplane on yaw support with wheel doors full open and wing flaps deflected 55°.

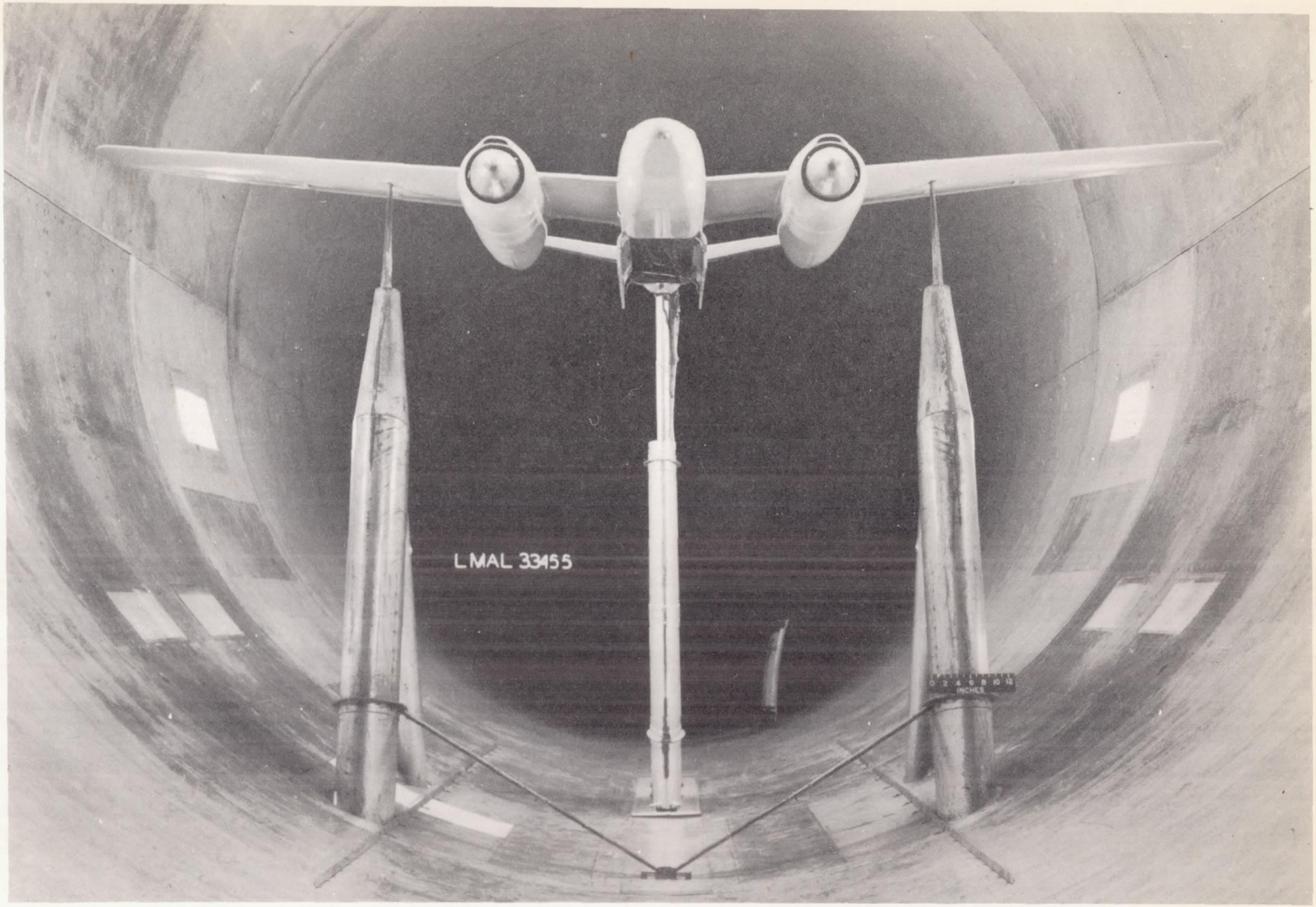

Figure 2(b).- 0.2375-scale model Douglas XA-26 airplane on normal, three-support system with bomb-bay doors full open.

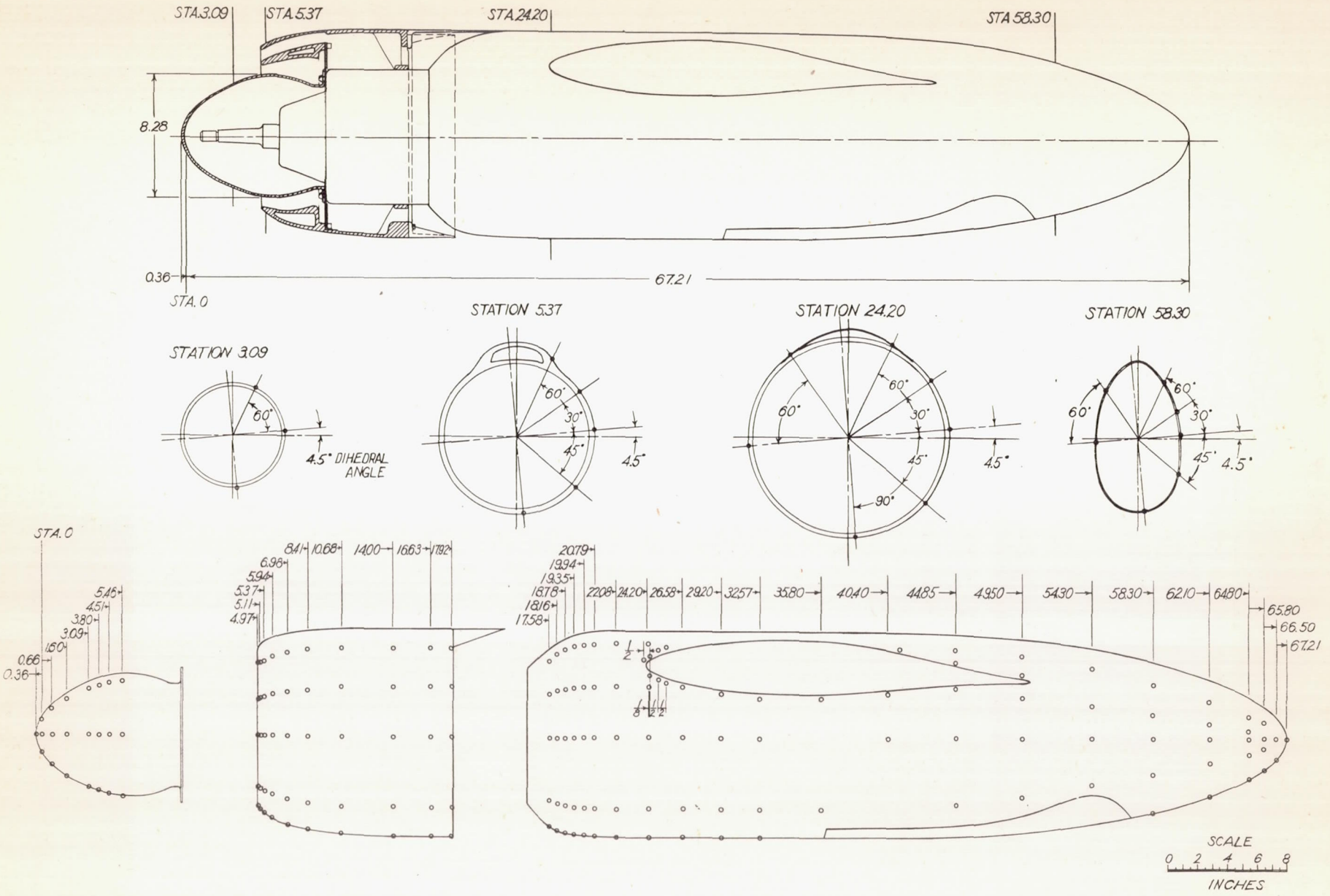

Figure 3.- Location of orifices on spinner, cowl, and nacelle of 0.2375-scale model Douglas XA-26 airplane

NATIONAL ADVISORY
COMMITTEE FOR AERONAUTICS

L-553

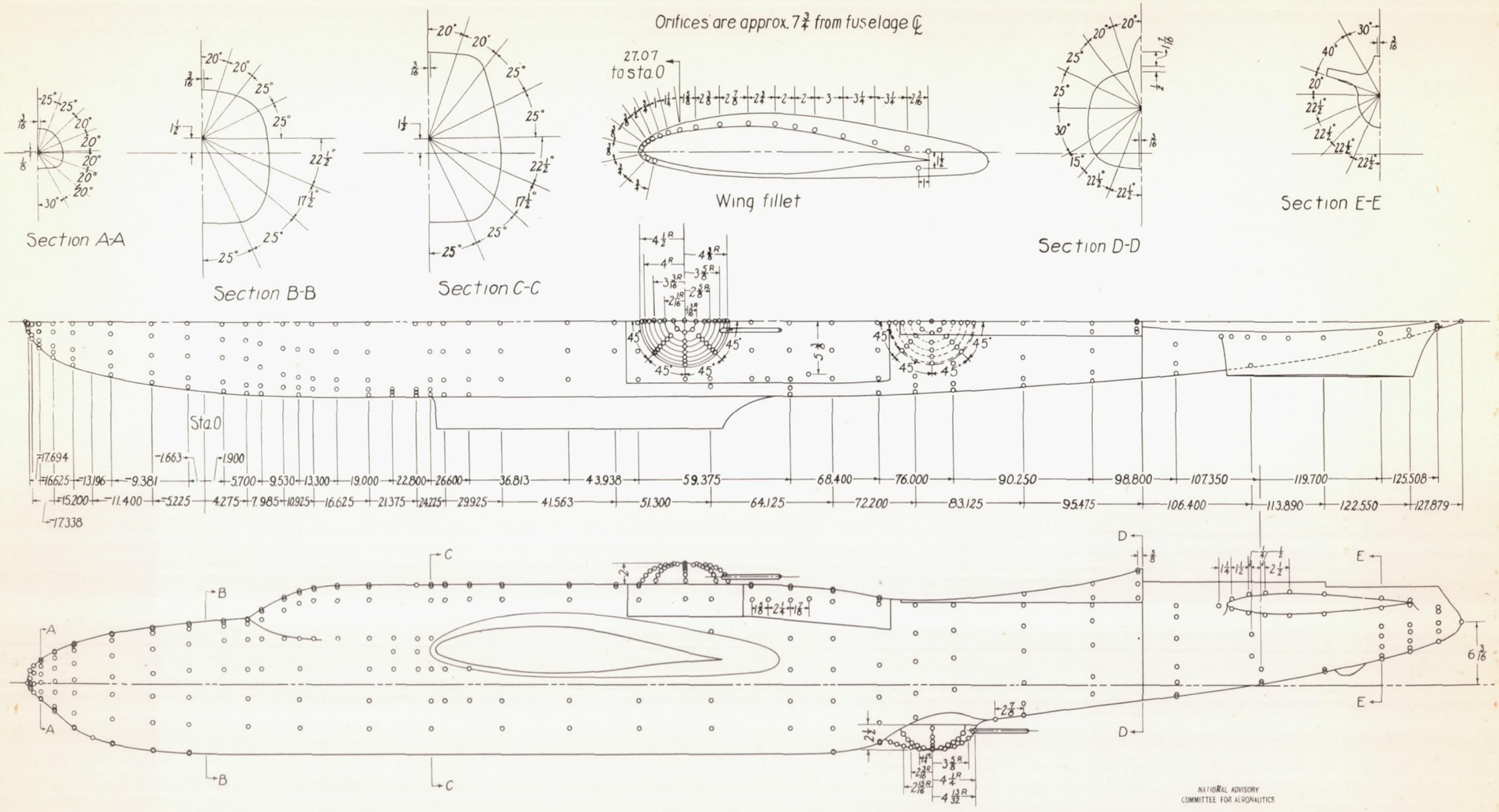

Figure 4.-Location of orifices on fuselage of 0.2375-scale model of Douglas XA-26 airplane

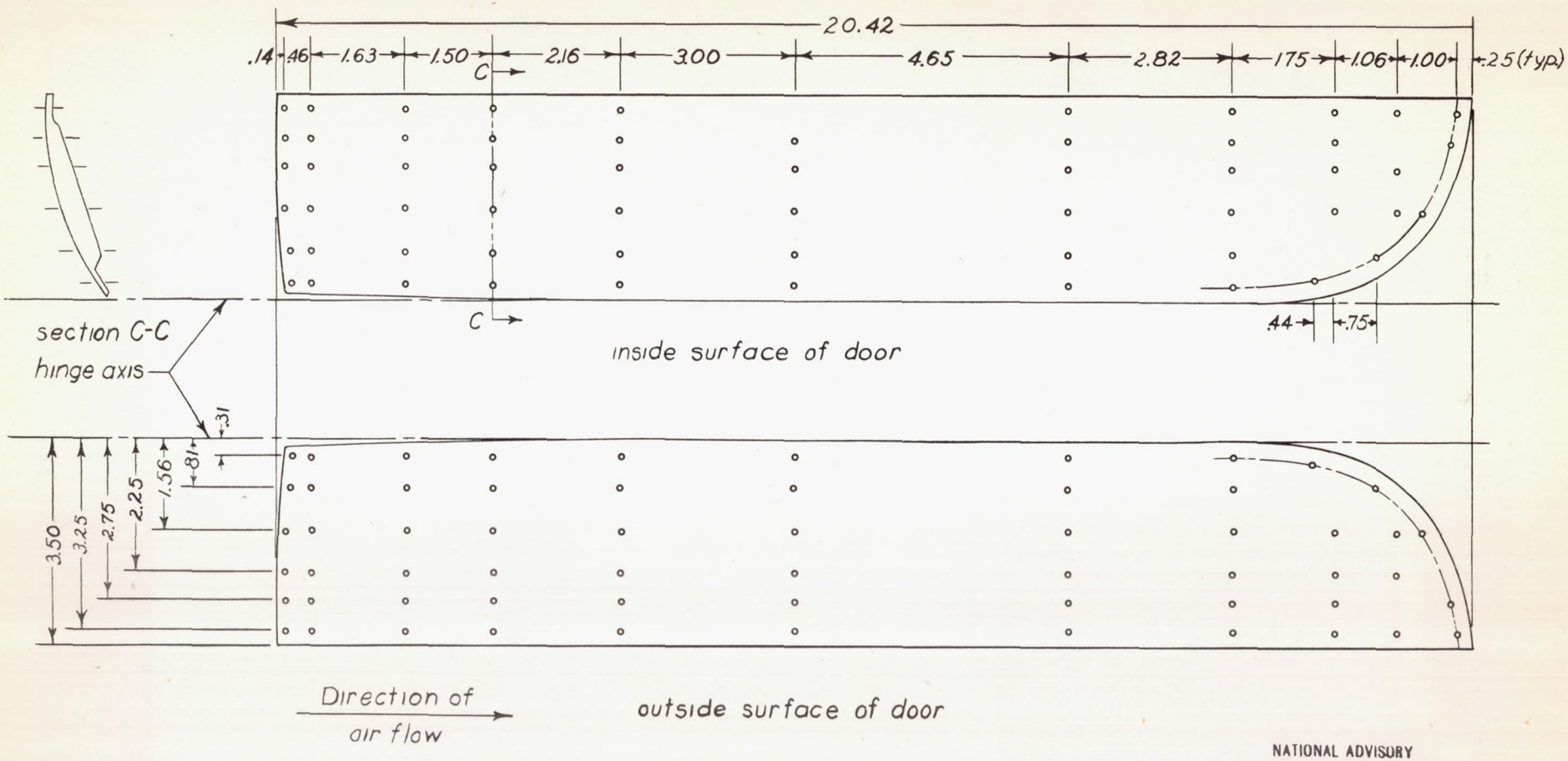

Figure 5 - Location of orifices on main wheel door of 0.2375-scale model Douglas XA-26 airplane

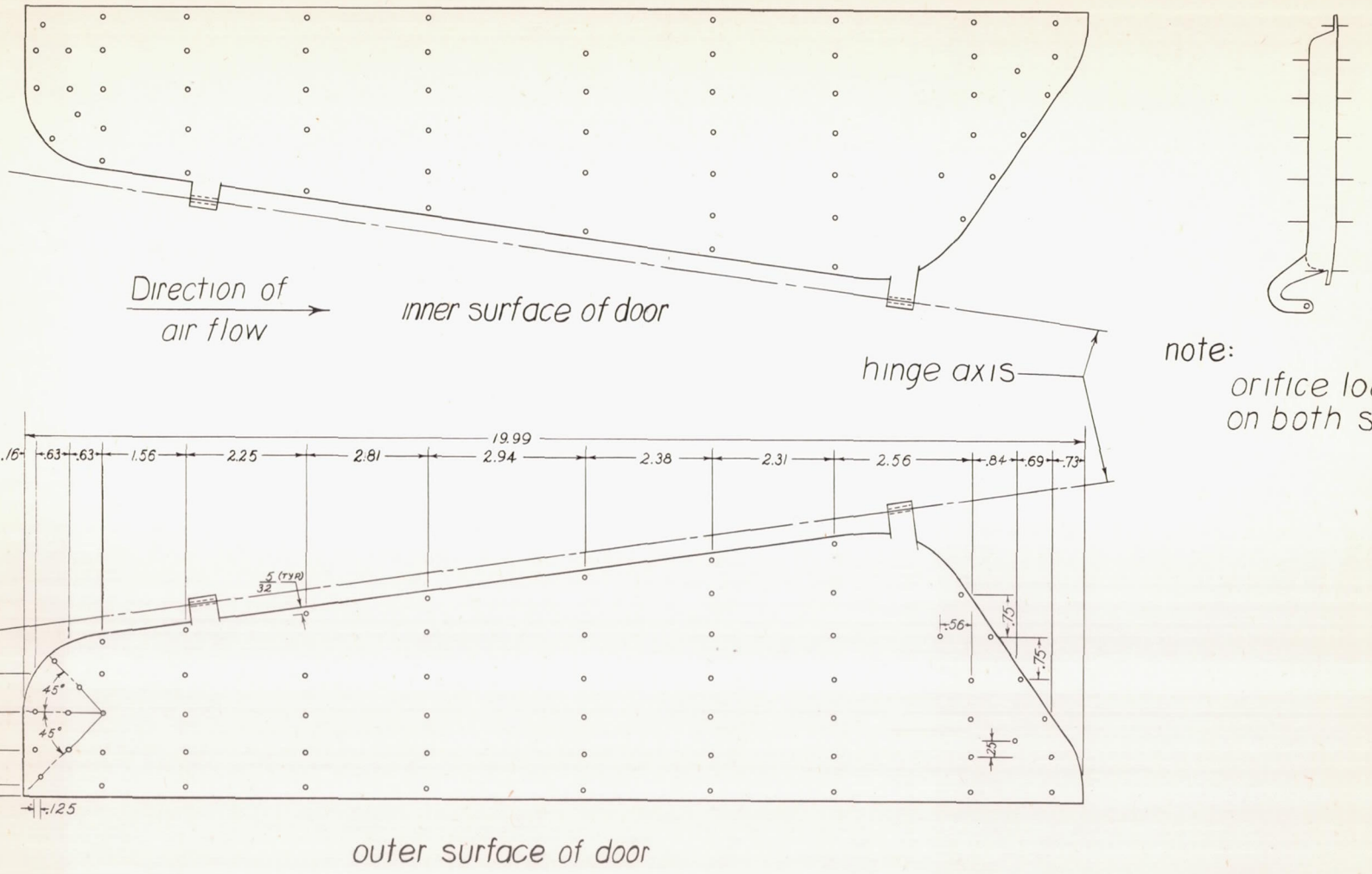

note:
orifice location same on both surfaces.

NATIONAL ADVISORY COMMITTEE FOR AERONAUTICS

Figure 6.-Location of orifices on nose wheel door of 0.2375-scale model Douglas XA-26 airplane

NATIONAL ADVISORY
COMMITTEE FOR AERONAUTICS

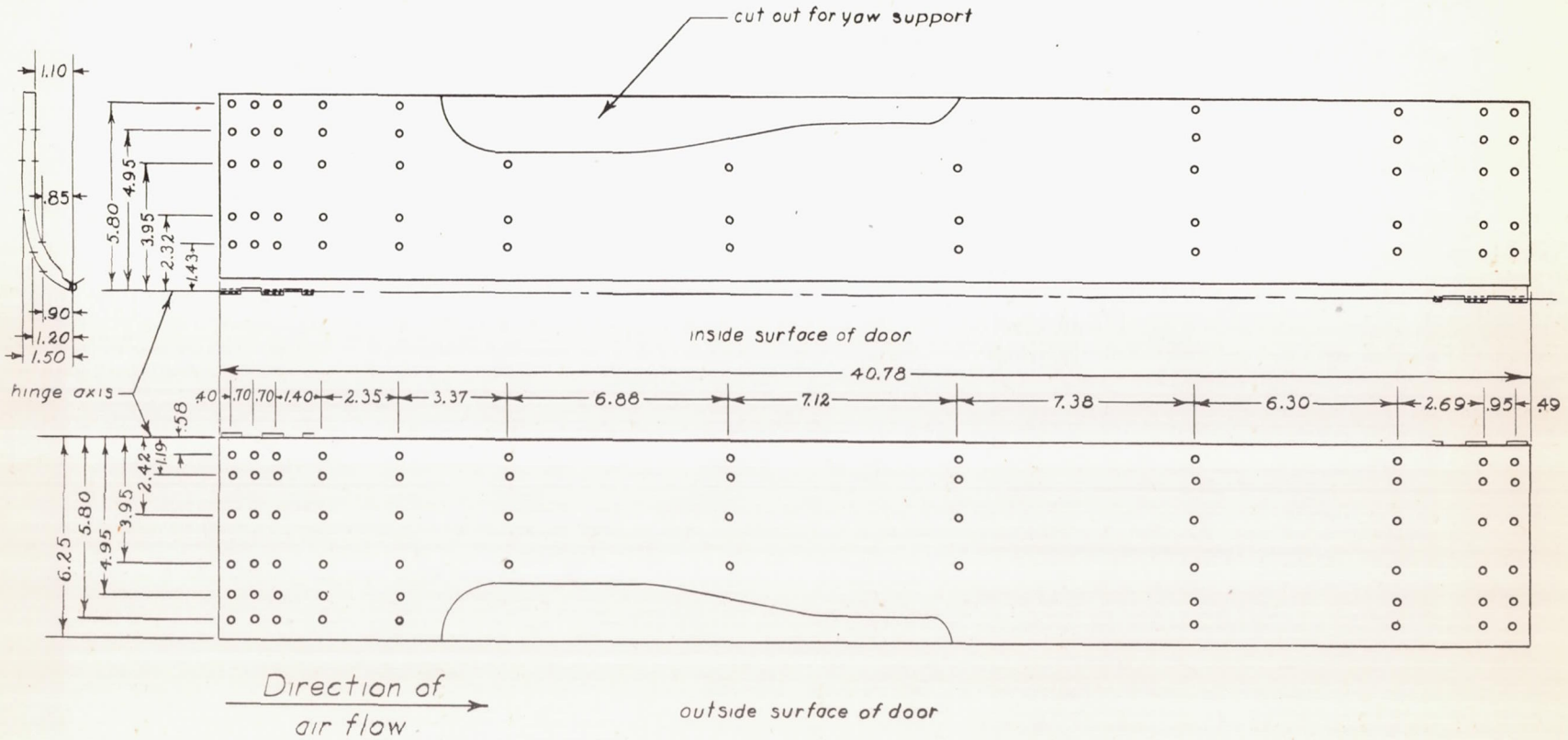

Figure 7.- Location of orifices on bomb bay door of 0.2375-scale model Douglas XA-26 airplane

L-553

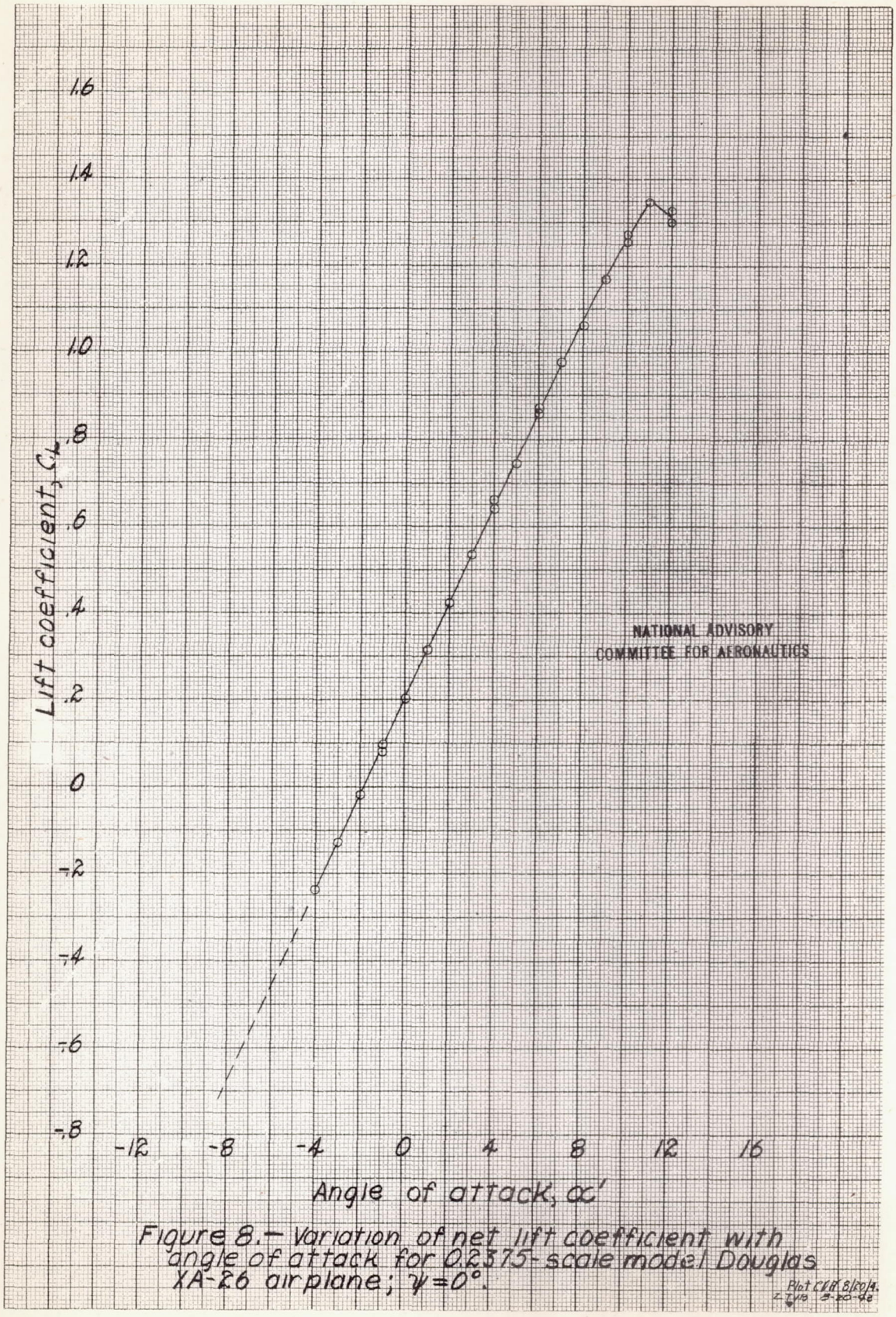

Figure 8.— Variation of net lift coefficient with angle of attack for 0.2375-scale model Douglas XA-26 airplane; $\psi = 0°$.

Plot C/A 8/10/A.
2-7/8 8-20-42

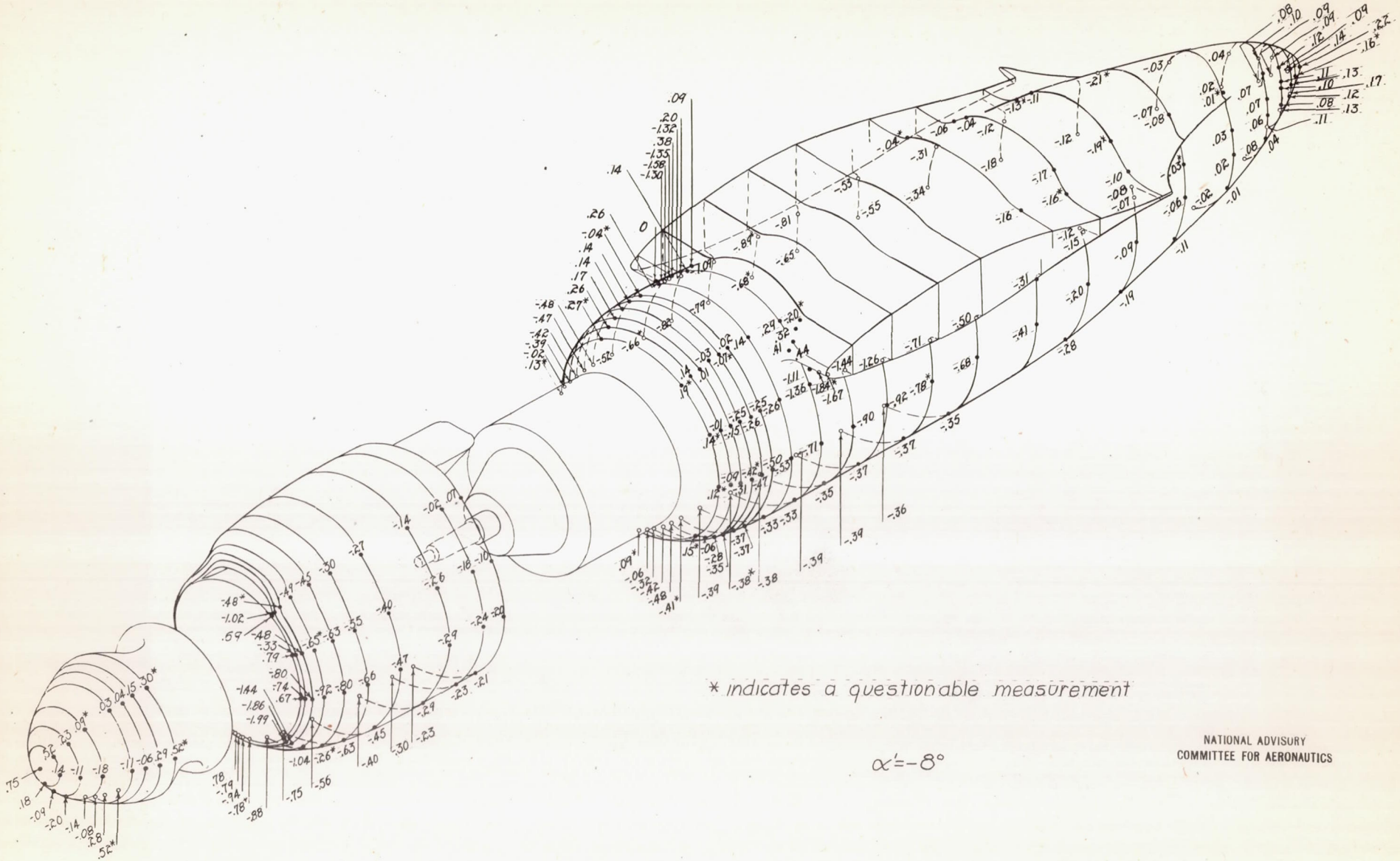

Figure 9a.—Pressure coefficients p/q on spinner, cowl, and nacelle of 0.2375-scale model Douglas XA-26 airplane; $\psi=-10°$; $q \approx 50$ lb/sq ft; $R \approx 3{,}900{,}000$; $M \approx 0.12$.

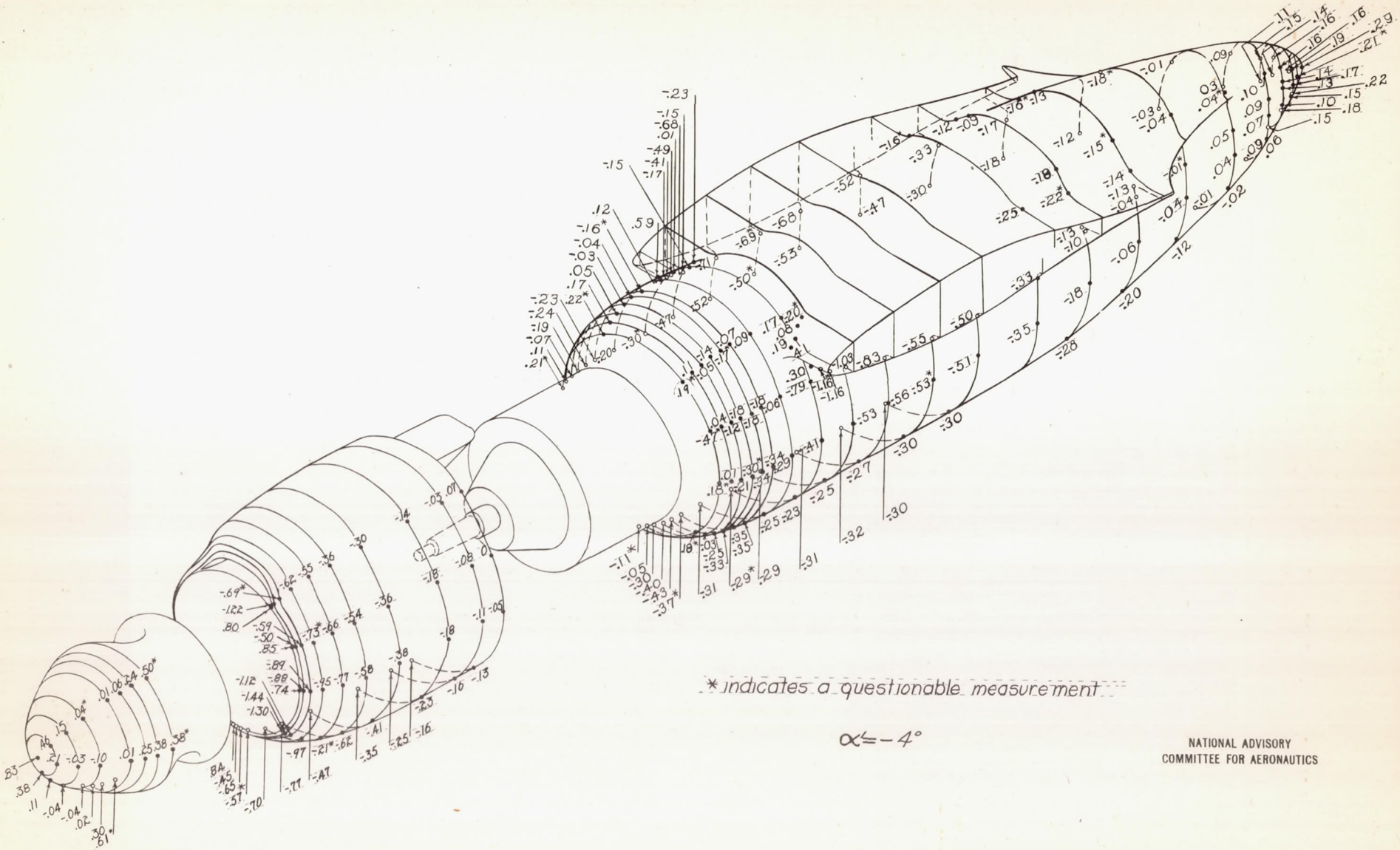

* indicates a questionable measurement

$\alpha = -4°$

NATIONAL ADVISORY
COMMITTEE FOR AERONAUTICS

Figure 9b.—continued

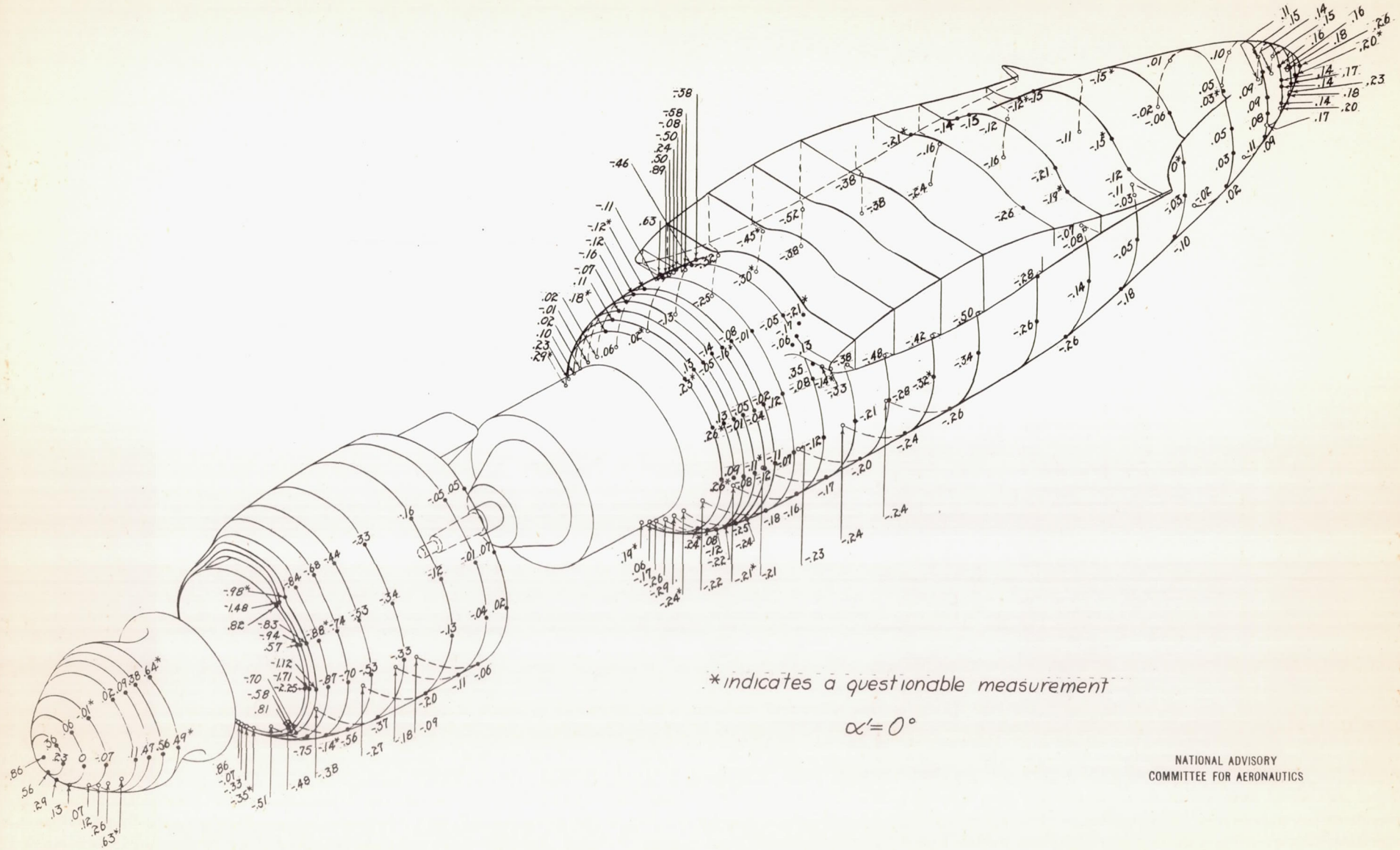

*indicates a questionable measurement

$\alpha' = 0°$

NATIONAL ADVISORY
COMMITTEE FOR AERONAUTICS

Figure 9c.—continued

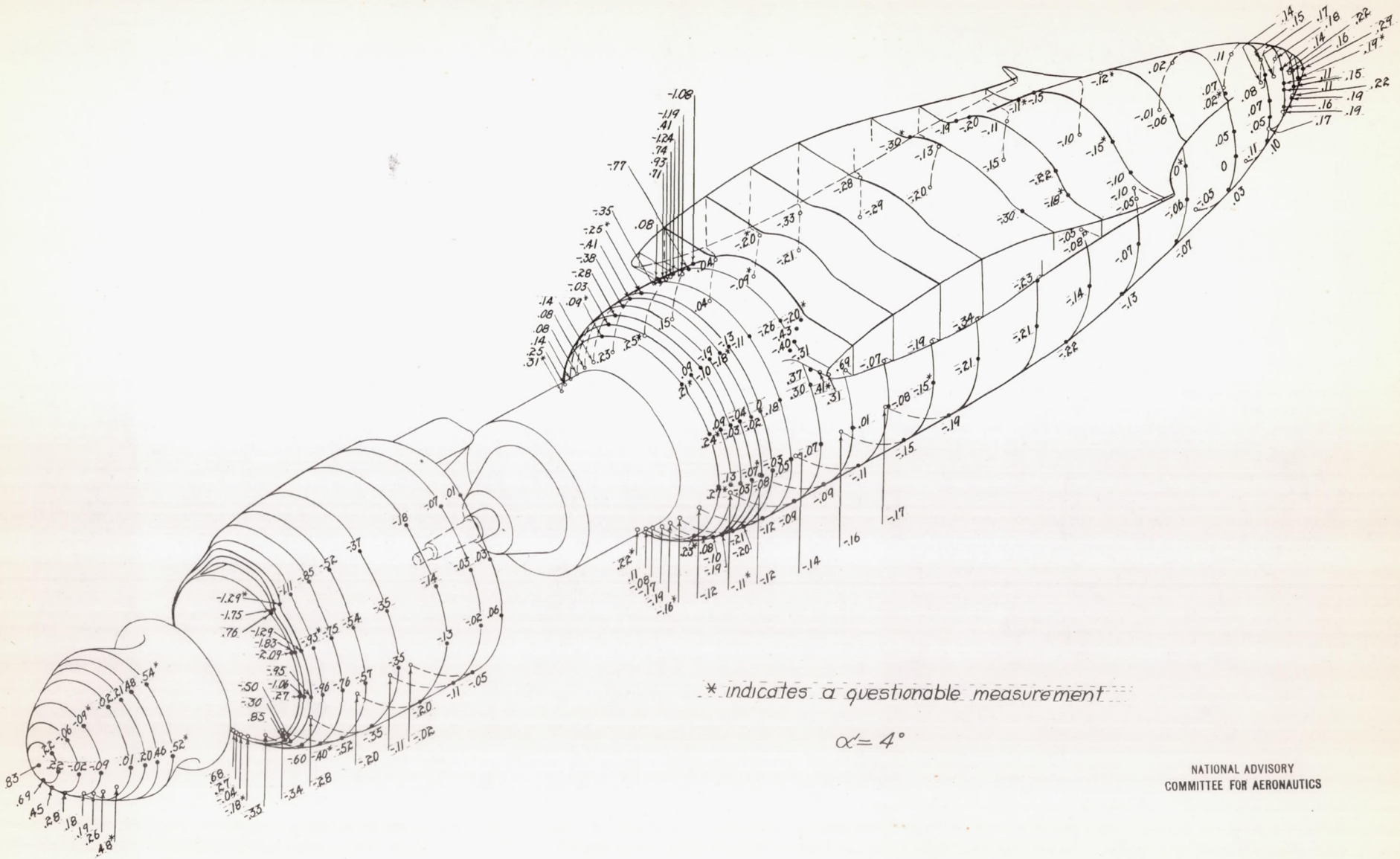

Figure 9d.—continued

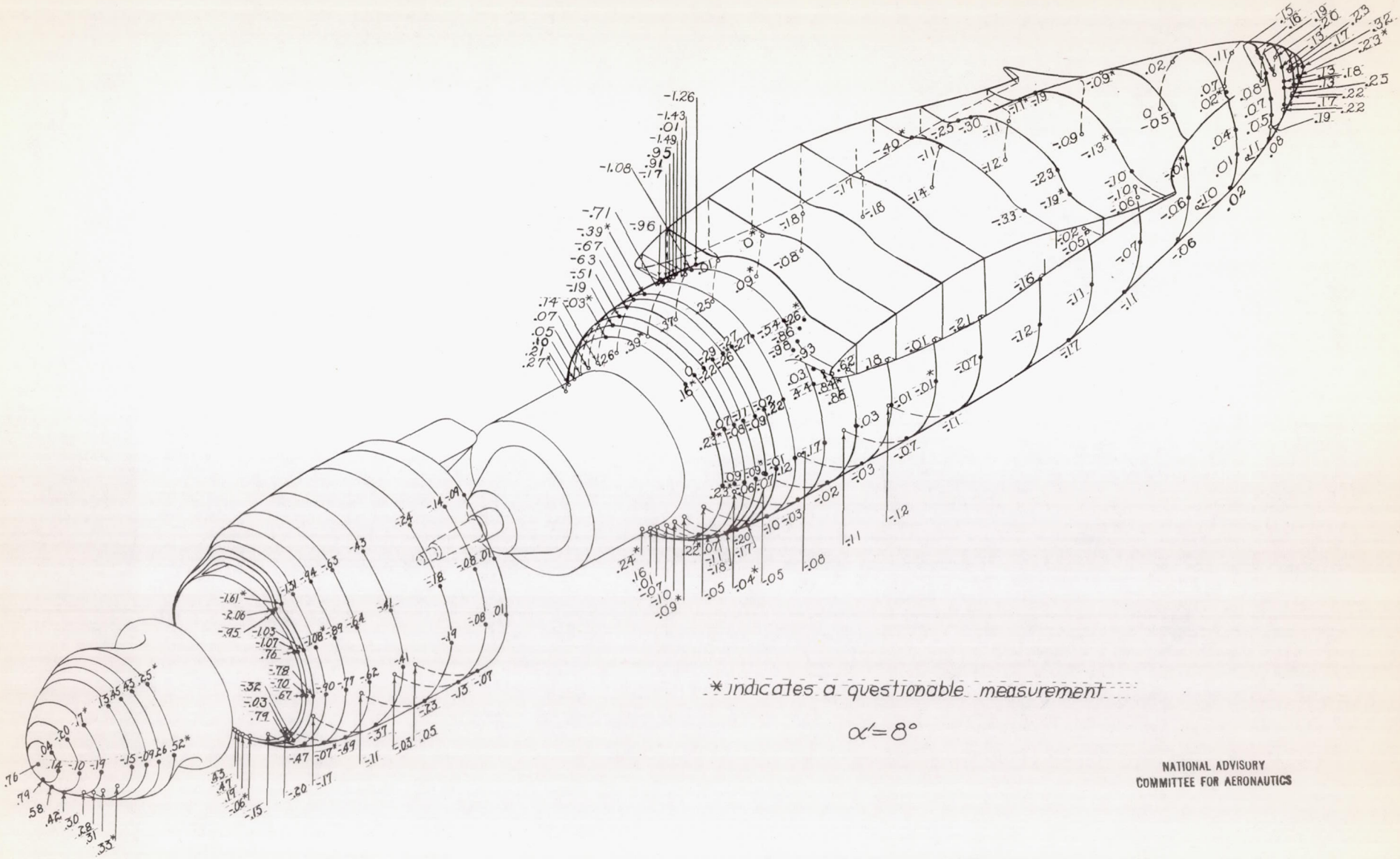

Figure 9e.—concluded

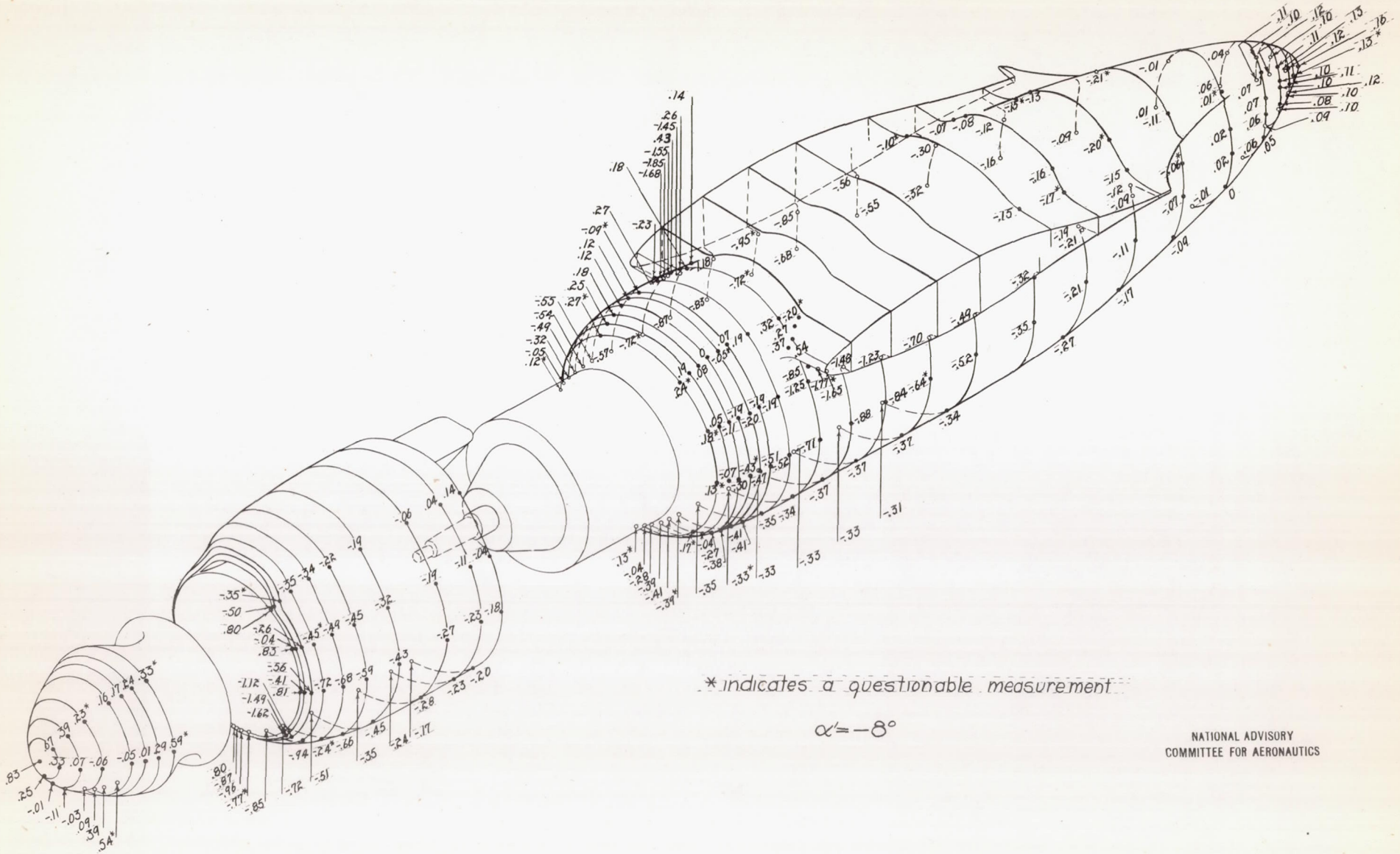

Figure 10a.—Pressure coefficients p/q on spinner, cowl, and nacelle of 0.2375—scale model Douglas XA-26 airplane; $\psi = -5°$; $q \approx 50$ lb/sq ft; $R \approx 3{,}910{,}000$; $M \approx 0.12$.

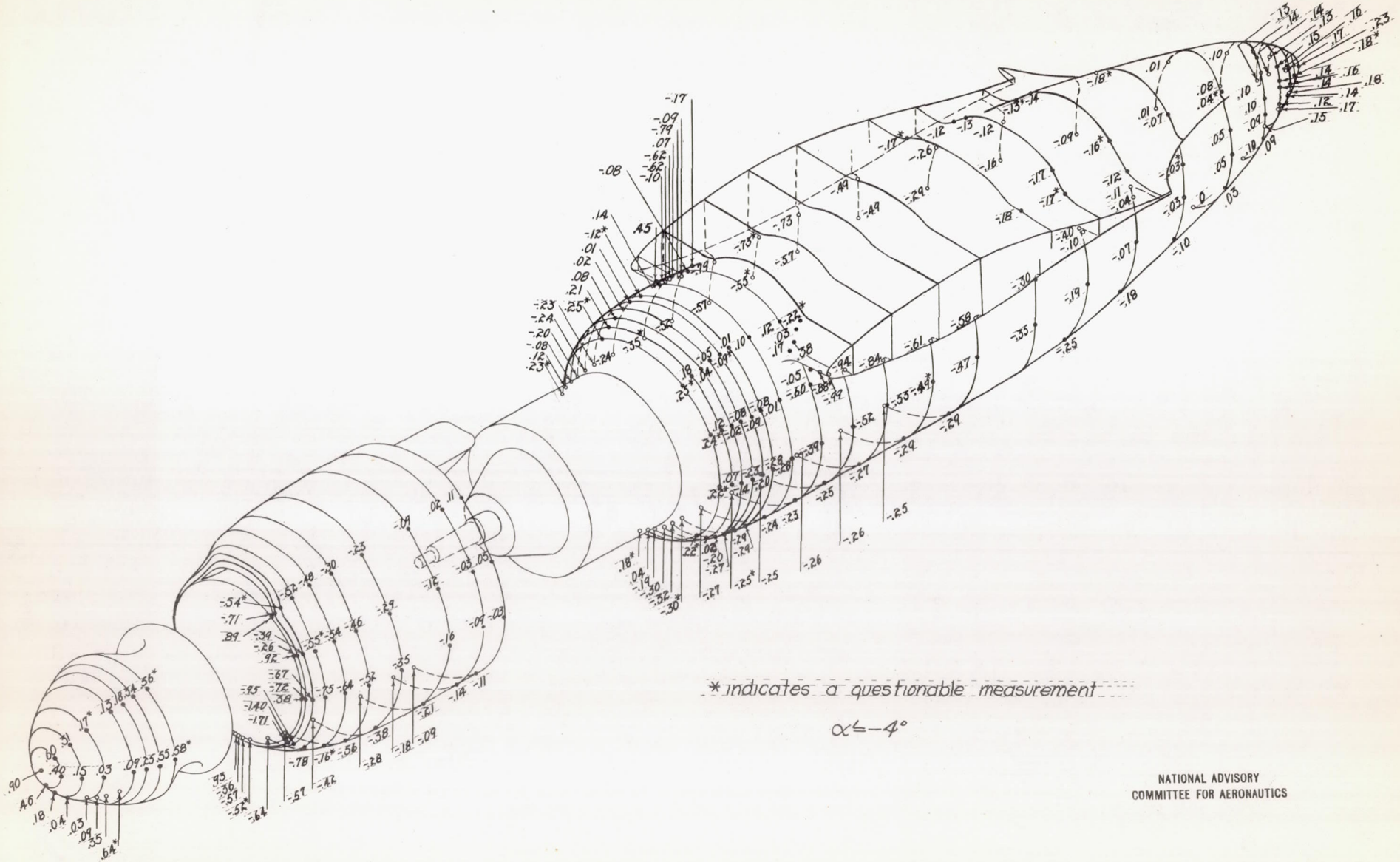

Figure 10b. —continued

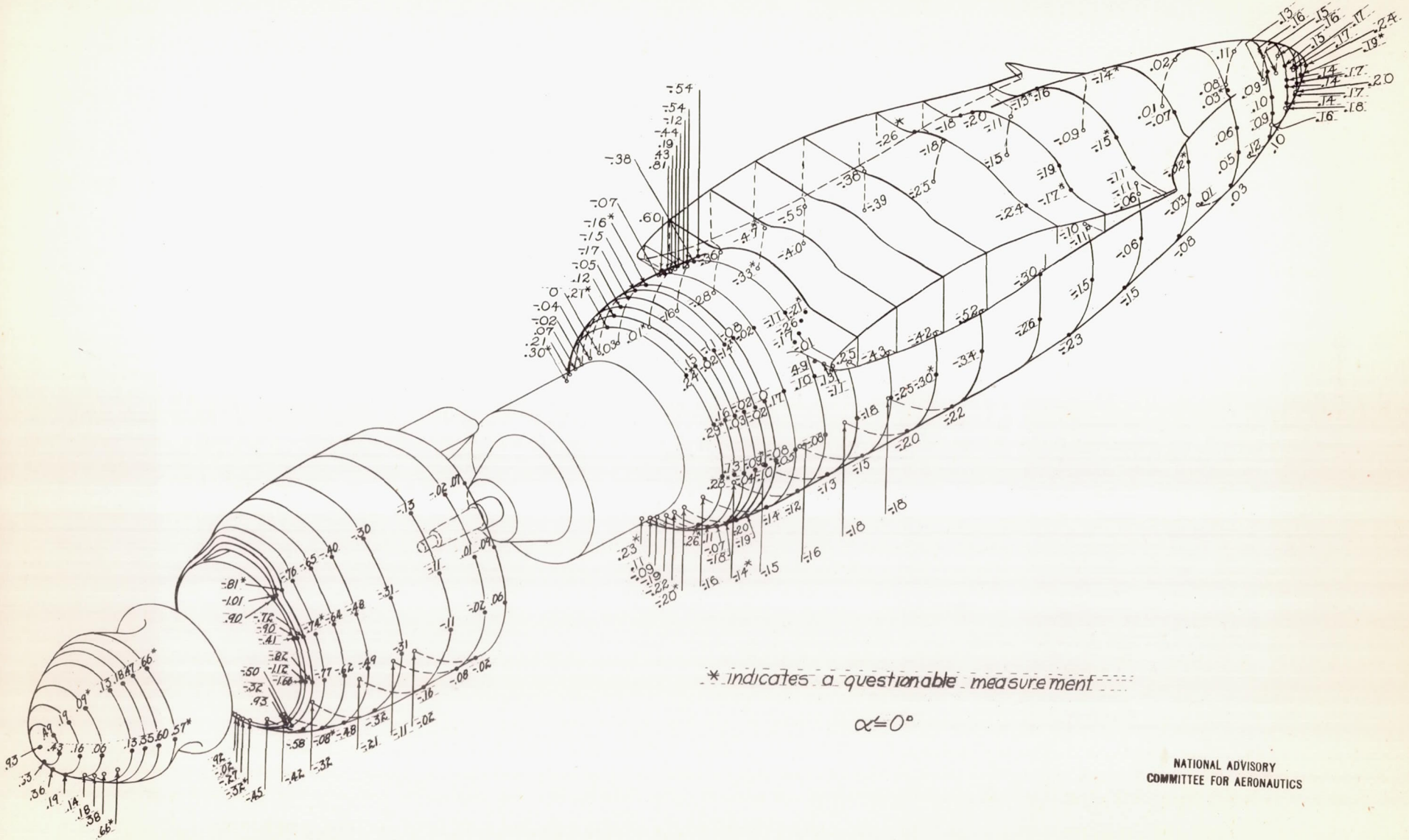

Figure 10c.—continued

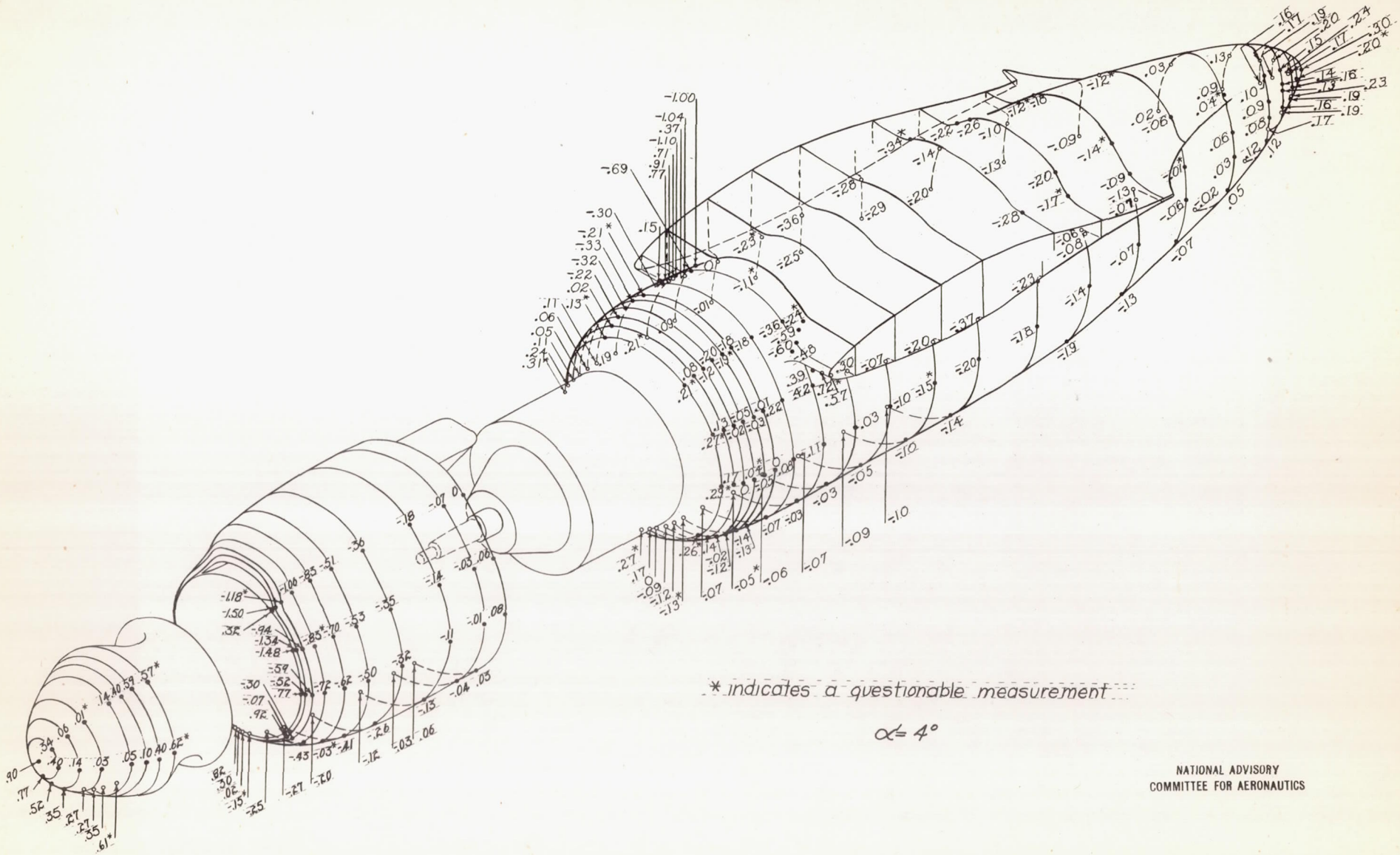

Figure 10d.—continued

L-553

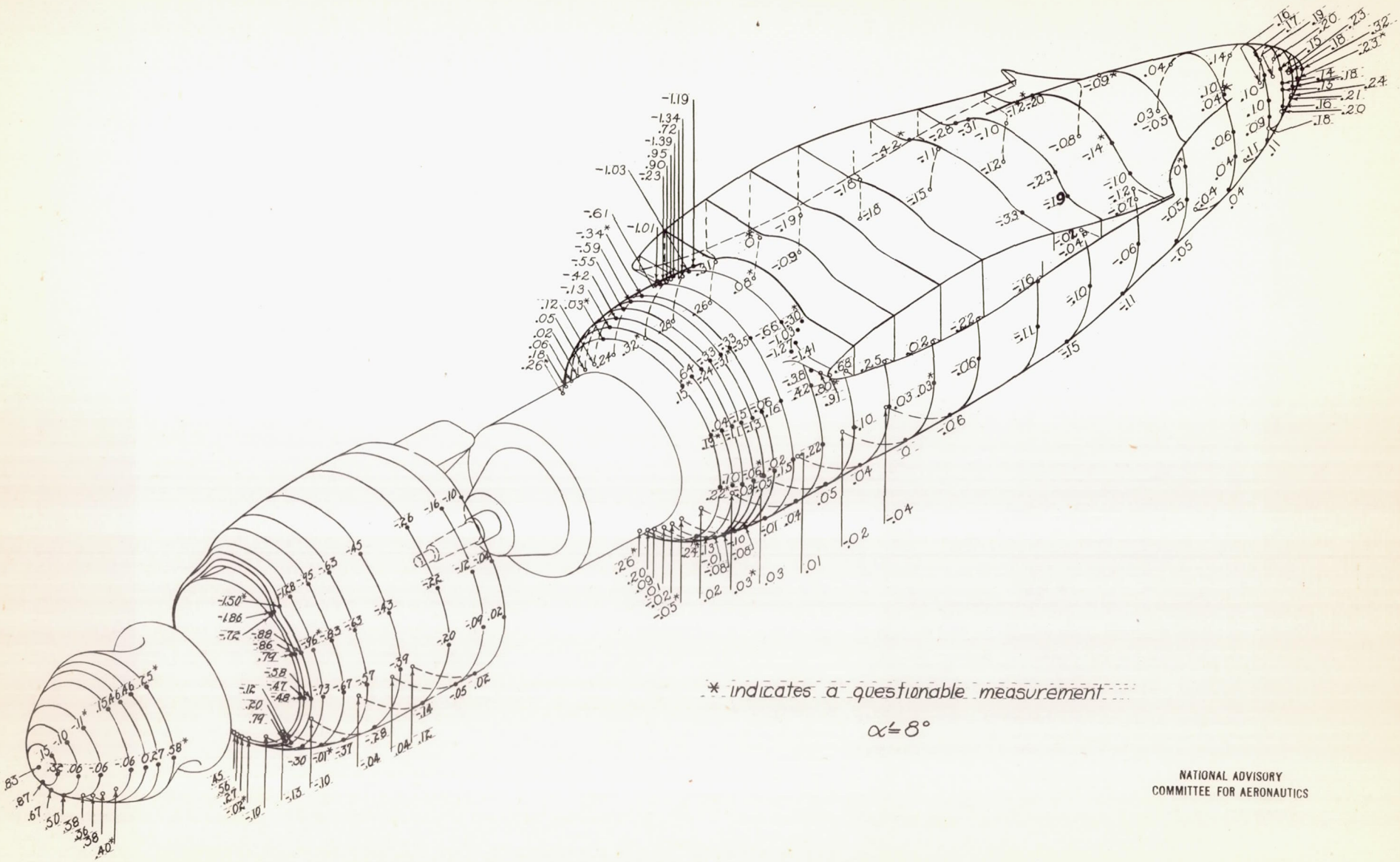

* indicates a questionable measurement

$\alpha \leq 8°$

NATIONAL ADVISORY
COMMITTEE FOR AERONAUTICS

Figure 10e.—concluded

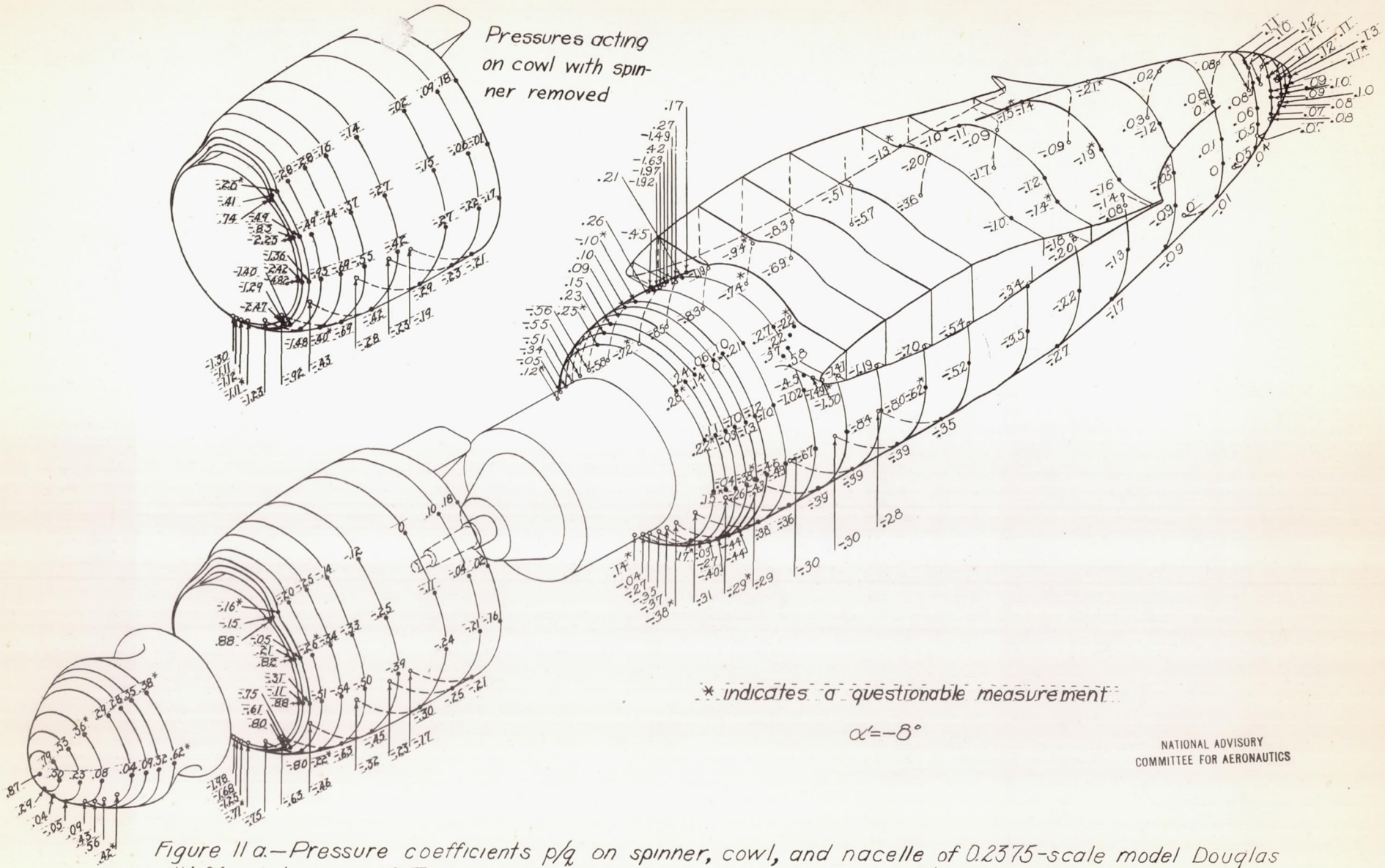

Figure 11 a.—Pressure coefficients p/q on spinner, cowl, and nacelle of 0.2375-scale model Douglas XA-26 airplane; ψ=0°. Test conditions with spinner installed; q≈50 lb/sq ft; R≈3,880,000; M≈0.12. Test conditions with spinner removed; q≈35 lb/sq ft; R≈3,300,000; M≈0.10.

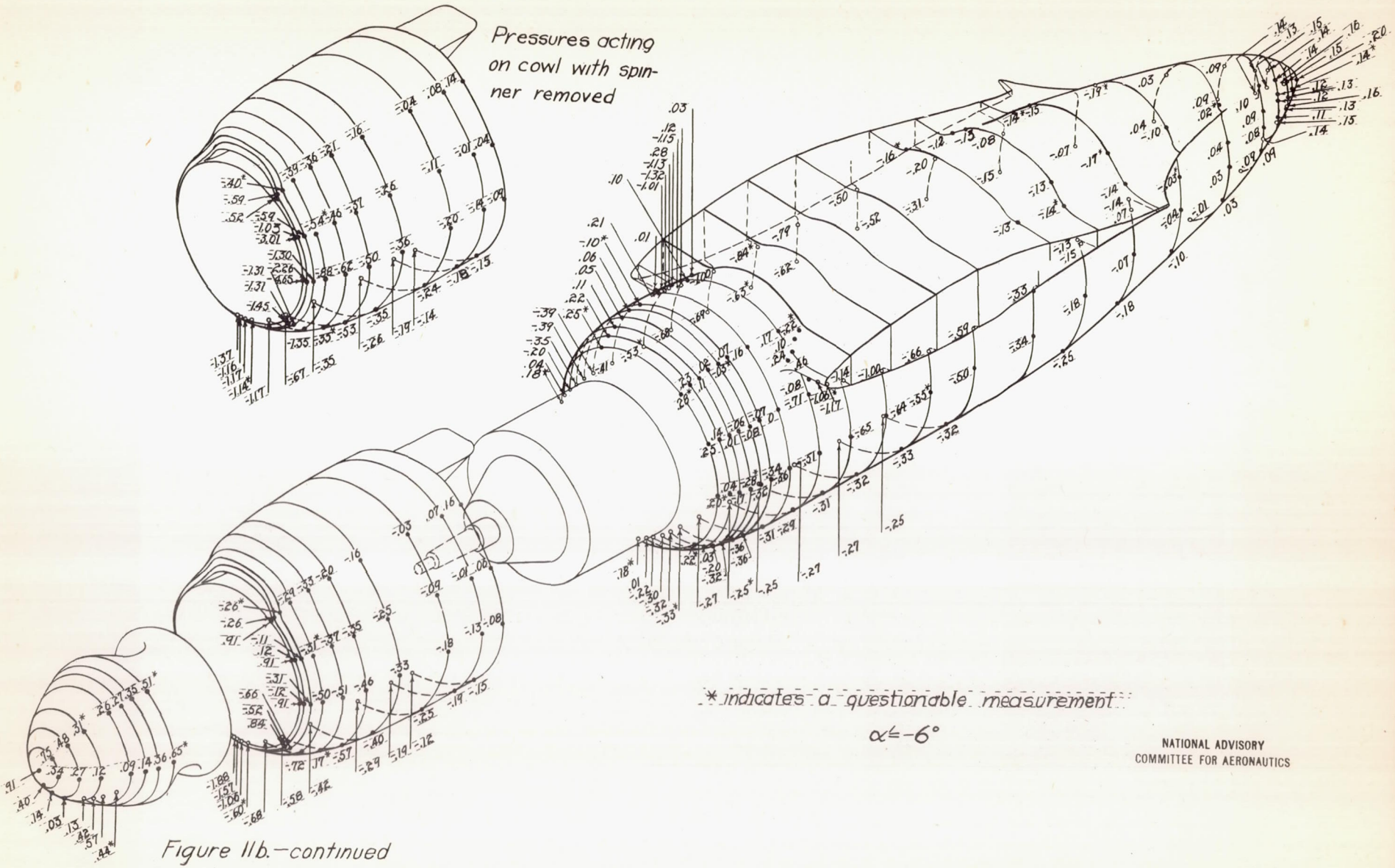

Figure 11b.—continued

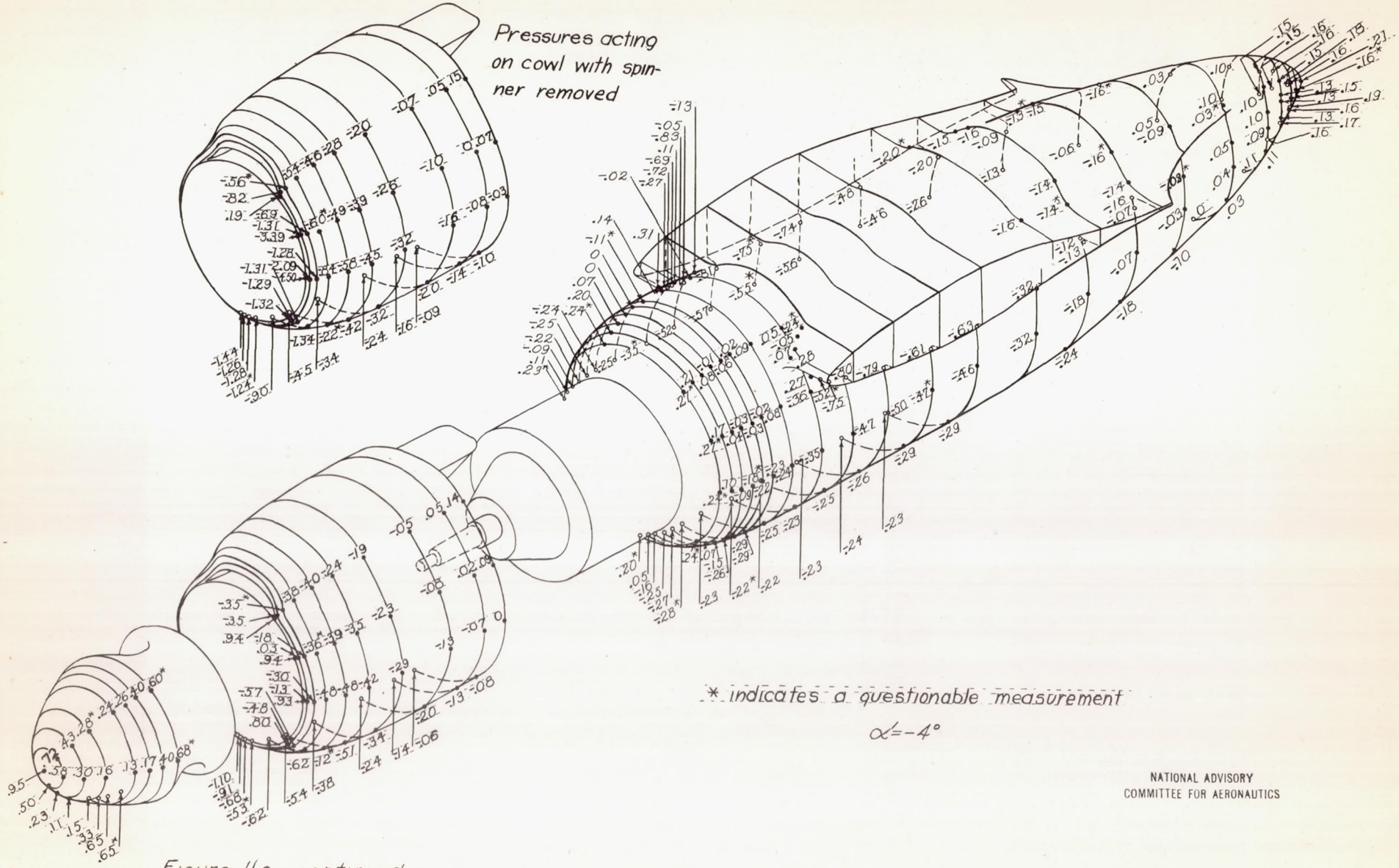

Figure 11c.—continued

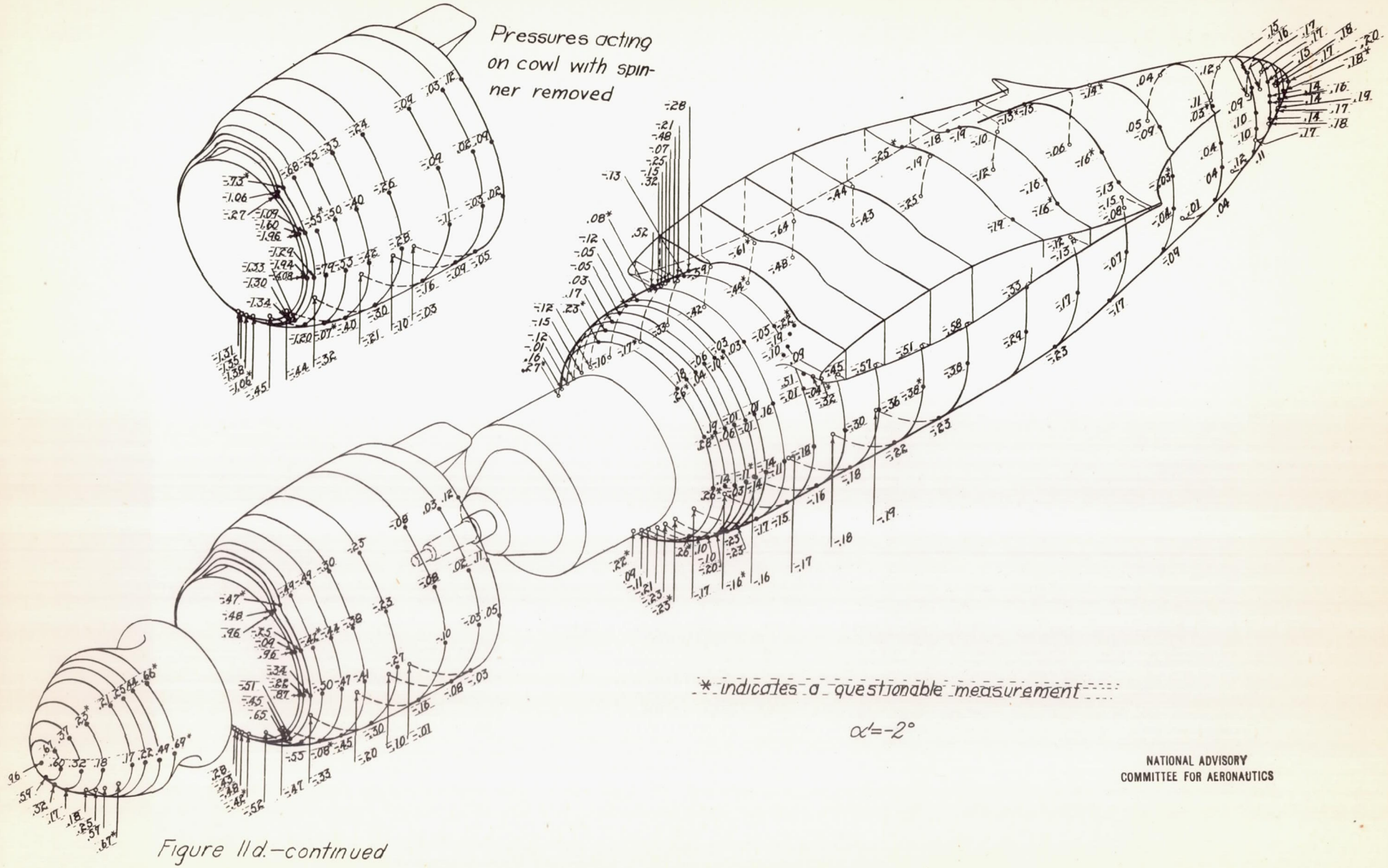

Figure 11d.—continued

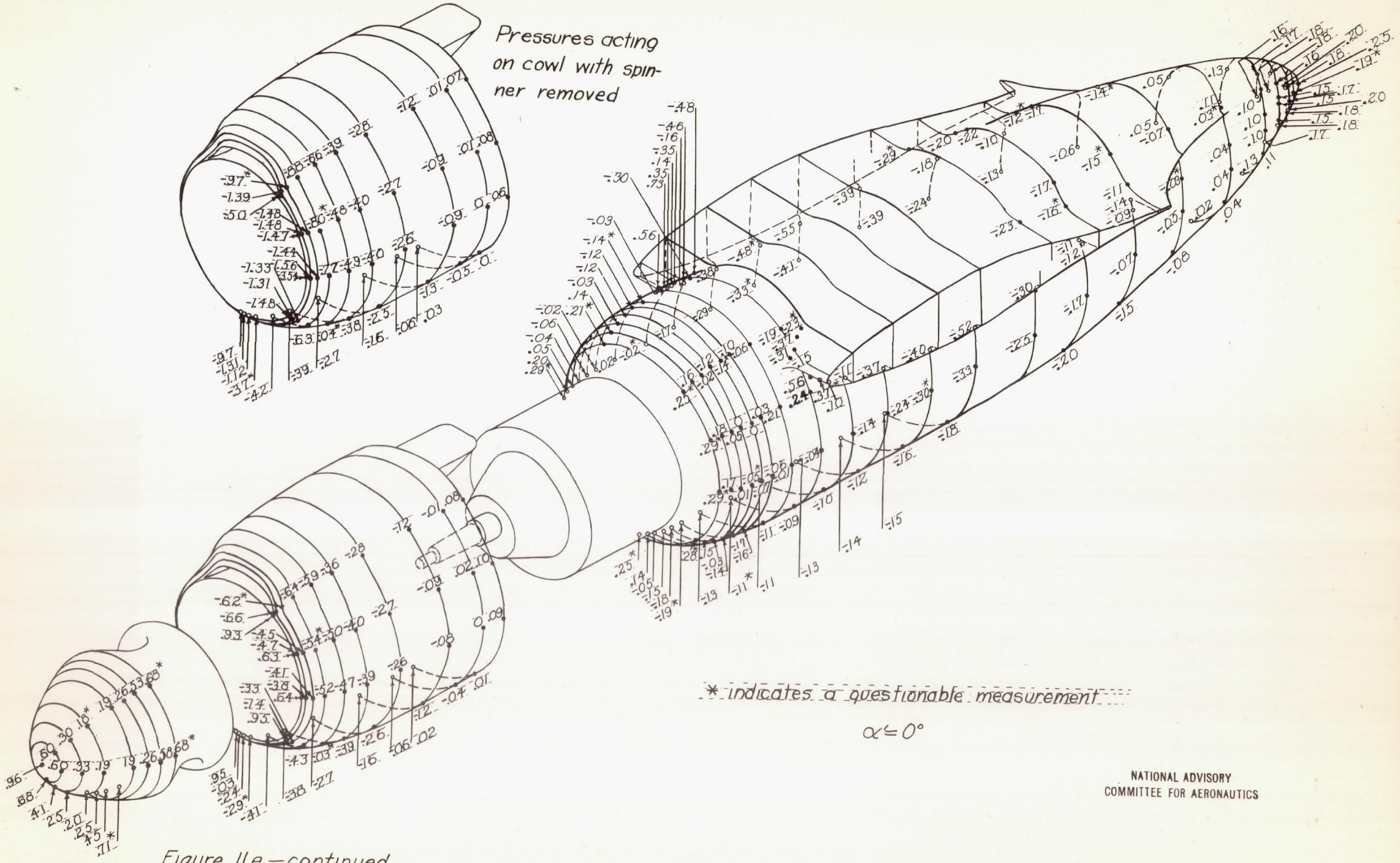

Figure 11e.—continued

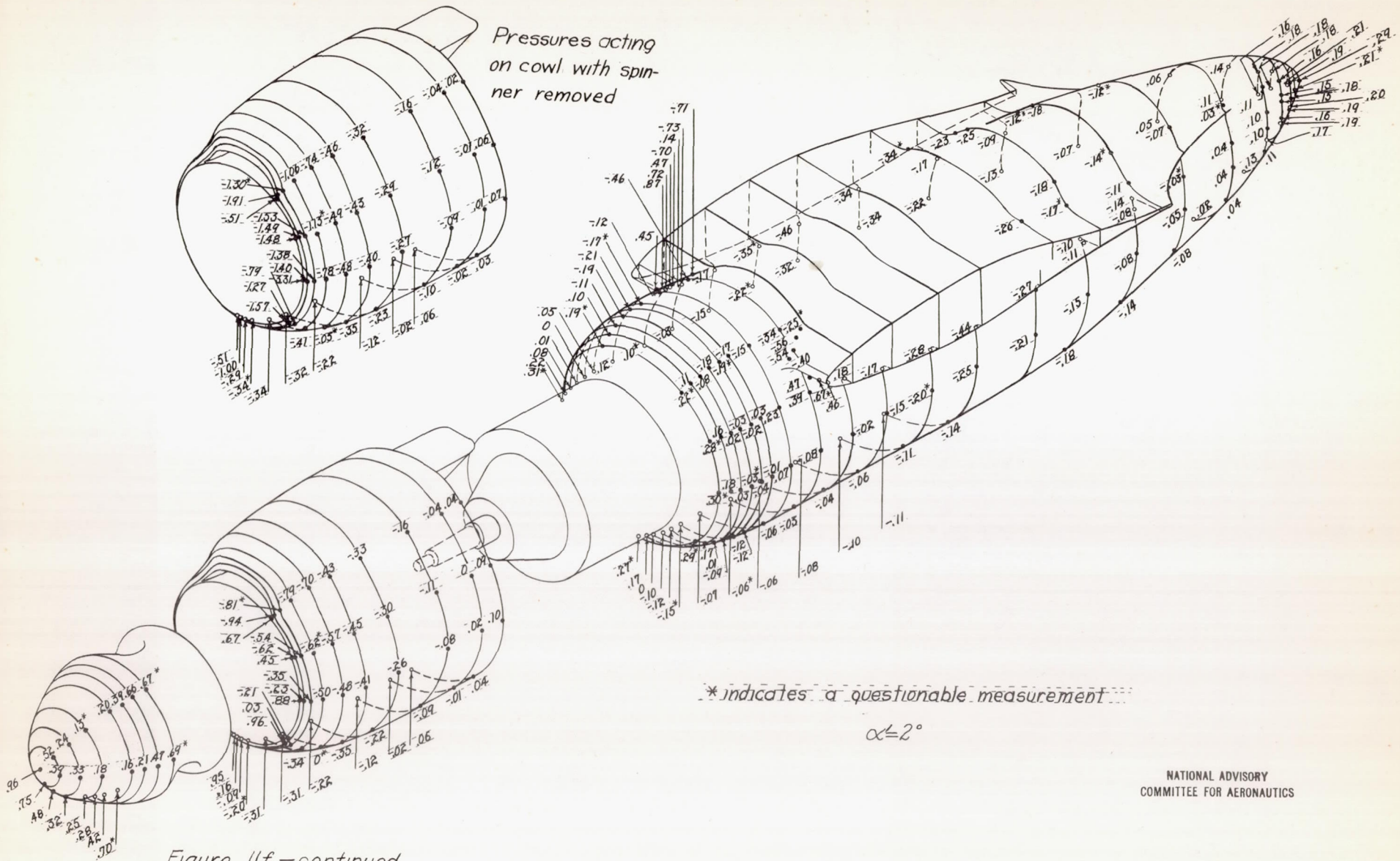

Figure 11f.—continued

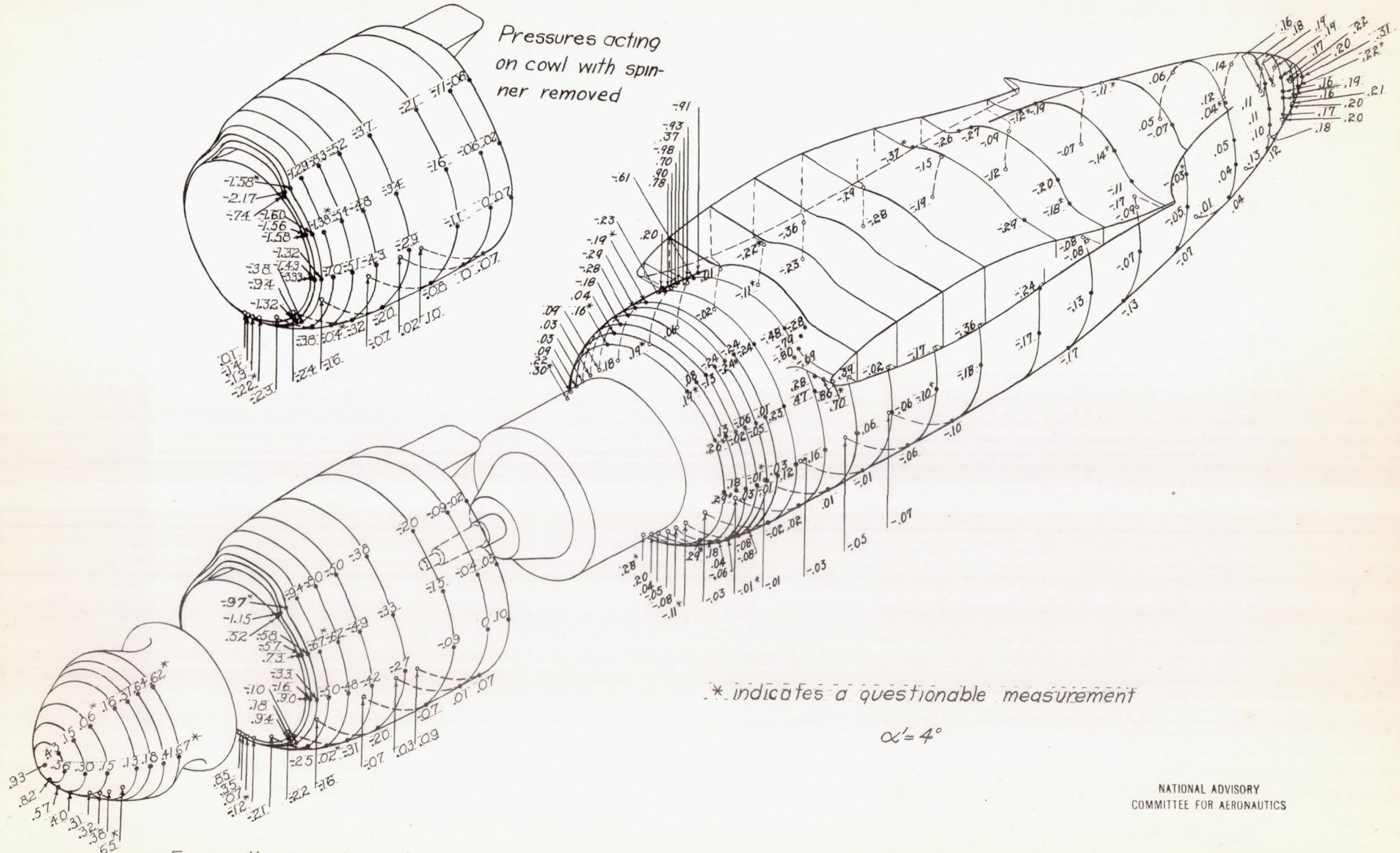

NATIONAL ADVISORY
COMMITTEE FOR AERONAUTICS

Figure 11g. – continued

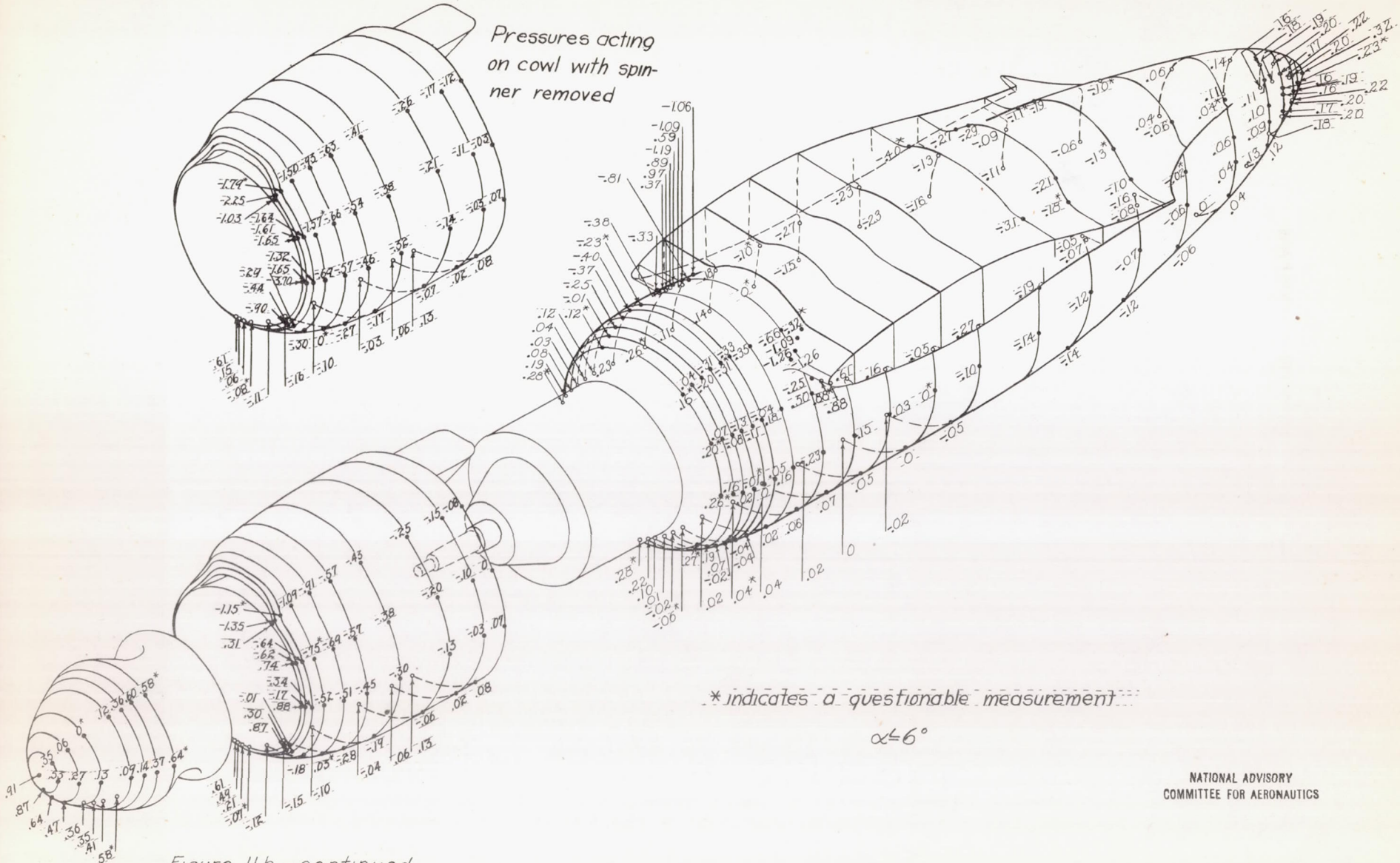

Figure 11h.—continued

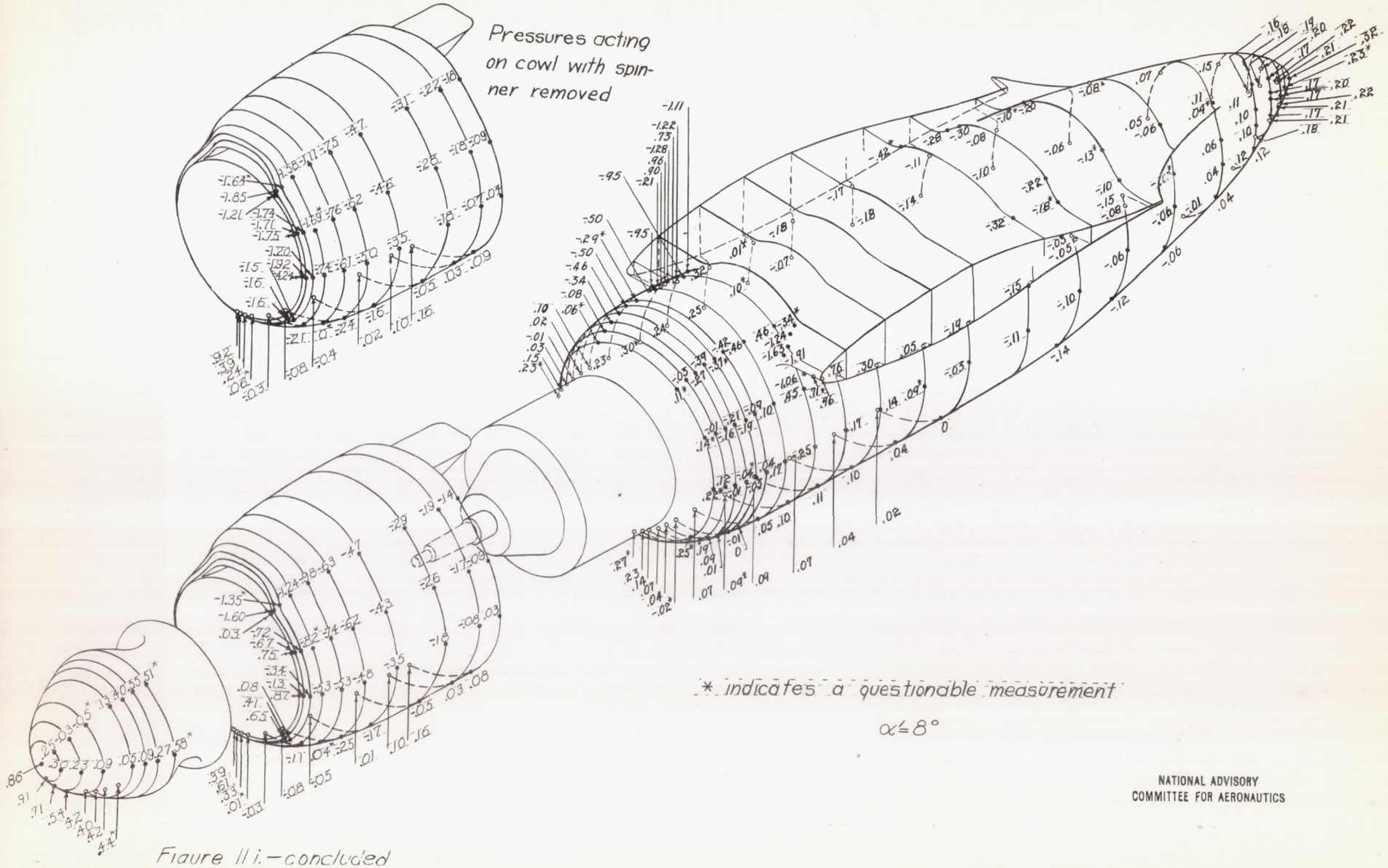

Figure 11 i.—concluded

NATIONAL ADVISORY
COMMITTEE FOR AERONAUTICS

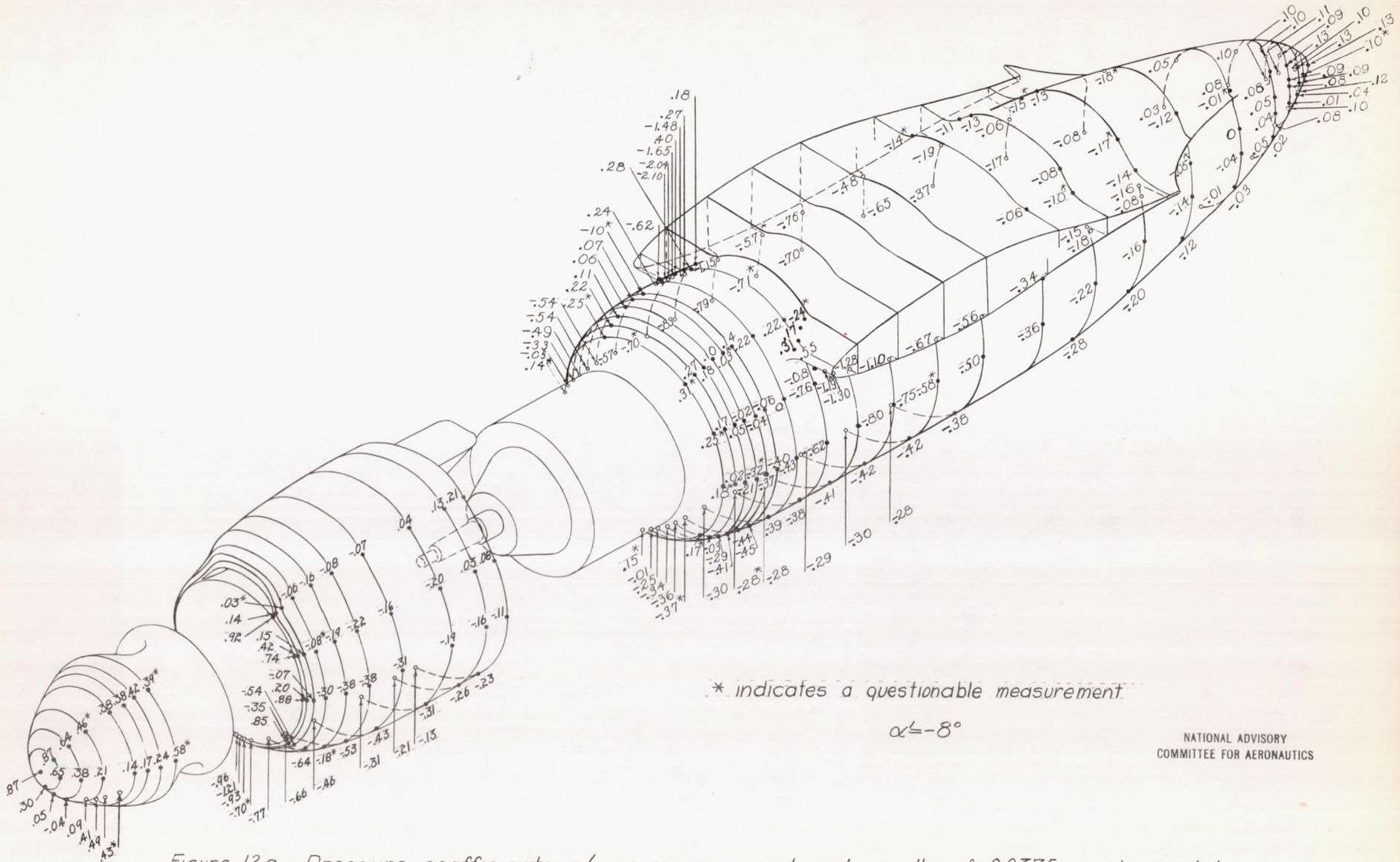

Figure 12 a.—Pressure coefficients p/q on spinner, cowl, and nacelle of 0.2375-scale model Douglas XA-26 airplane; $\psi = 5°$; $q \approx 50$ lb/sq ft; $R \approx 3{,}870{,}000$; $M \approx 0.12$.

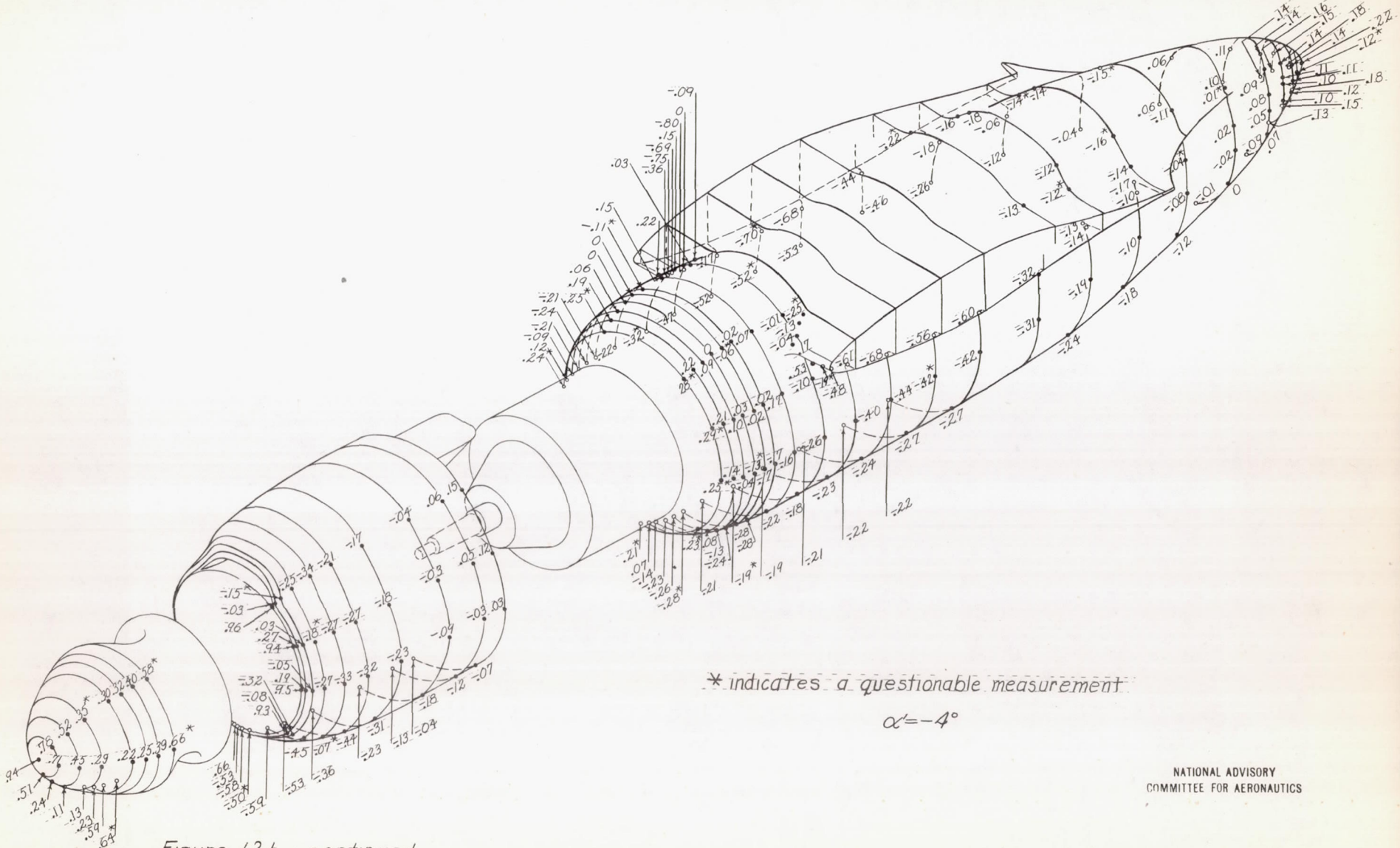

* indicates a questionable measurement

$\alpha = -4°$

NATIONAL ADVISORY
COMMITTEE FOR AERONAUTICS

Figure 12 b.—continued

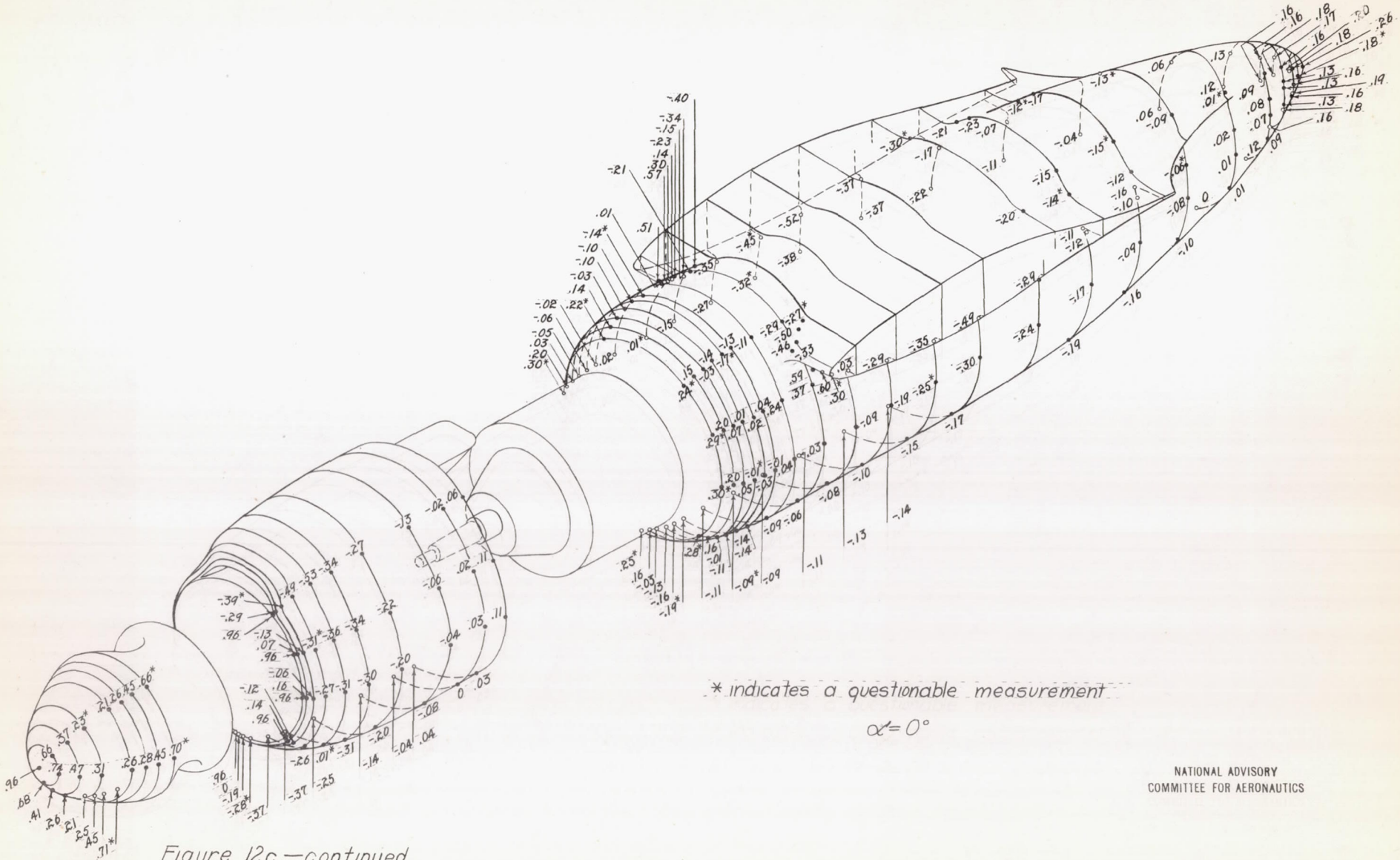

* indicates a questionable measurement

$\alpha = 0°$

NATIONAL ADVISORY
COMMITTEE FOR AERONAUTICS

Figure 12c.—continued

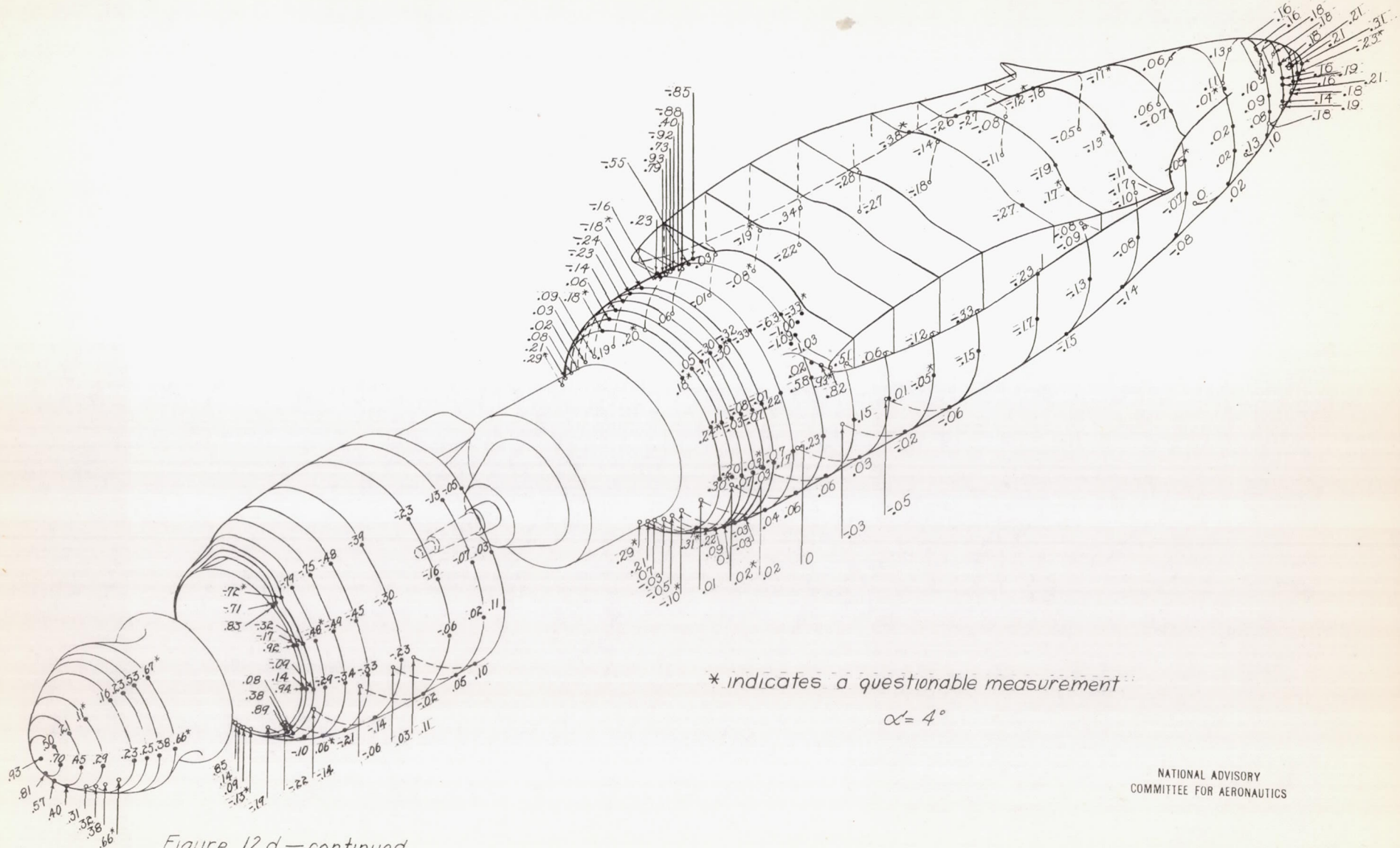

* indicates a questionable measurement

$\alpha = 4°$

NATIONAL ADVISORY
COMMITTEE FOR AERONAUTICS

Figure 12 d.—continued

* indicates a questionable measurement

$\alpha = 8°$

Data incomplete due to missing photograph.

Figure 12 e. — concluded

NATIONAL ADVISORY
COMMITTEE FOR AERONAUTICS

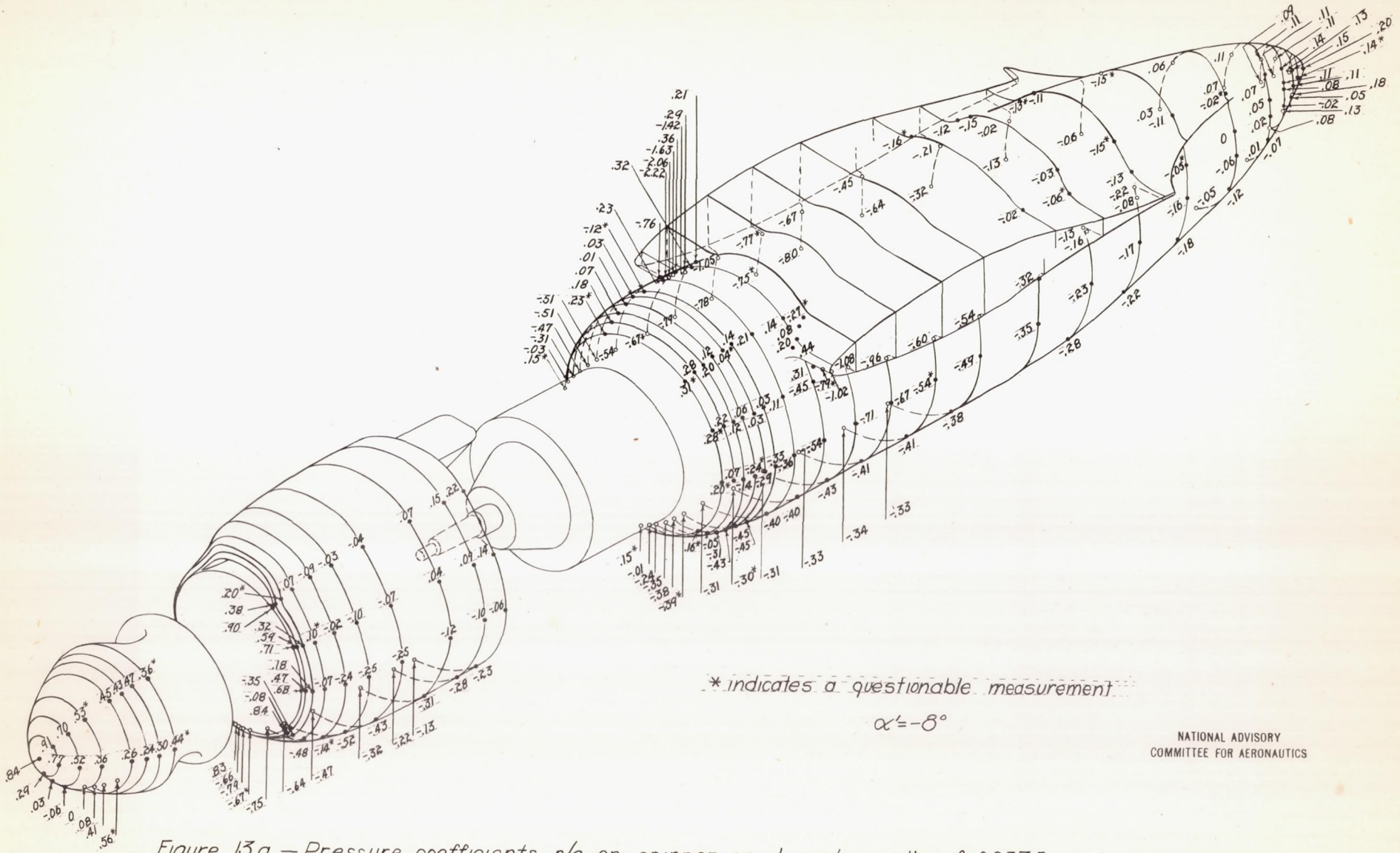

Figure 13a. — Pressure coefficients p/q on spinner, cowl, and nacelle of 0.2375-scale model Douglas XA-26 airplane; ψ = 10°; q ≈ 50 lb/sq ft; R ≈ 3,870,000; M ≈ 0.12.

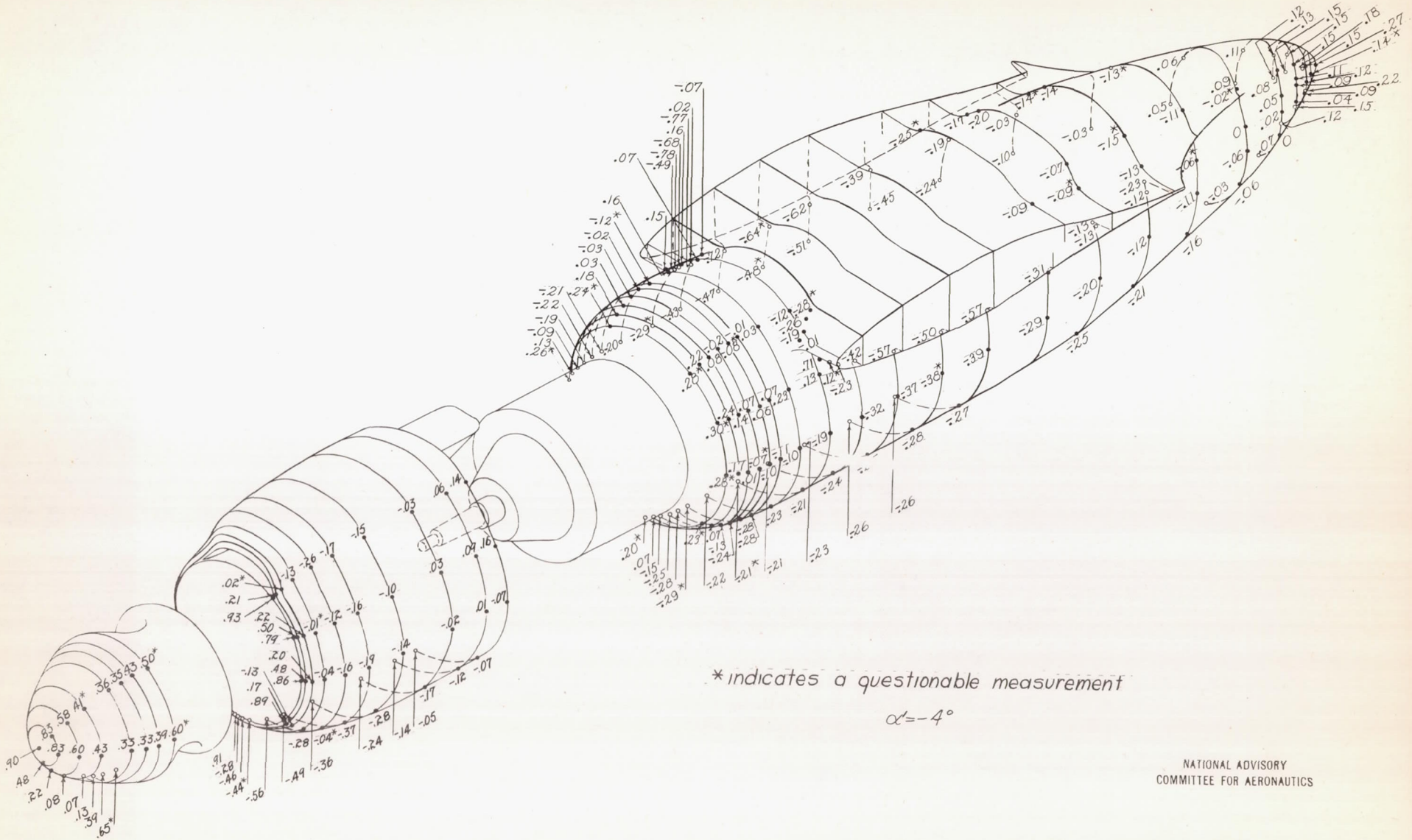

Figure 13b.—continued

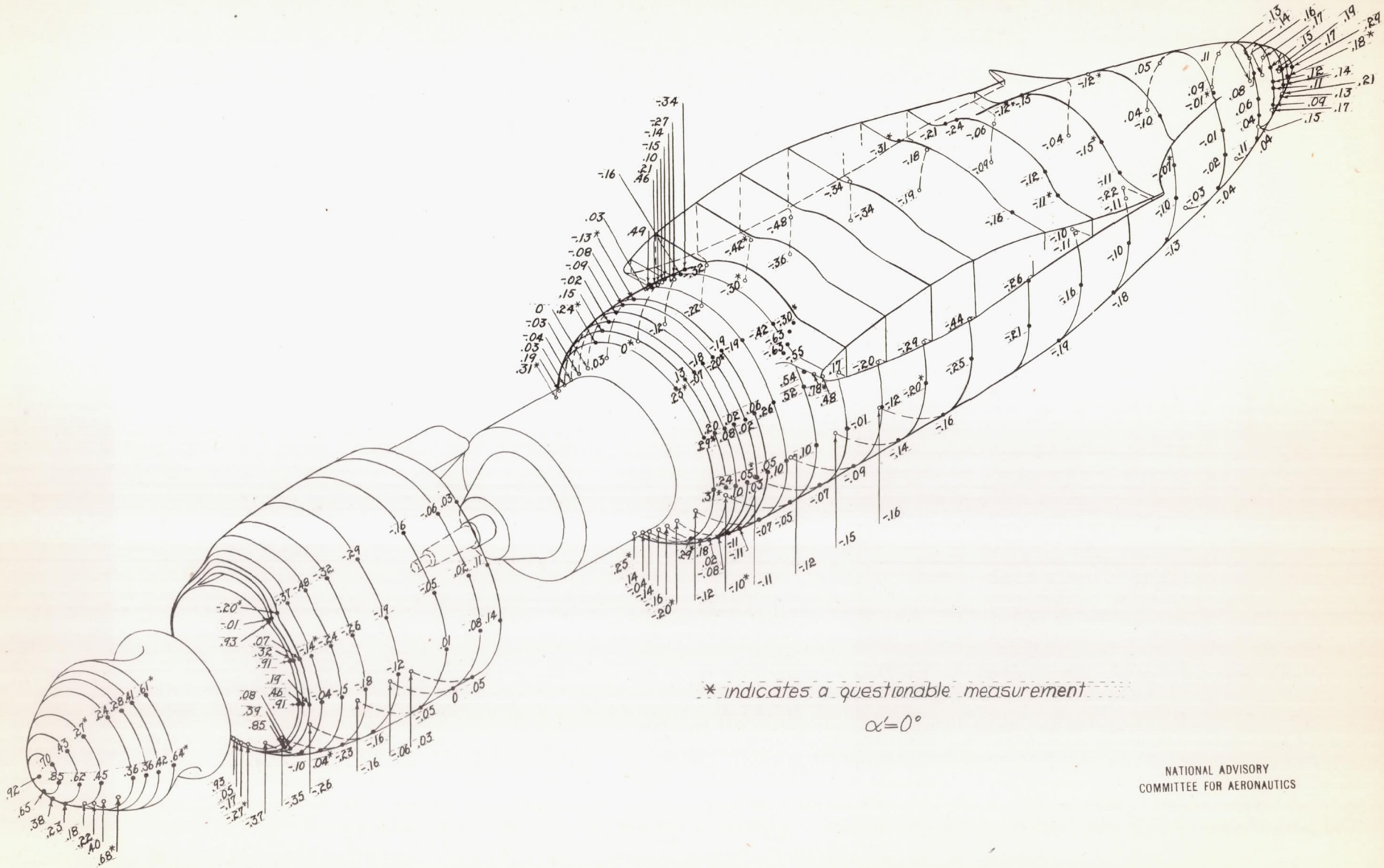

Figure 13c.— continued

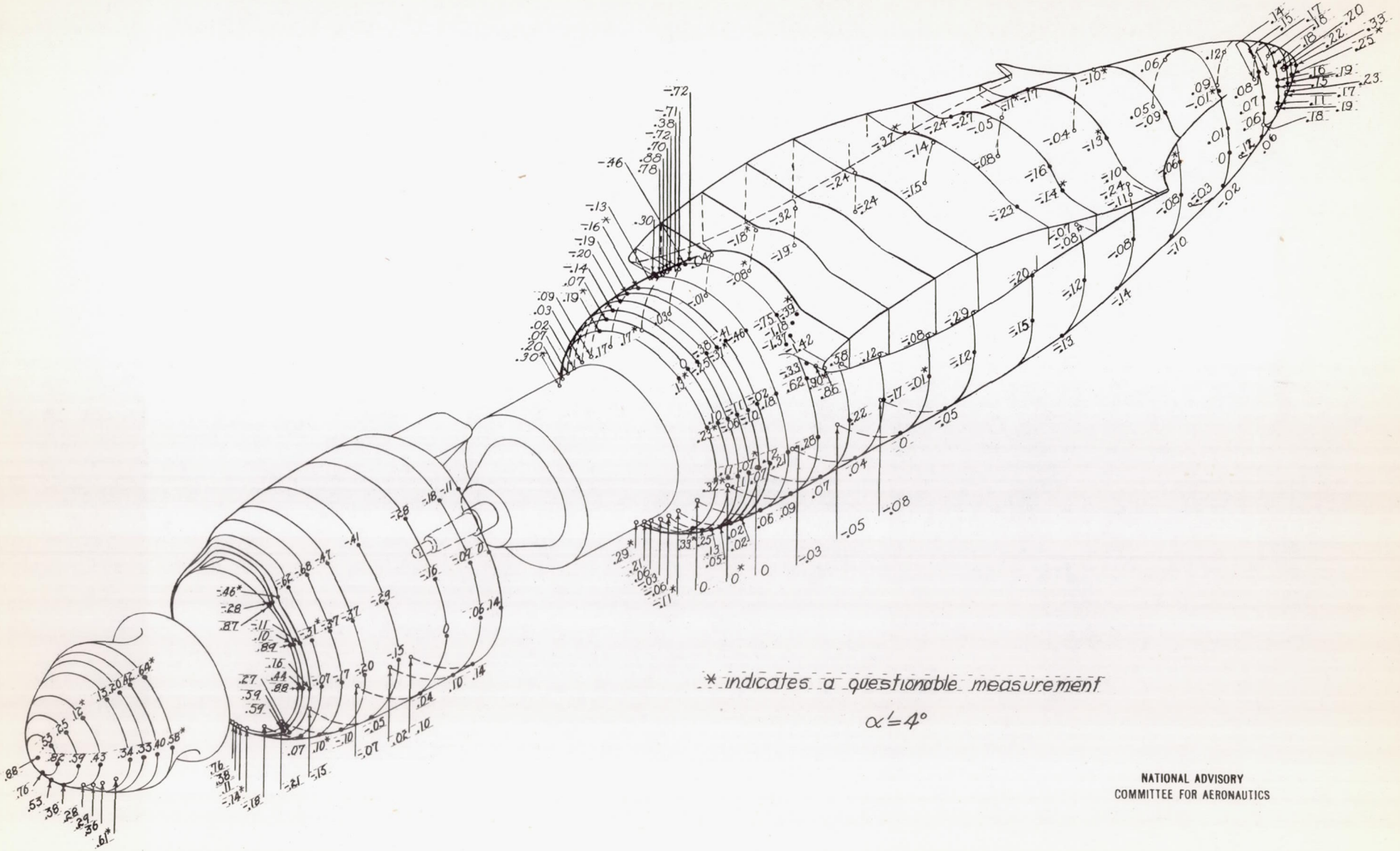

* indicates a questionable measurement

$\alpha \doteq 4°$

NATIONAL ADVISORY
COMMITTEE FOR AERONAUTICS

Figure 13 d.—continued

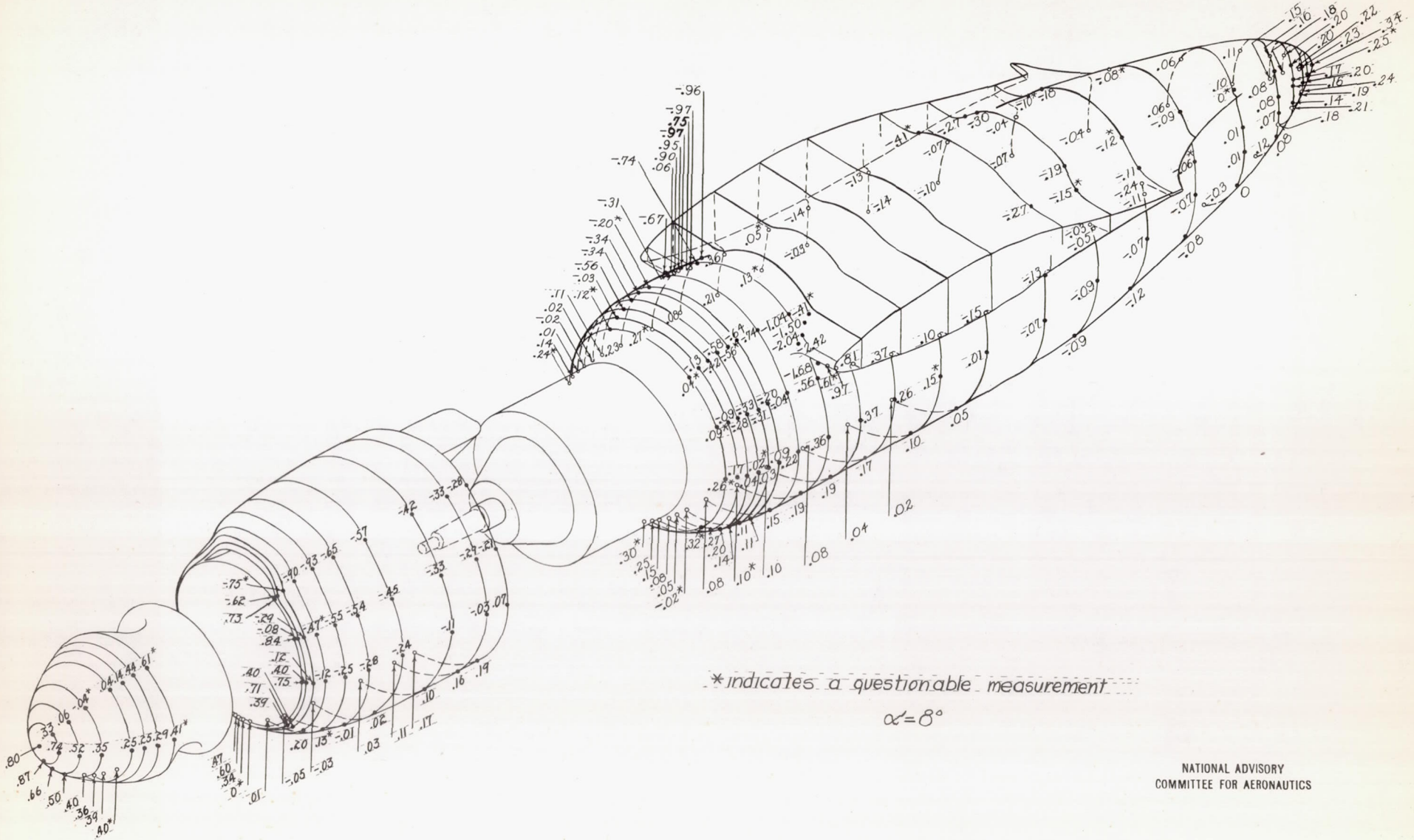

Figure 13e.—concluded

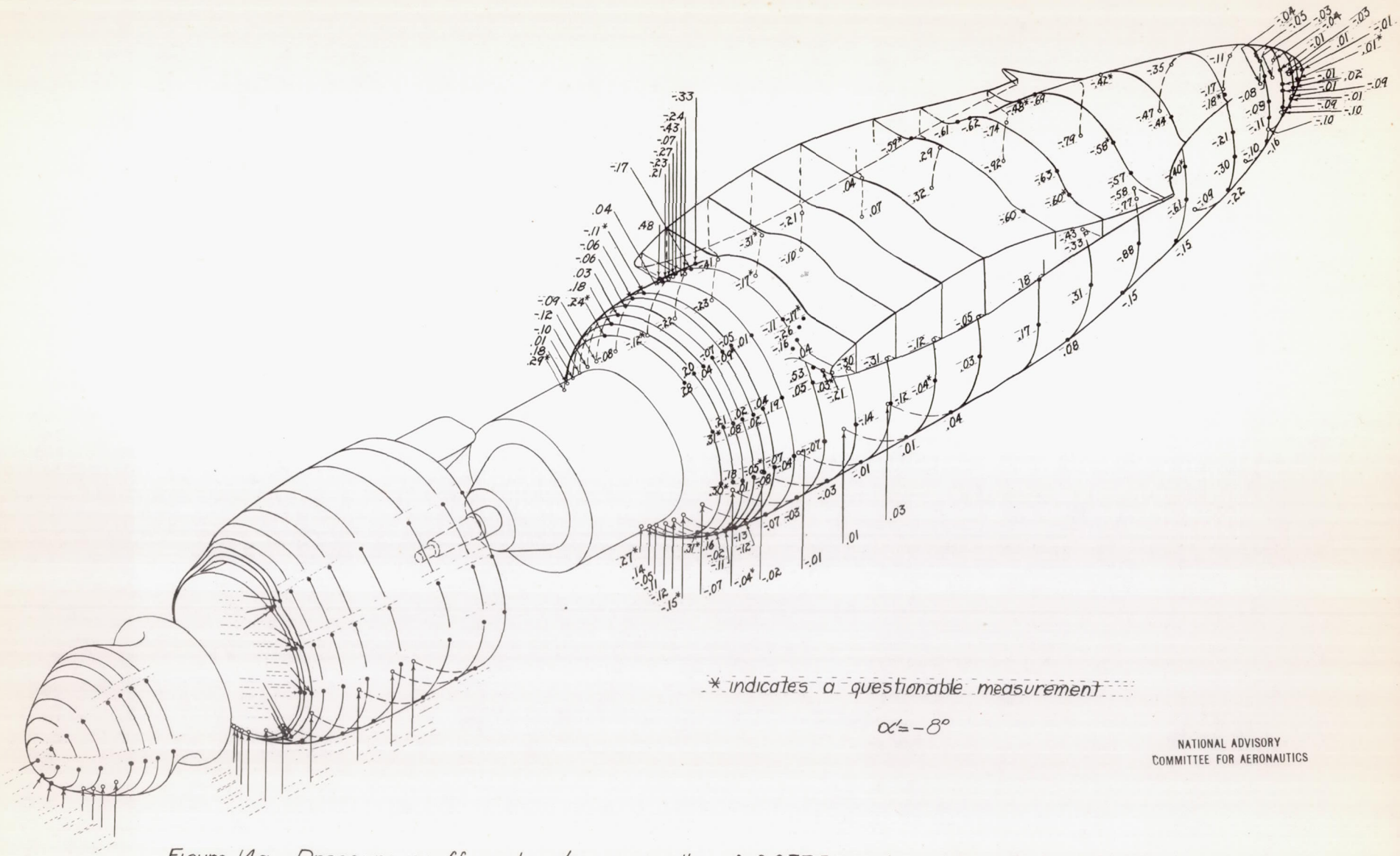

Figure 14a.—Pressure coefficients p/q on nacelle of 0.2375-scale model Douglas XA-26 airplane; $\psi = 0°$; $\delta_f = 55°$; $q \approx 50$ lb/sq ft; $R \approx 3{,}720{,}000$; $M \approx 0.12$.

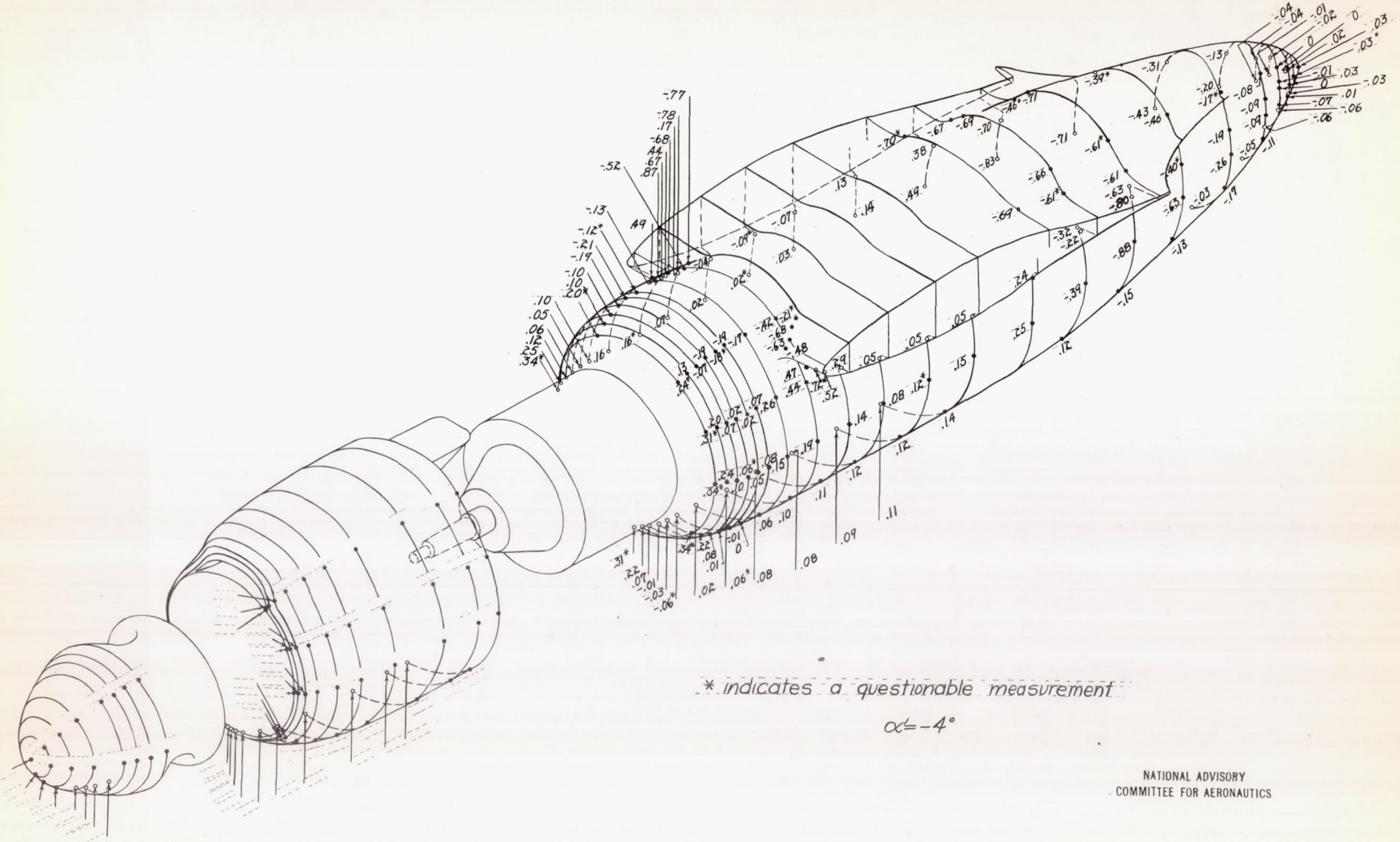

Figure 14b.—continued

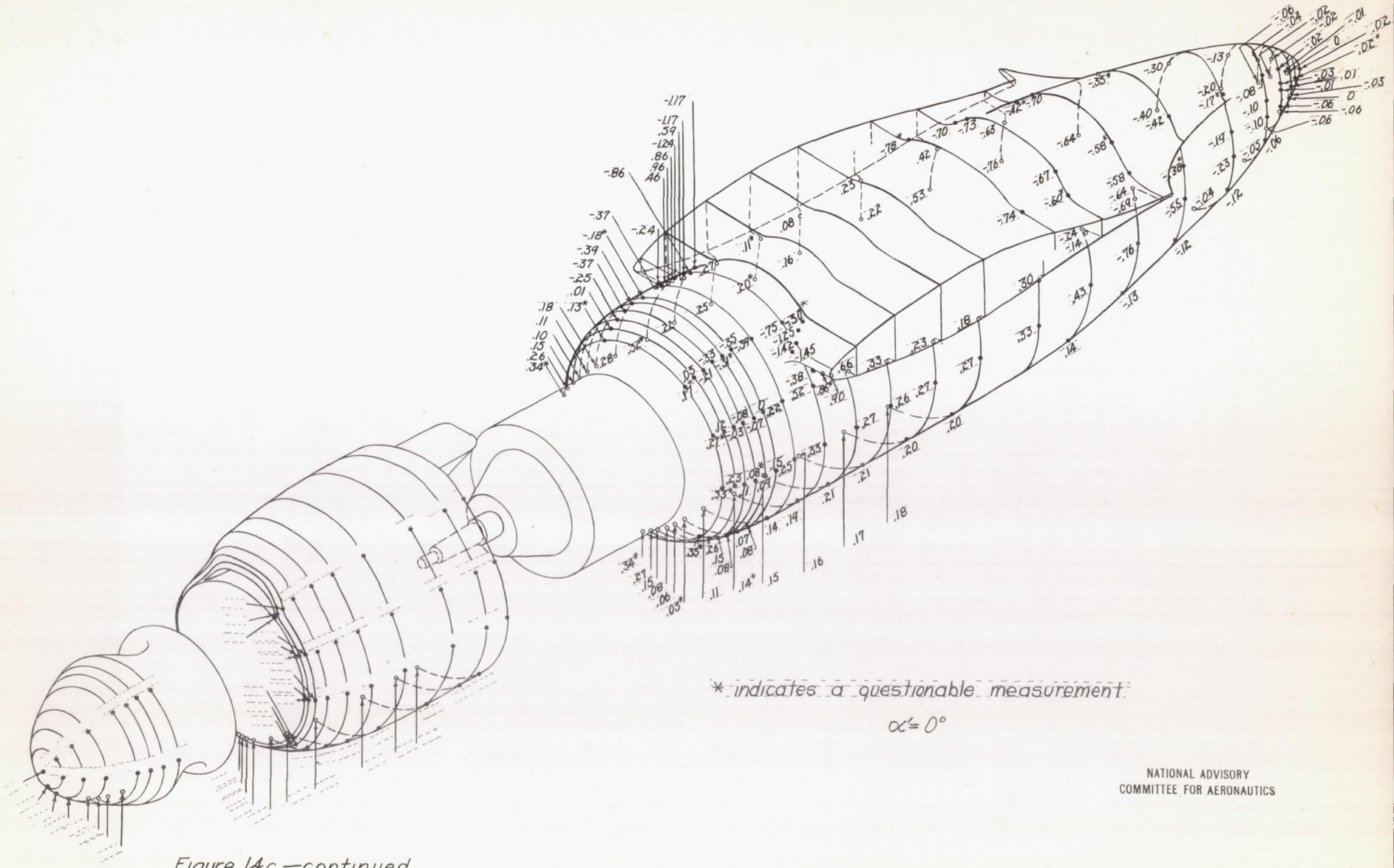

Figure 14c.—continued

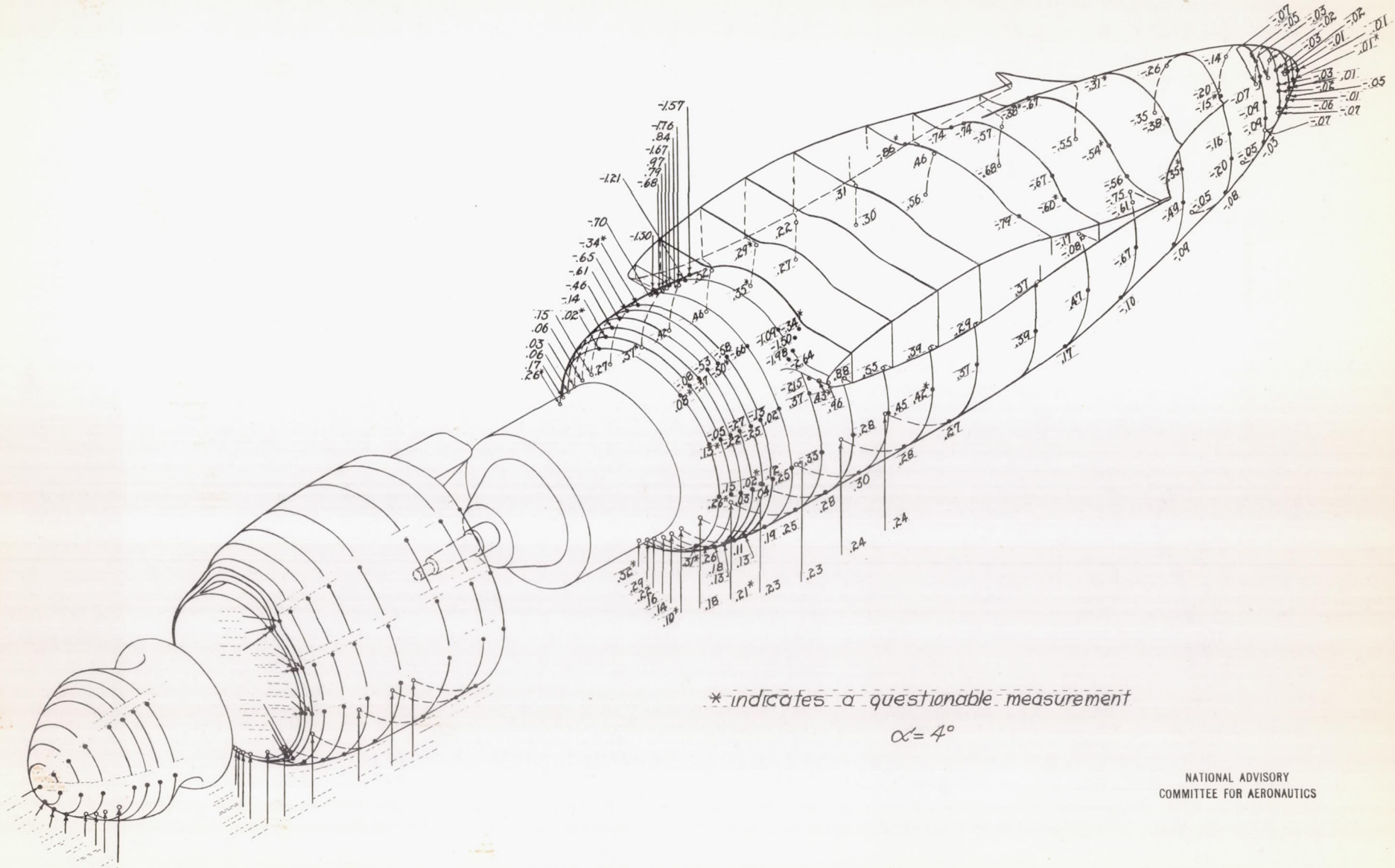

Figure 14d.—continued

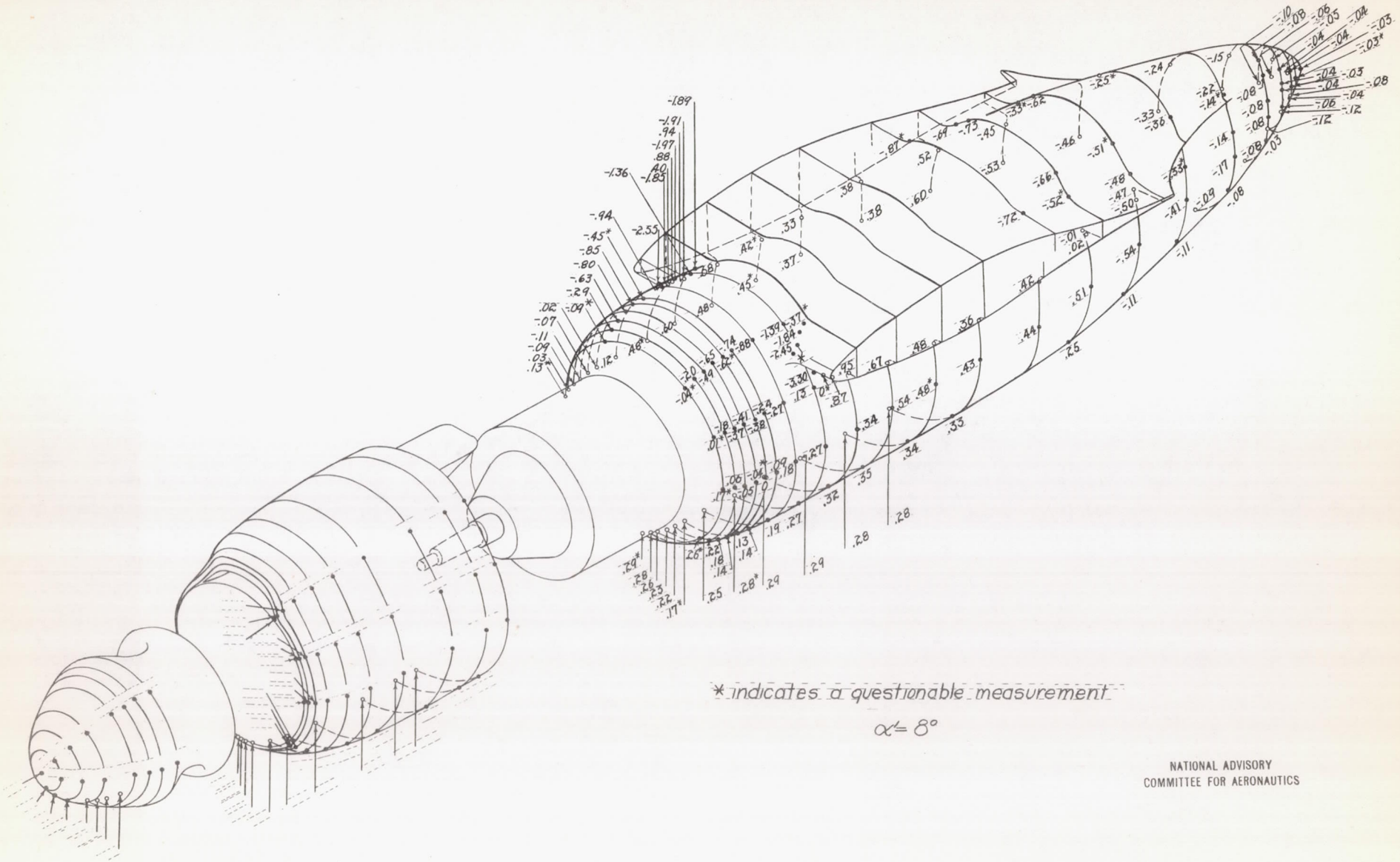

Figure 14e.— concluded

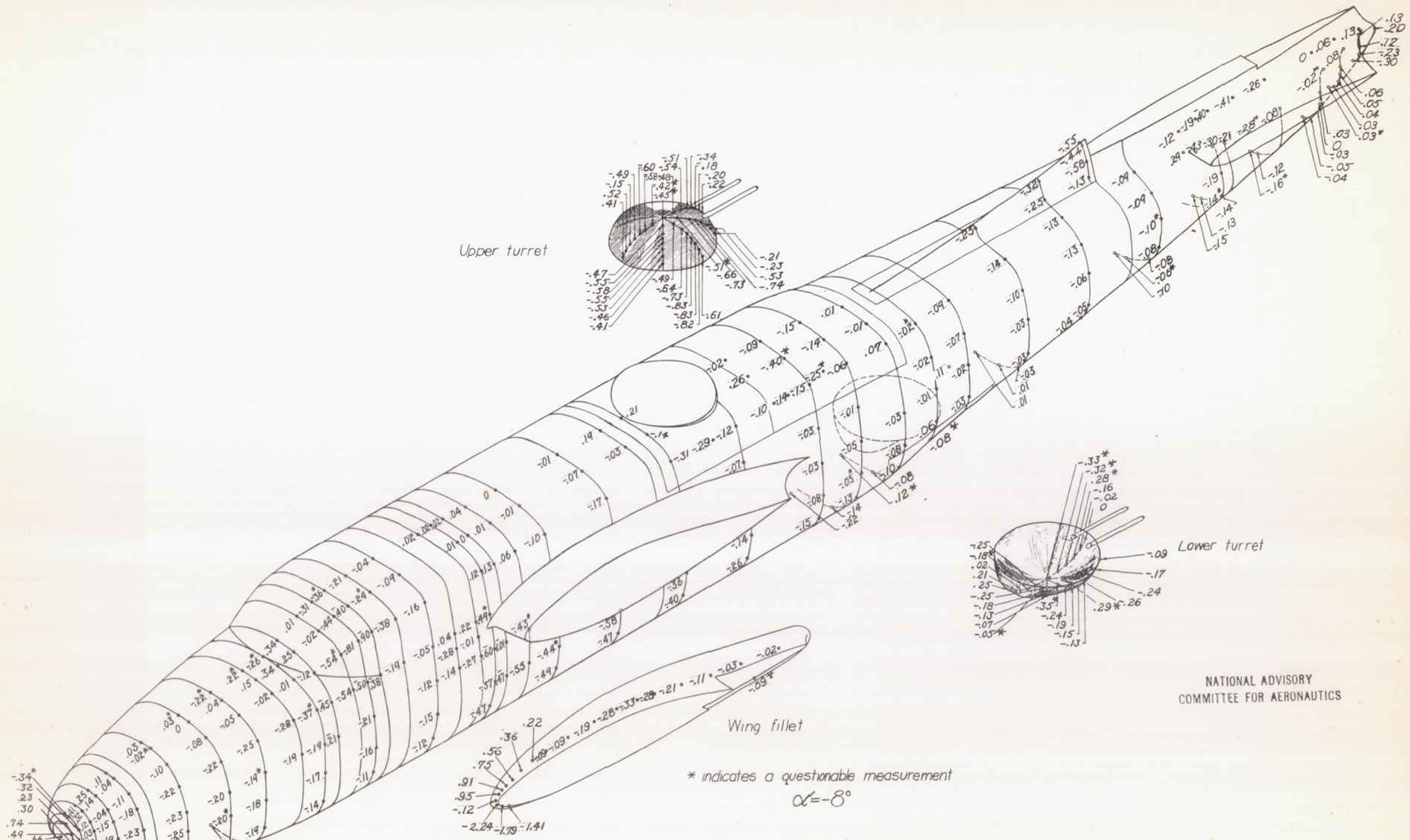

Figure 15a.—Pressure coefficients p/q on fuselage of 0.2375-scale model Douglas XA-26 airplane; ψ=-10°; q≈50 lb/sq ft; R≈4,000,000; M≈0.12.

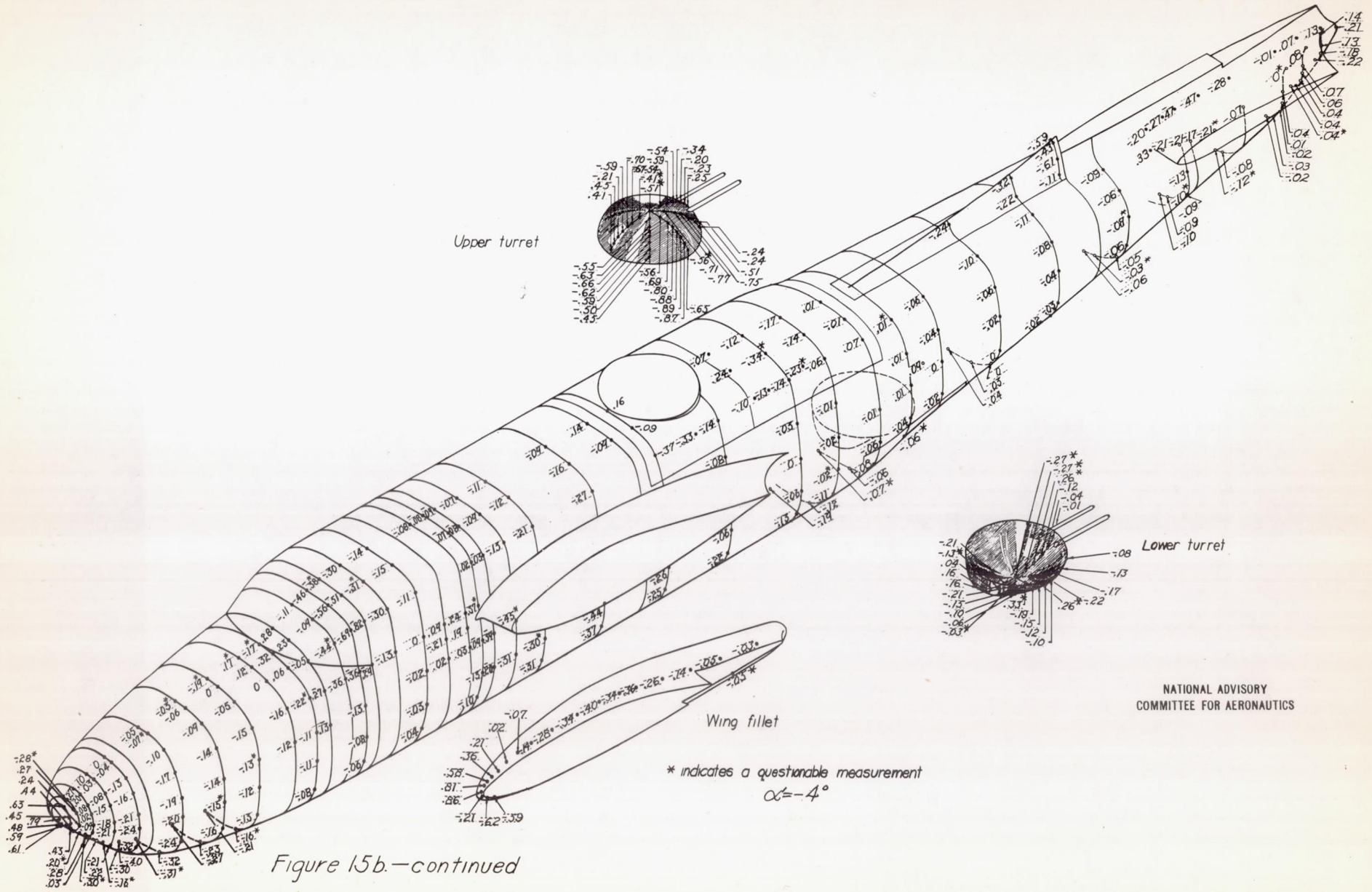

Figure 15b.—continued

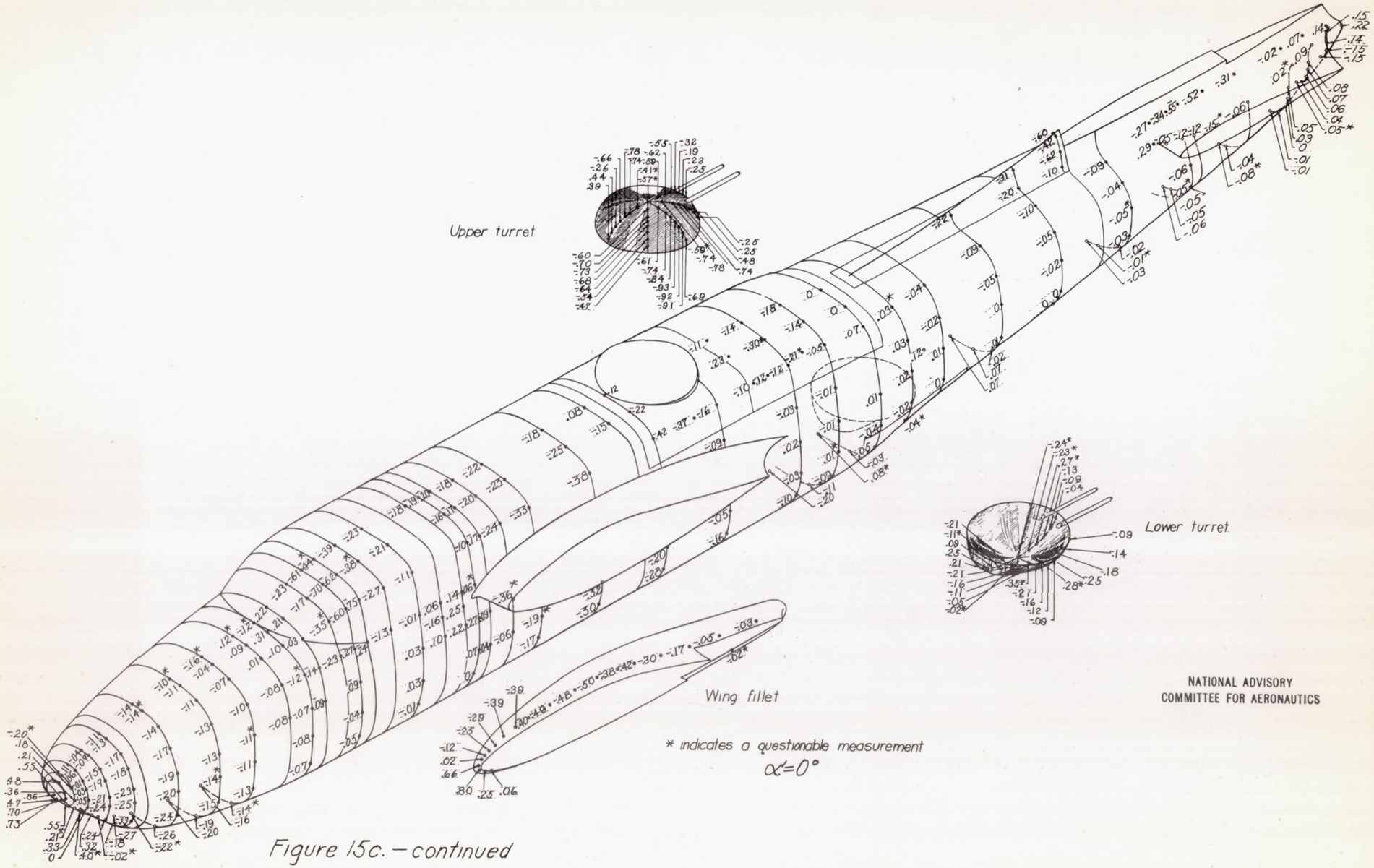

Figure 15c. — continued

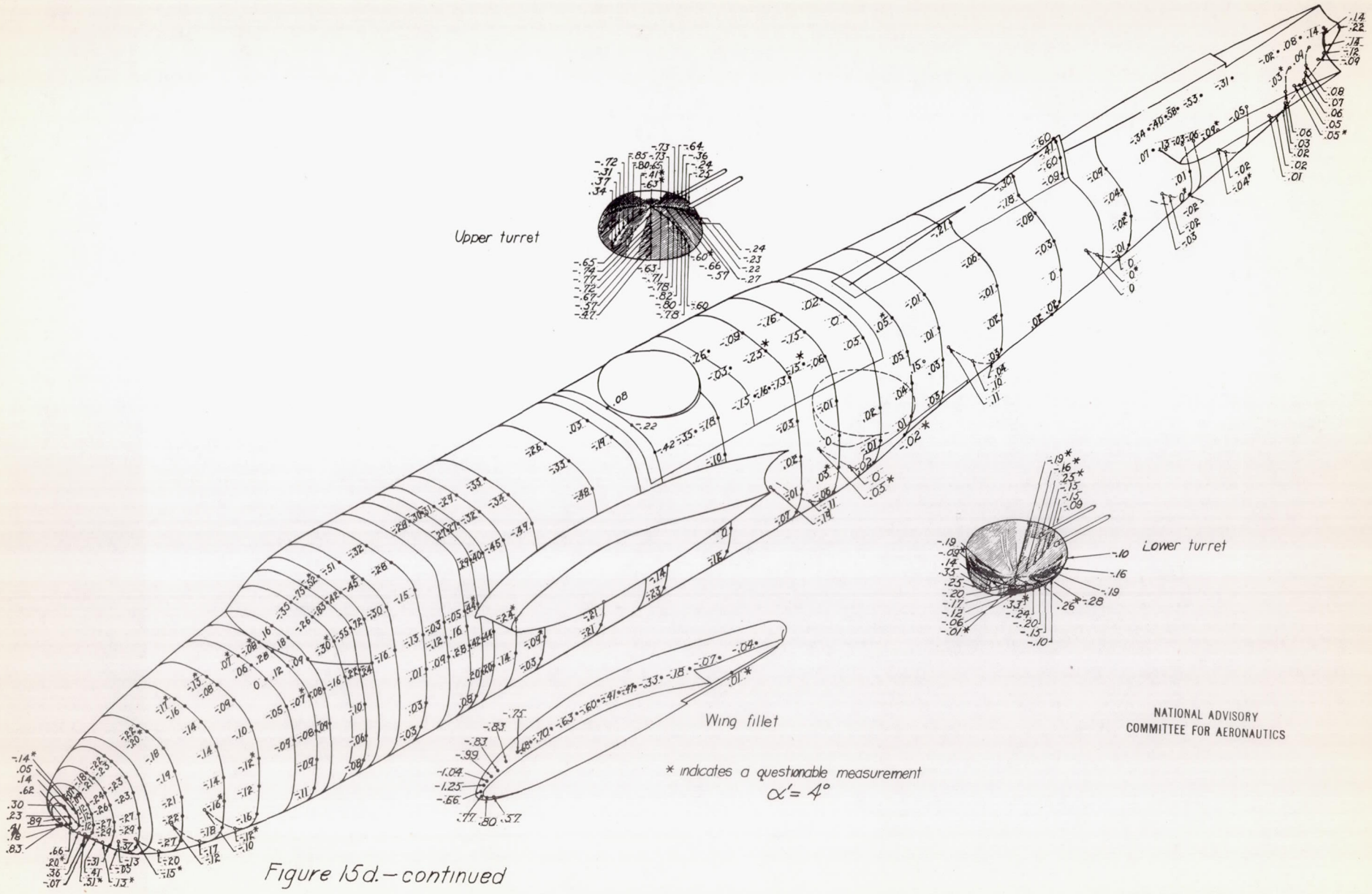

Figure 15d.—continued

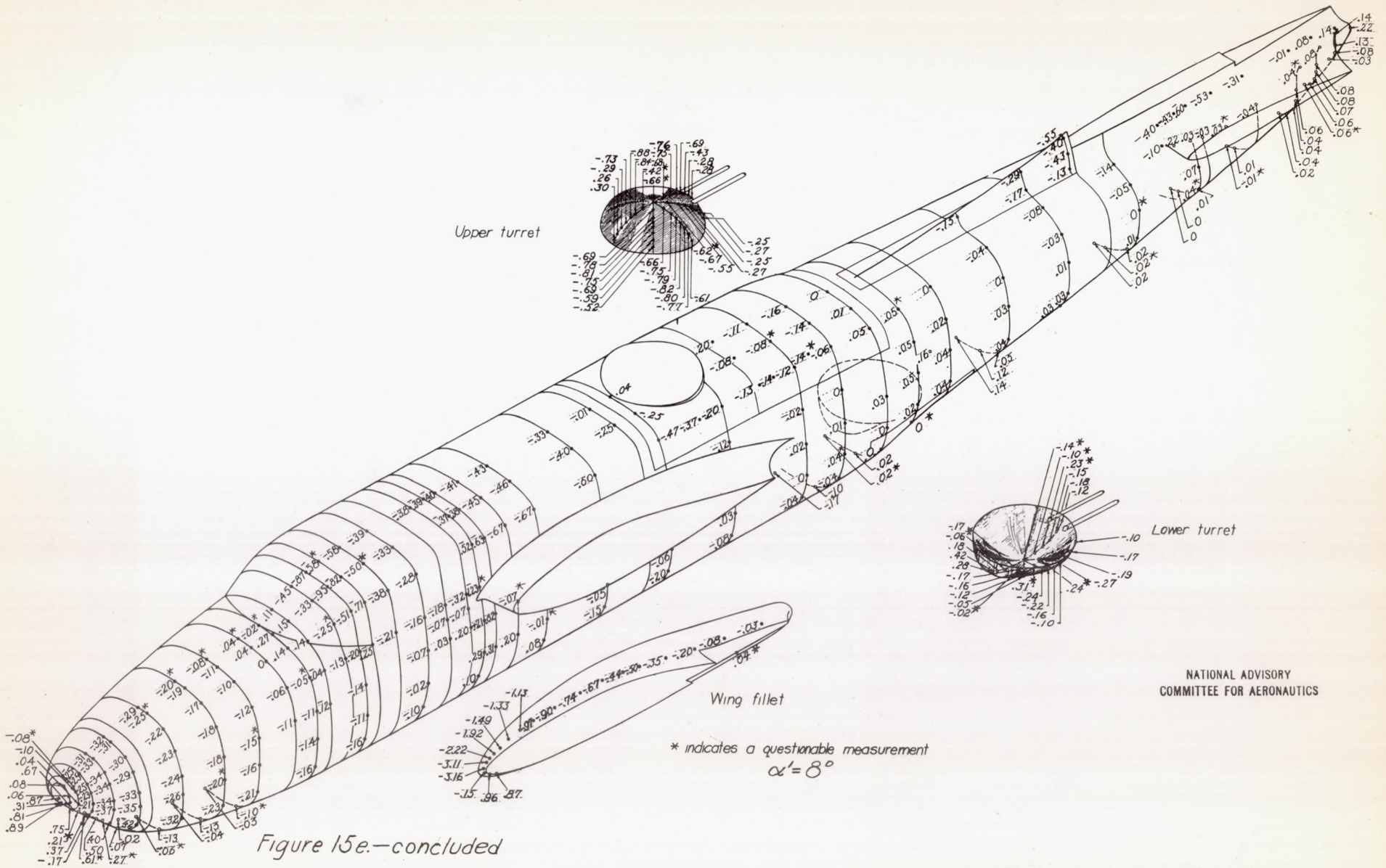

Figure 15e.—concluded

NATIONAL ADVISORY
COMMITTEE FOR AERONAUTICS

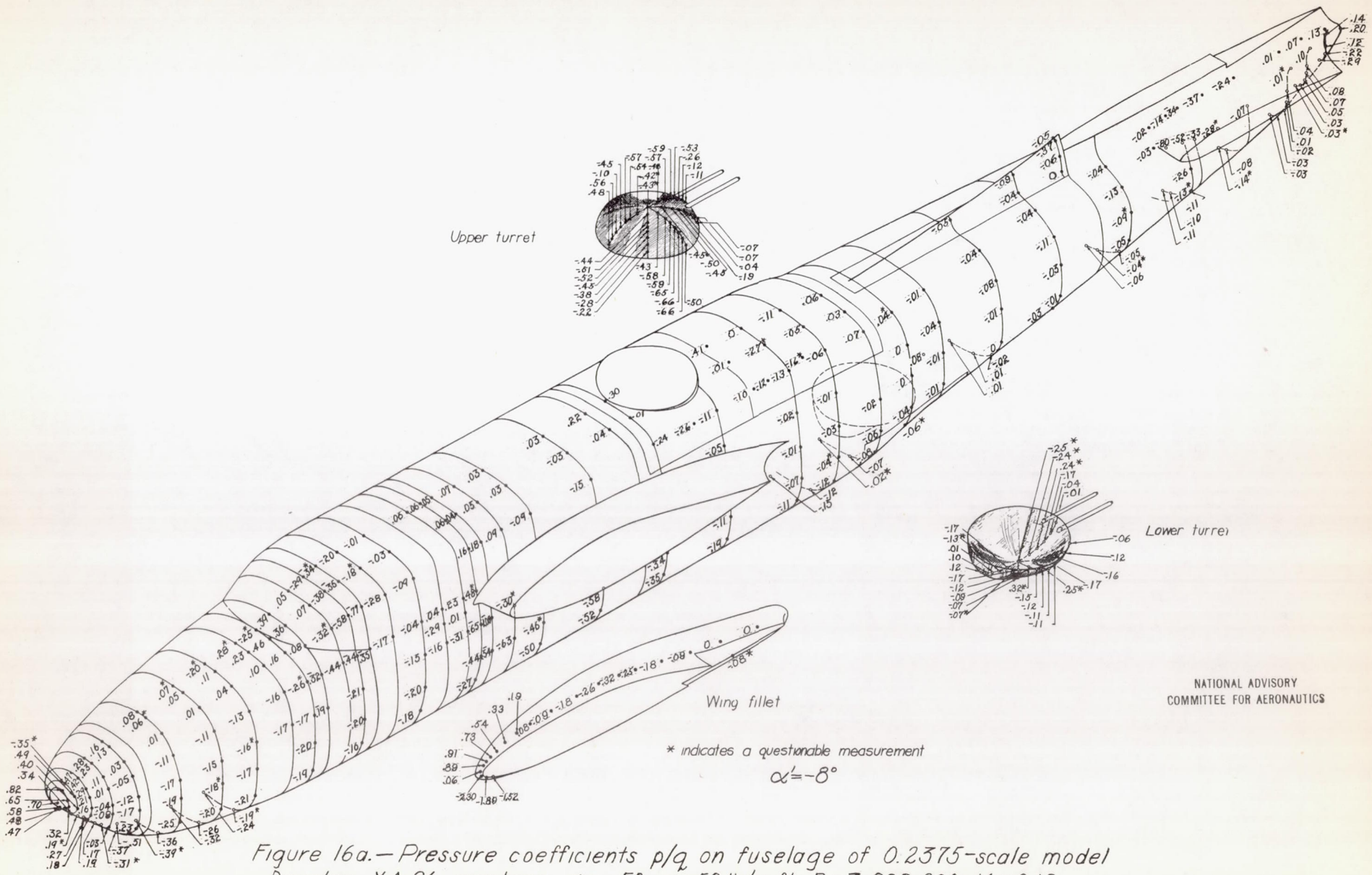

Figure 16a.—Pressure coefficients p/q on fuselage of 0.2375-scale model Douglas XA-26 airplane; $\psi=-5°$; $q\approx 50$ lb/sq ft; $R\approx 3{,}990{,}000$; $M\approx 0.12$.

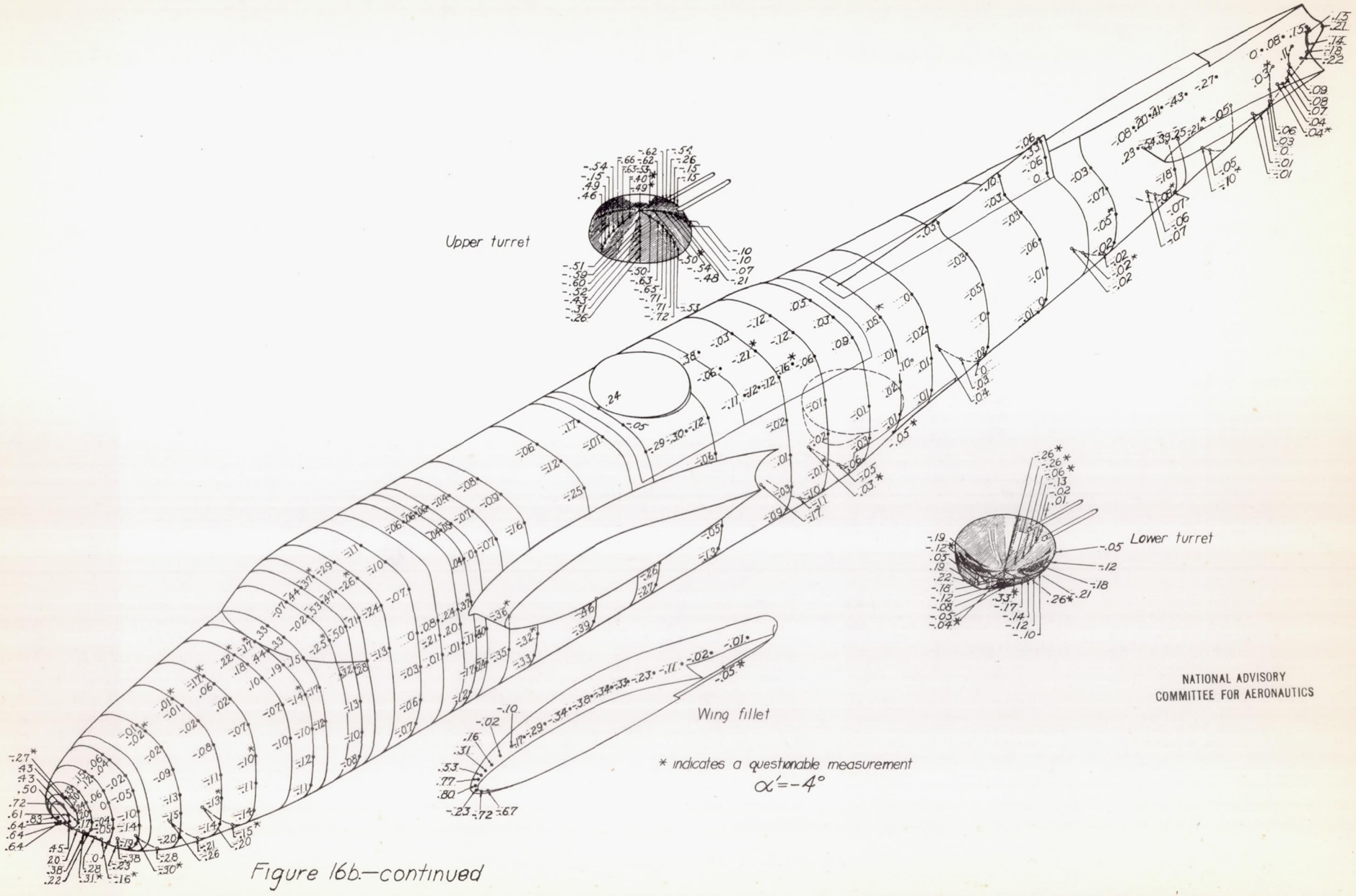

Figure 16b.—continued

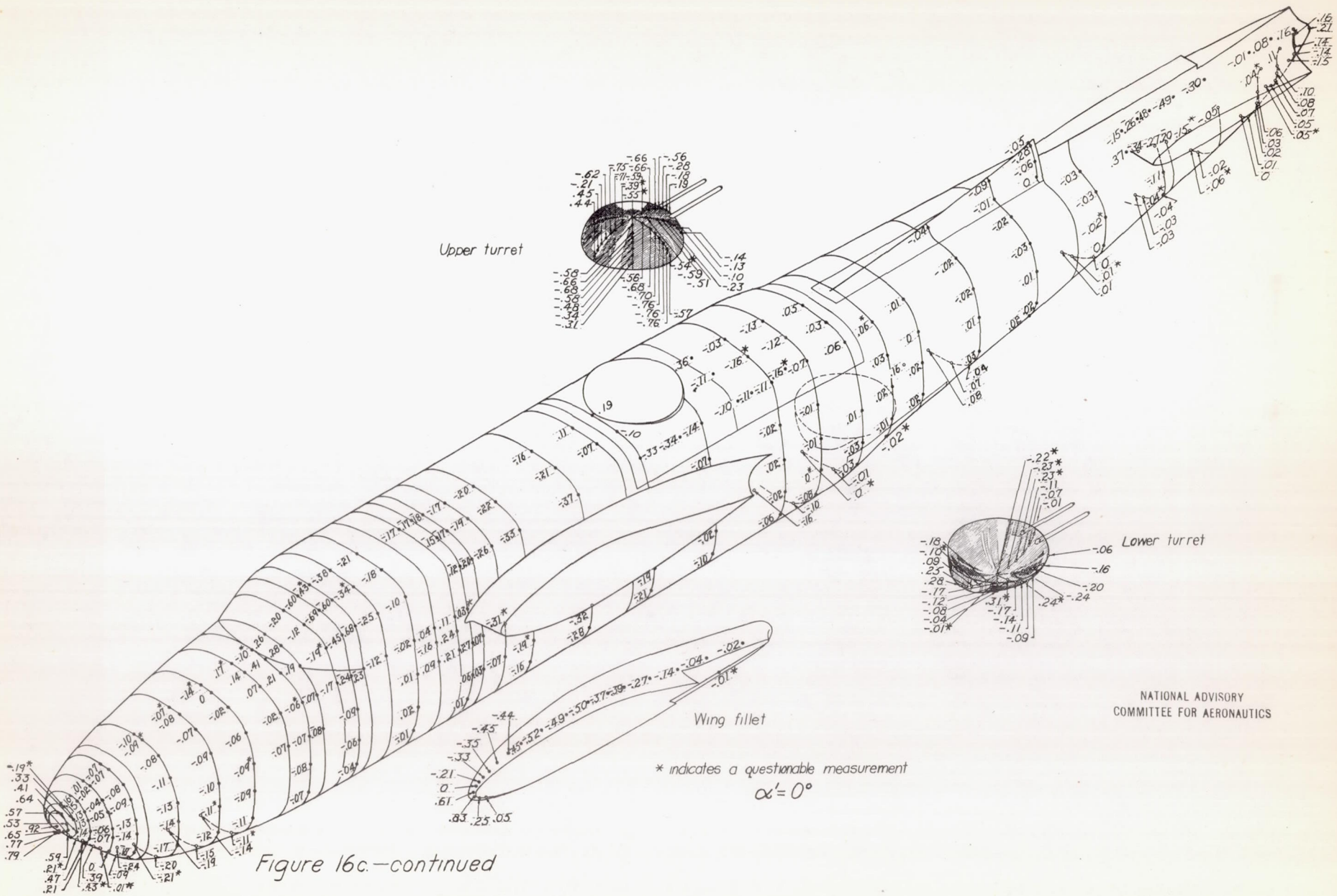

Figure 16c.—continued

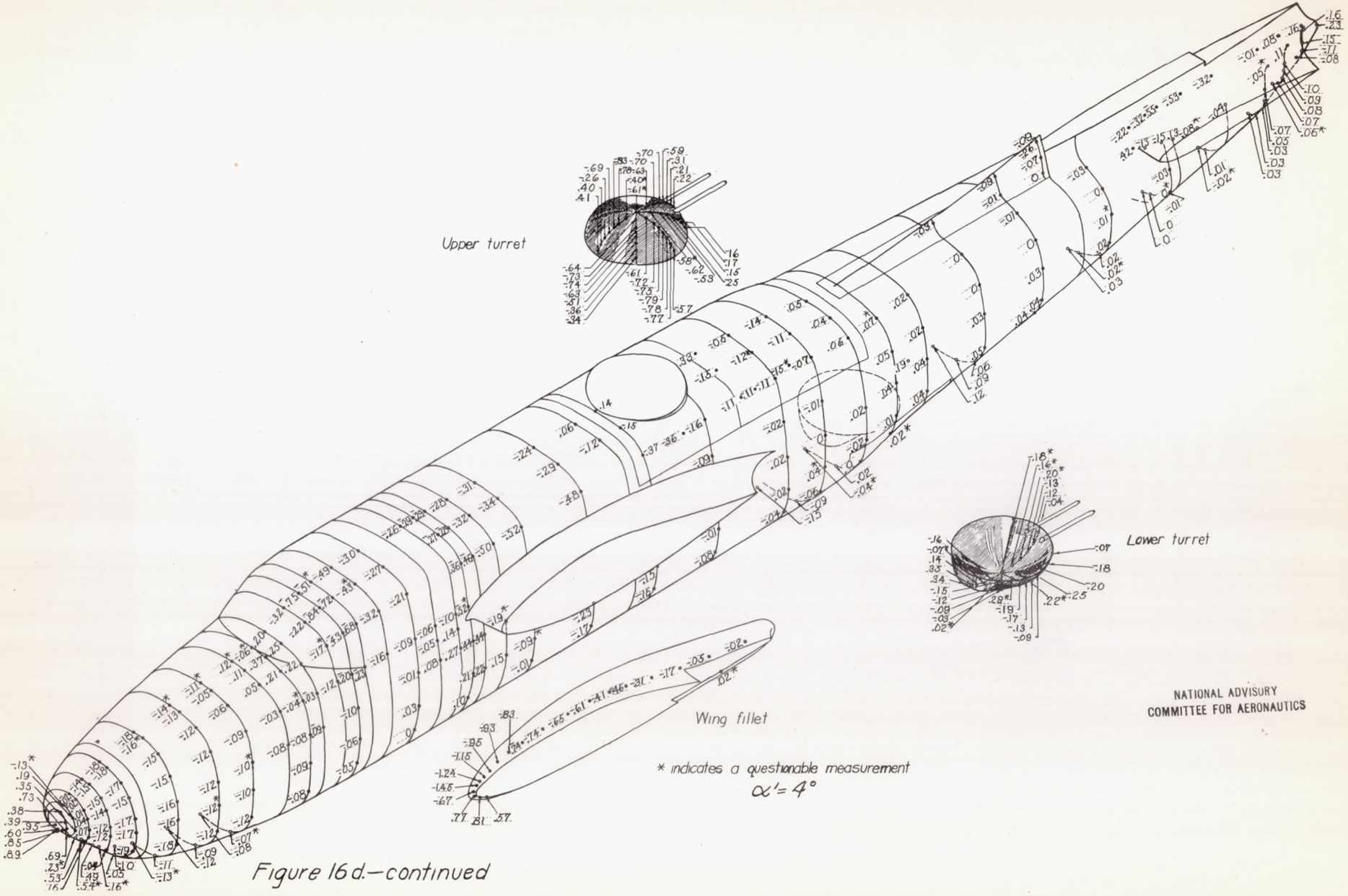

Figure 16 d.—continued

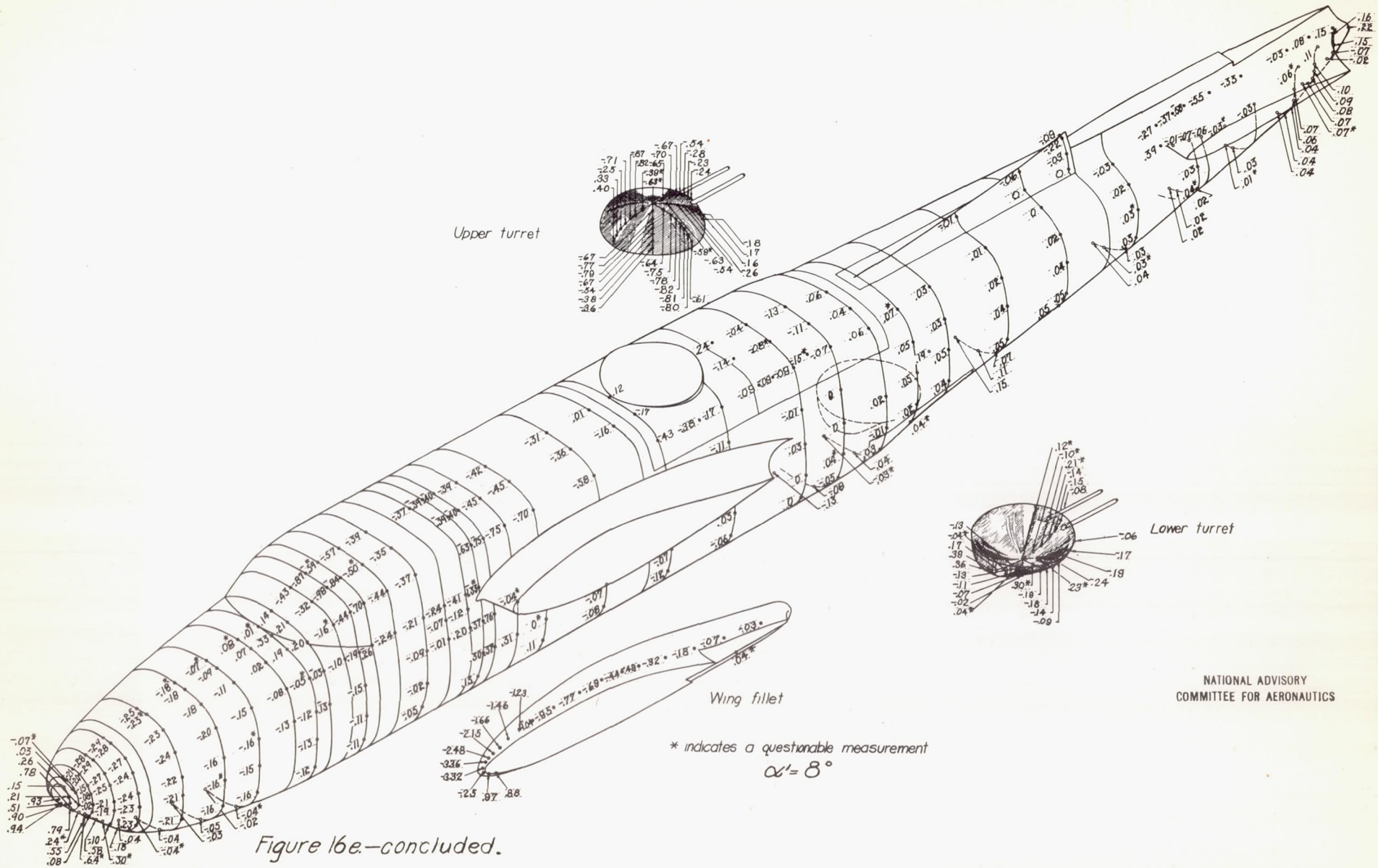

Figure 16e.—concluded.

NATIONAL ADVISORY
COMMITTEE FOR AERONAUTICS

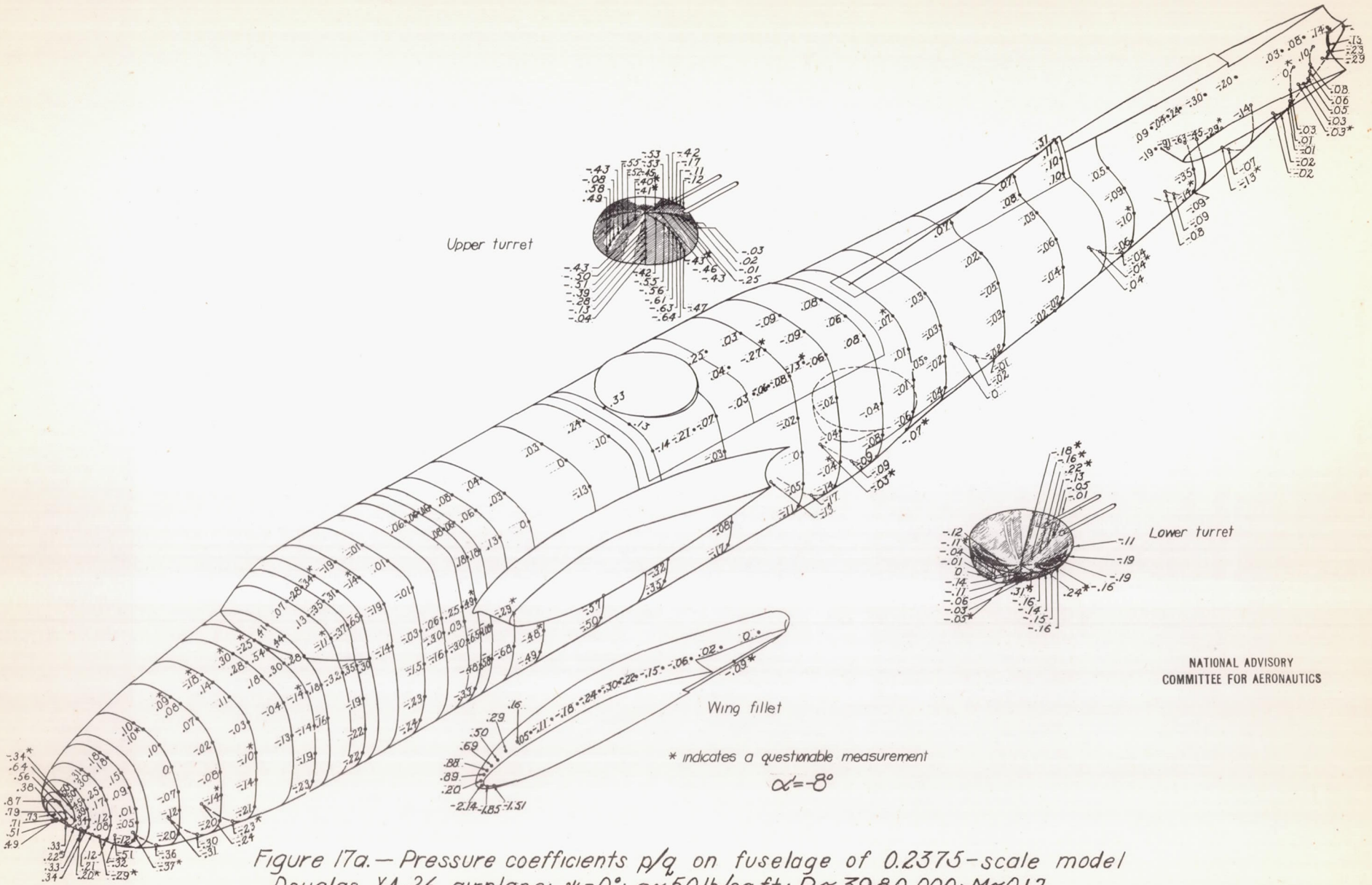

Figure 17a.—Pressure coefficients p/q on fuselage of 0.2375-scale model Douglas XA-26 airplane; ψ=0°; q≈50 lb/sq ft; R≈3,980,000; M≈0.12.

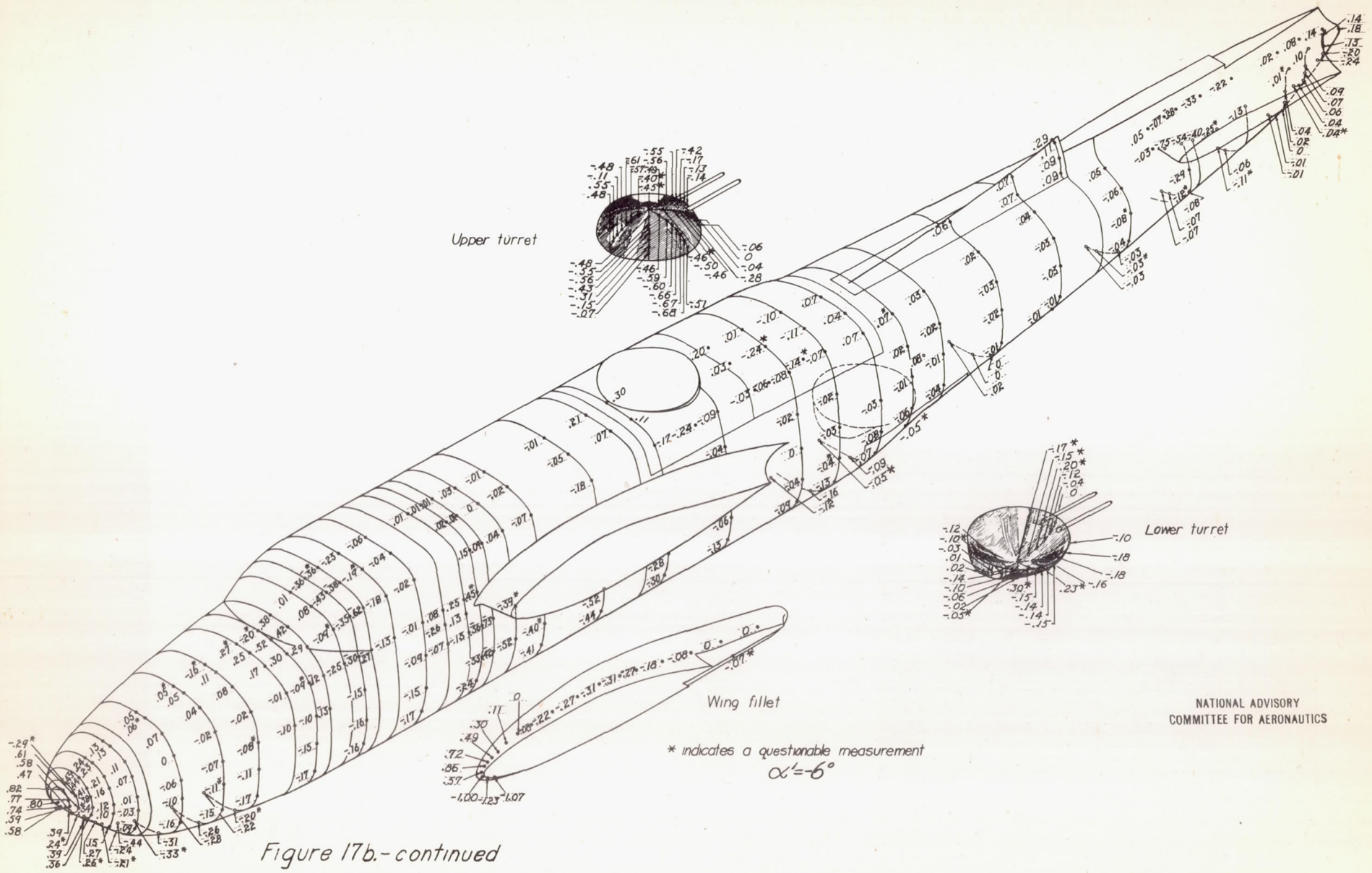

Figure 17b.- continued

NATIONAL ADVISORY
COMMITTEE FOR AERONAUTICS

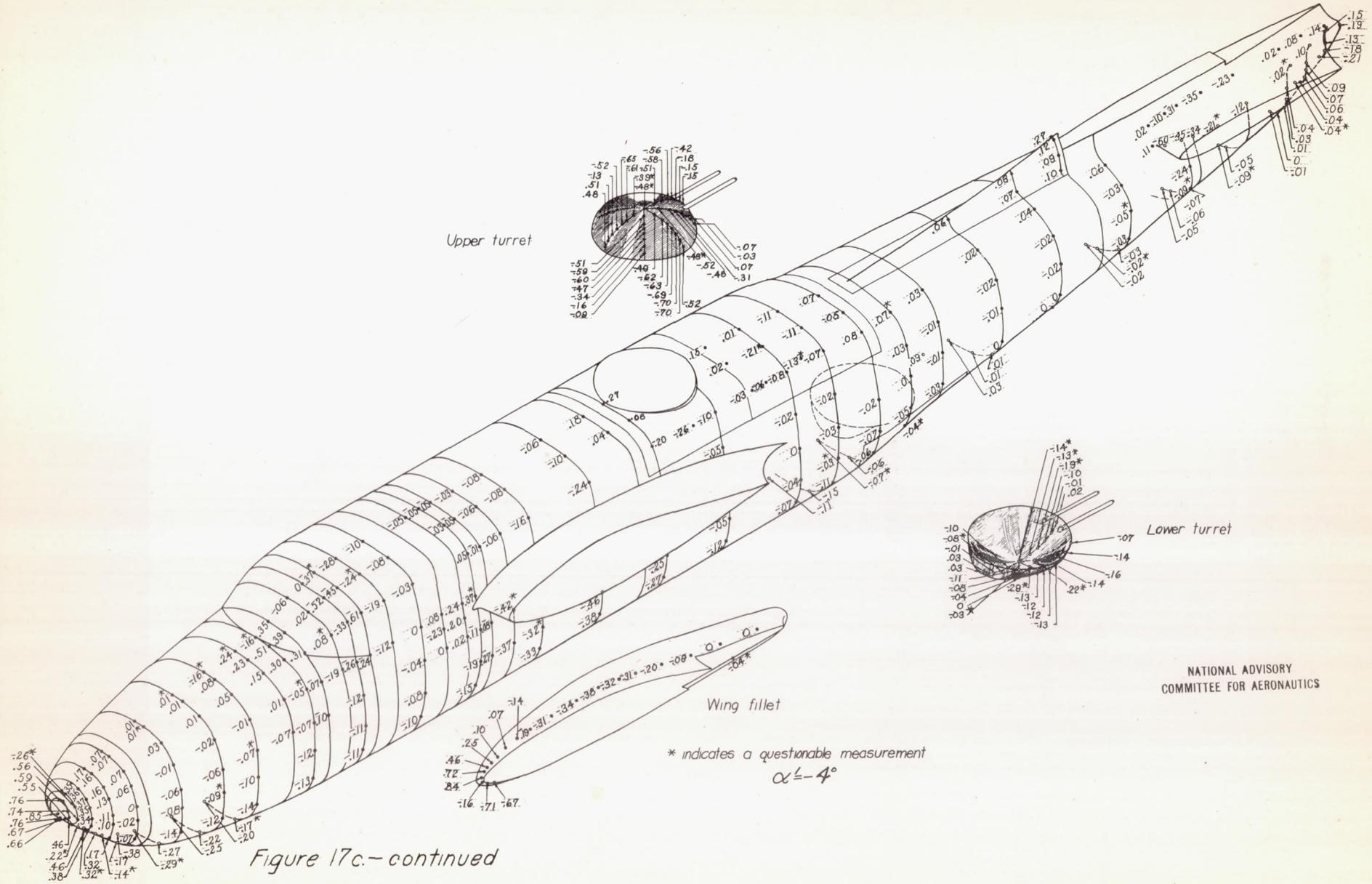

Figure 17c.- continued

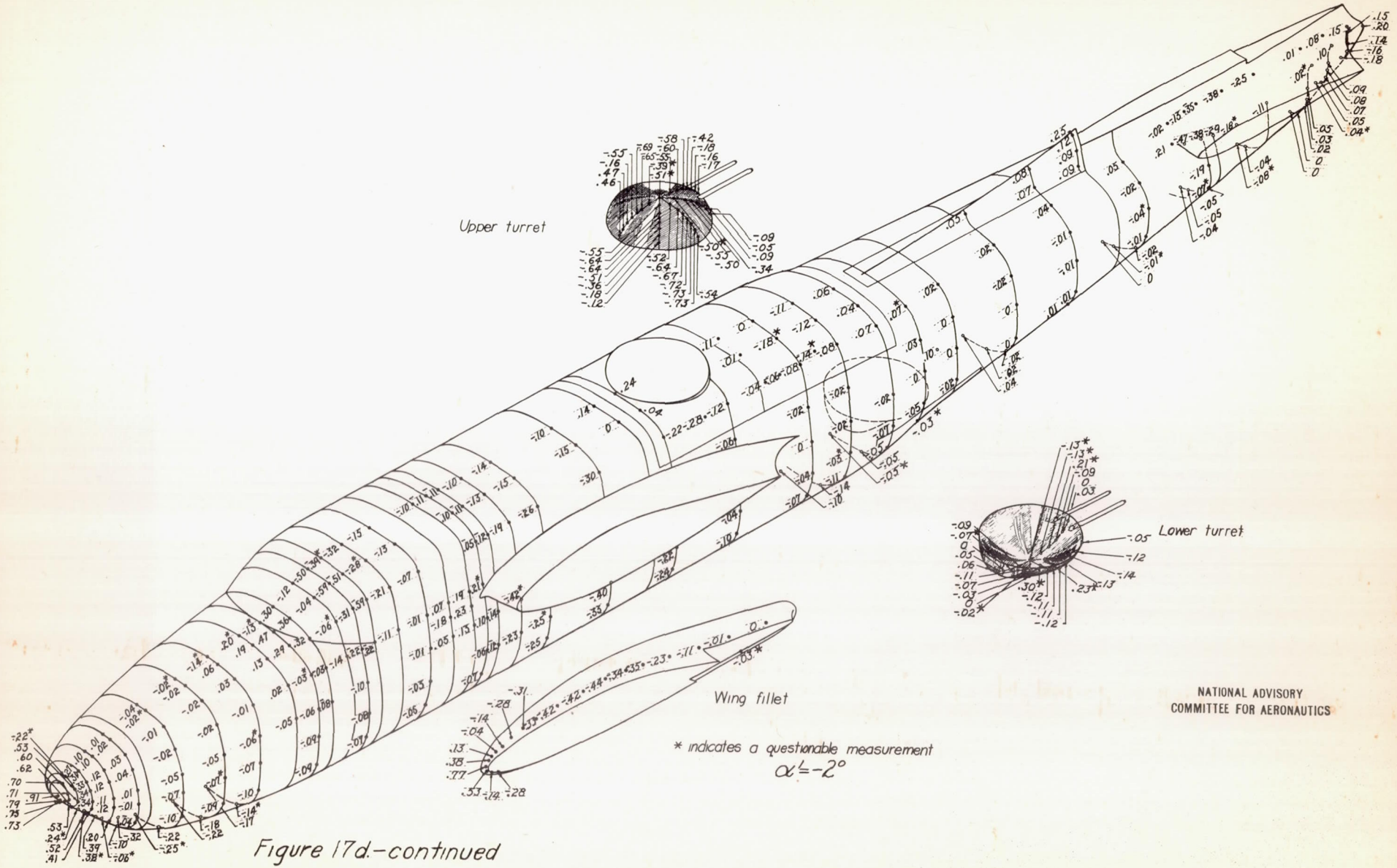

Figure 17d.-continued

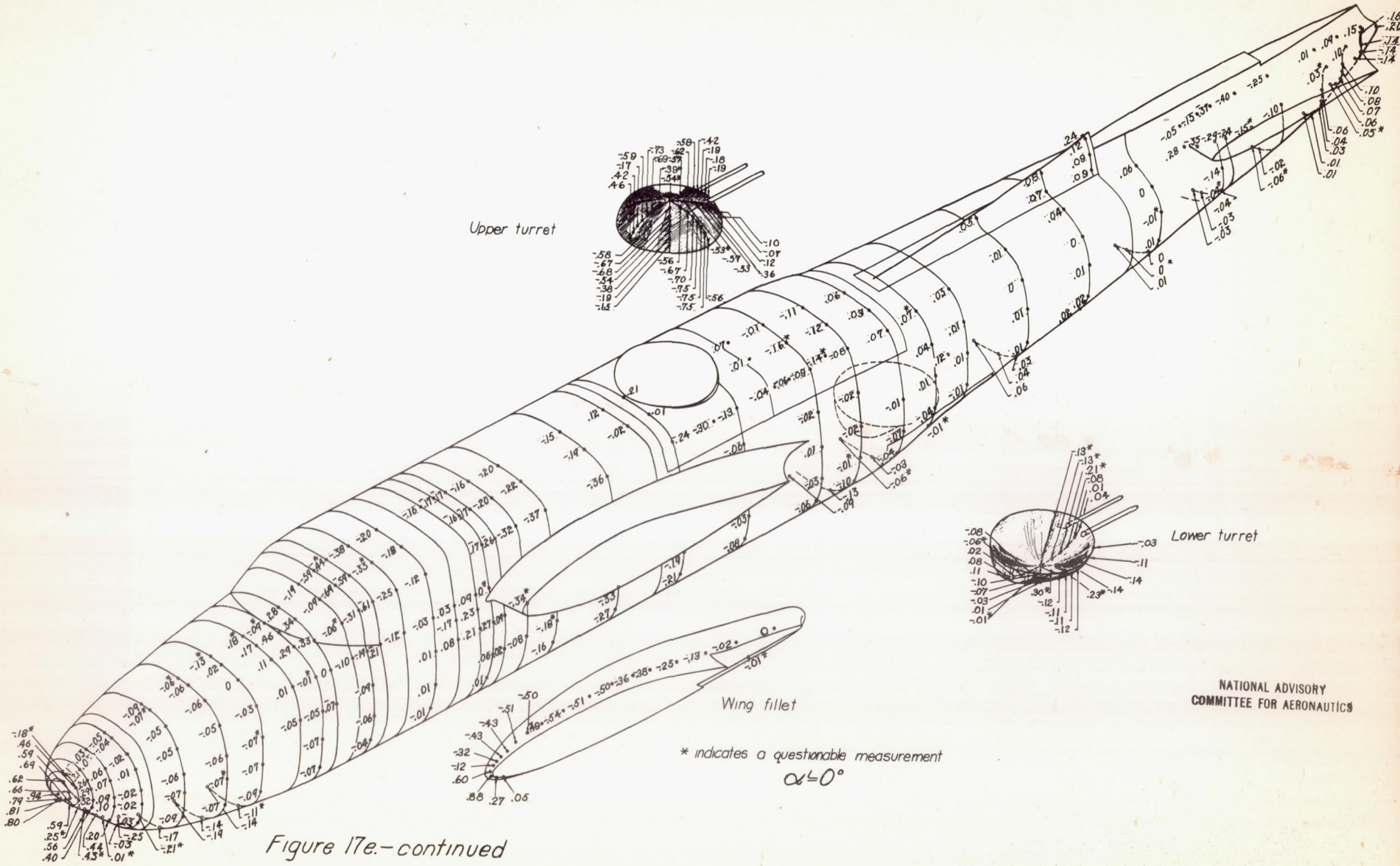

Figure 17e.- continued

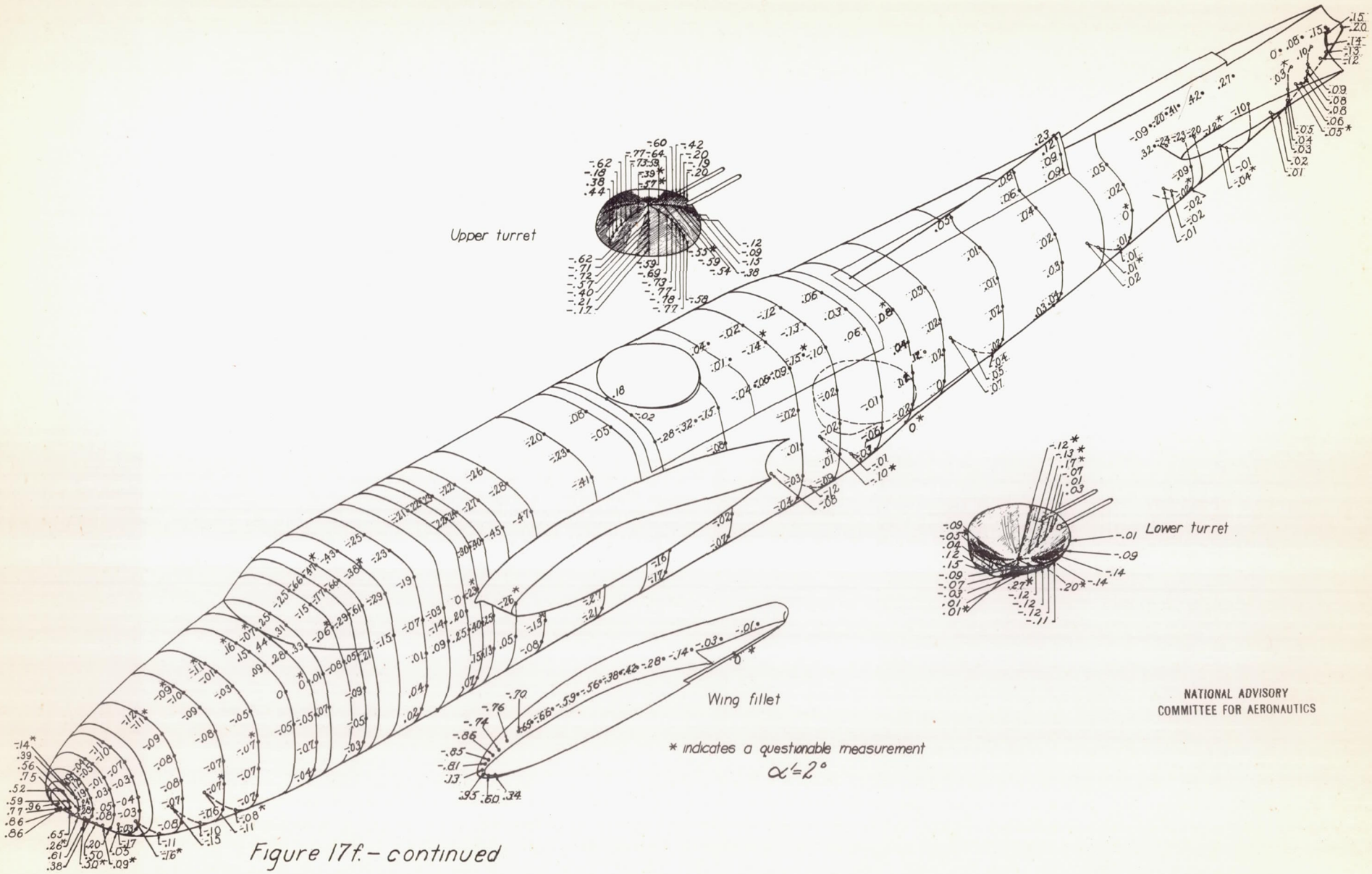

Figure 17f.- continued

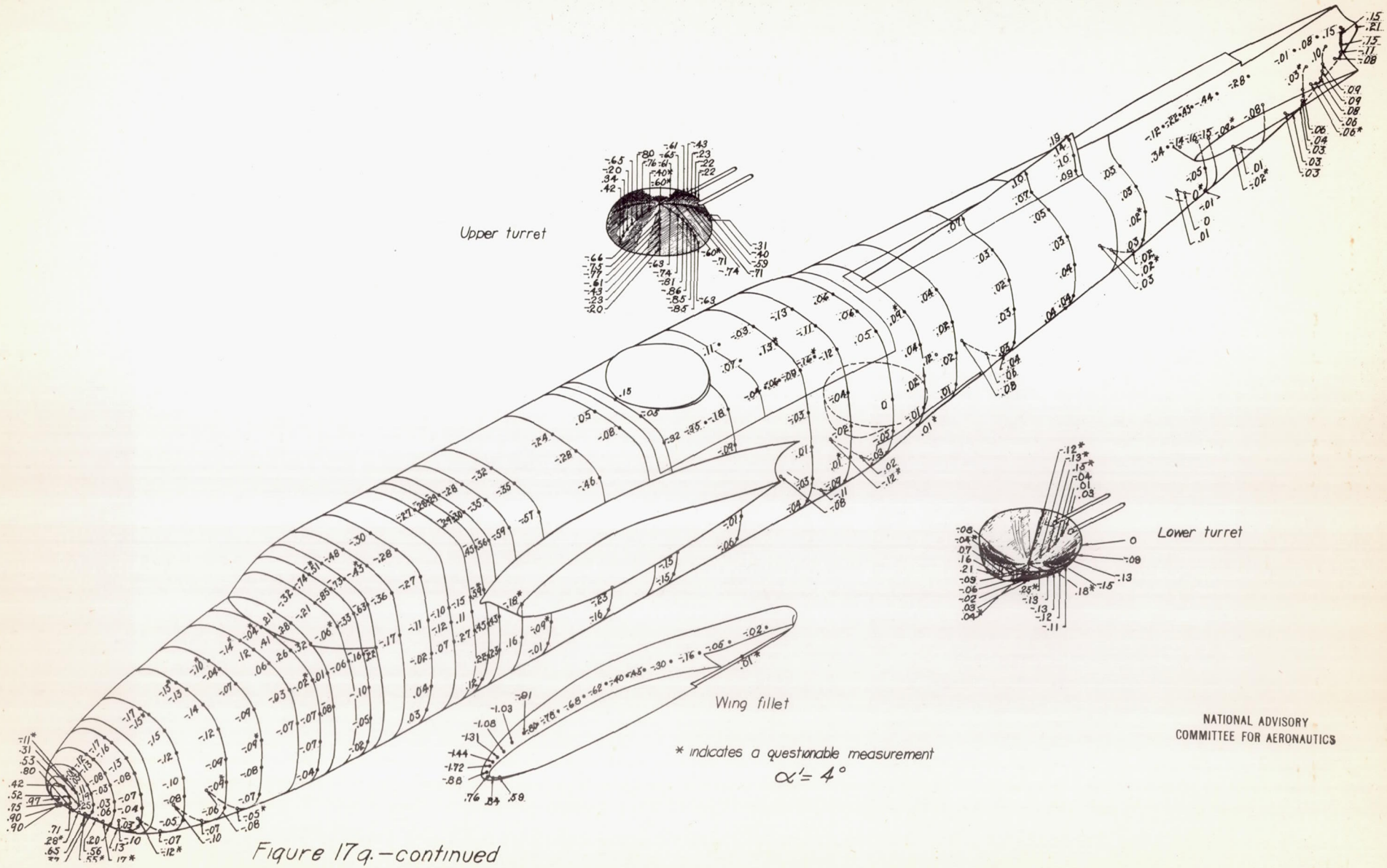

Figure 17q.—continued

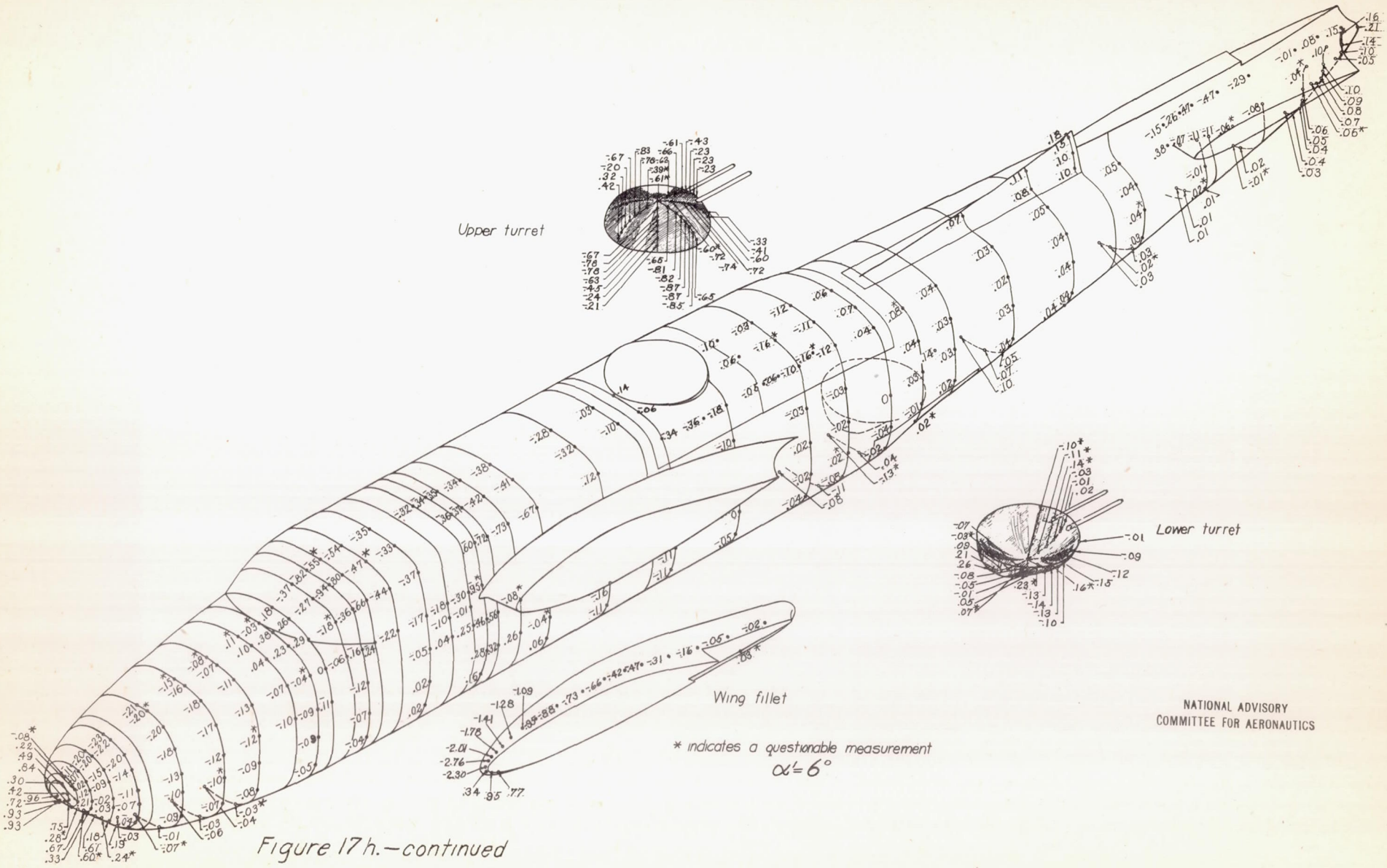

Figure 17h.—continued

NATIONAL ADVISORY
COMMITTEE FOR AERONAUTICS

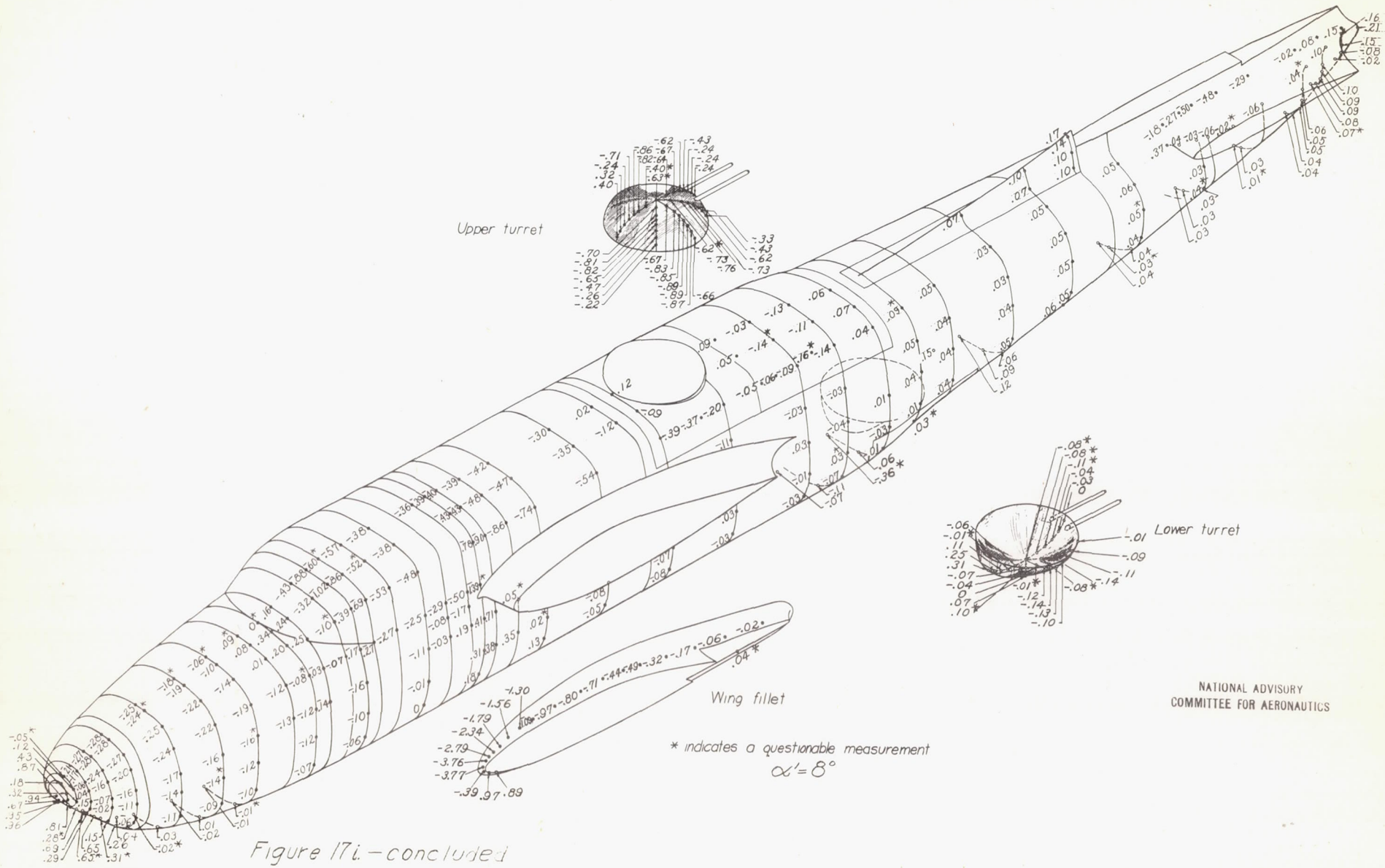

Figure 17i.—concluded

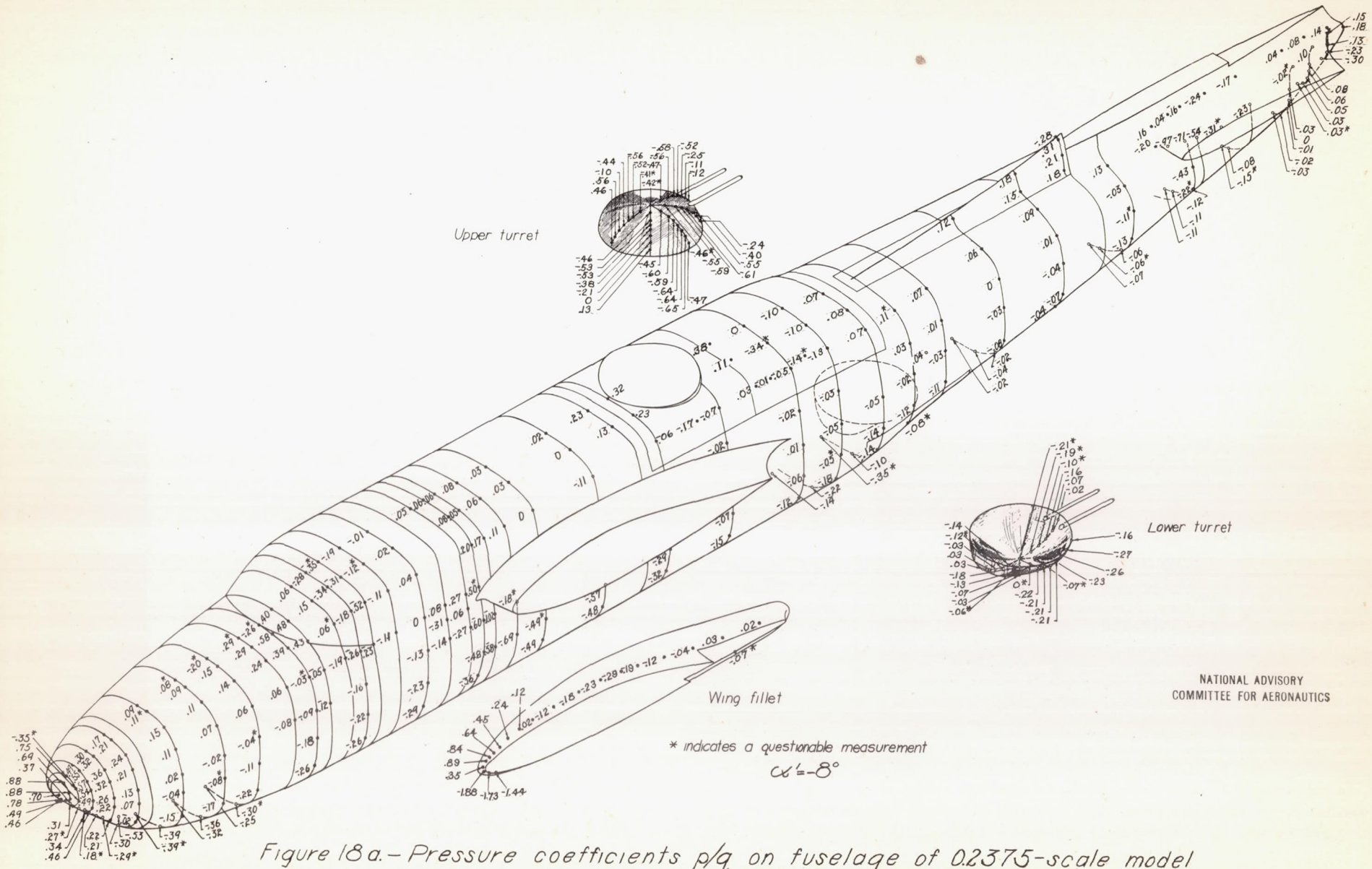

Figure 18a.– Pressure coefficients p/q on fuselage of 0.2375-scale model Douglas XA-26 airplane; $\psi=5°$; $q\approx 50 lb/sq ft$; $R\approx 3{,}970{,}000$; $M\approx 0.12$.

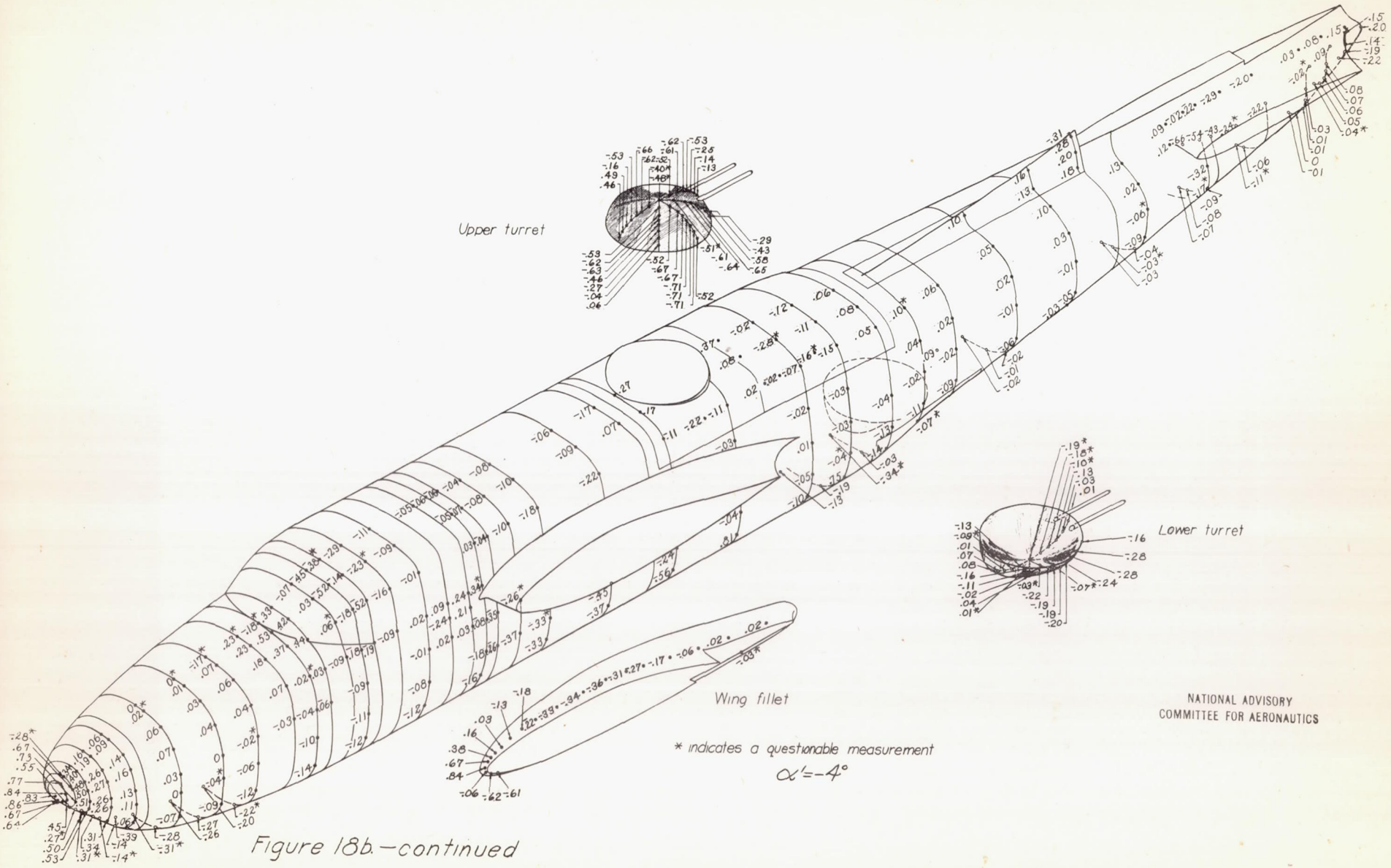

Figure 18b.—continued

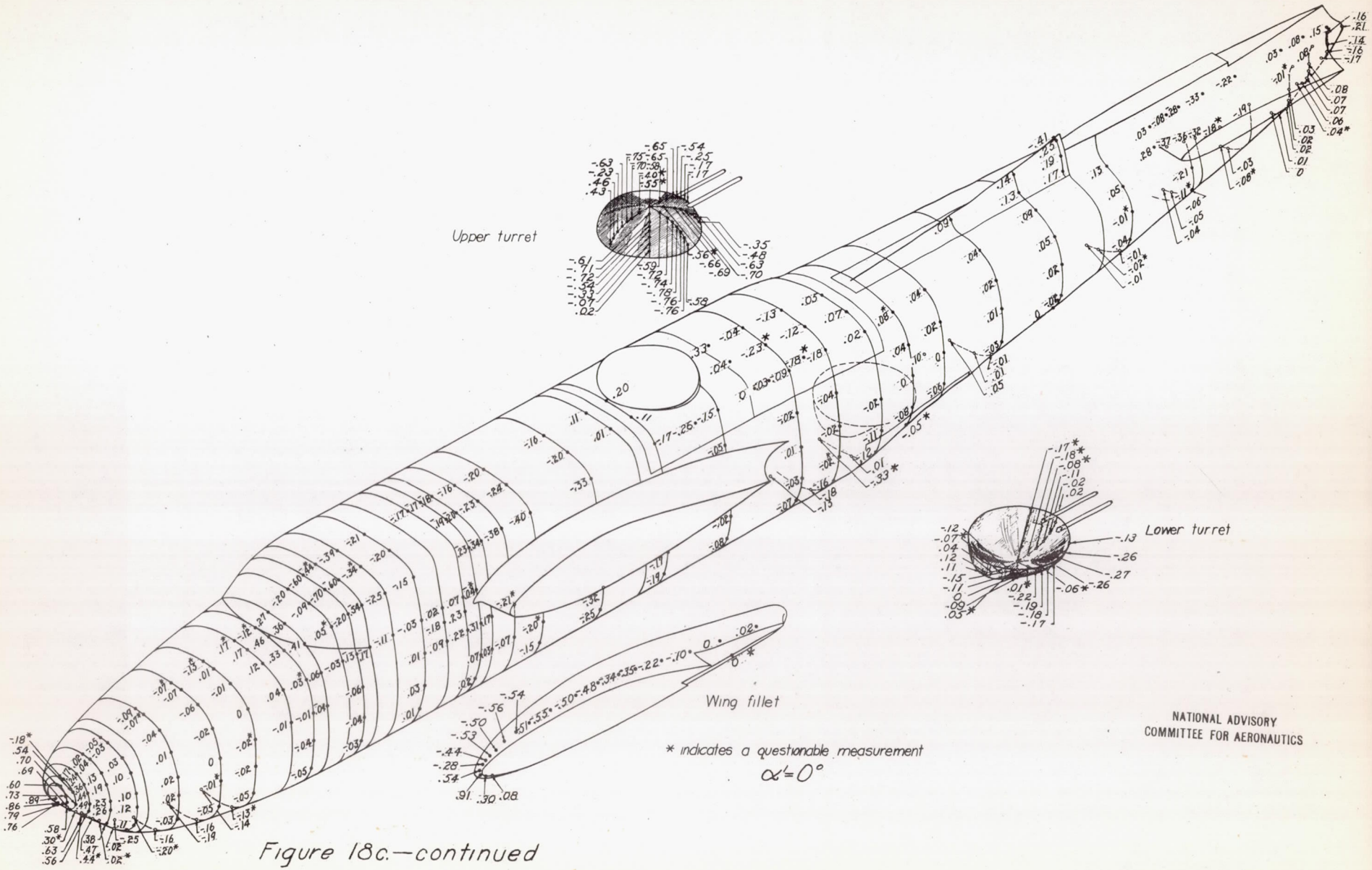

Figure 18c.—continued

NATIONAL ADVISORY
COMMITTEE FOR AERONAUTICS

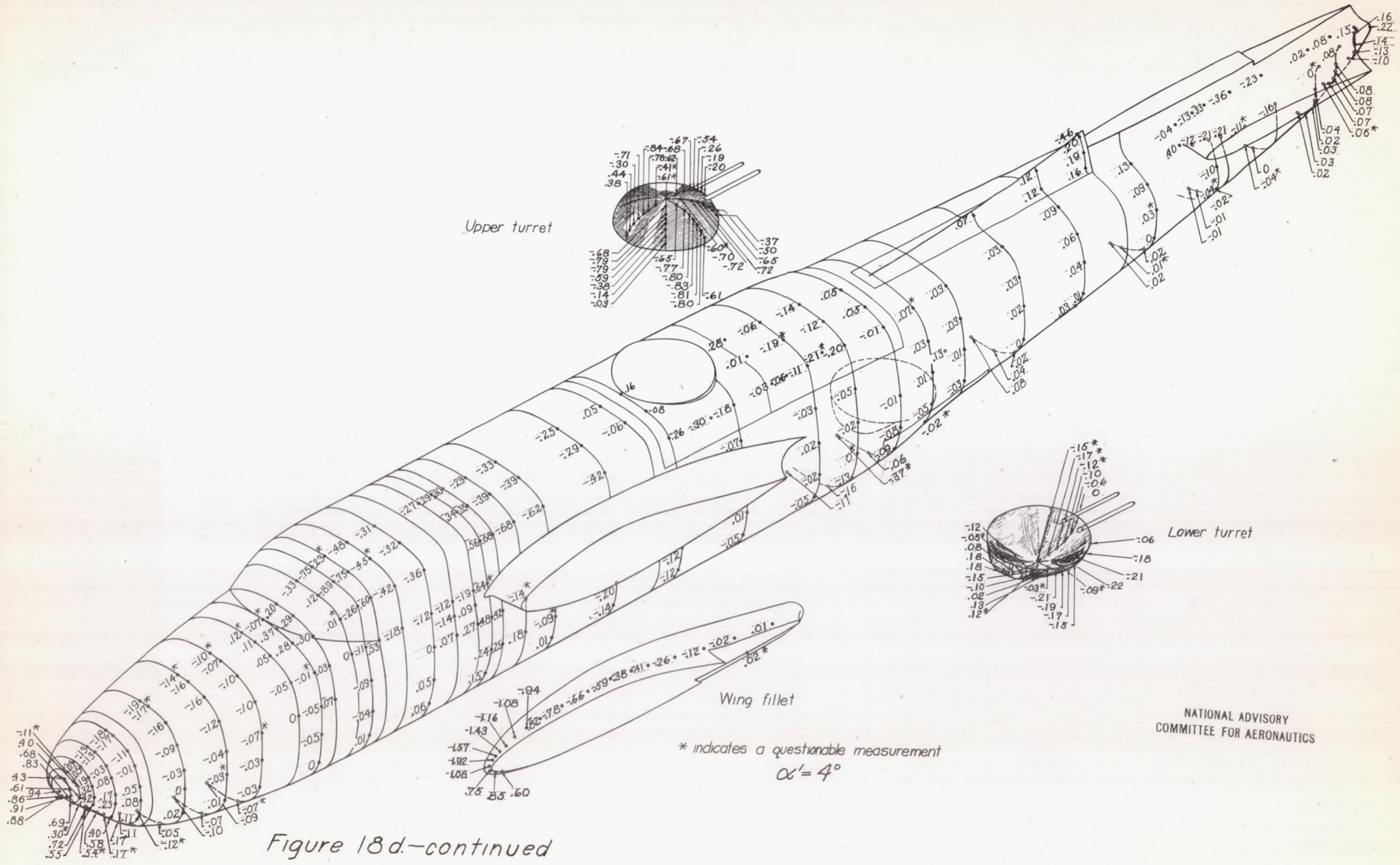

Figure 18d.—continued

L-553

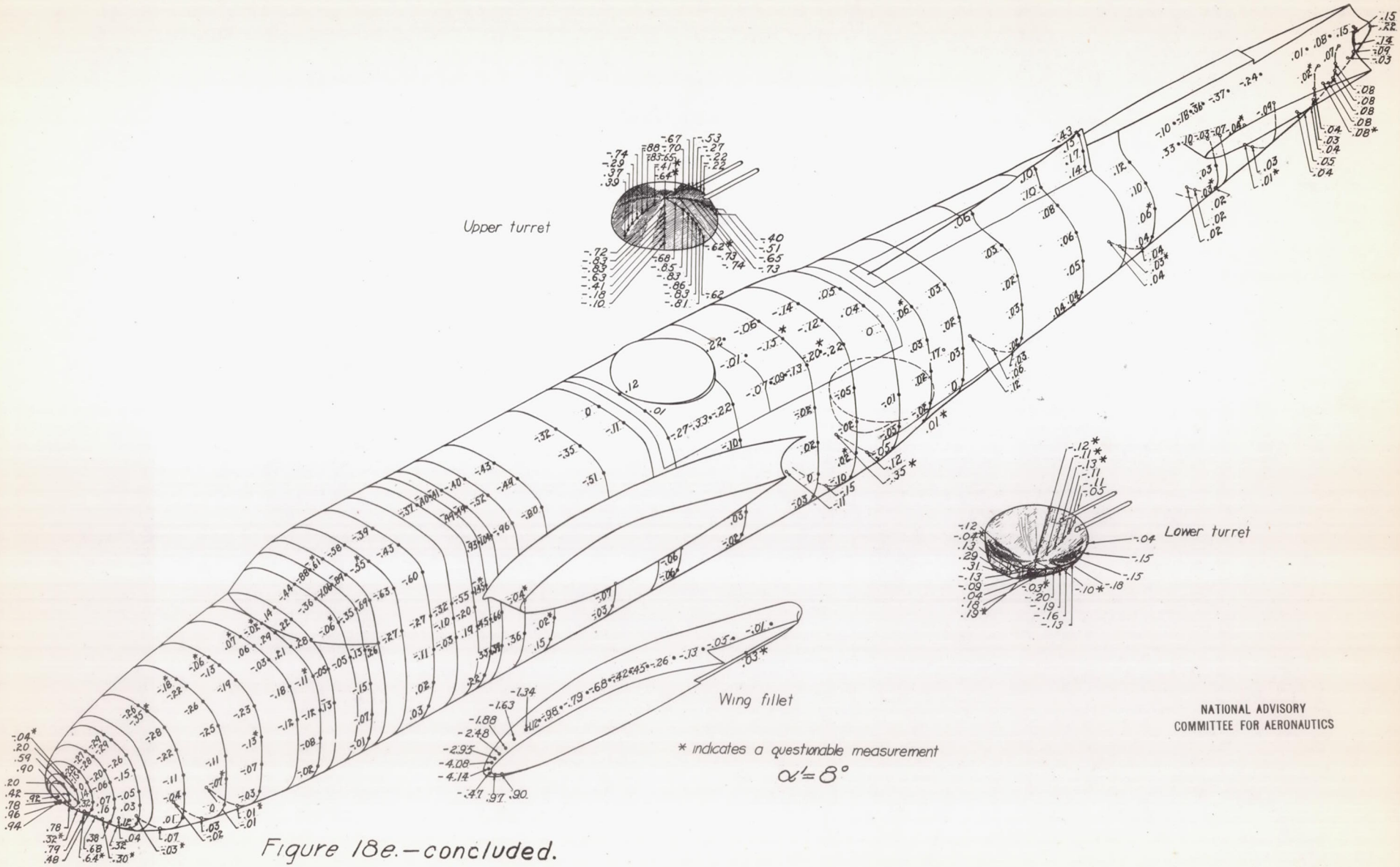

* indicates a questionable measurement

$\alpha' = 8°$

Figure 18e.—concluded.

NATIONAL ADVISORY
COMMITTEE FOR AERONAUTICS

L-553

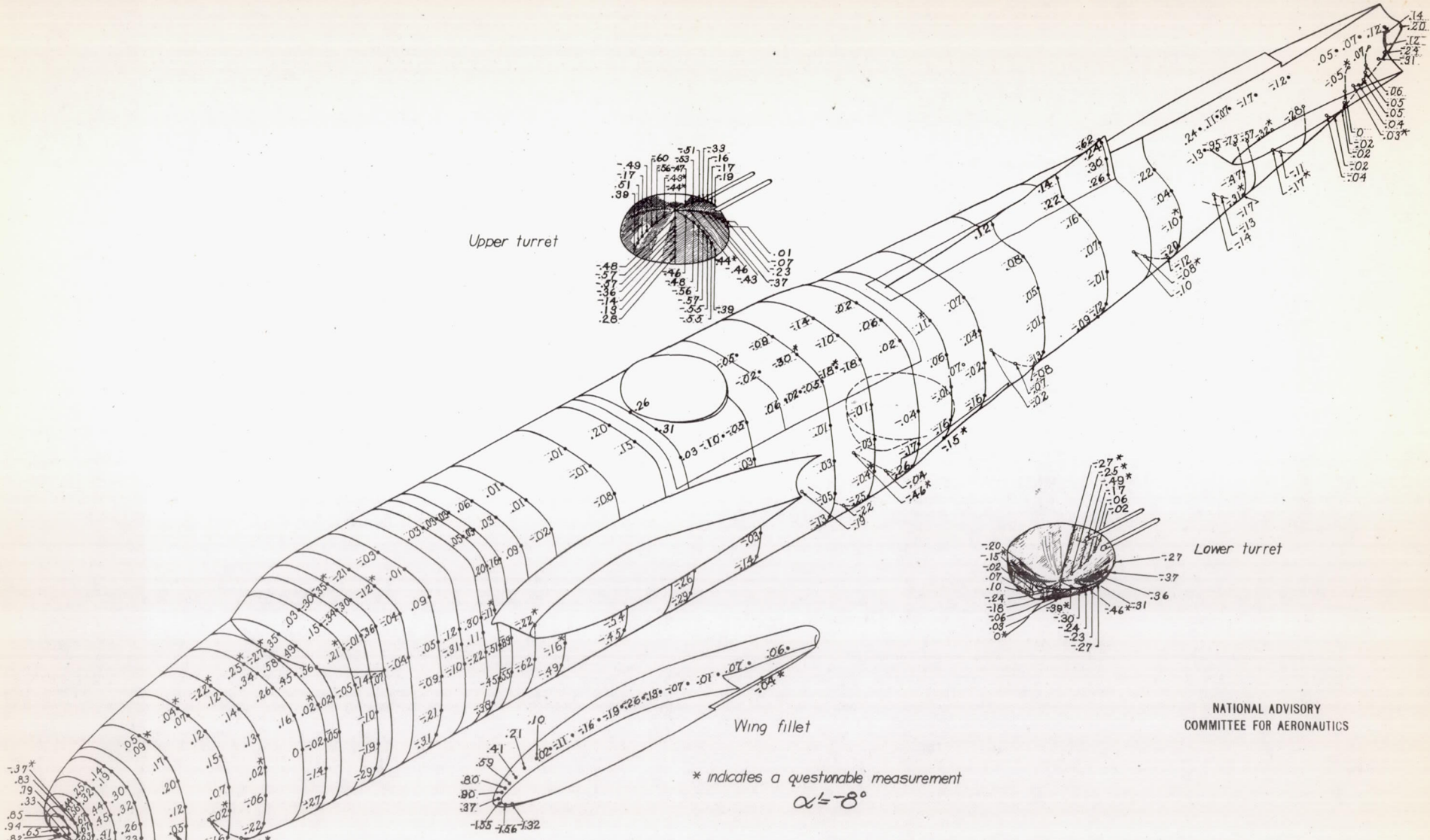

Figure 19a.—Pressure coefficients p/q on fuselage of 0.2375-scale model Douglas XA-26 airplane; $\psi = 10°$; $q \approx 50$ lb/sq ft; $R \approx 3{,}950{,}000$; $M \approx 0.12$.

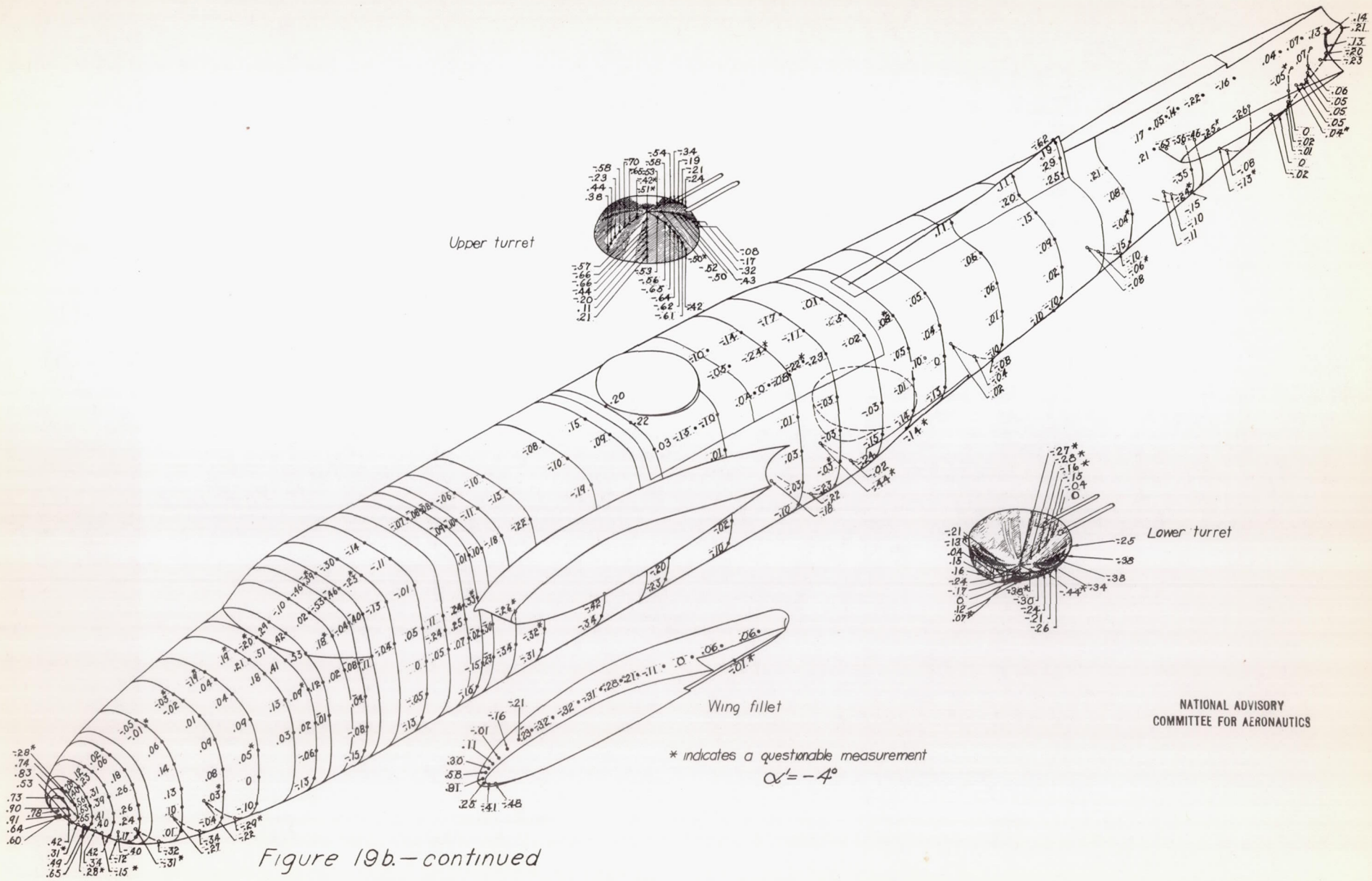

Figure 19b.—continued

NATIONAL ADVISORY
COMMITTEE FOR AERONAUTICS

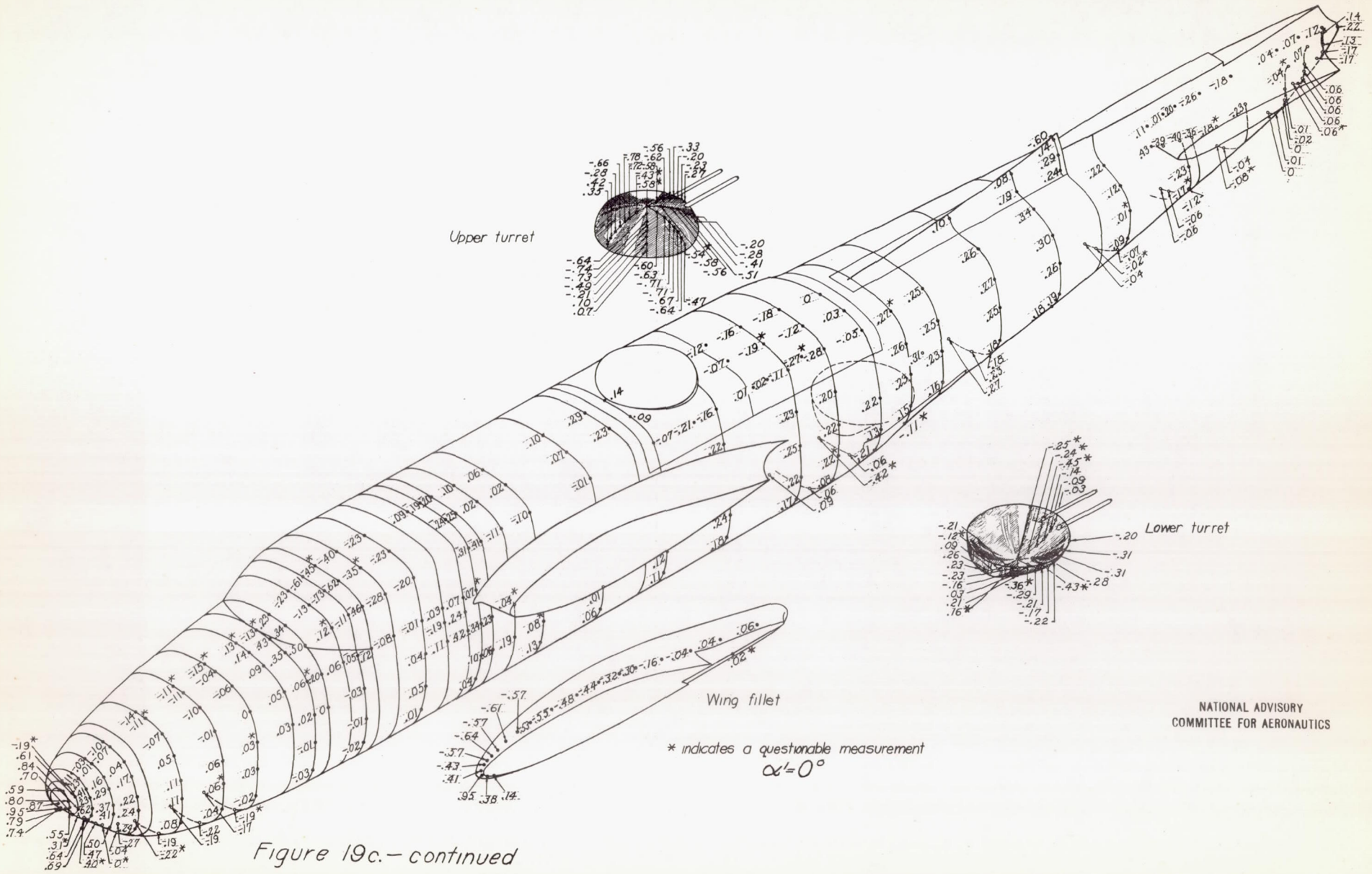

Figure 19c.— continued

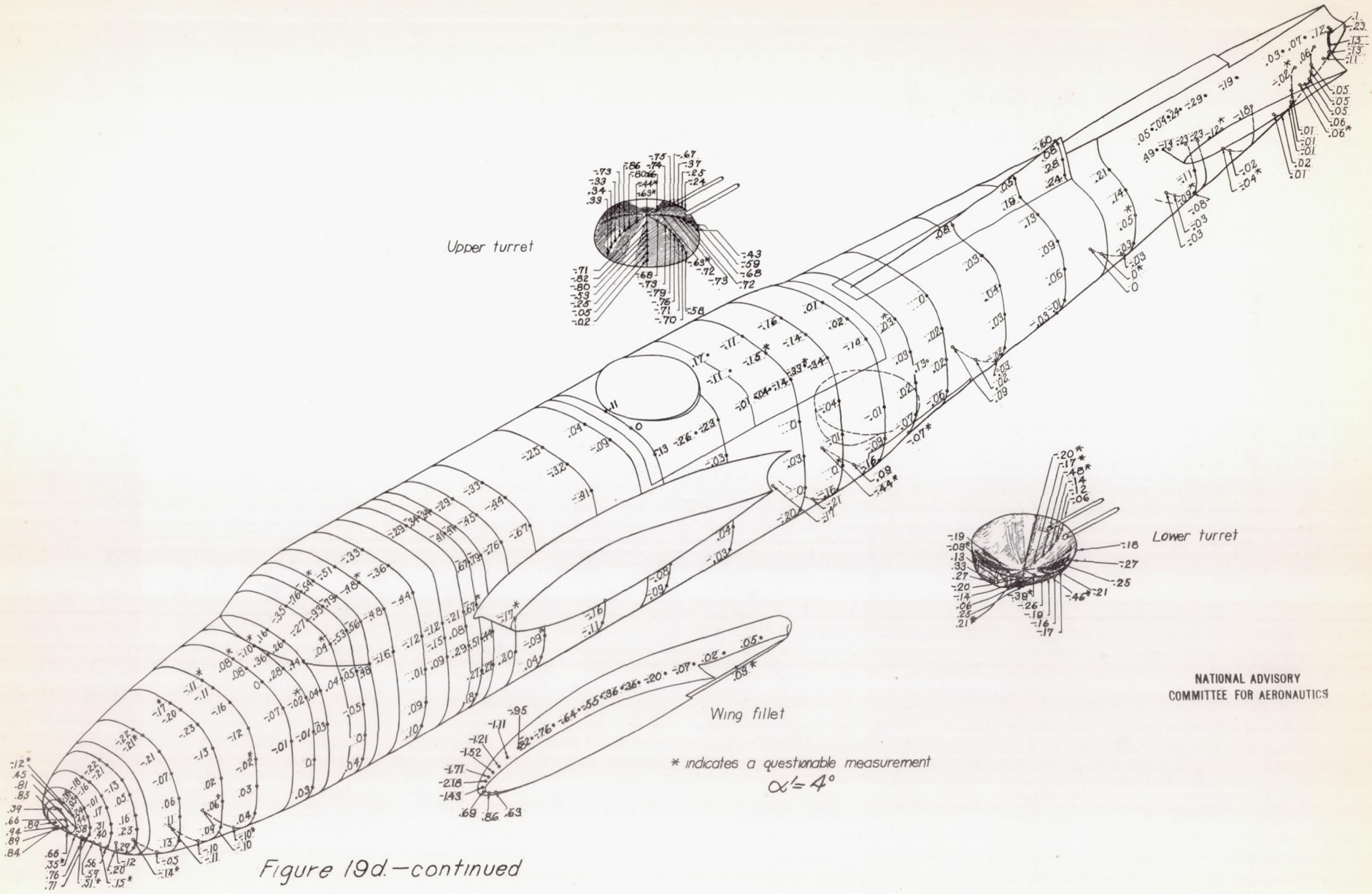

Figure 19d.—continued

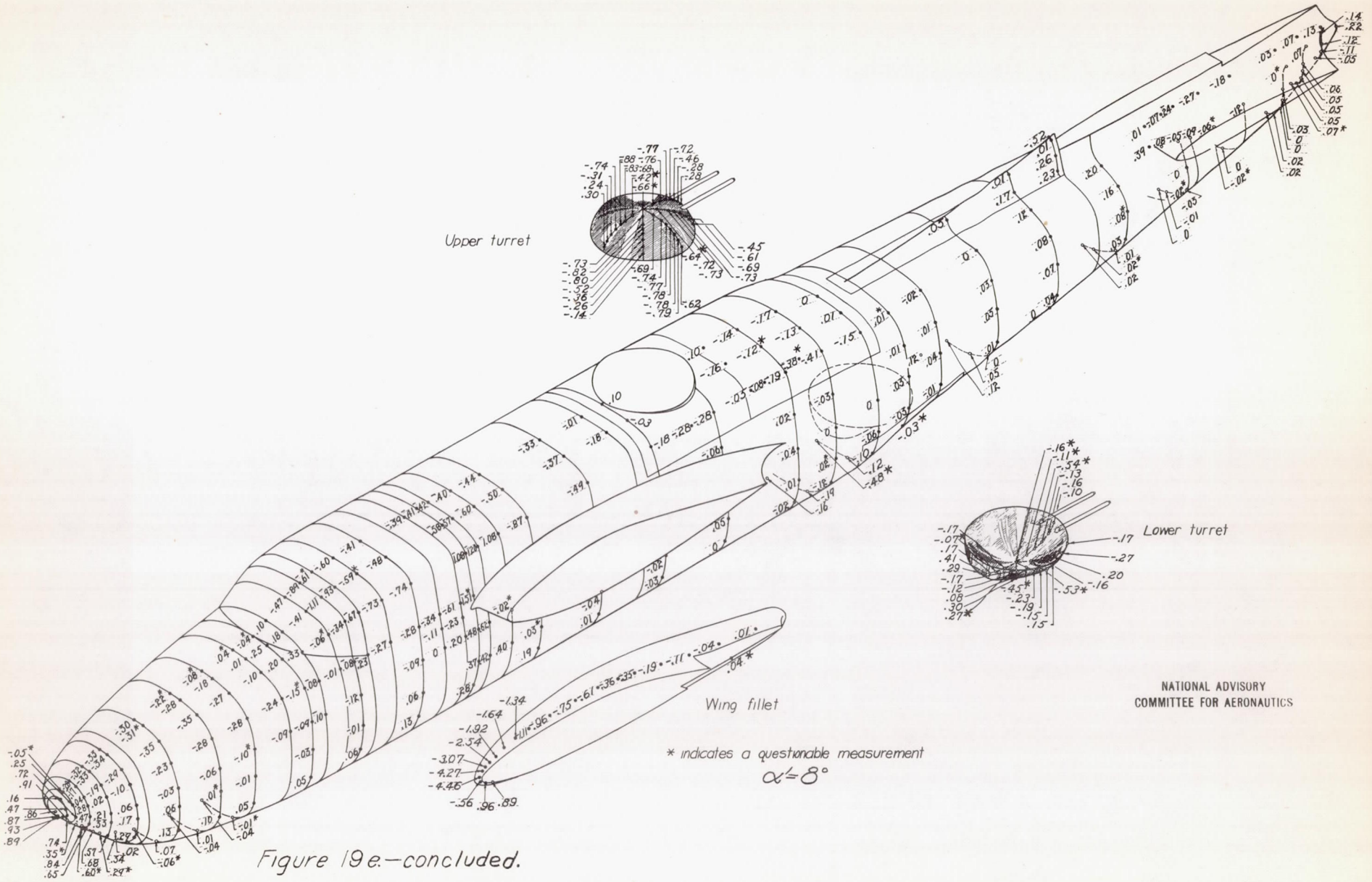

Figure 19e.—concluded.

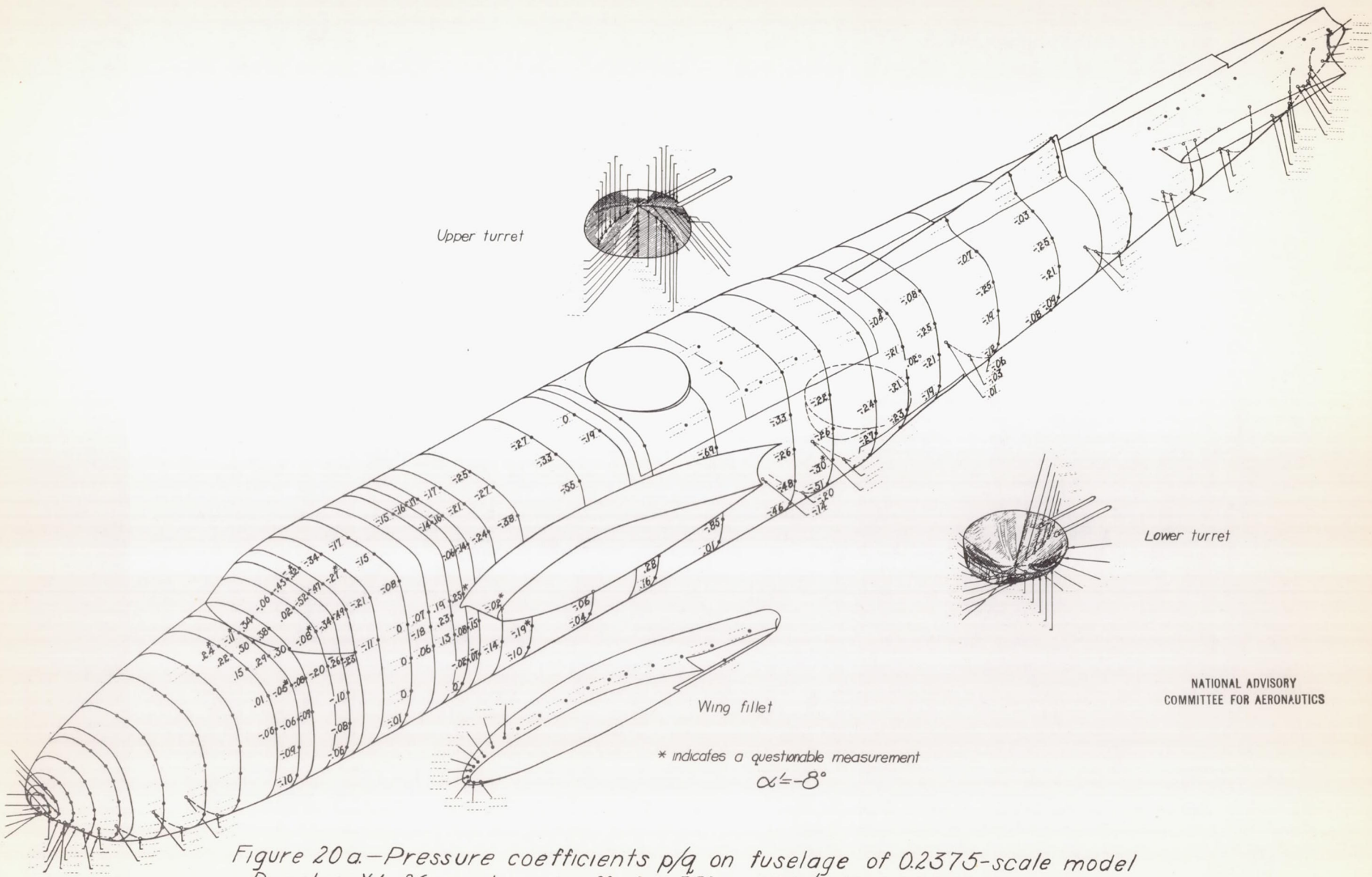

Figure 20a.—Pressure coefficients p/q on fuselage of 0.2375-scale model Douglas XA-26 airplane; $\psi = 0°$; $\delta_f = 55°$; $q \approx 50$ lb/sq ft; $R \approx 3{,}750{,}000$; $M \approx 0.12$.

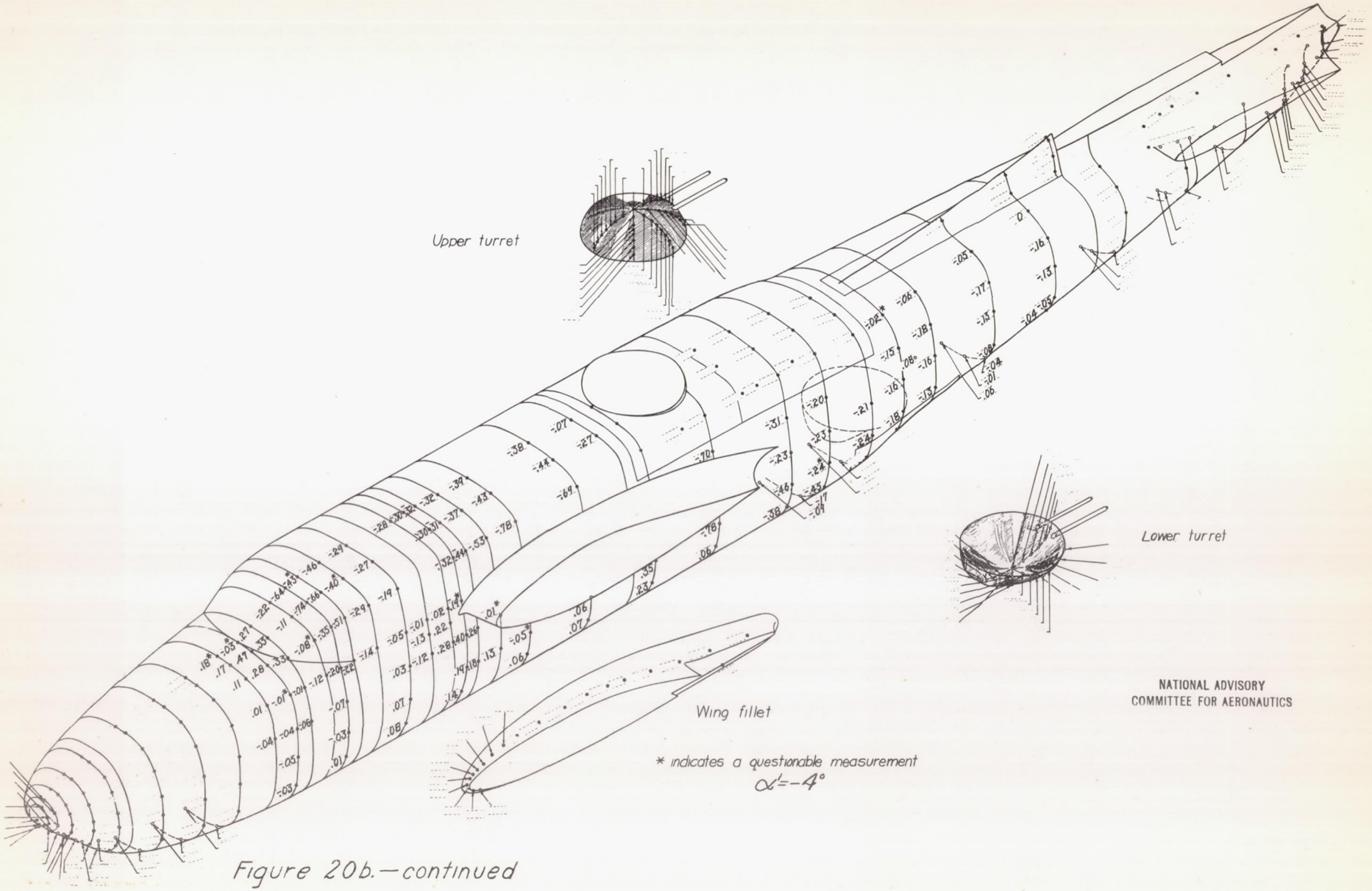

Figure 20b.—continued

L-553

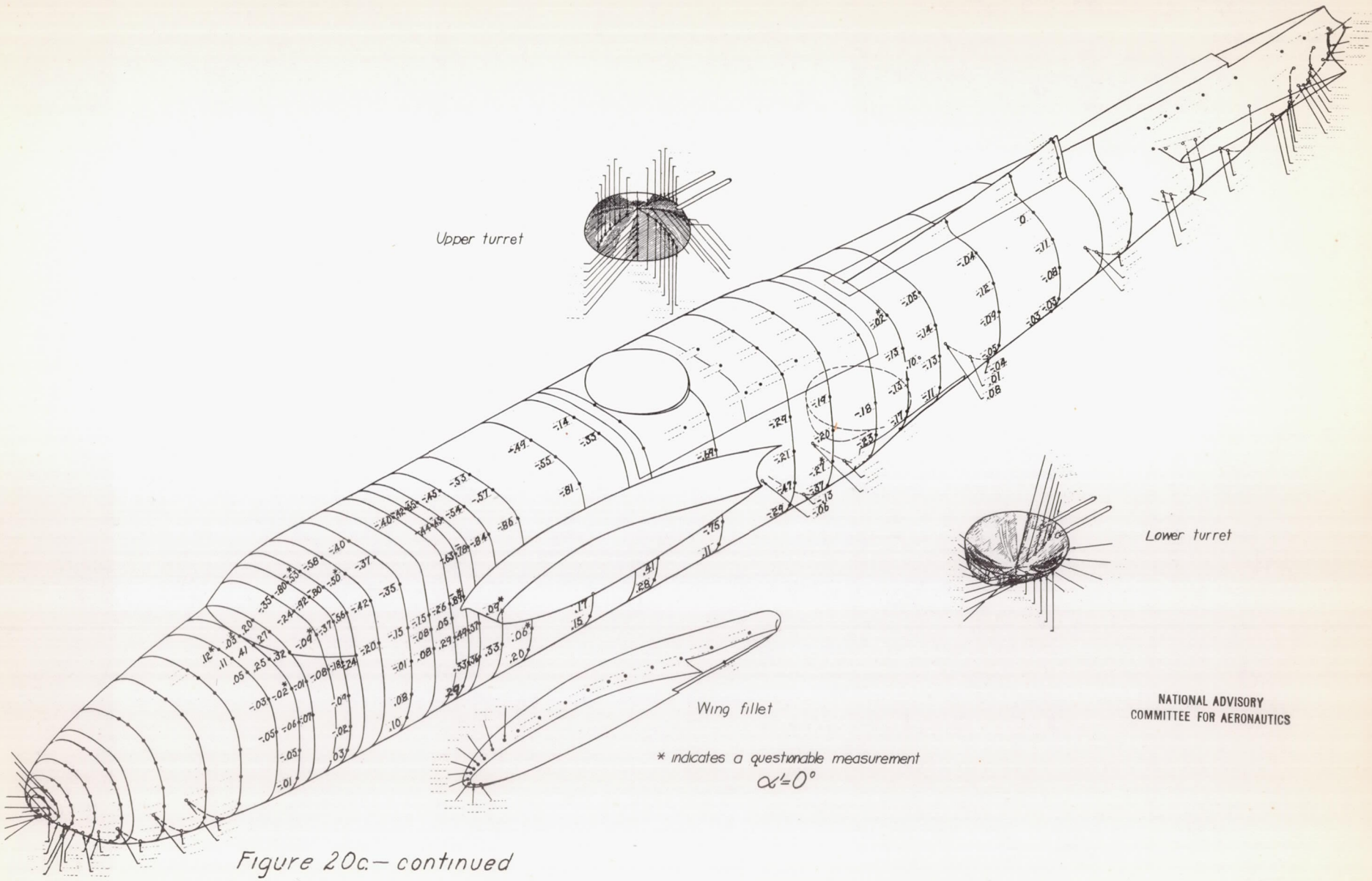

NATIONAL ADVISORY
COMMITTEE FOR AERONAUTICS

Figure 20c.— continued

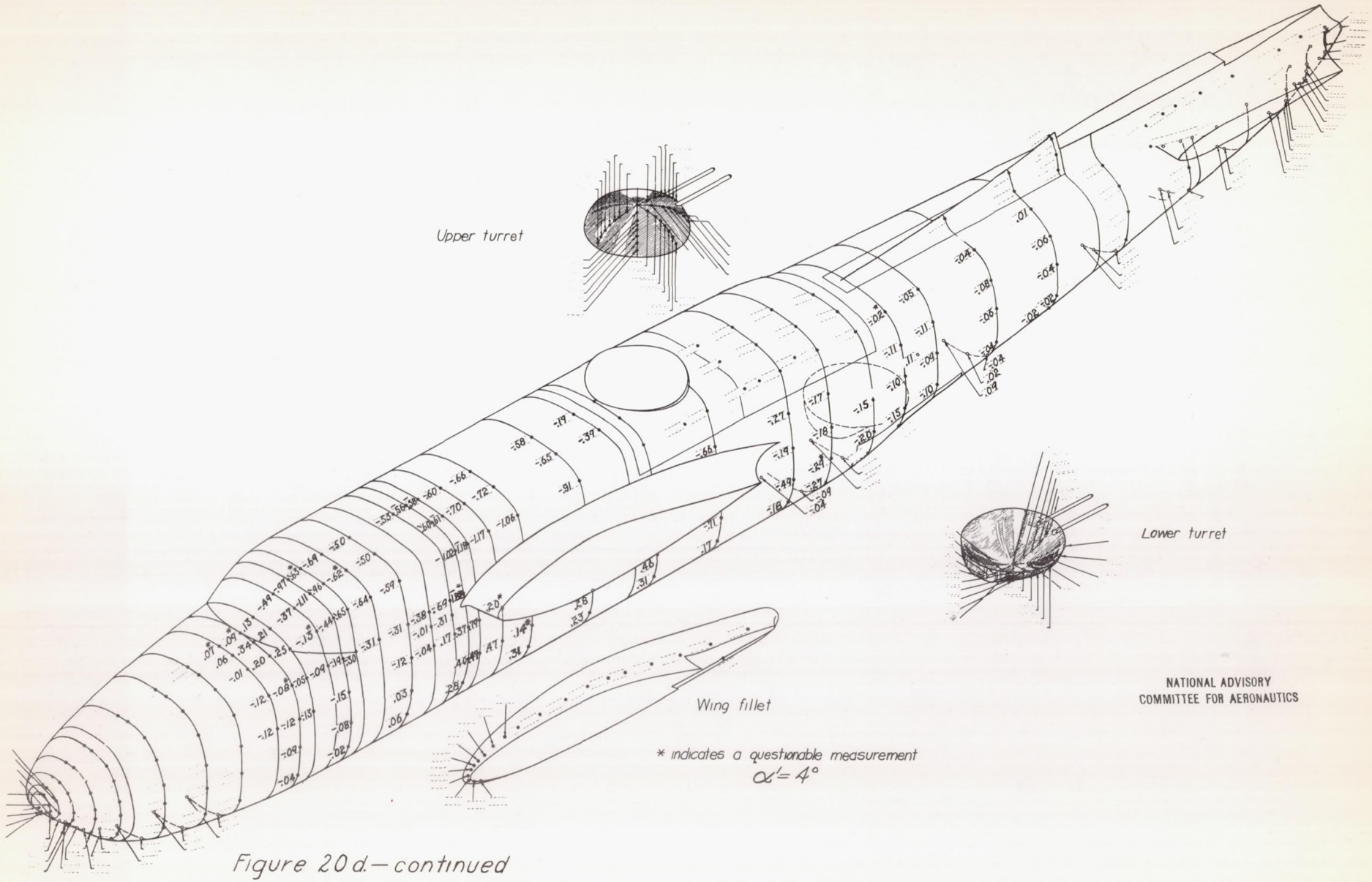

NATIONAL ADVISORY
COMMITTEE FOR AERONAUTICS

Figure 20 d.—continued

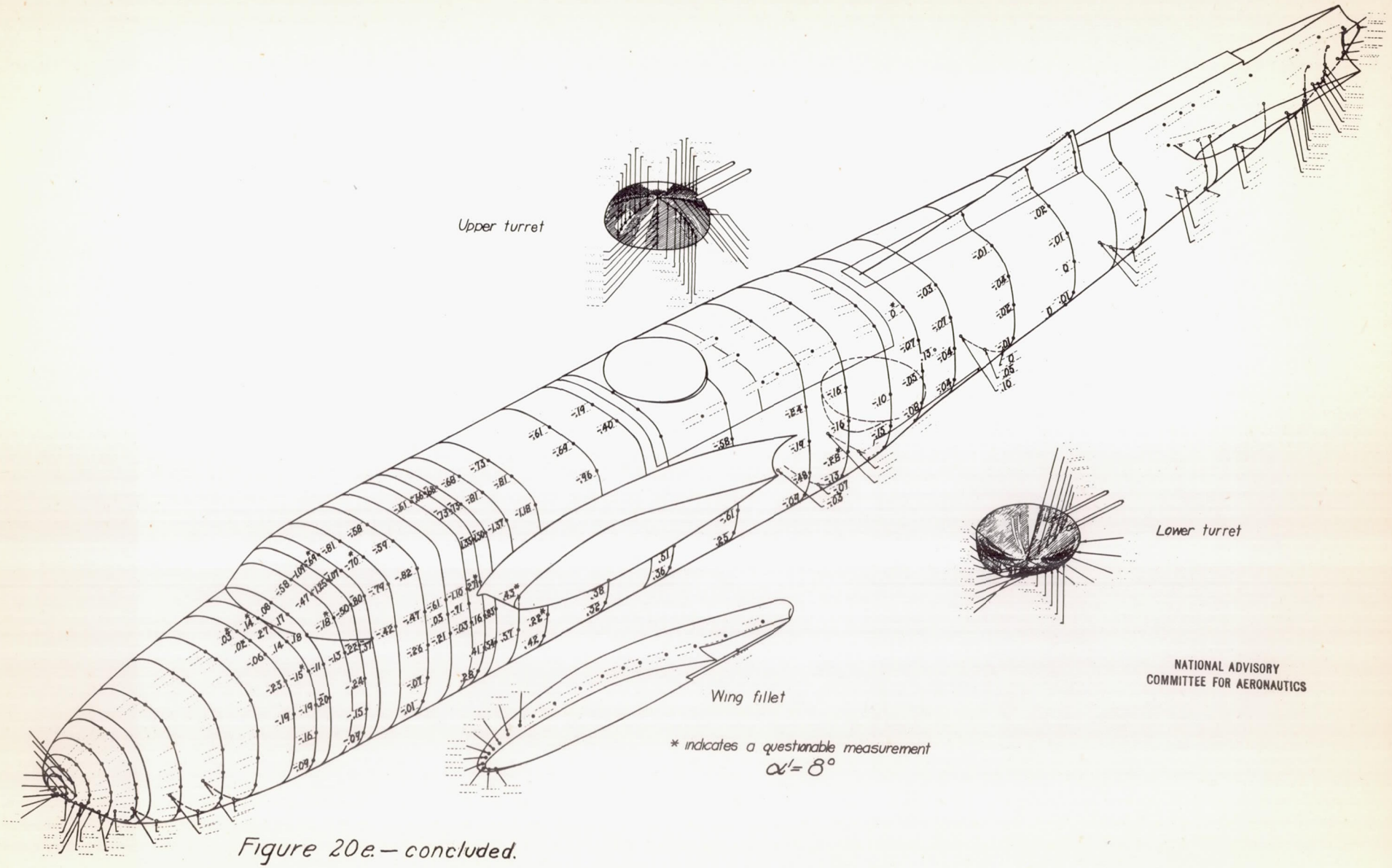

Figure 20e.—concluded.

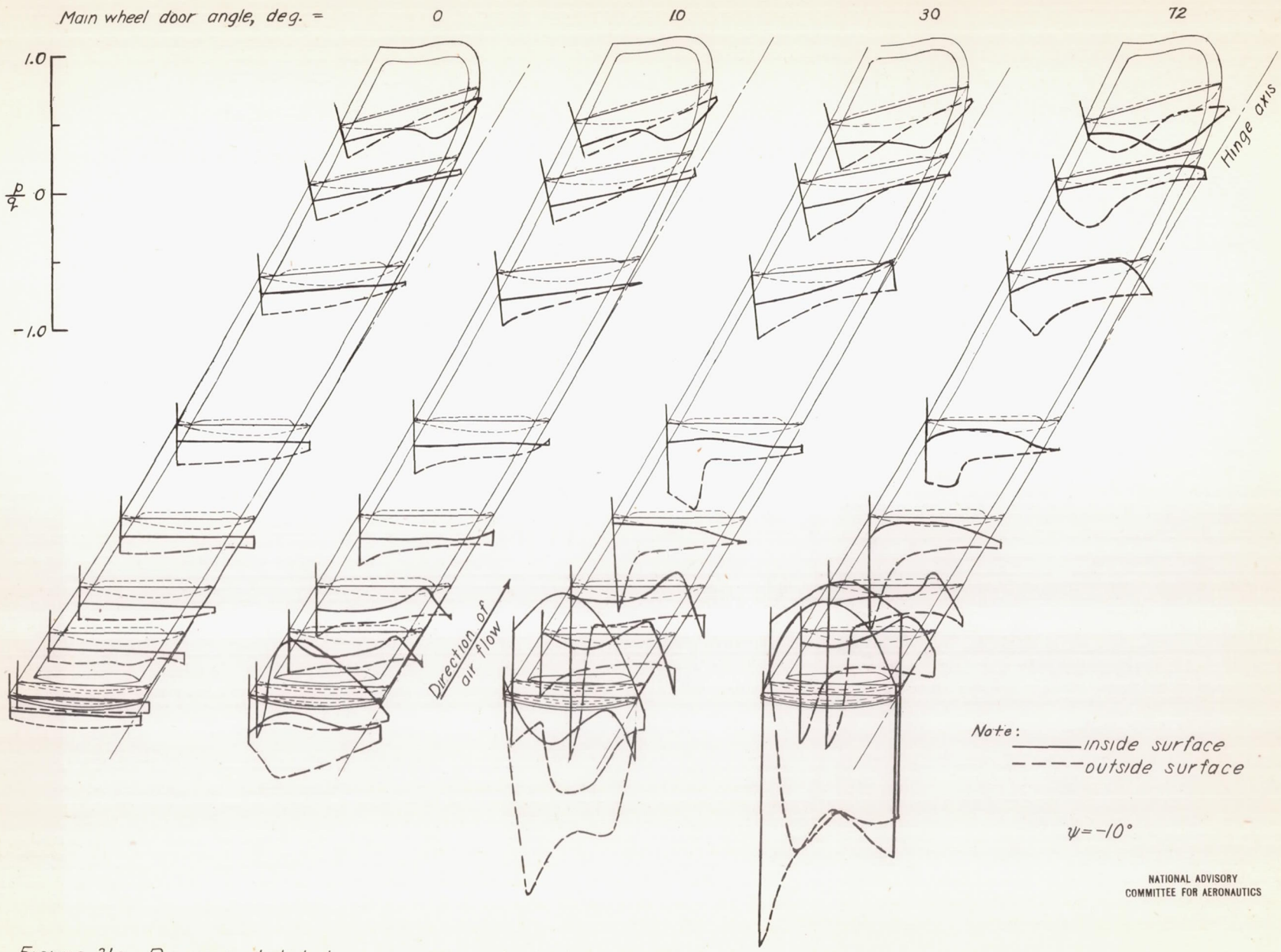

Figure 21a.—Pressure distribution over main wheel door of 0.2375-scale model Douglas XA-26 airplane; $\alpha = 4°$; $q \approx 50$ lb/sq ft; $R \approx 3,950,000$; $M \approx 0.12$.

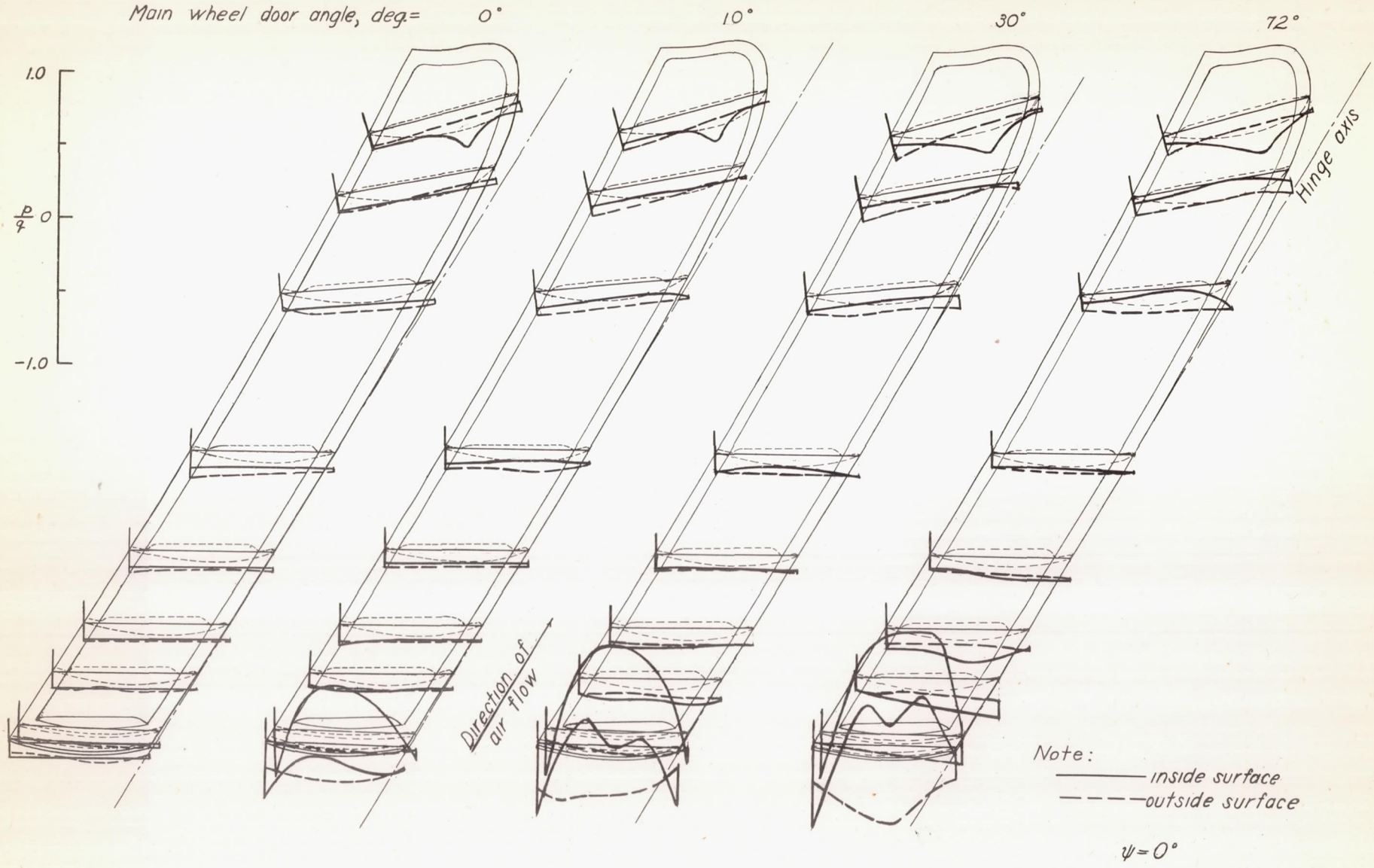

NATIONAL ADVISORY COMMITTEE FOR AERONAUTICS

Figure 21b.—continued

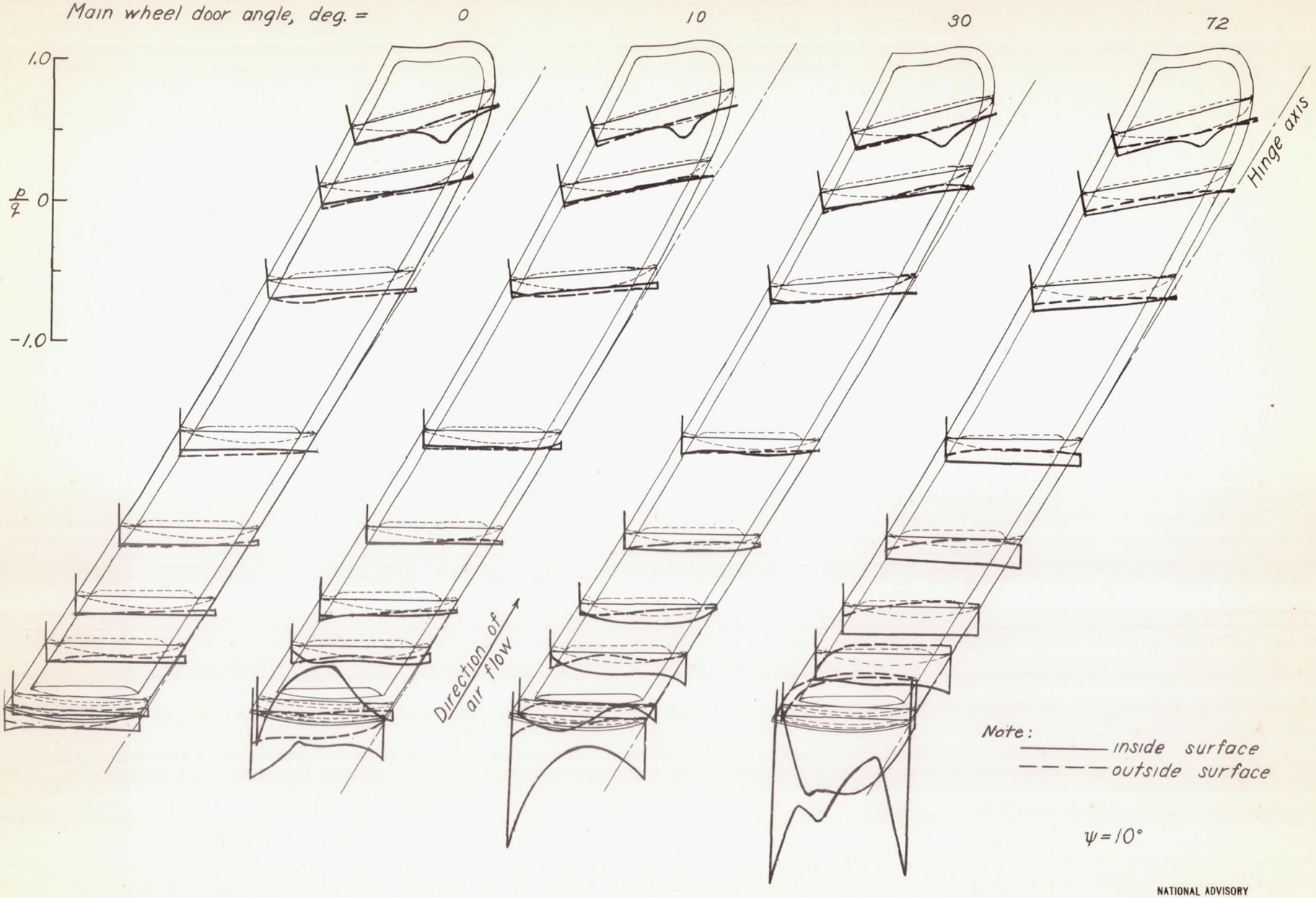

Figure 21c. concluded.

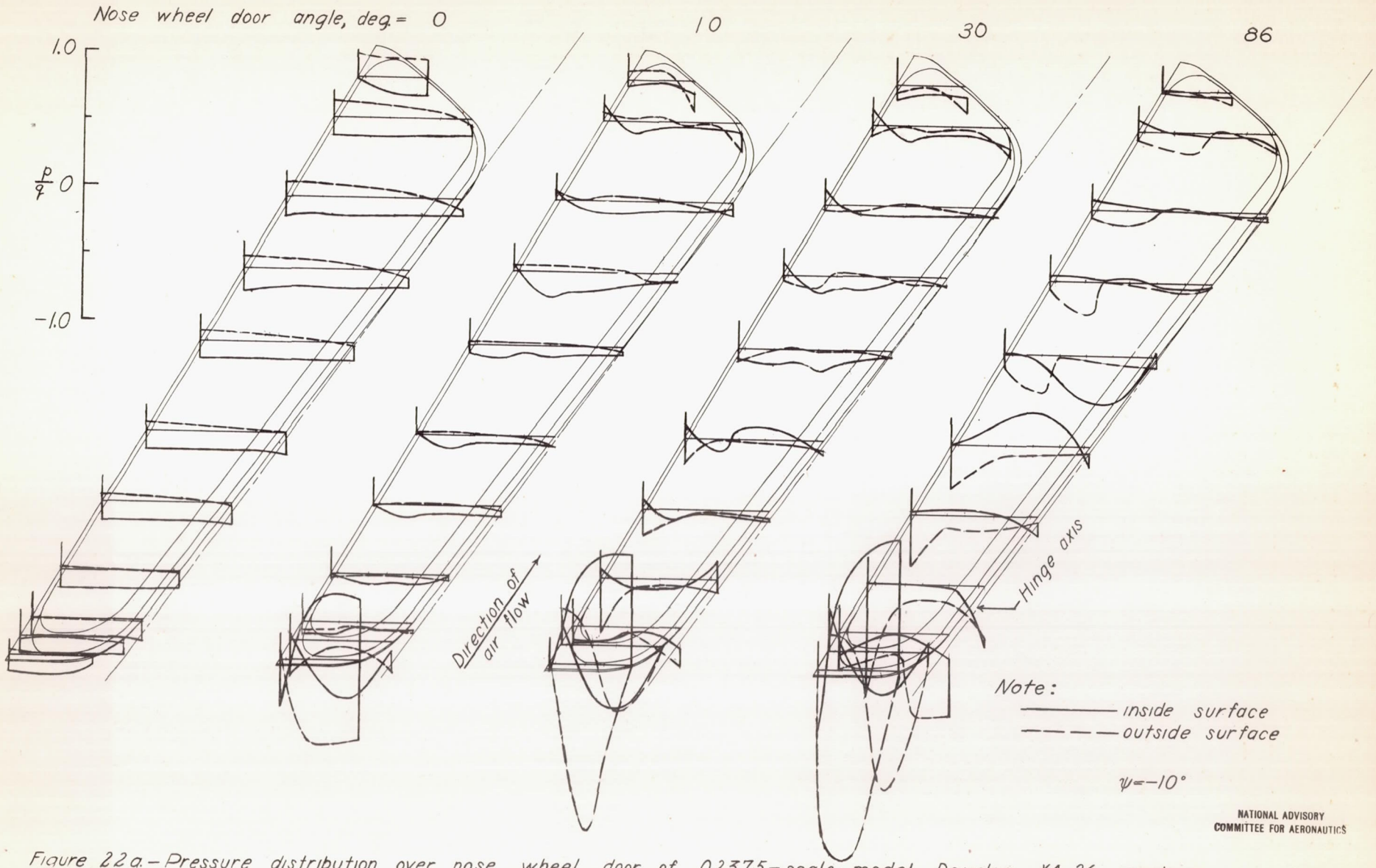

Figure 22a.—Pressure distribution over nose wheel door of 0.2375-scale model Douglas XA-26 airplane; $\alpha = 4°$; $q \approx 50$ lb/sq ft; $R \approx 3,940,000$; $M \approx 0.12$.

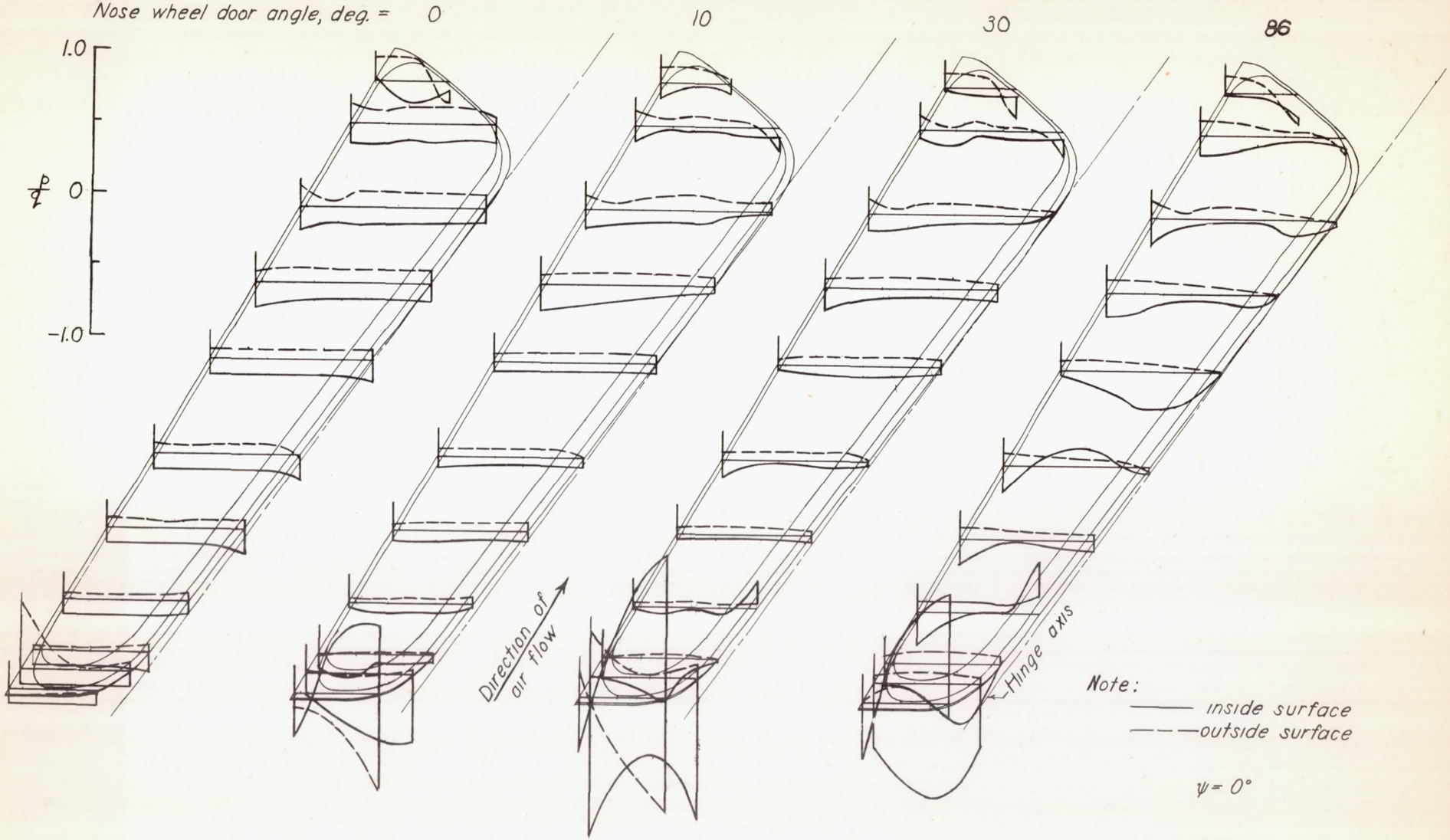

Figure 22b.— continued

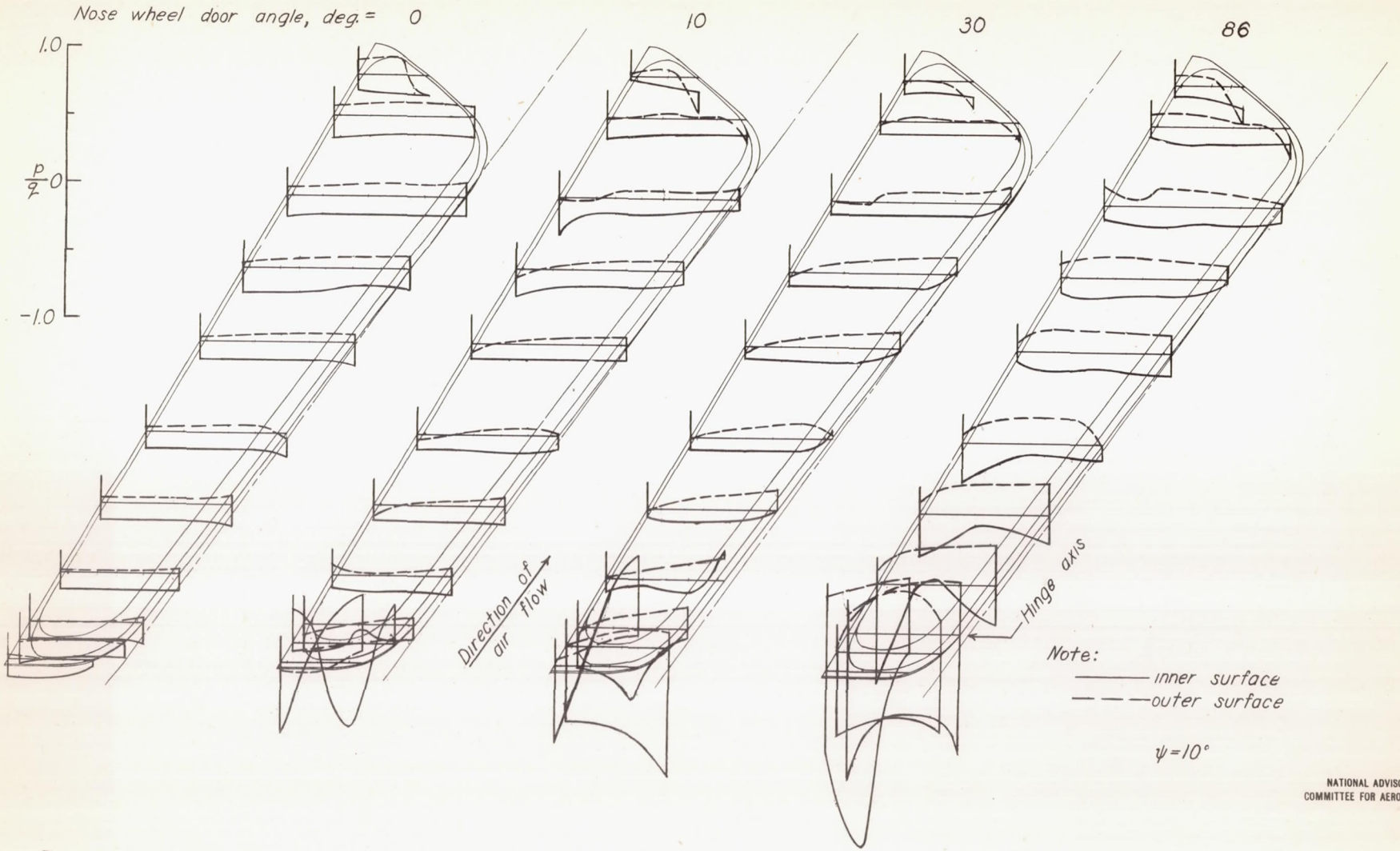

Figure 22c. – concluded.

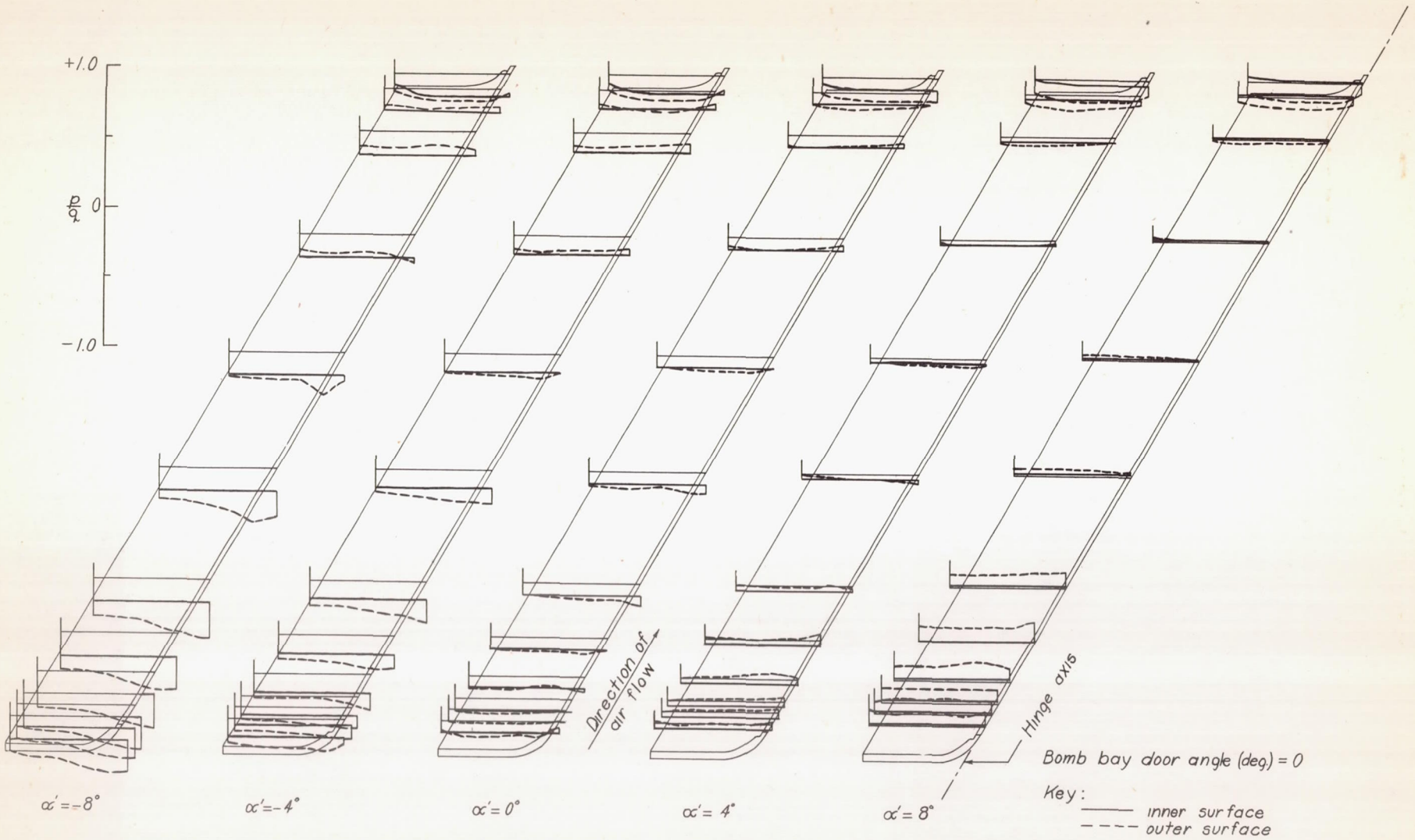

Figure 23a .— Pressure distribution over bomb bay door of 0.2375-scale model Douglas XA-26 Airplane; $\psi = 0°$; $q \approx 50$ lb/sq ft; $R \approx 3{,}640{,}000$; $M \approx 0.18$.

NATIONAL ADVISORY COMMITTEE FOR AERONAUTICS

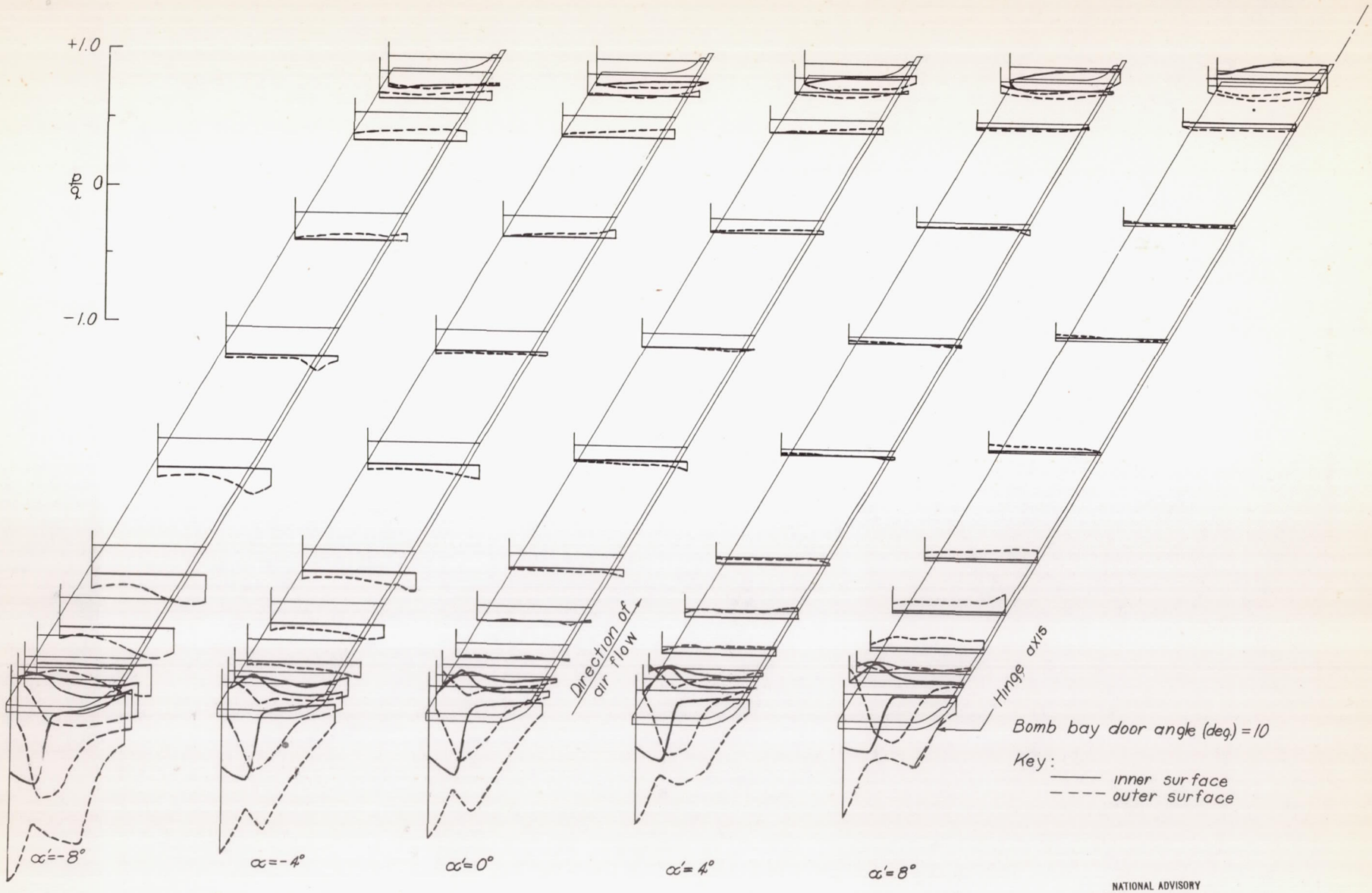

NATIONAL ADVISORY COMMITTEE FOR AERONAUTICS

Figure 23b.— Continued

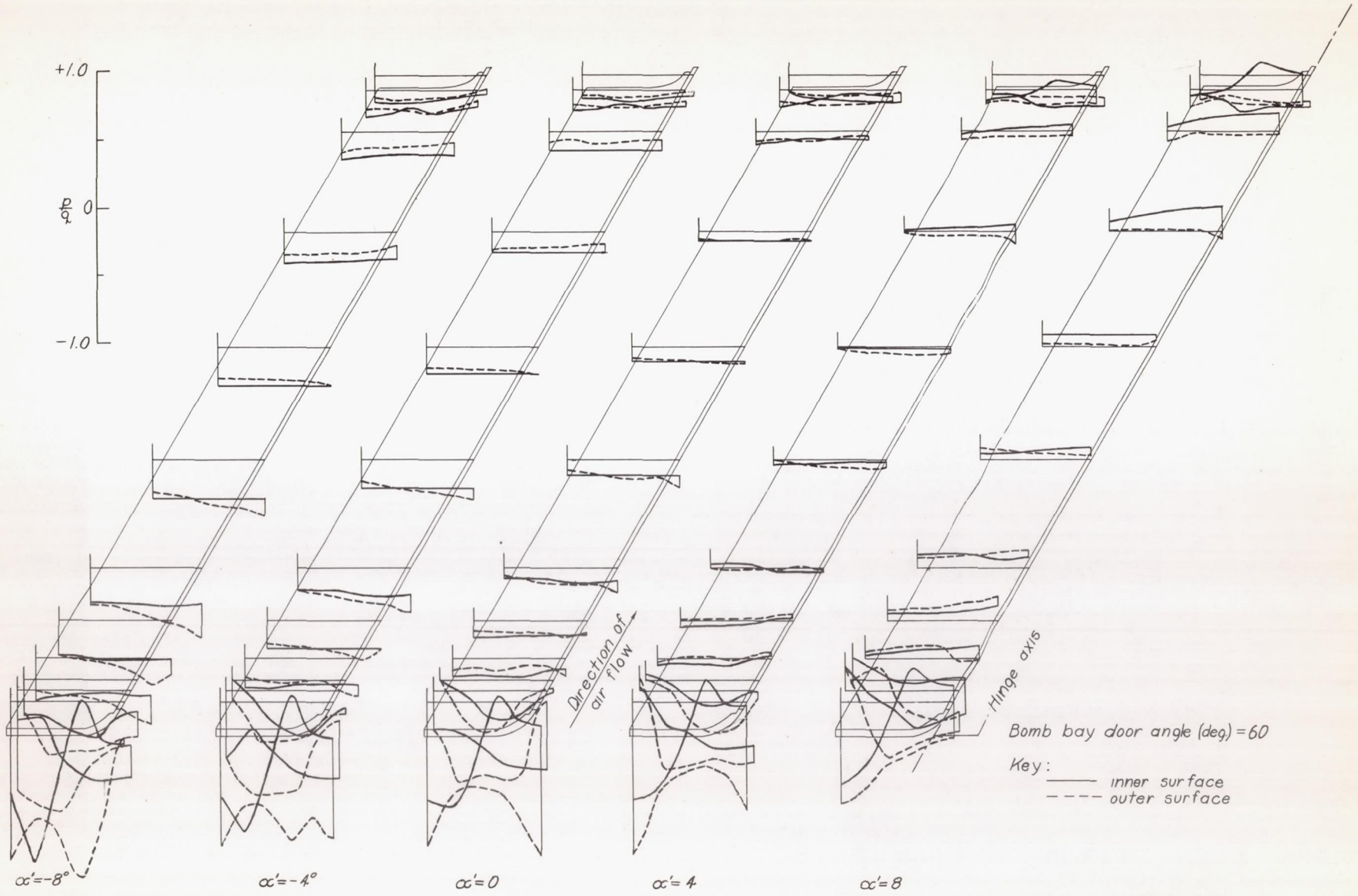

NATIONAL ADVISORY COMMITTEE FOR AERONAUTICS

Figure 23c.- Concluded.

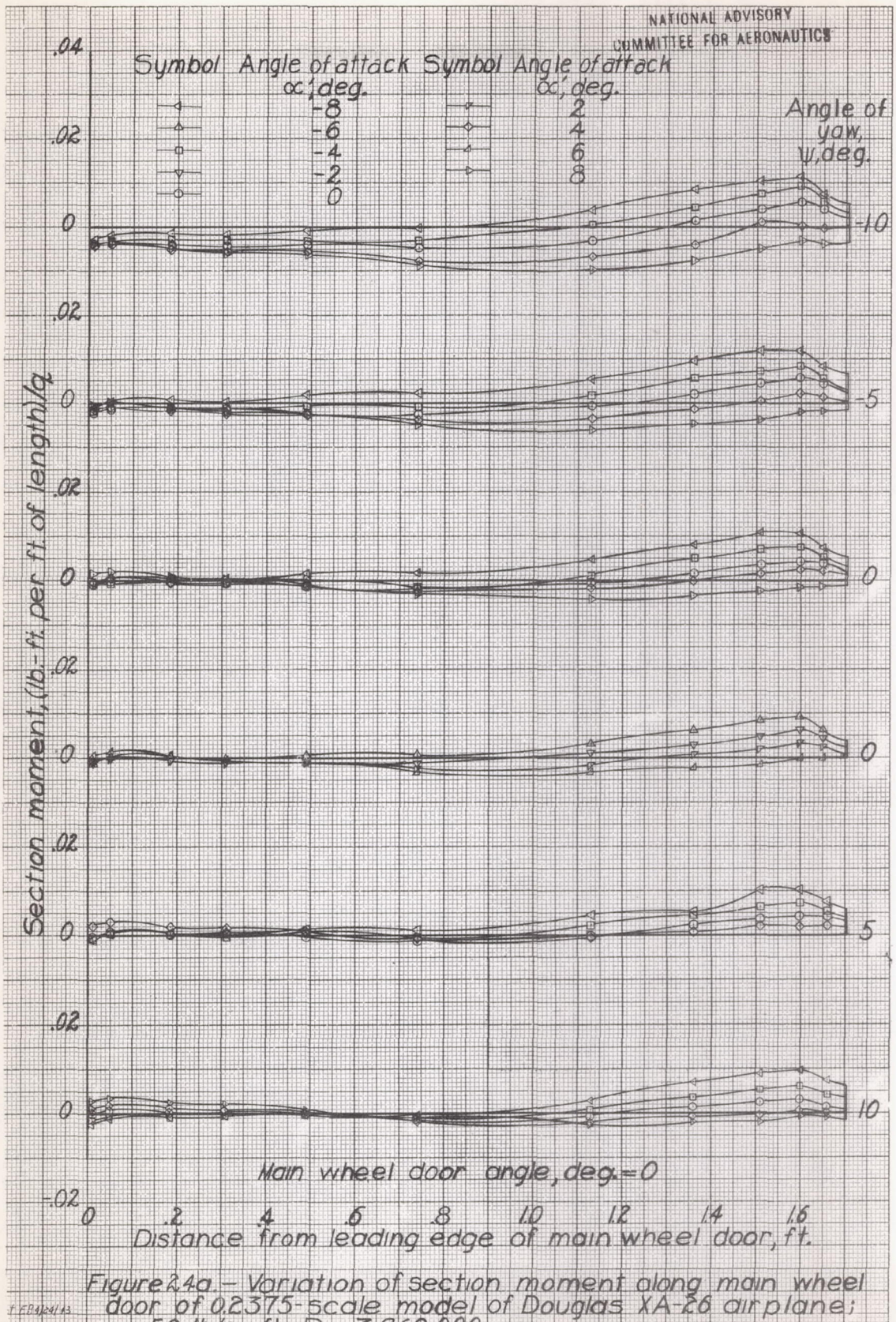

Figure 24a. – Variation of section moment along main wheel door of 0.2375-scale model of Douglas XA-26 airplane; $q \approx 50$ lb/sq ft; $R \approx 3,960,000$.

F-FB-4124-43
RMA 4126 43

NATIONAL ADVISORY
COMMITTEE FOR AERONAUTICS

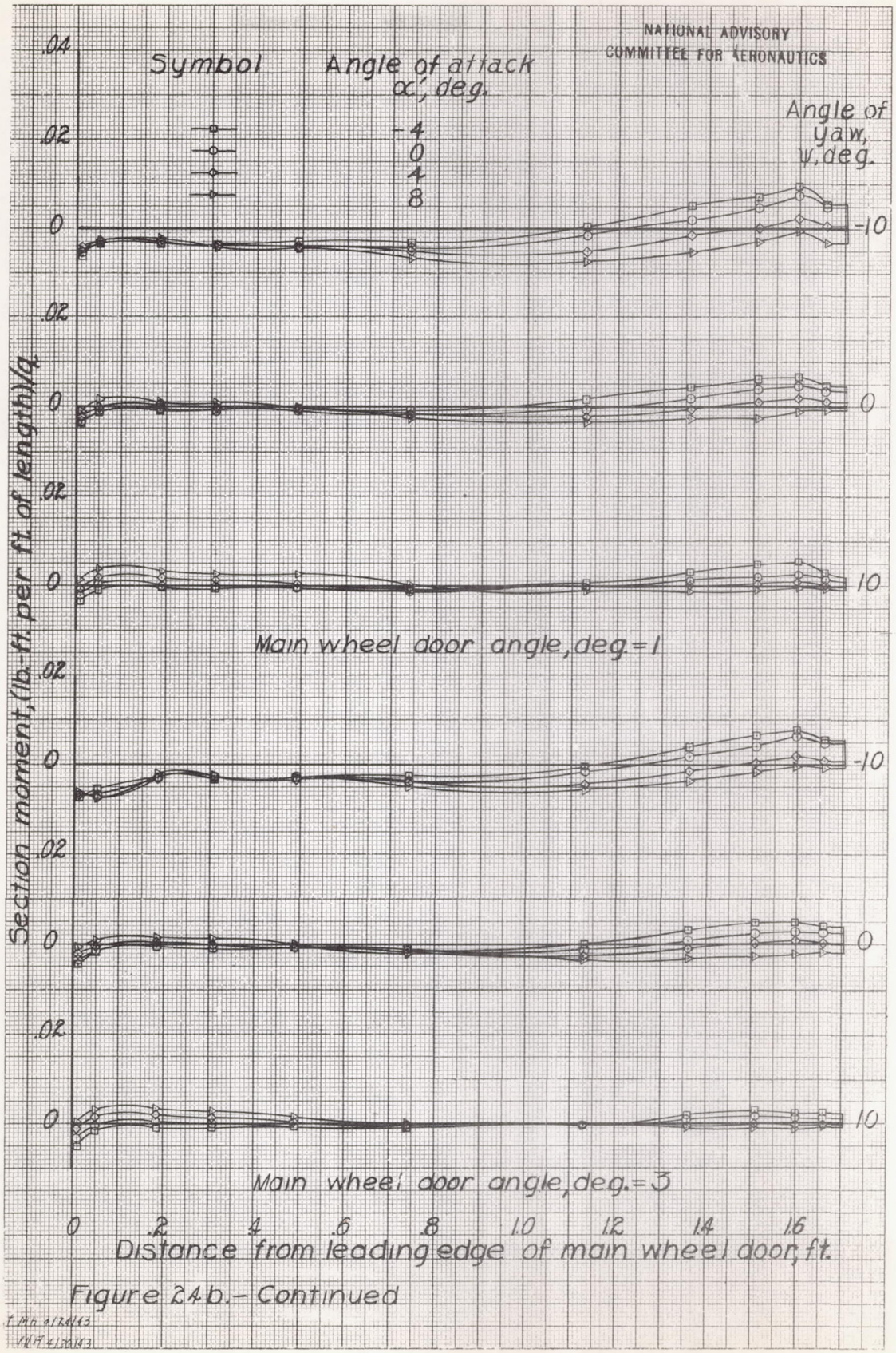

Figure 24b.- Continued

L-553

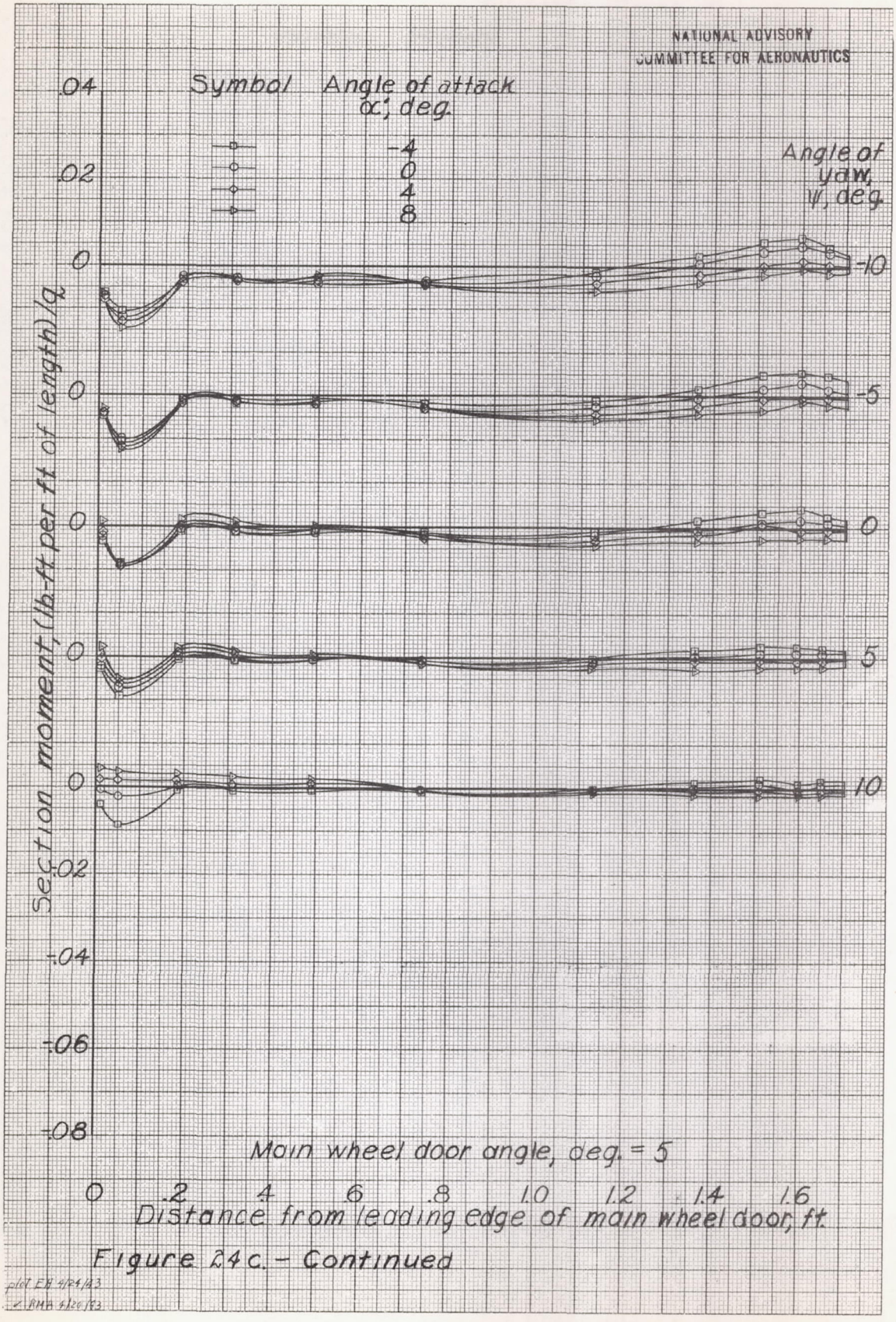

Figure 24c. - Continued

plot EB 4/24/43
ck RMA 4/26/43

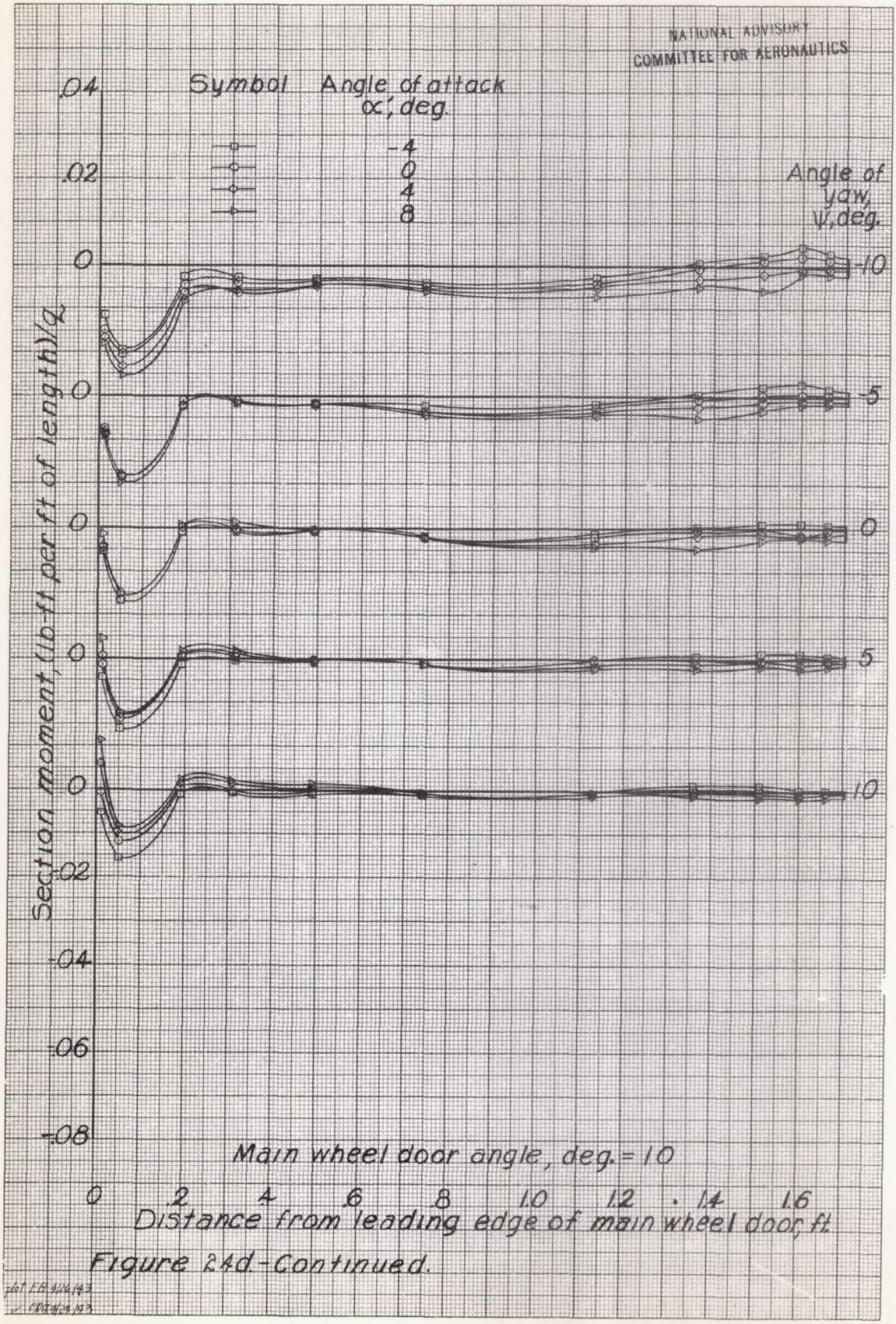

Figure 24d - Continued.

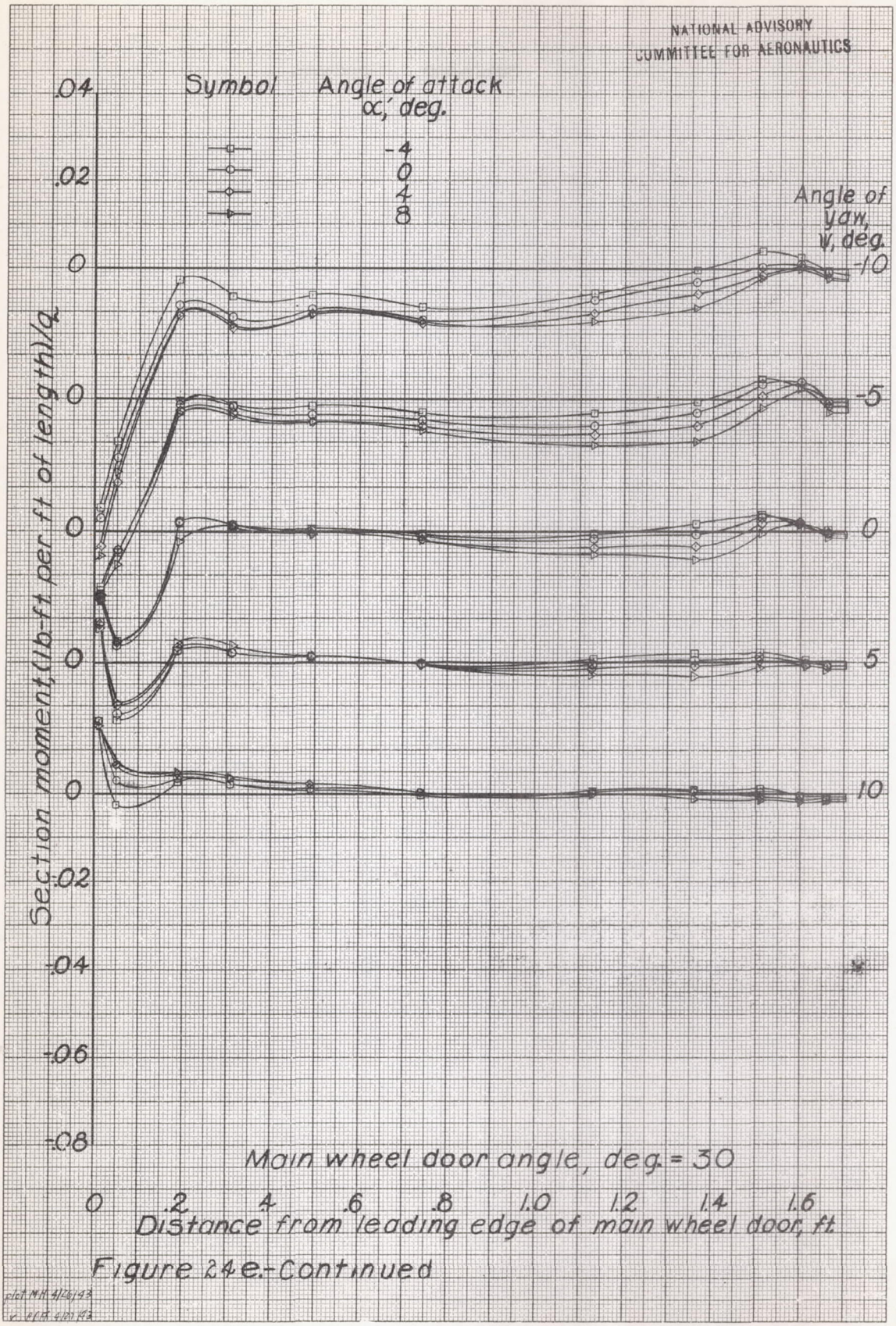

Figure 24e.- Continued

L-553

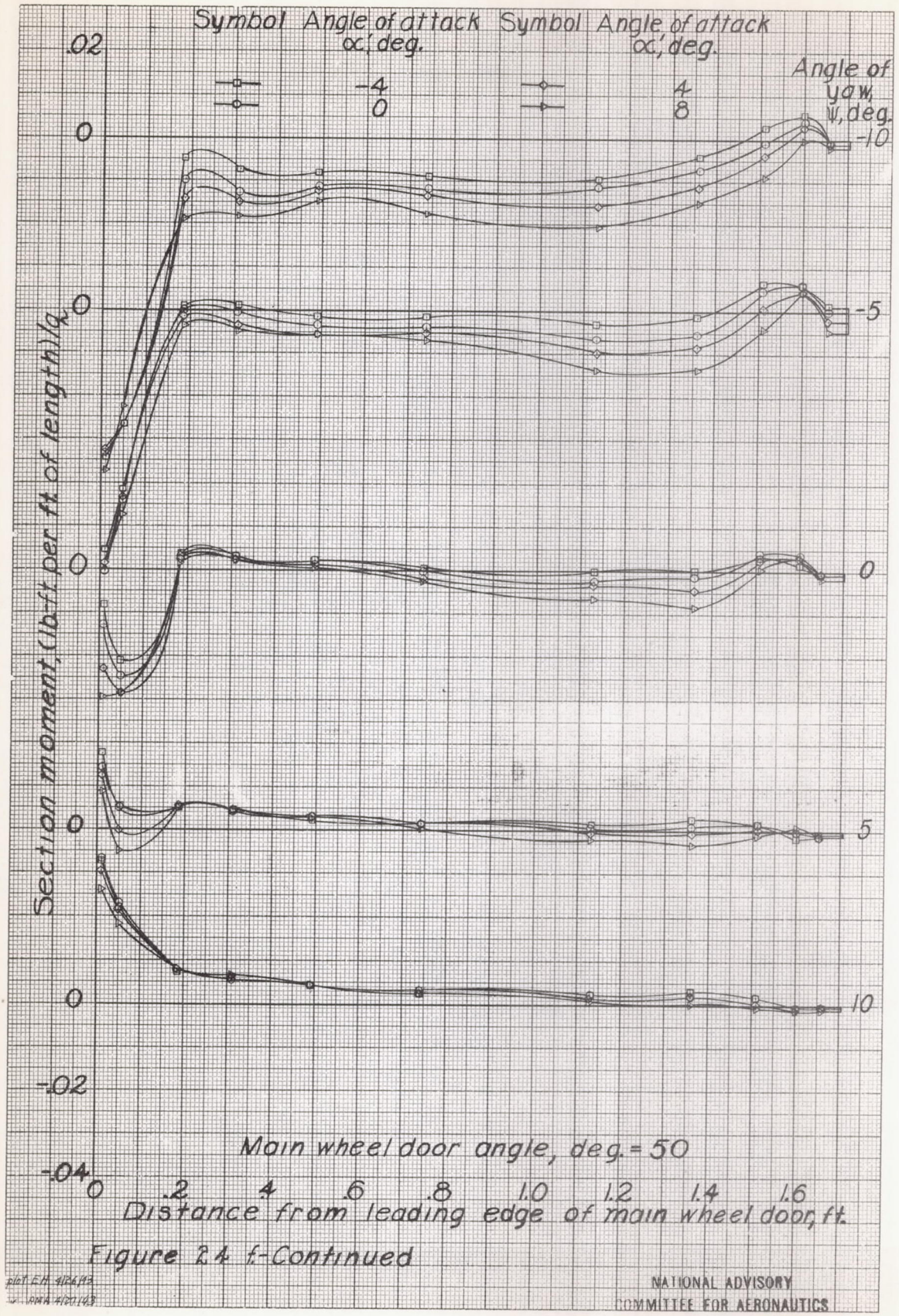

Figure 24 f-Continued

NATIONAL ADVISORY COMMITTEE FOR AERONAUTICS

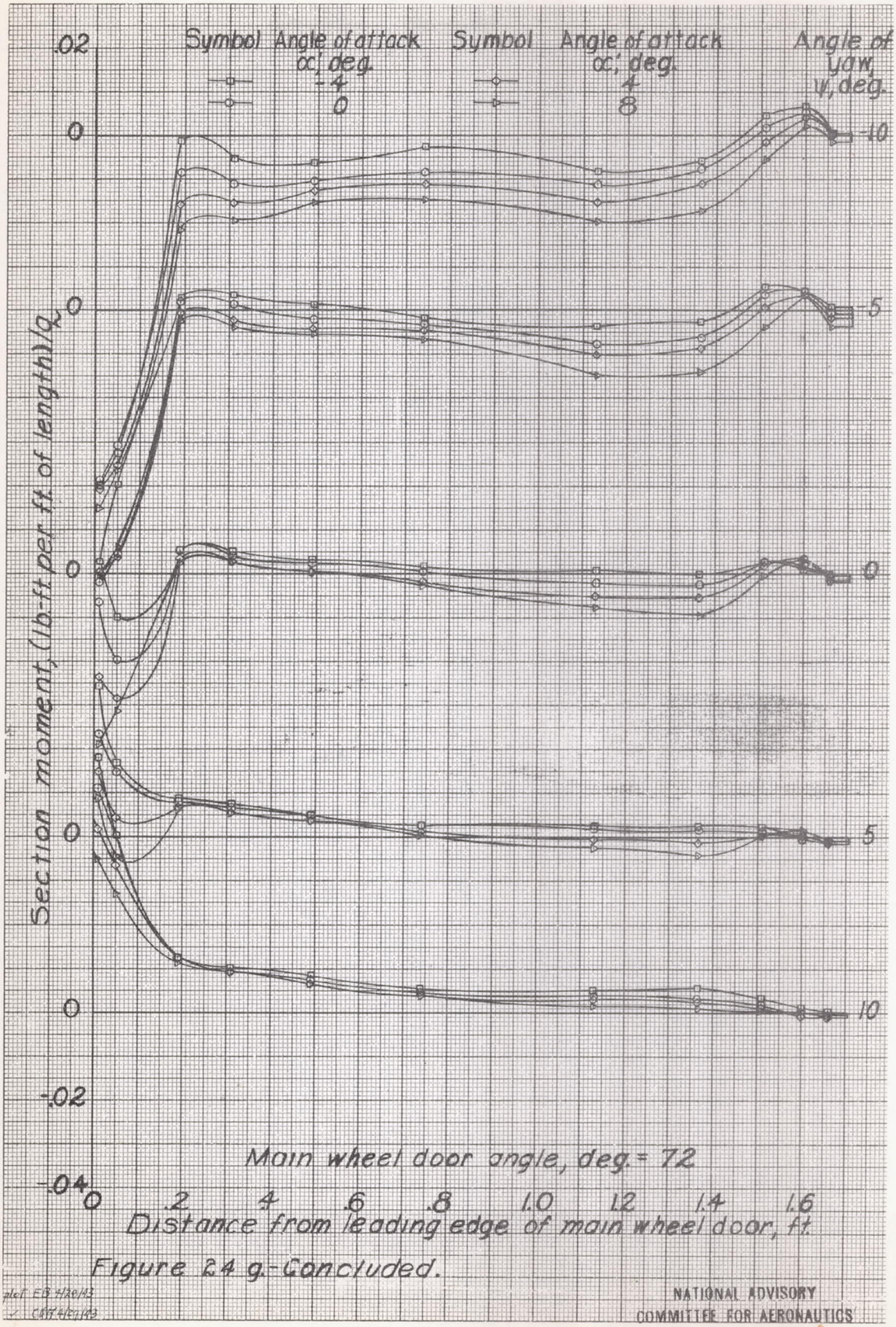

Figure 24 g.- Concluded.

plot EB 4/20/43
✓ CHT 4/20/43

NATIONAL ADVISORY
COMMITTEE FOR AERONAUTICS

NATIONAL ADVISORY
COMMITTEE FOR AERONAUTICS

L-553

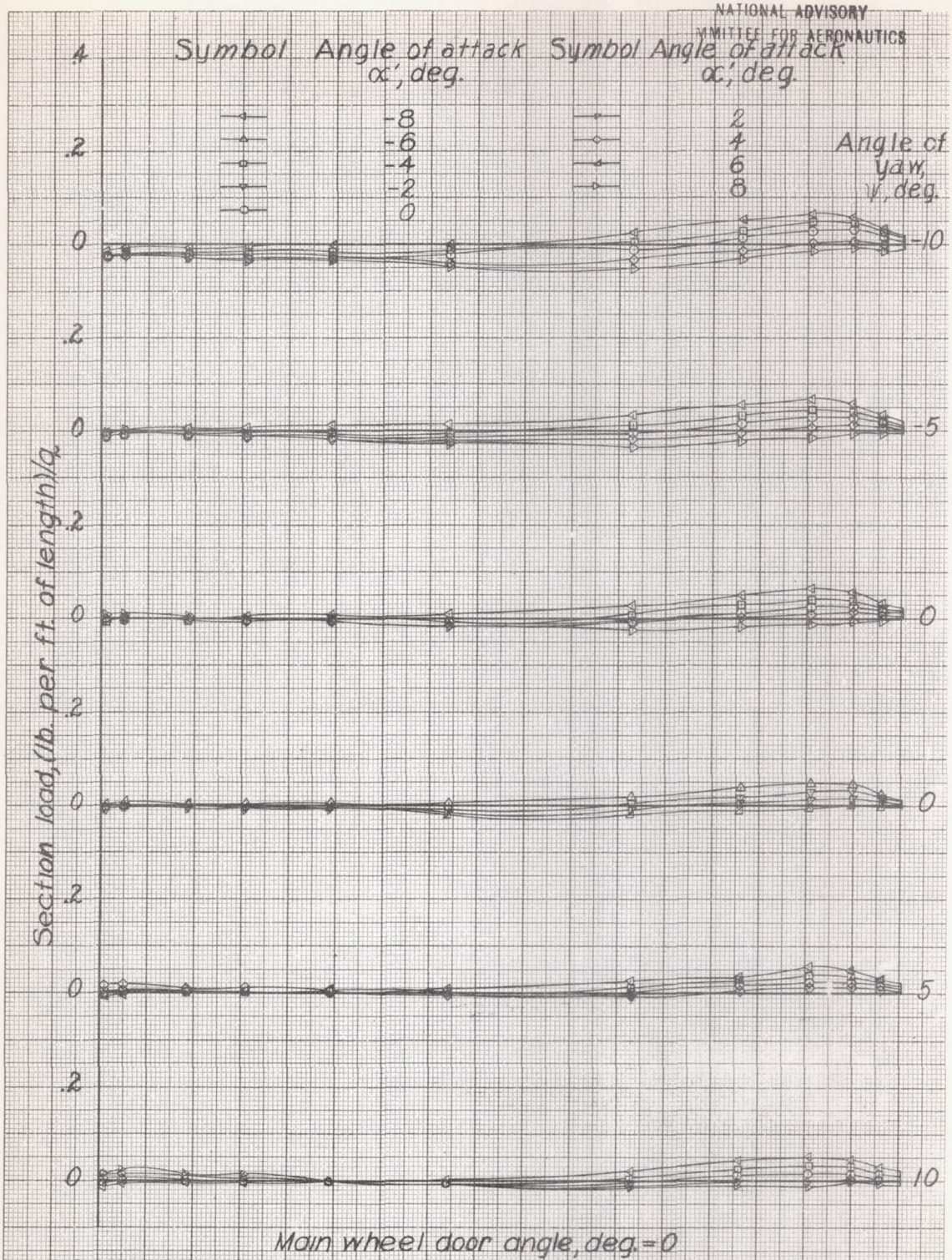

Figure 25a. – Variation of section load along main wheel door of 0.2375-scale model of Douglas XA-26 airplane; $q \approx 50$ lb./sq ft; $R \approx 3,960,000$.

NACA-Langley - 4-28-43 - 1000

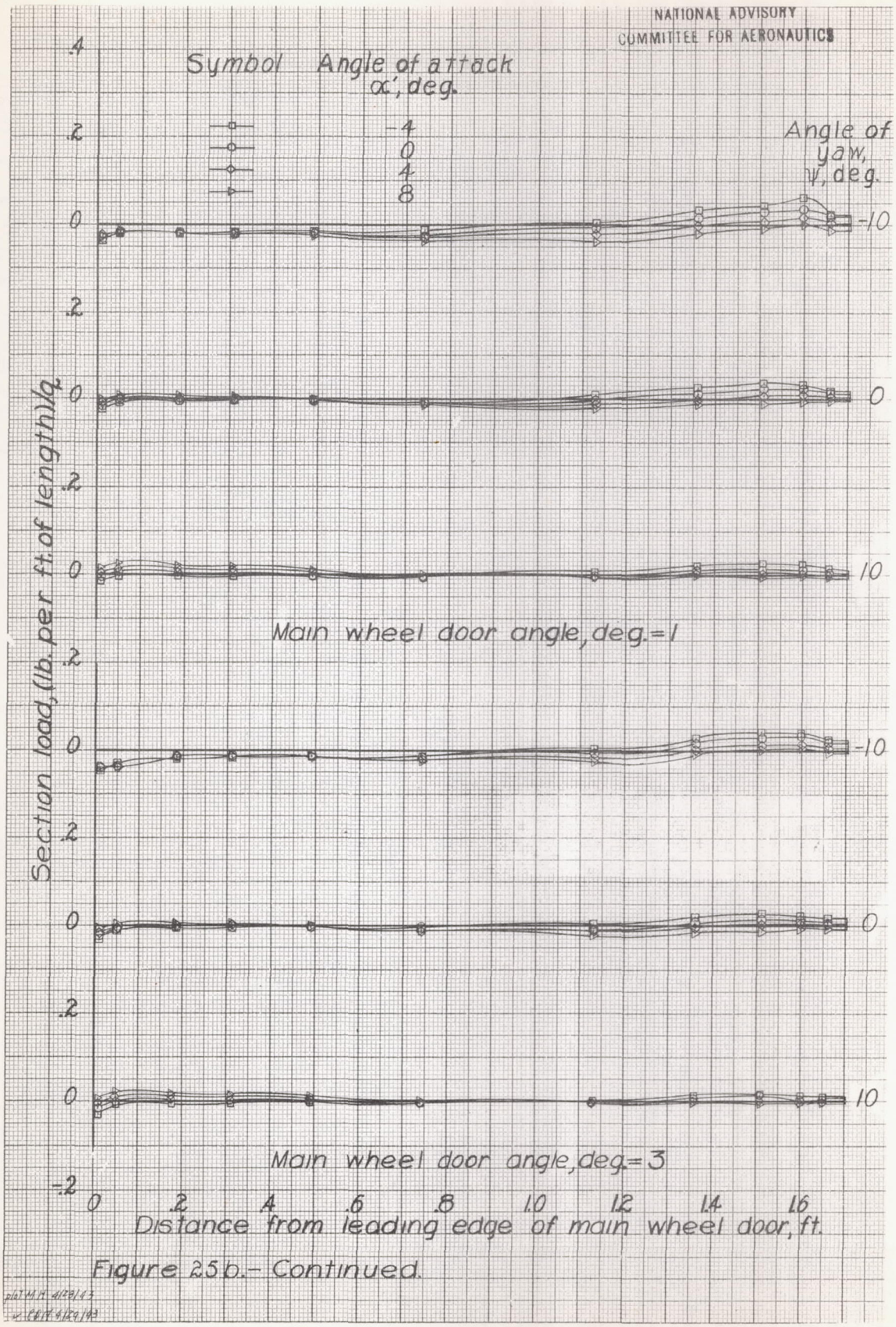

Figure 25.b.- Continued.

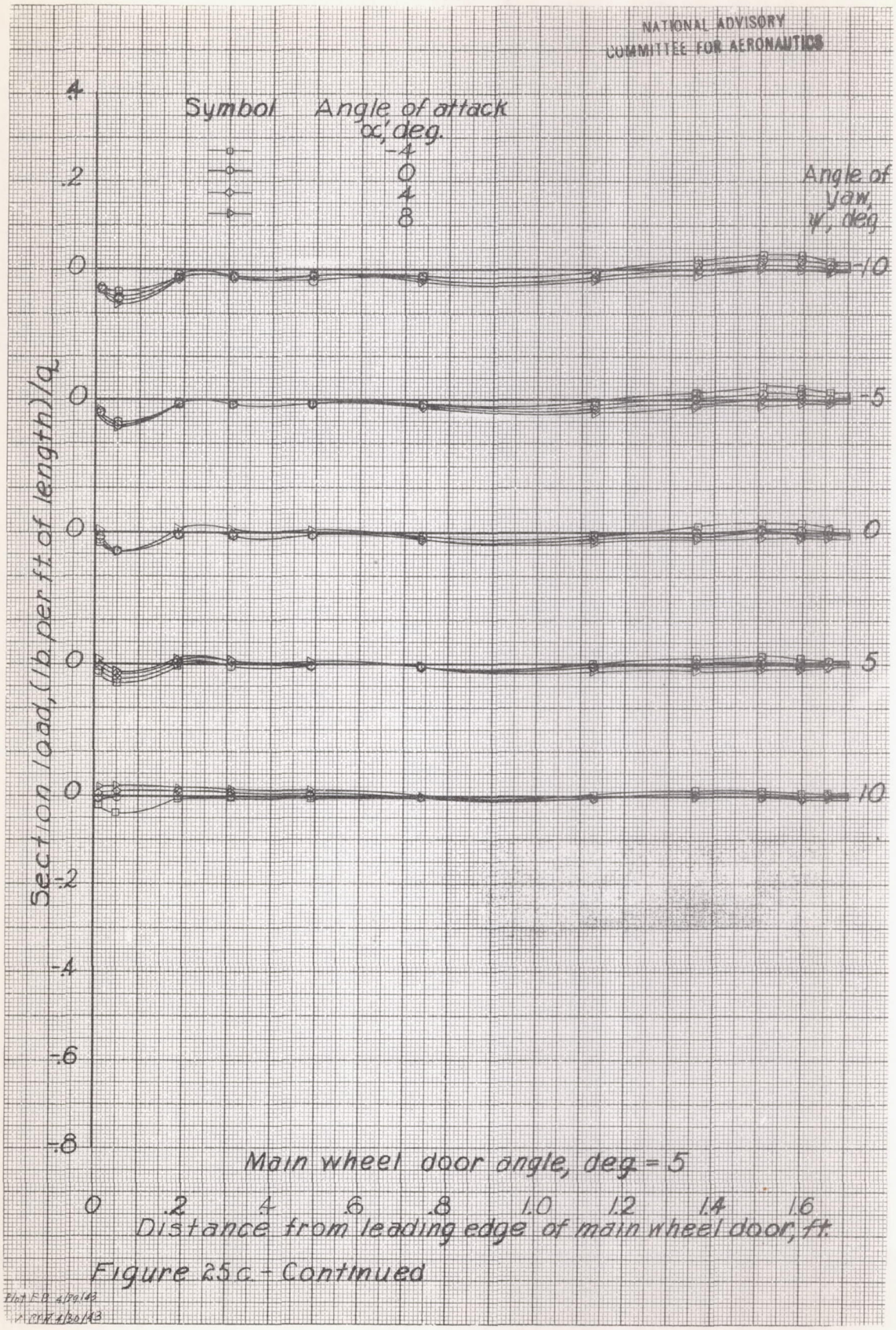

Figure 25c - Continued

L-553

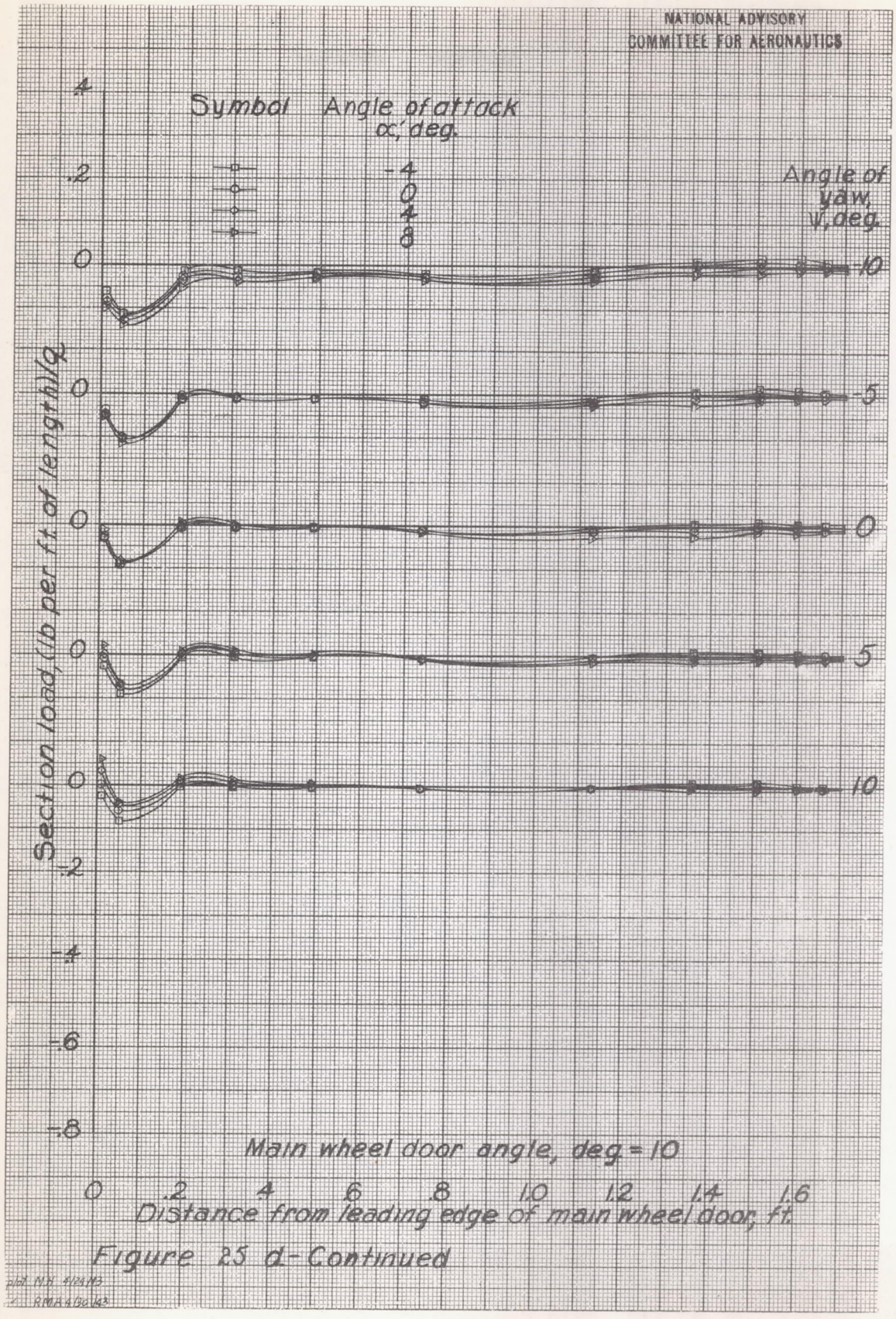

Figure 25 d- Continued

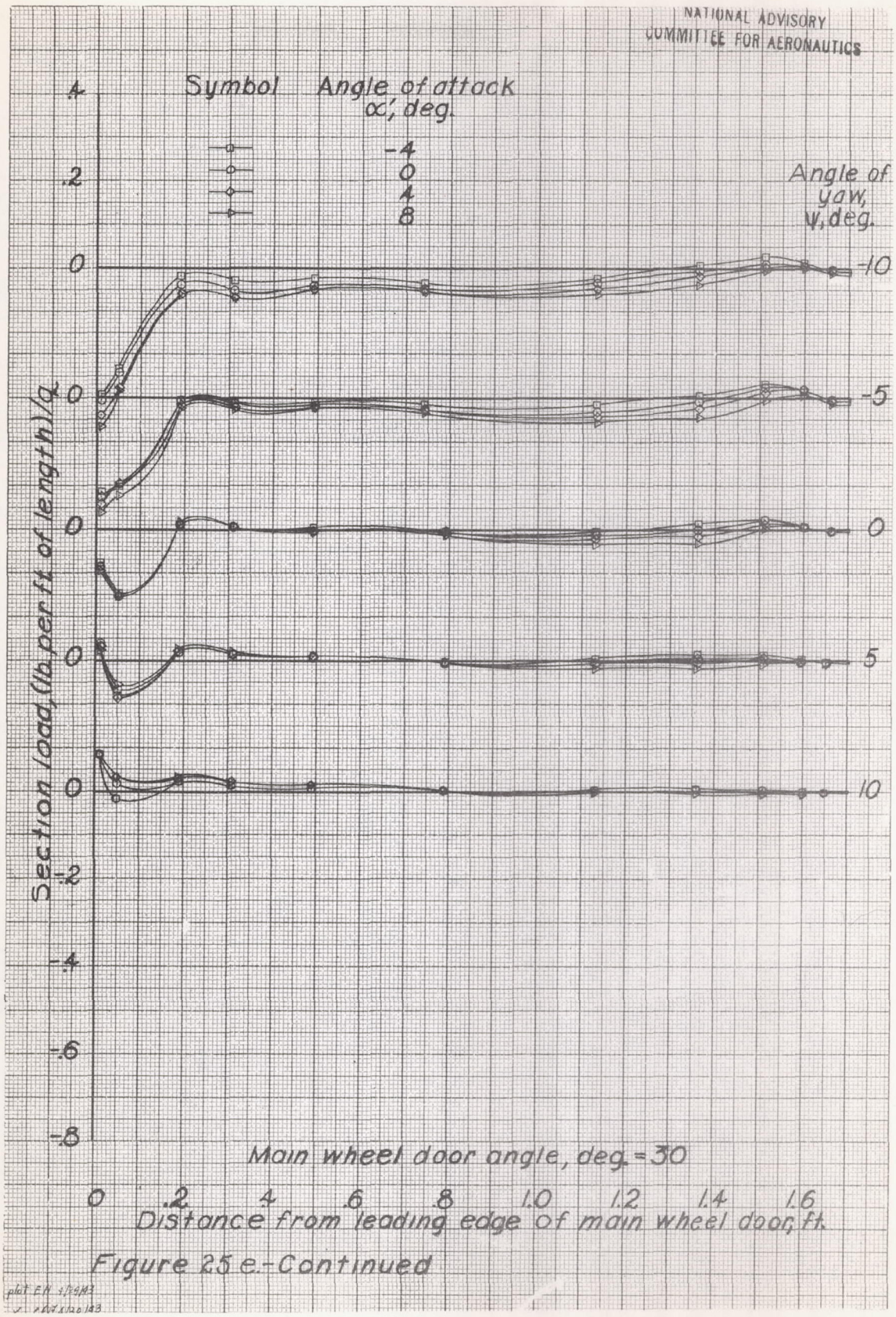

Figure 25 e.-Continued

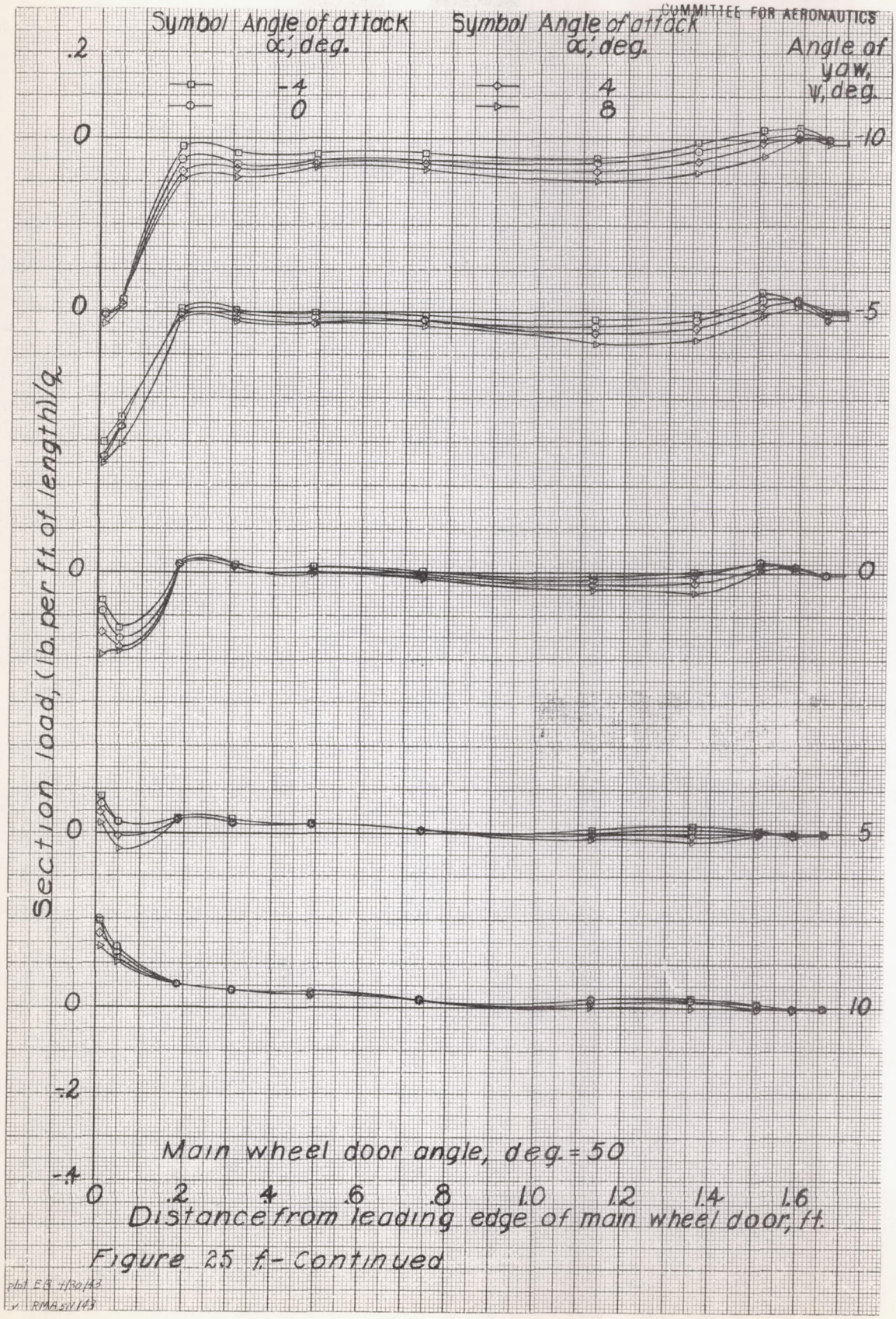

Figure 25 f- Continued

plot E.B. 4/30/43
✓ RMA-SW 143

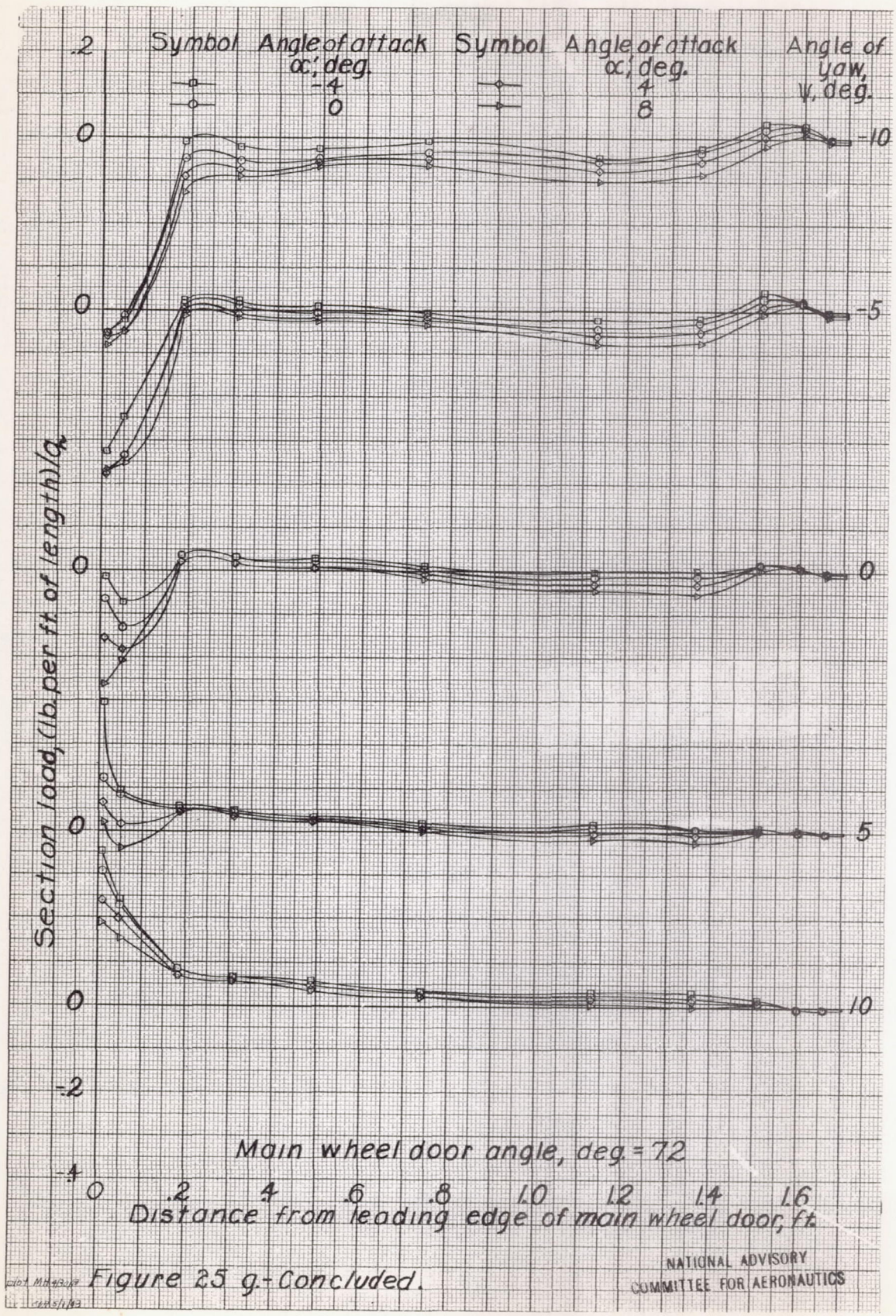

Figure 25 g.- Concluded.

NATIONAL ADVISORY COMMITTEE FOR AERONAUTICS

L-553

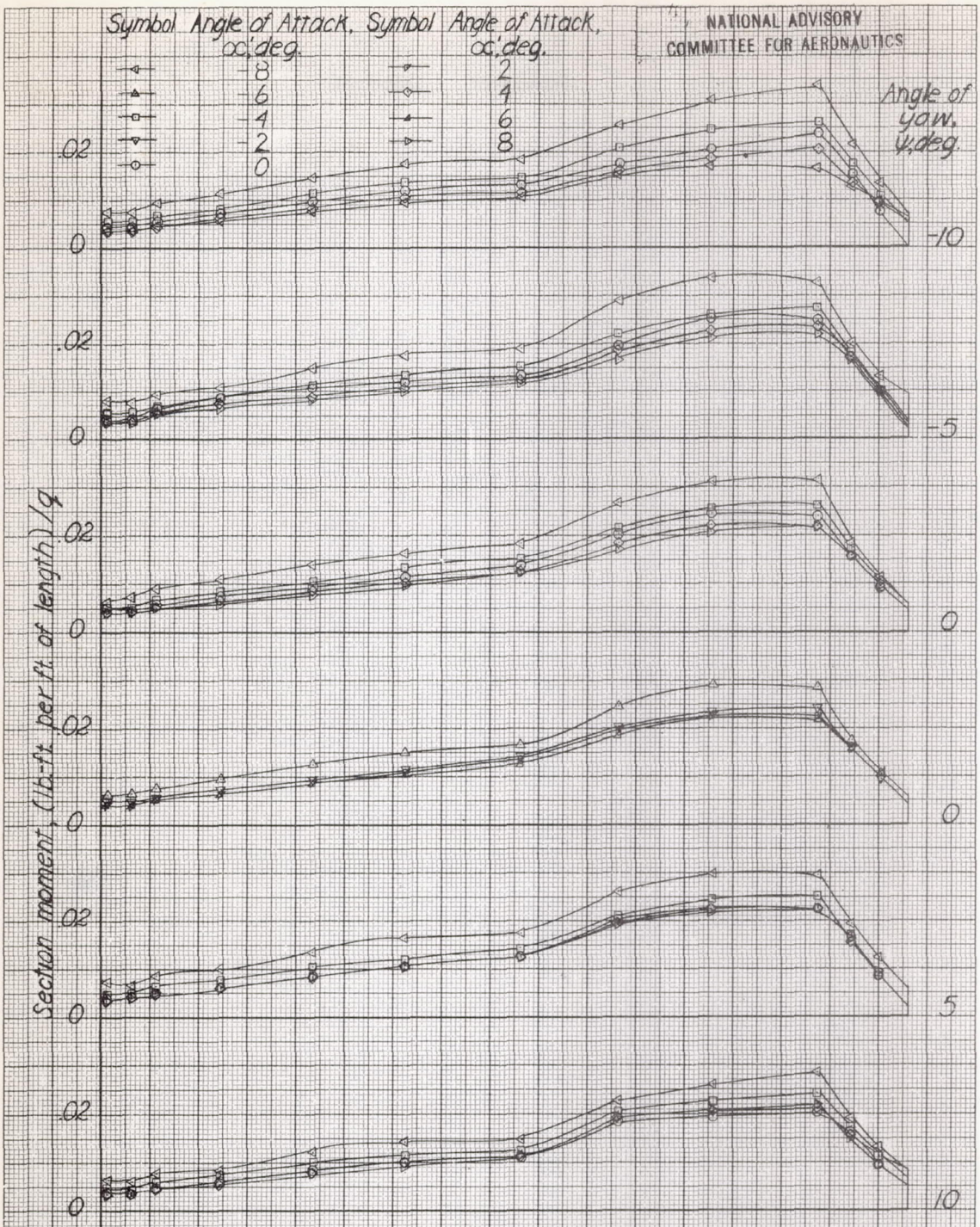

Figure 26a. - Variation of section moment along nose wheel door of 0.2375 - scale model of Douglas XA-26 airplane; $q \approx 50$ lb/sq-ft; $R \approx 3,950,000$

Plot TB 3/25/43
EH 4/1/43

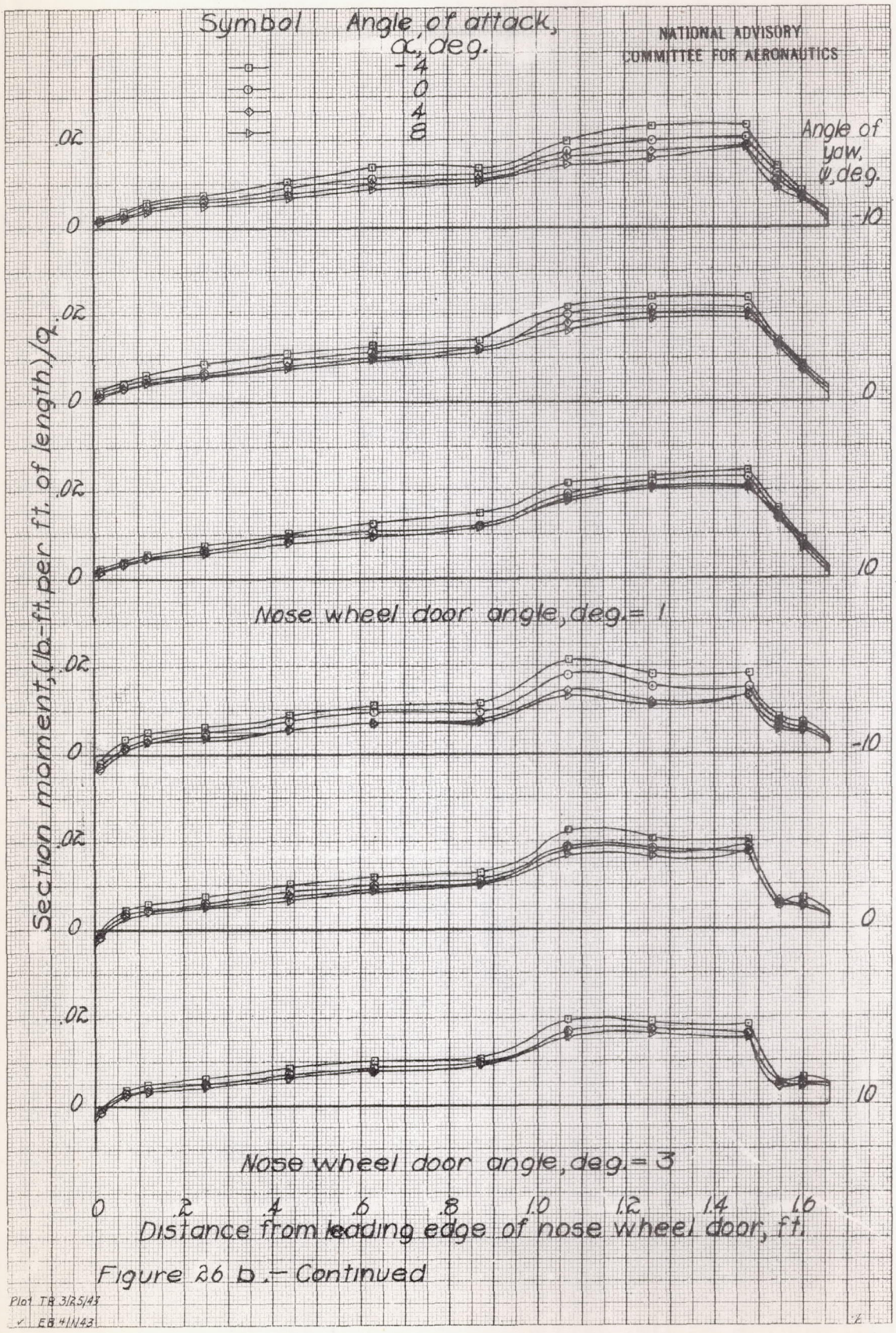

Figure 26 b.- Continued

Plot TB 3/25/43
✓ EB 4/1/43

L-553

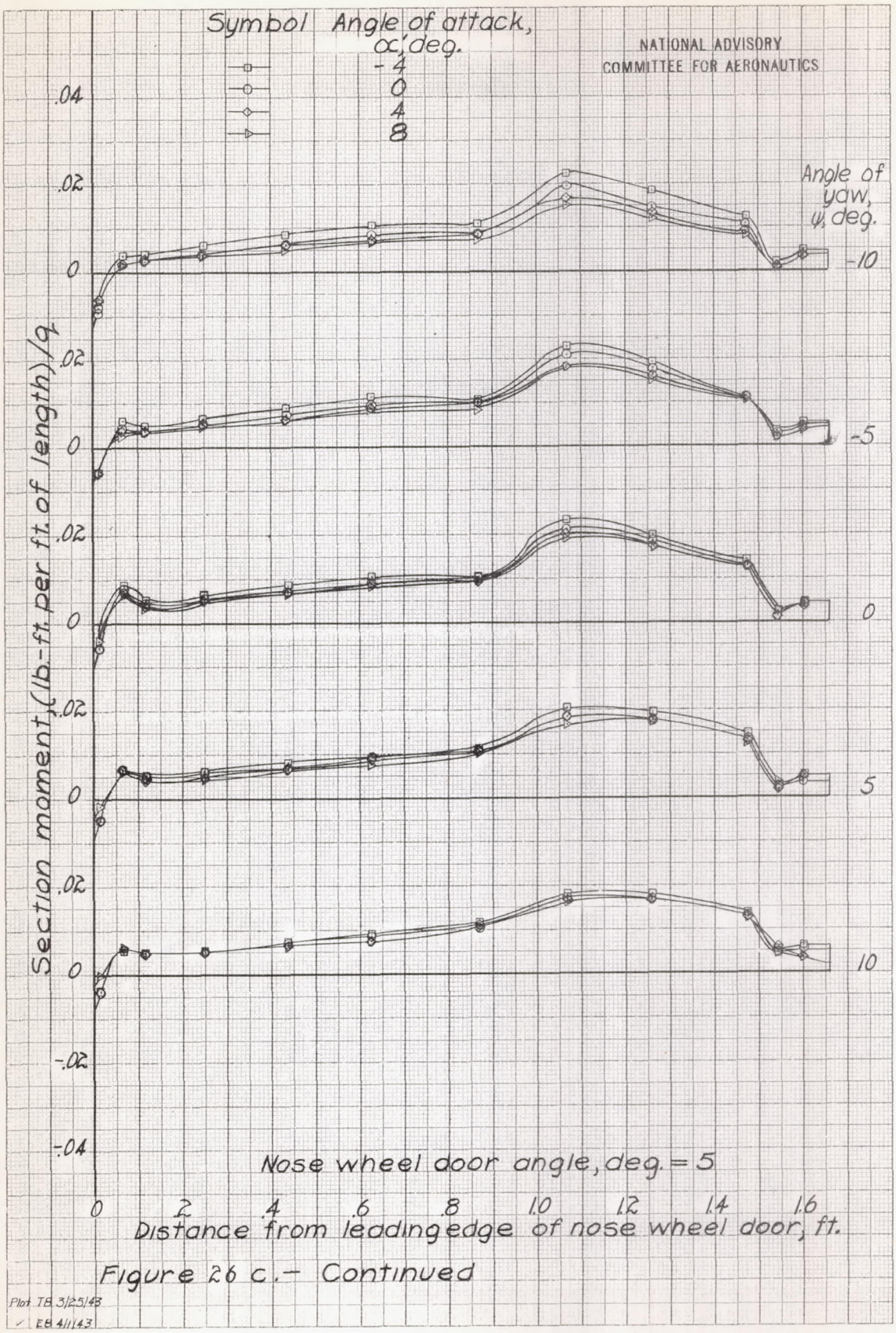

Figure 26 c.- Continued

Plot TB 3/25/43
✓ EB 4/1/43

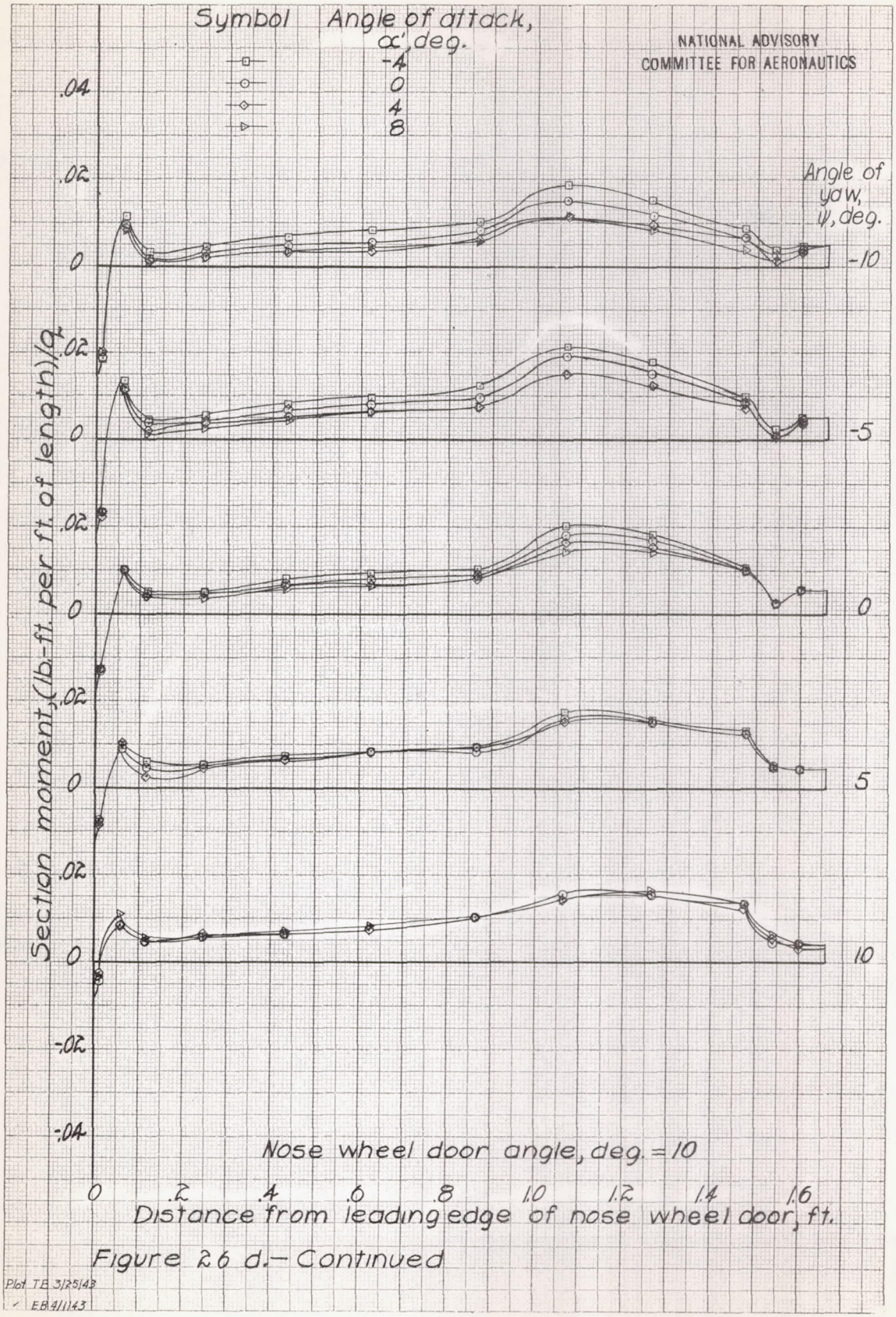

Figure 26 d.- Continued

Plot TB 3/25/43
EB 3/11/43

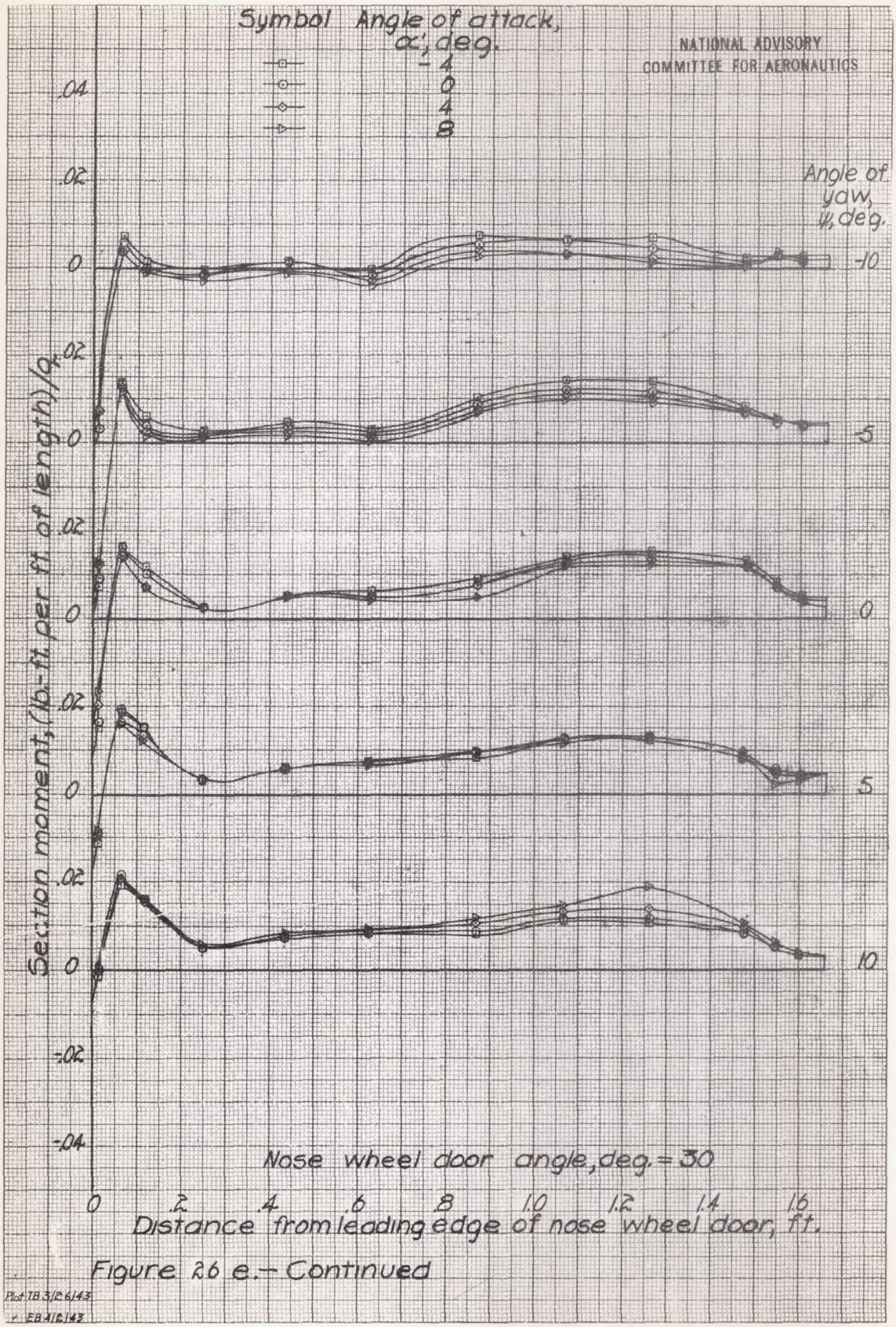

Figure 26 e.- Continued

Plot TB 3/26/43
r. FB 4/6/43

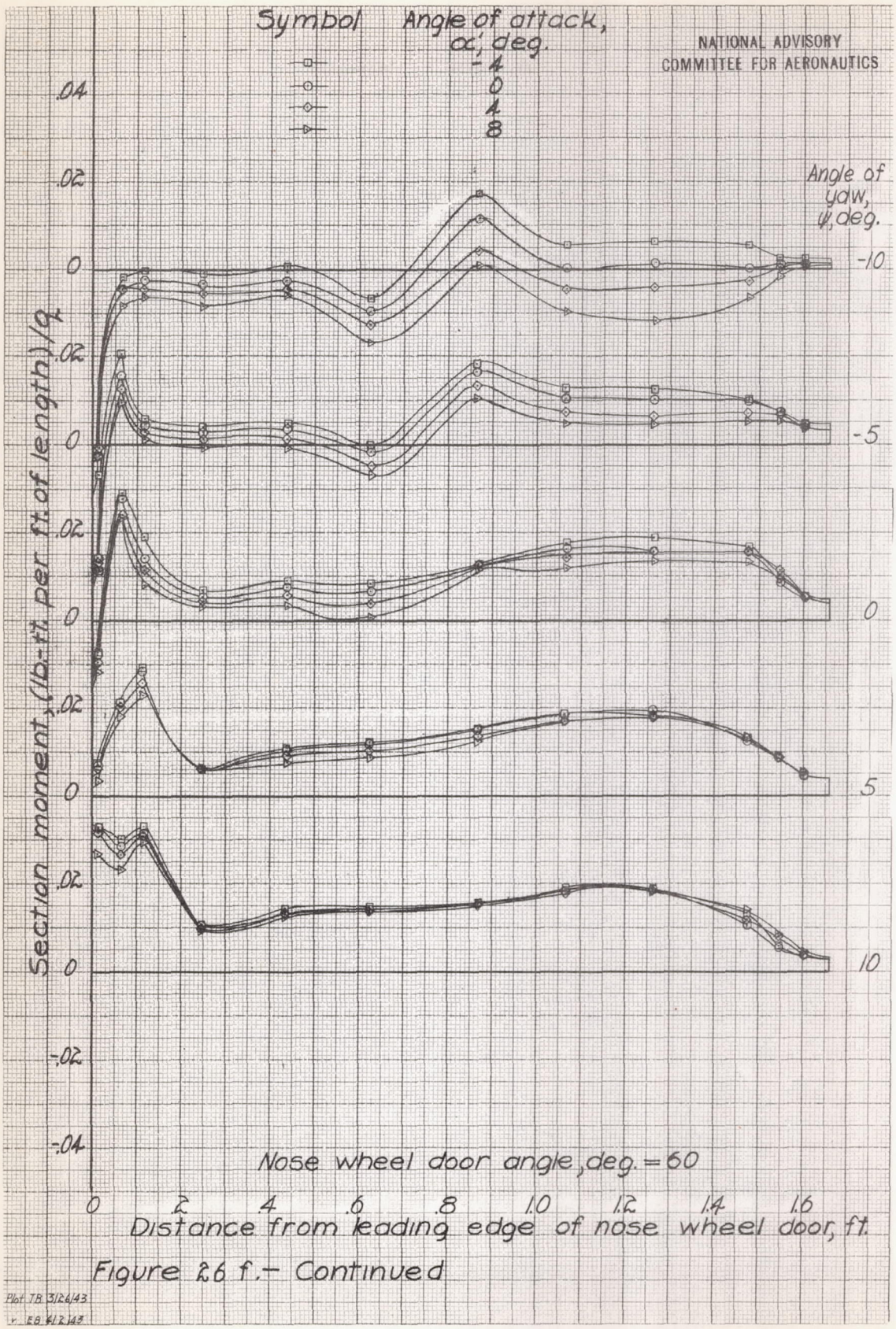

Figure 26 f.- Continued

Plot TB 3/26/43
r. EB 4/2/43

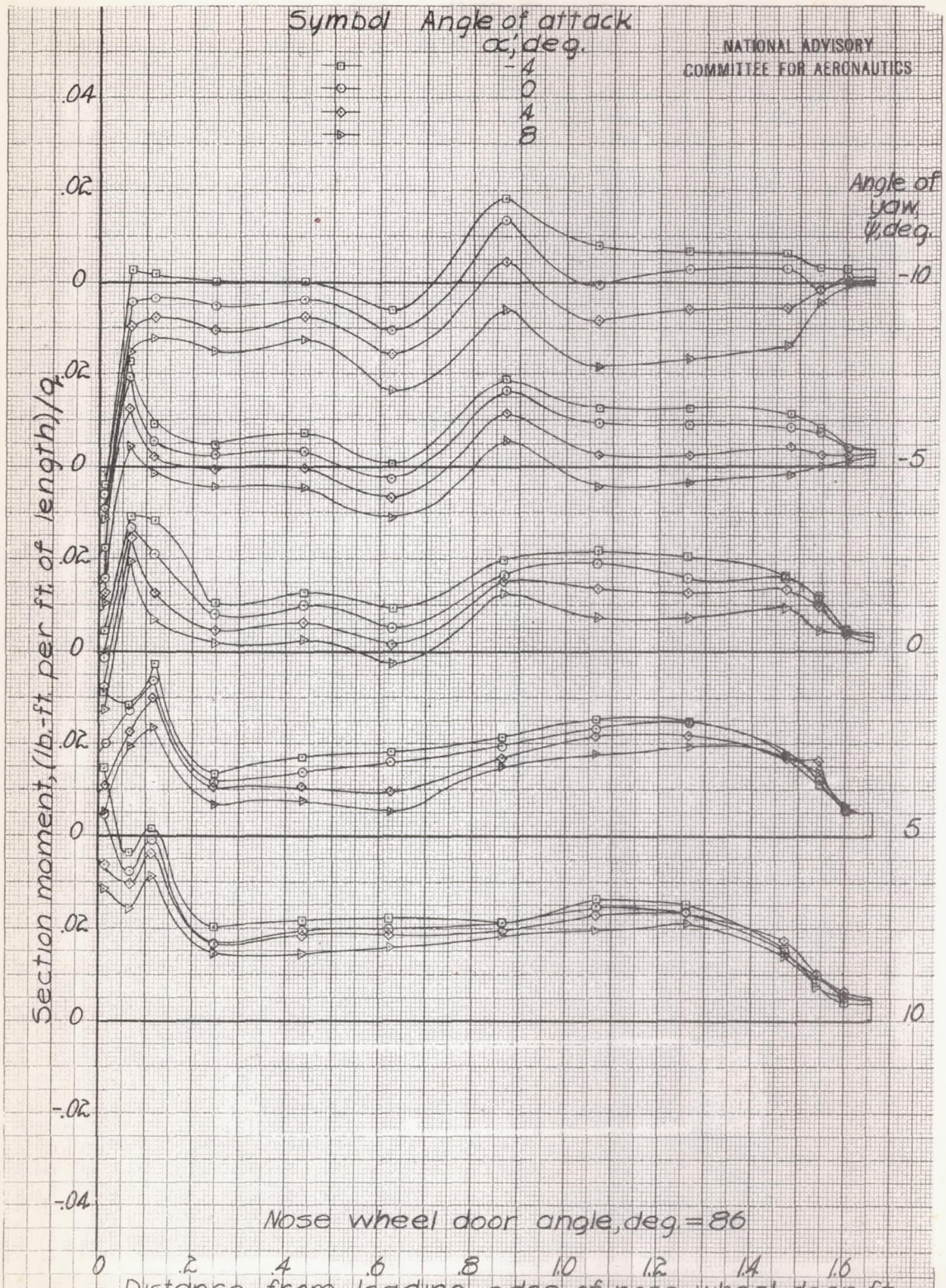

Figure 26 g.- Concluded.

Plot TB 3/26/43
A EB 4/2/43

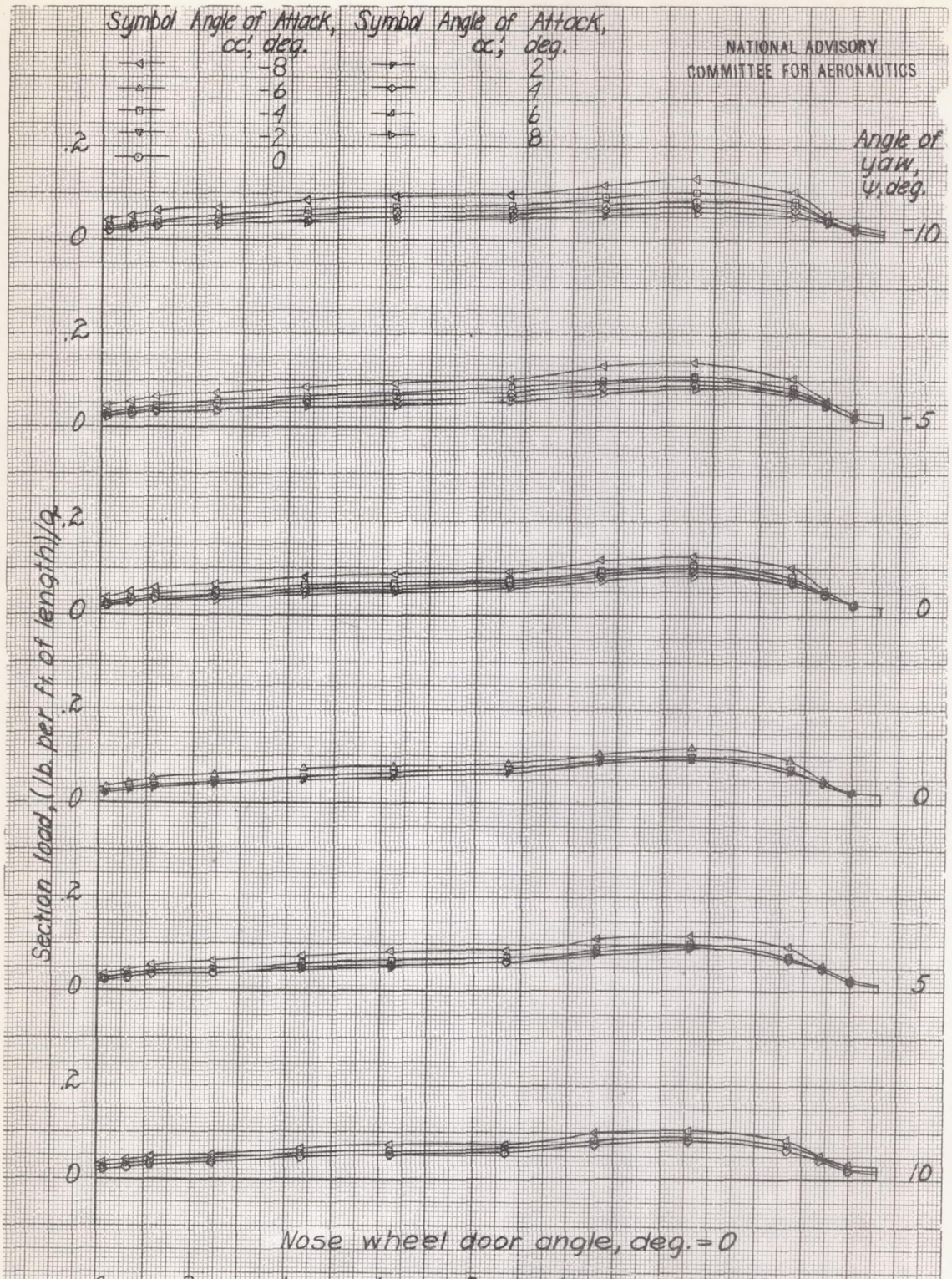

Figure 27a — Variation of section load along nose wheel door of 0.2375-scale model of Douglas XA-26 airplane; $q \approx 50$ lb/sq ft ; $R \approx 3,950,000$.

Plot TB 3/27/43
v EB 4/13/43

L-553

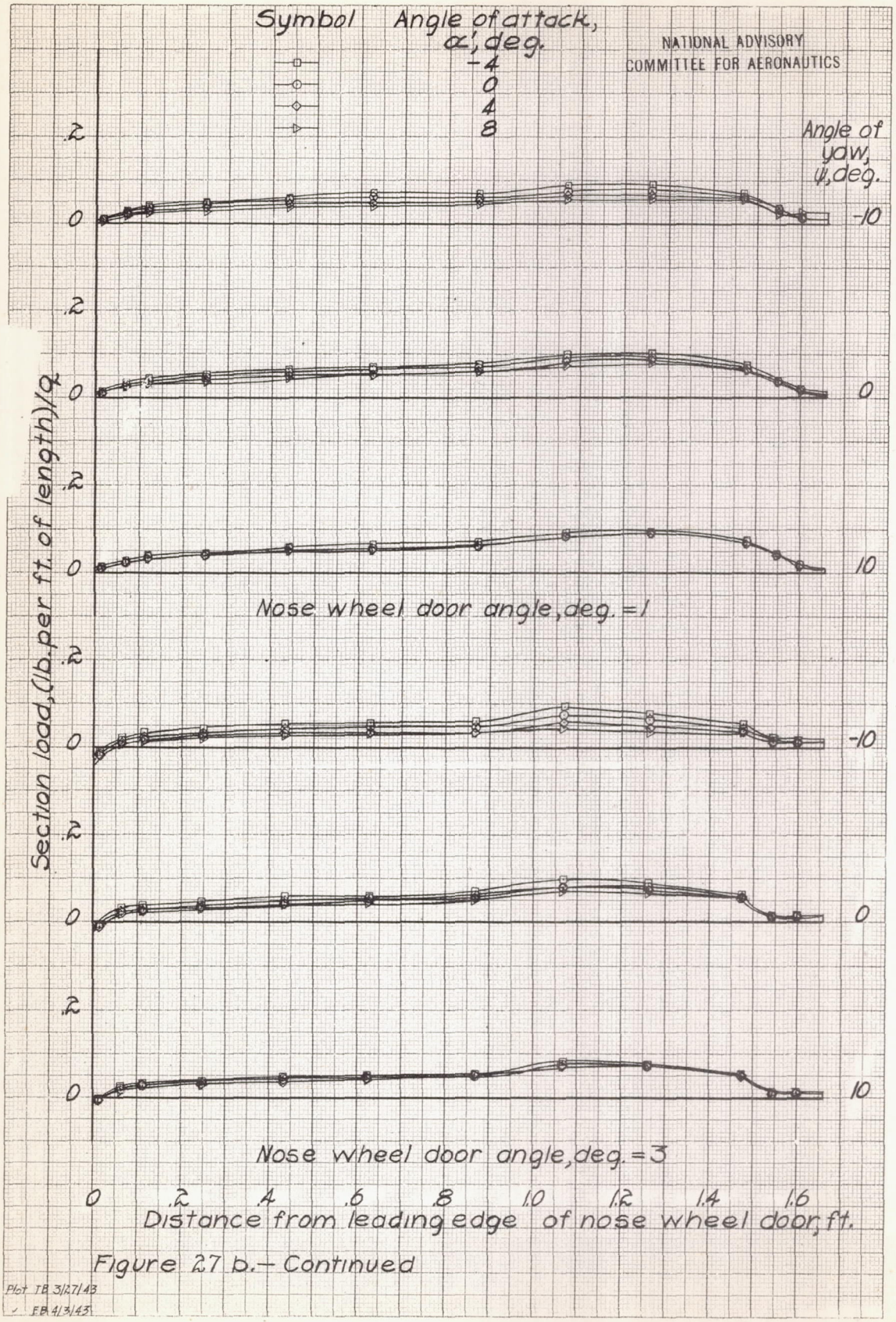

Figure 27 b.- Continued

Plot TB 3/27/43
✓ EB 4/3/43

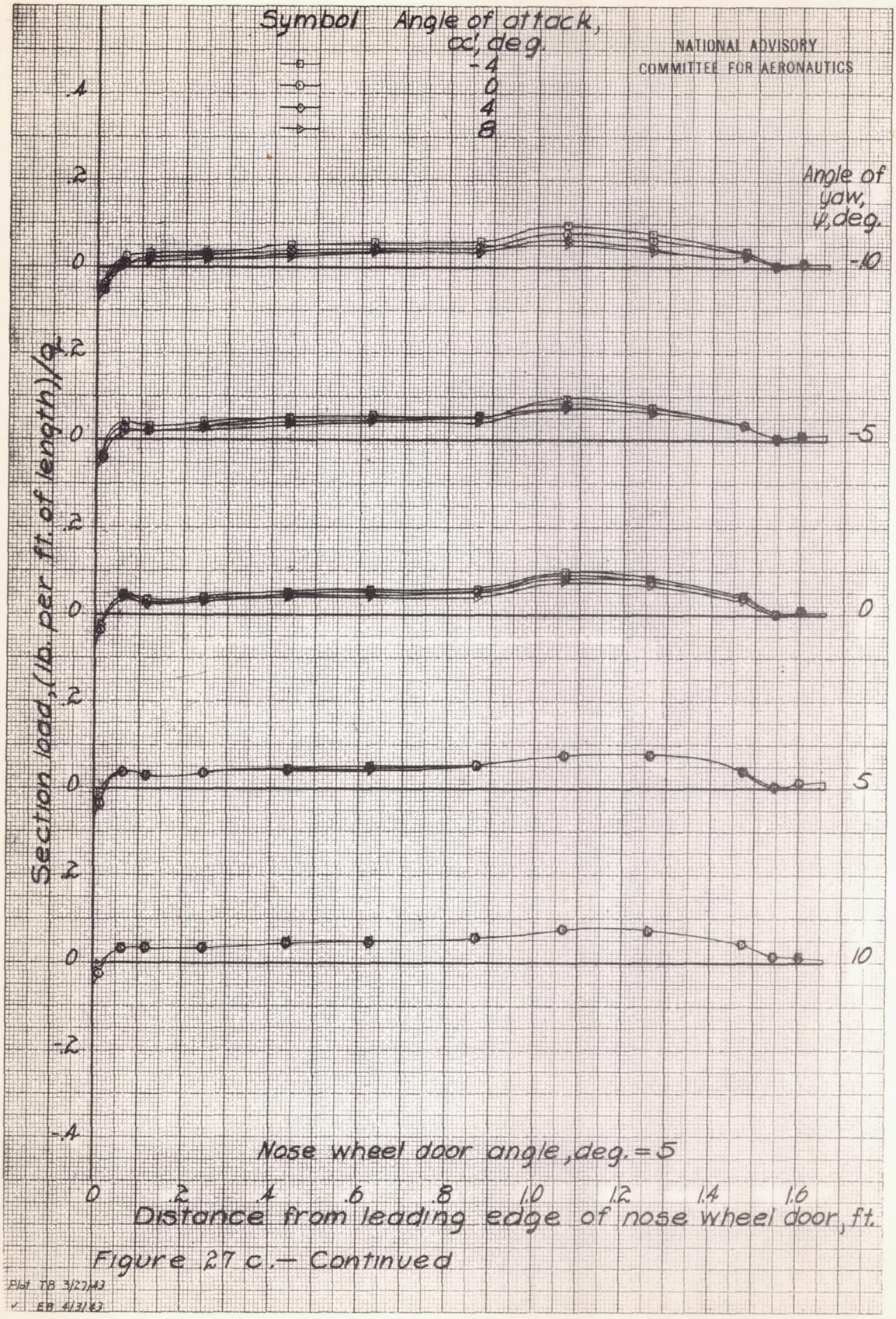

Figure 27 c.— Continued

Plot TB 3/27/43
✓ EB 4/3/43

L-553

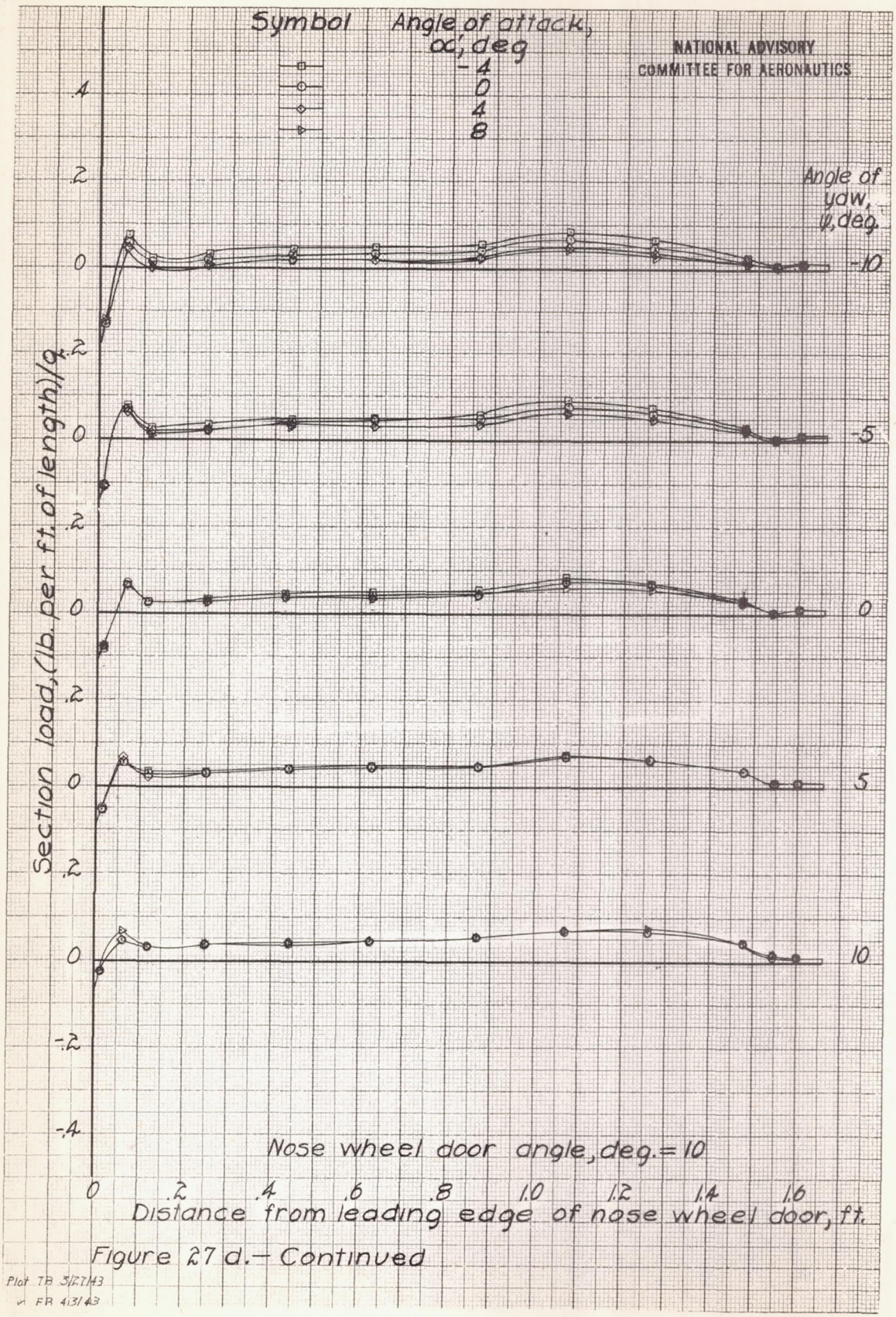

Figure 27 d.— Continued

Plot TB 3/27/43
FR 4/3/43

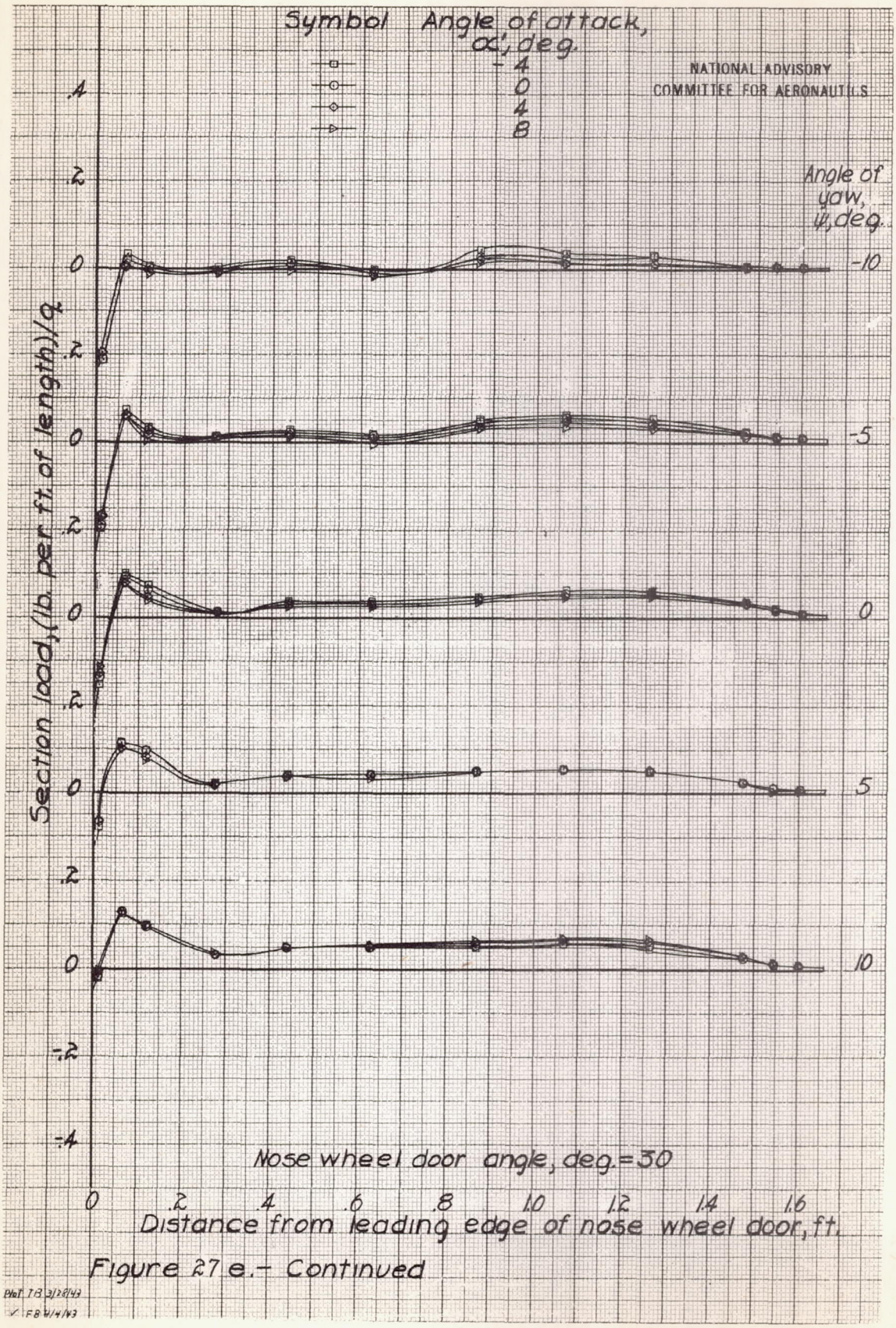

Figure 27 e.- Continued

Plot TB 3/26/43
✓ FB 4/4/43

L-553

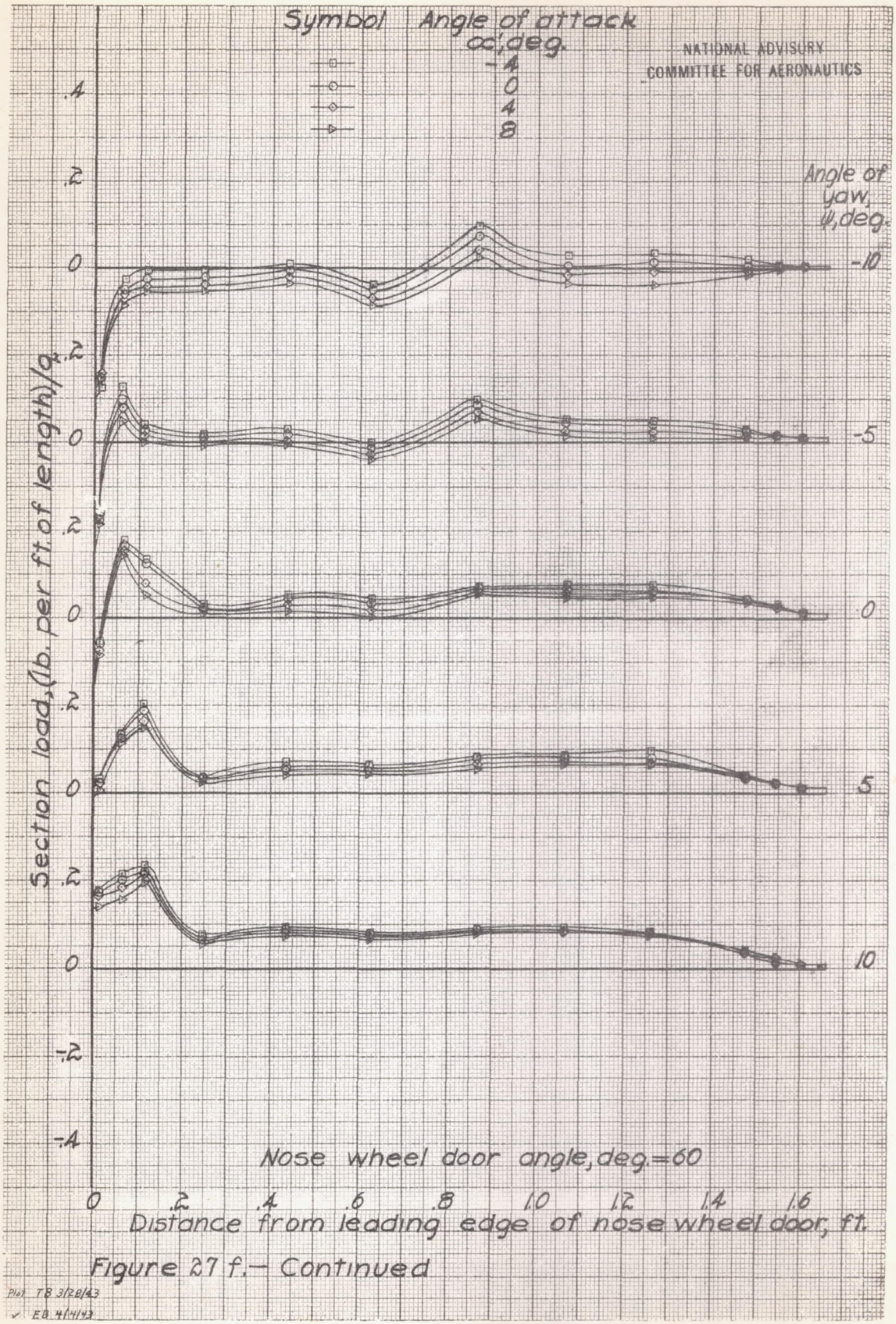

Figure 27 f.— Continued

Pict TB 3/28/43
✓ EB 4/14/43

L-553

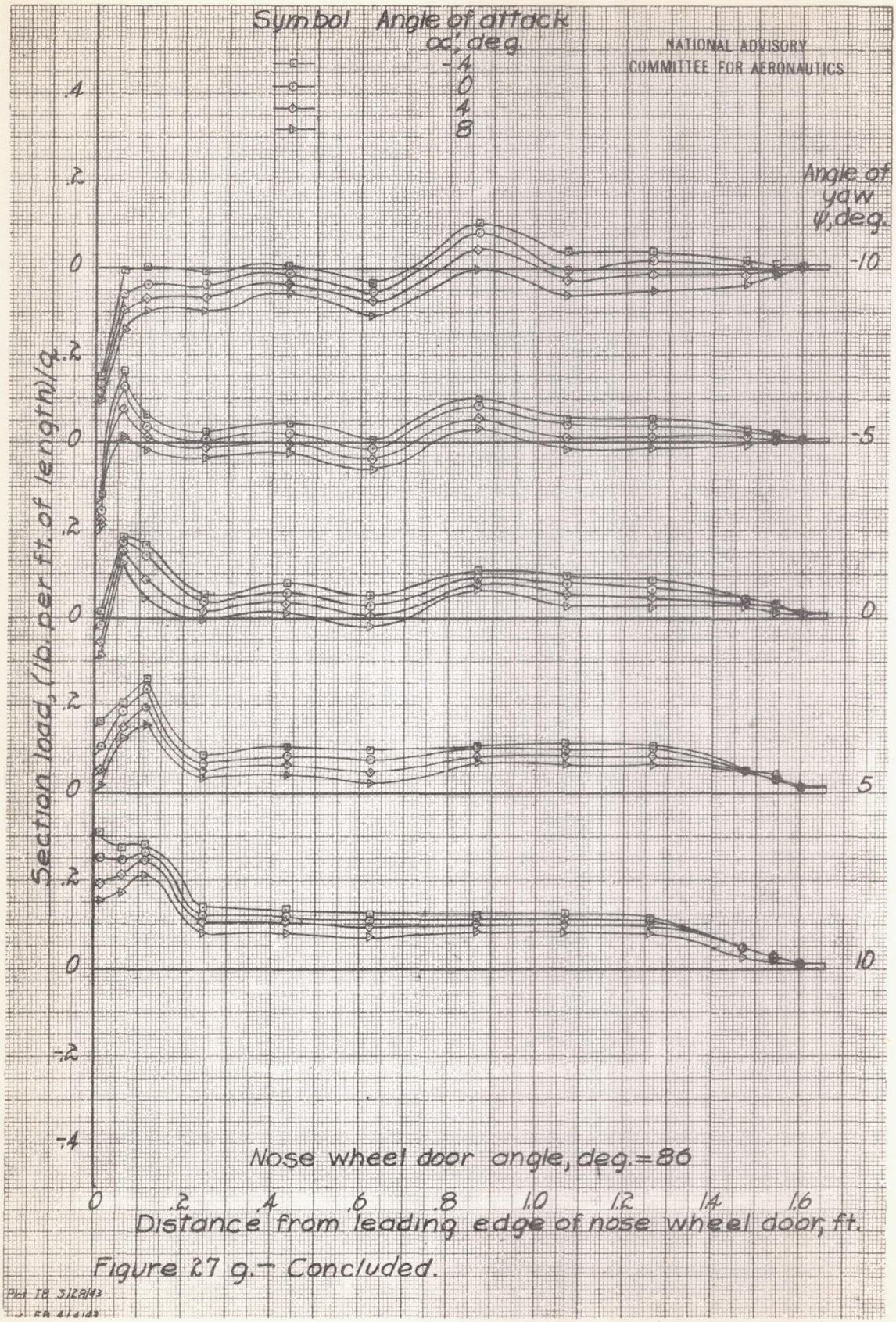

Figure 27 g.- Concluded.

Pict TB 3/28/43
FB 4/14/43

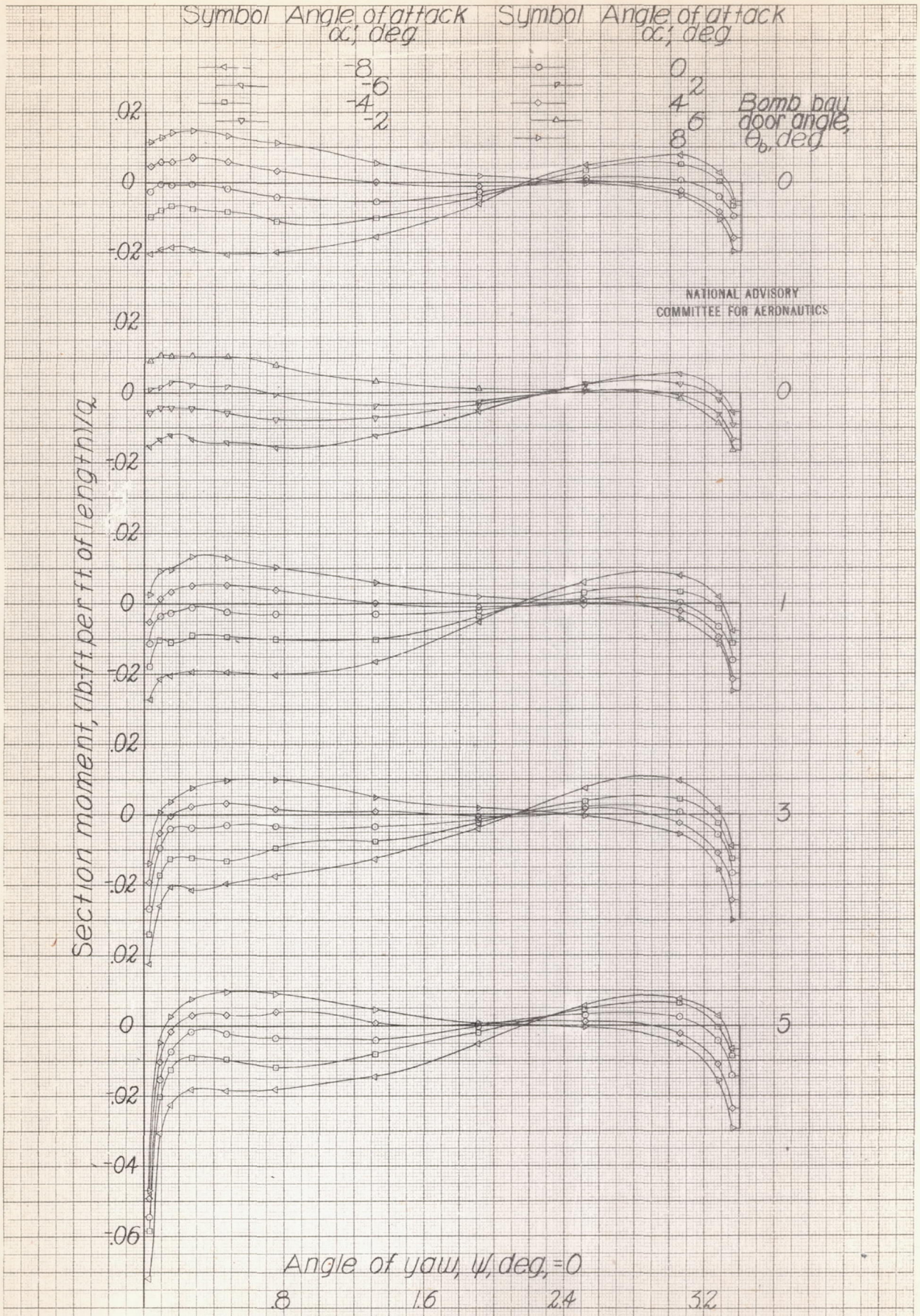

Figure 28a- Variation of section moment along bomb bay door of 0.2375 scale model of Douglas XA-26 airplane; q≈ 50 lb/sq ft; R≈ 3,640,000; M≈ 0.12.

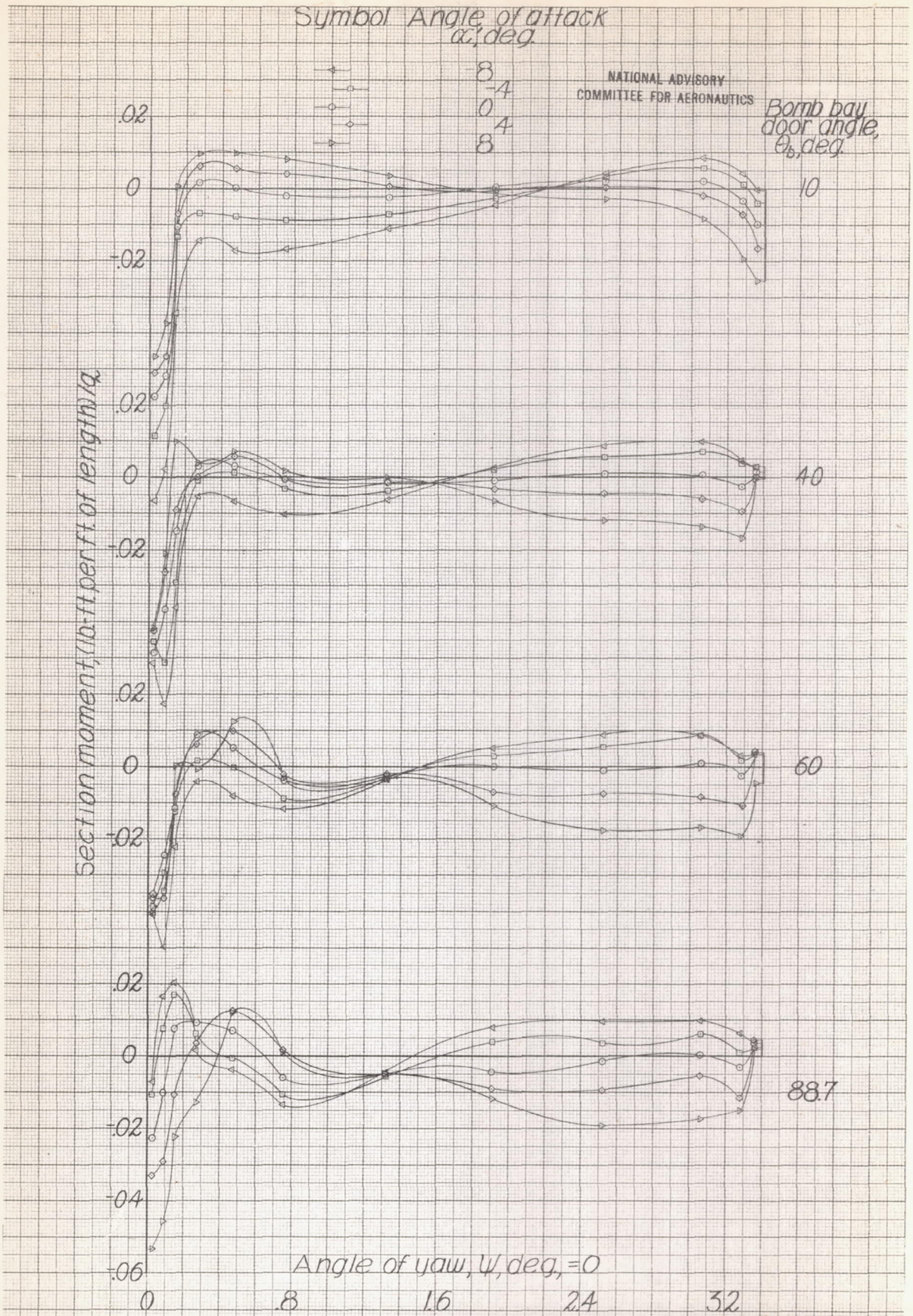

Figure 28b - concluded.

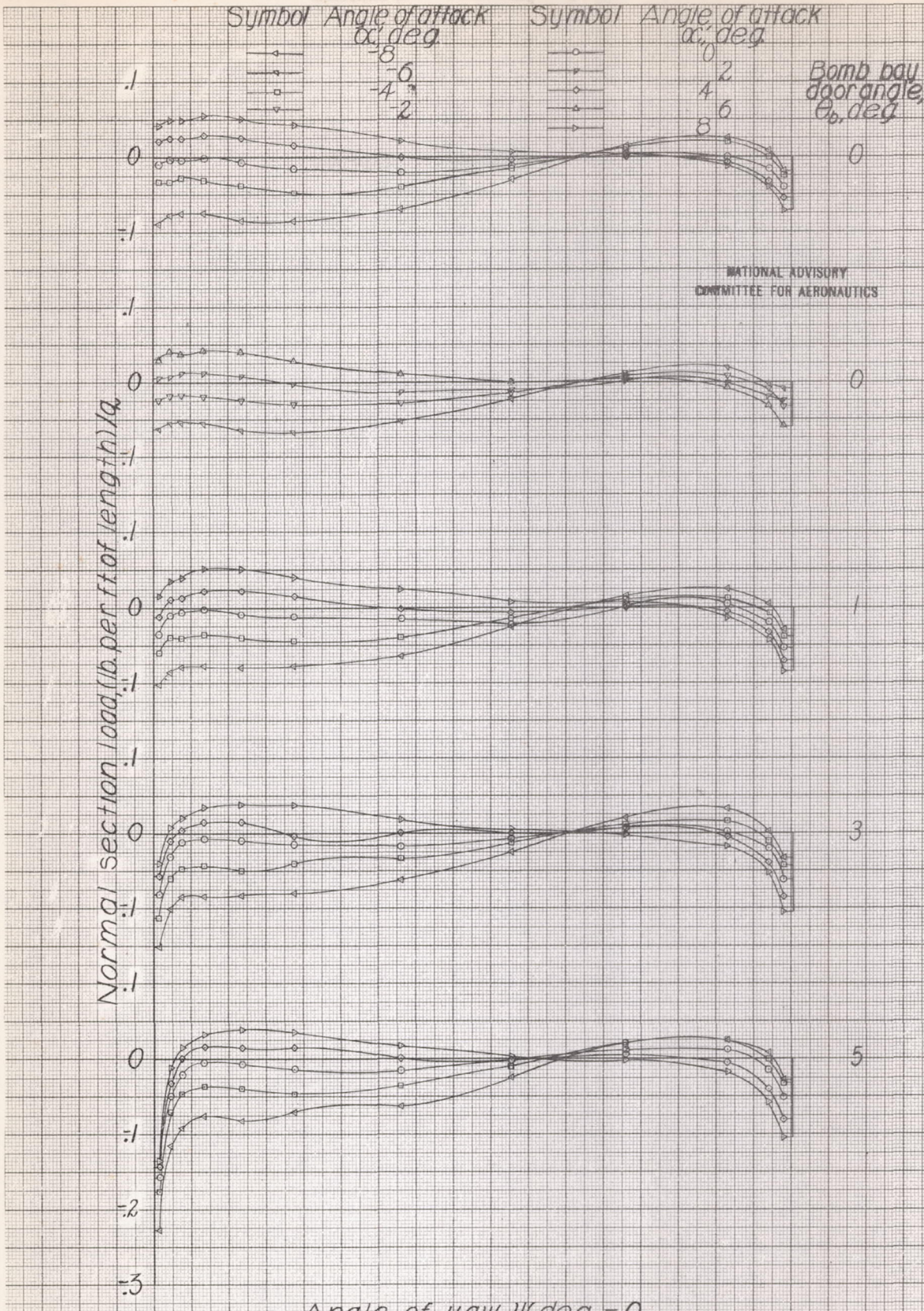

Figure 29a - Variation of normal section load along bomb bay door of 0.2375-scale model of Douglas XA-26 airplane; q ≈ 50 lb/sq ft.; R ≈ 3,640,000; M ≈ 0.12

55-7-53

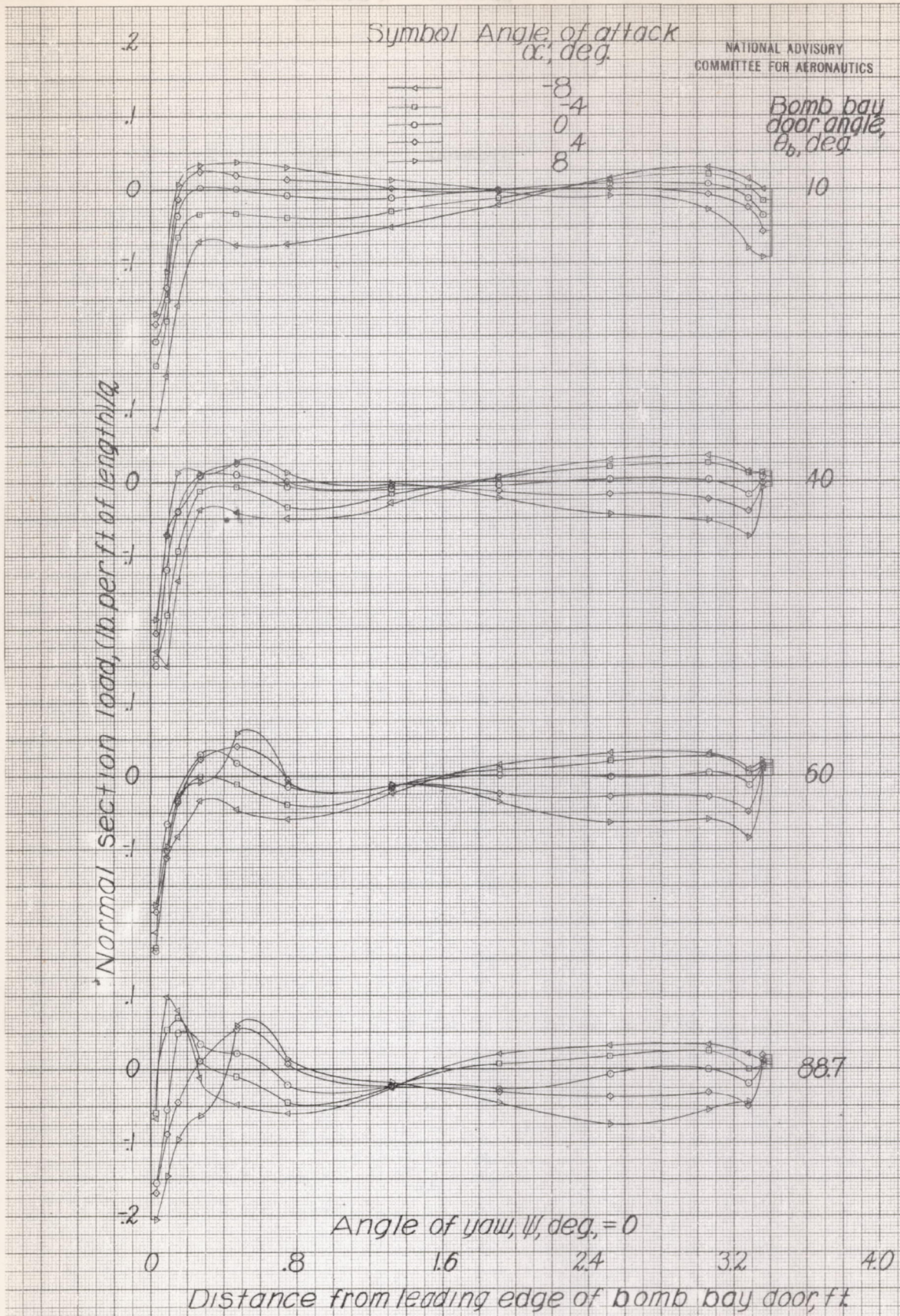

Figure 29b-continued.

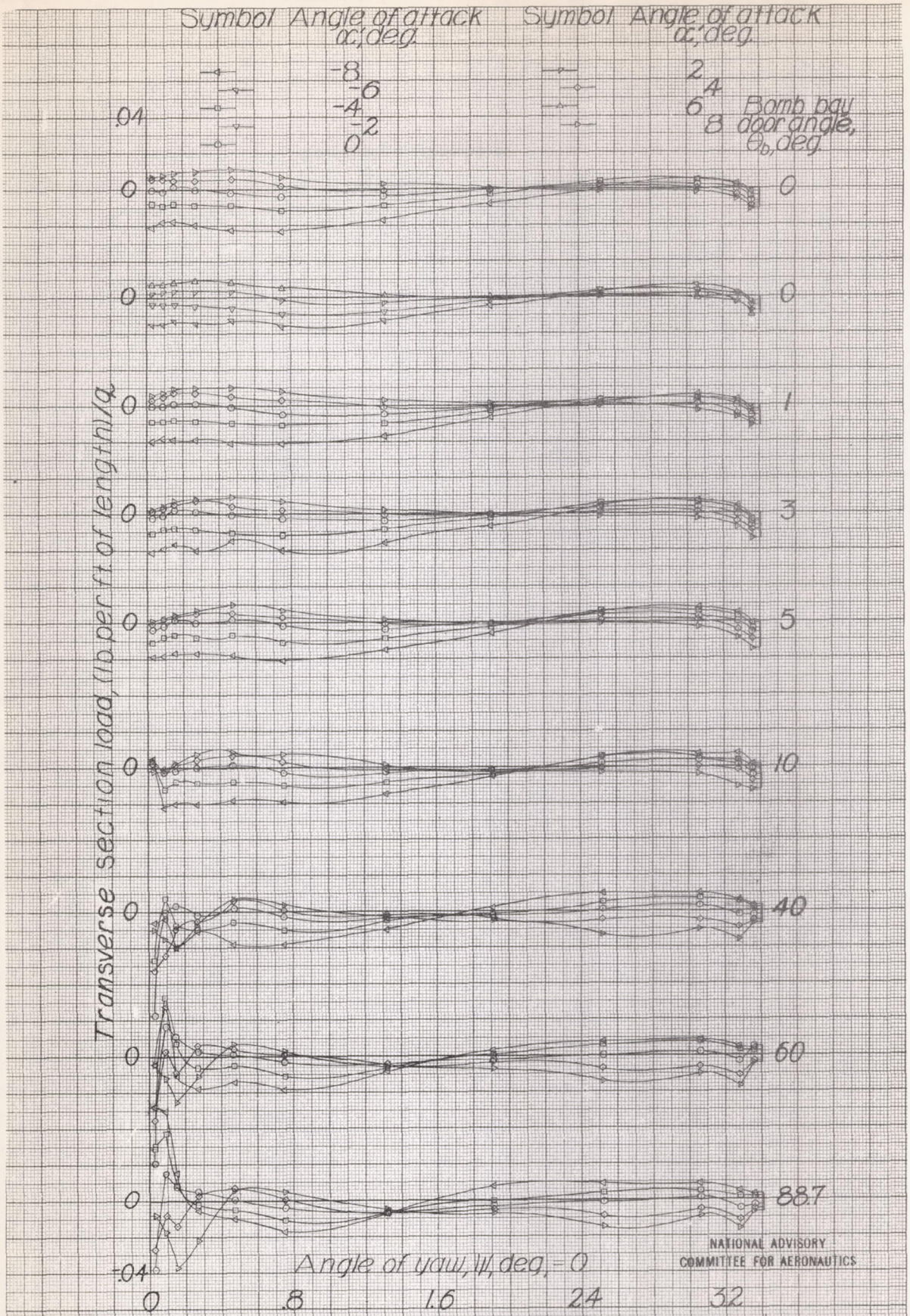

Figure 29c.-Variation of transverse section load along bomb bay door of 0.2375-scale model of Douglas XA-26 airplane; $q \approx 50$ lb/sq ft; $R \approx 3,640,000$; $M \approx 0.12$.

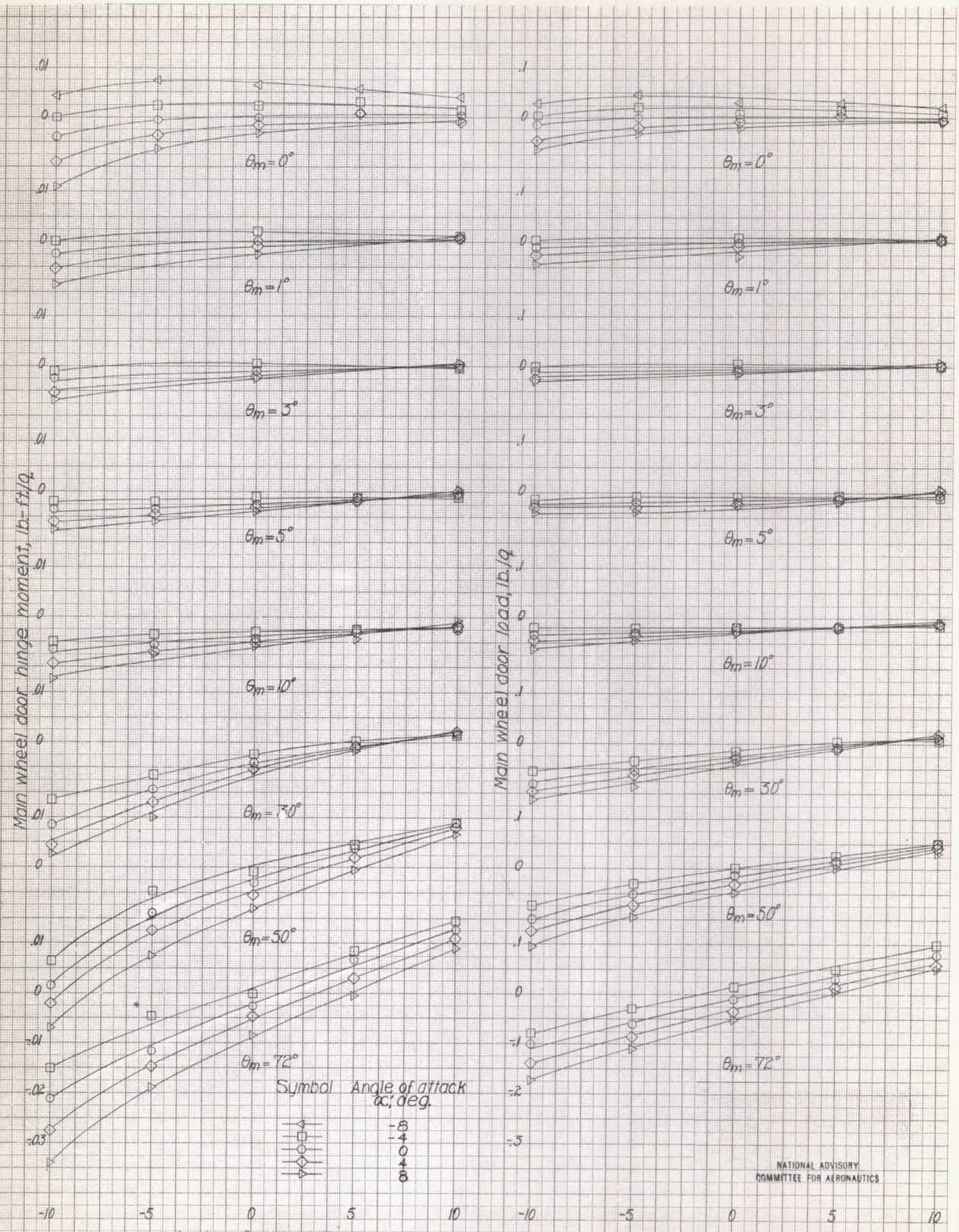

Figure 30.– Hinge moments and loads on main wheel door of 0.2375-scale model of Douglas XA-26 airplane; $q \approx 50$ lb/sq ft; $R \approx 3,960,000$.

L-553

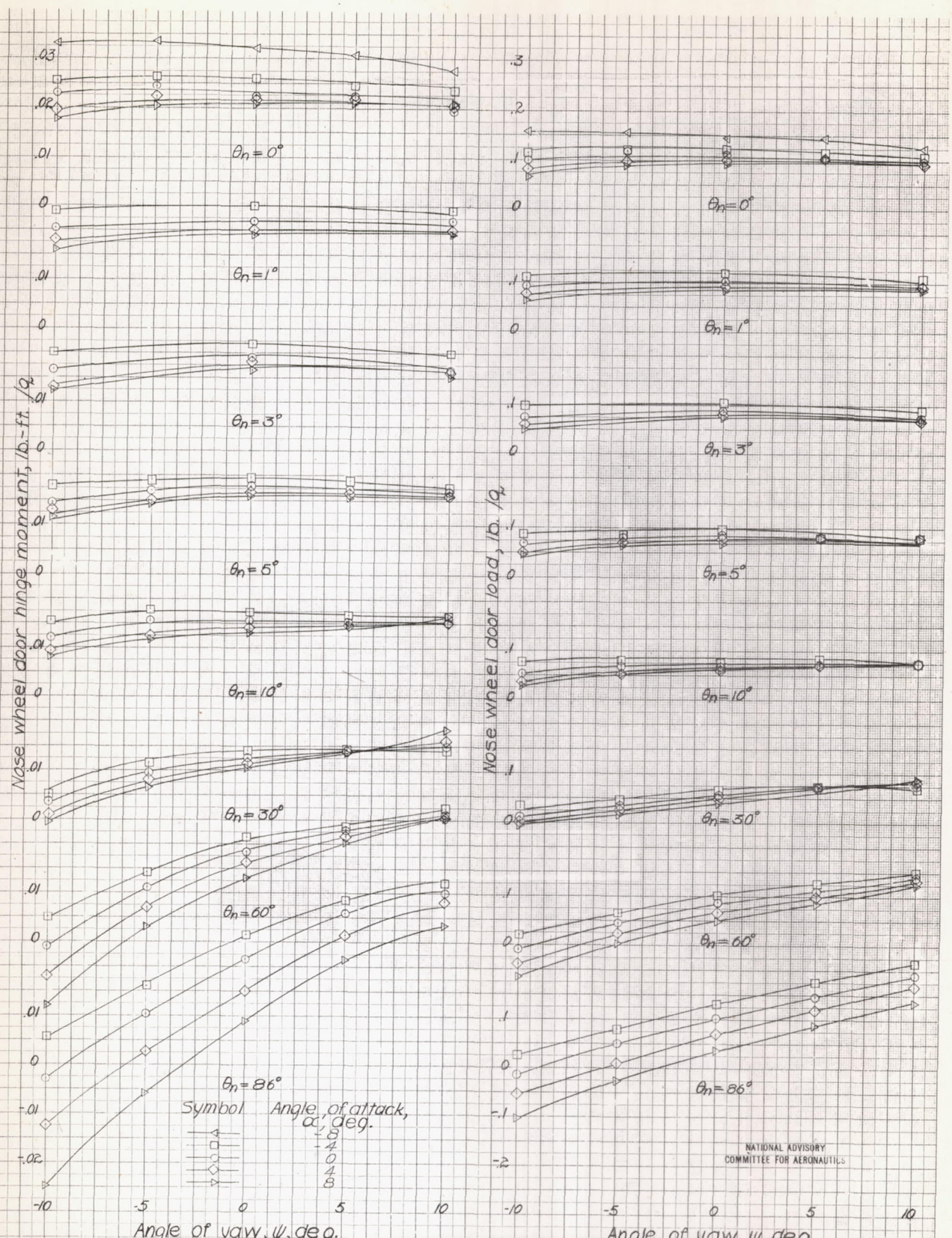

Figure 31 .— Hinge moments and loads on nose wheel door of 0.2375-scale model of Douglas XA-26 airplane; $q \approx 50$ lb/sq ft; $R \approx 3,950,000$.

L-553

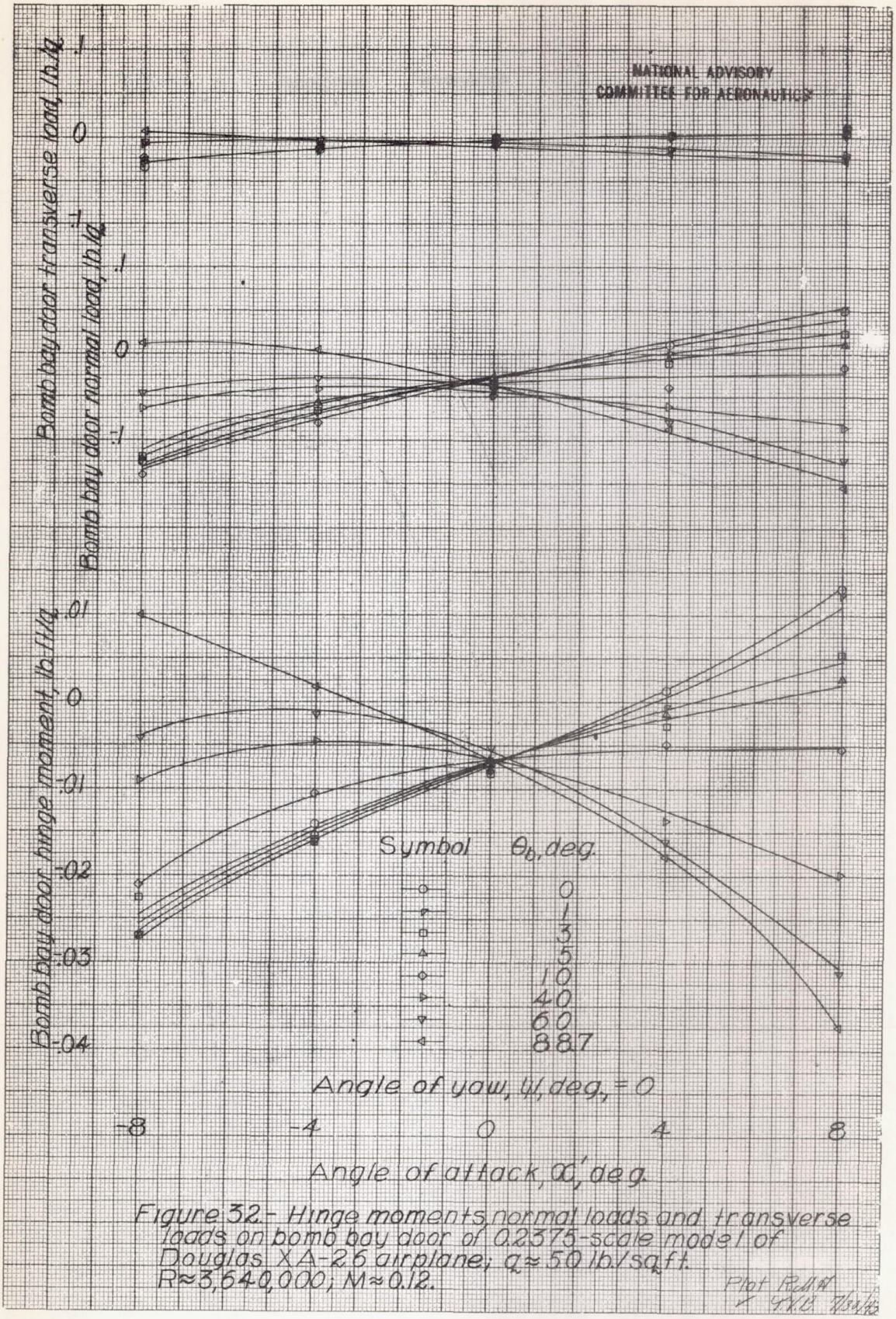

Figure 32.- Hinge moments, normal loads and transverse loads on bomb bay door of 0.2375-scale model of Douglas XA-26 airplane; $q \approx 50$ lb./sq.ft. $R \approx 3,640,000$; $M \approx 0.12$.

Plot Read by N.A.C.A. 7/24/42